Innate Mechanisms of Antimicrobial Defense Associated with the Avian Eggshell

Megan Rose-Martel

Thesis submitted to the
Faculty of Graduate and Postdoctoral Studies
in partial fulfillment of the requirements
for the Doctorate in Philosophy degree in
Cellular and Molecular Medicine

Department of Cellular and Molecular Medicine
Faculty of Medicine
University of Ottawa

Dedication

This thesis is dedicated to the loving memory of my father. He was a man in constant pursuit of knowledge. I was constantly reminded of how proud he was of my accomplishments, both personal and scientific. He read every article I published, every poster I created and inquired constantly about the research I was conducting, wanting to know every detail. His unwavering support and encouragement was invaluable to the completion of this thesis. I am extremely saddened that he is not here with us to see the completion of this chapter of my life which would have never been possible without him.

I also dedicate this thesis to my loving husband, my wonderful mother and my darling daughter for their endless love, patience and support that they show towards me every day of my life. They have helped me through the most difficult times by listening to me, making me laugh and always having faith that I could make it. They are and will always be a constant source of comfort, love and happiness.

Acknowledgments

I would like to express my sincere gratitude to my supervisor and mentor, Dr. Maxwell Hincke, for the opportunity to work in his laboratory. His encouragement, guidance and motivation throughout my Ph.D. studies have made this research possible. I would also like to thank the members of my thesis advisory committee, Dr. Simon Lemaire, Dr. Alain Stintzi and Dr. Franco Pagotto for their advice and insightful discussions.

I would also like to thank all my labmates for making the duration of my studies so enjoyable. I am especially grateful to the friendship provided by Jennifer Major, with whom lively discussions about life and science have helped me maintain good mental health.

I would like to thank Dr. Syed Sattar from the Centre for Research on Environmental Microbiology (CREM) for the generous donation of bacterial cultures which were crucial for this research.

This research was funded by the Natural Sciences and Engineering Research Council of Canada (NSERC), the Poultry Industry Council (PIC) and the Agriculture and Agri-Food Canada (AAFC)–Canadian Poultry Research Council (CPRC) poultry cluster.

Abstract

During the course of evolution, the avian egg has developed multiple physical and chemical barriers in order to resist microbial challenges. These barriers are essential for the successful reproduction of avian species as well as to maintain safe and nutritious food for human consumption of the table egg. The calcified eggshell is a biomineralized barrier with an integrated organic matrix containing antimicrobial proteins, a hallmark of sophisticated biological structures. Calcium carbonate is deposited onto the outer shell membranes to form the calcified mammillary, palisade and vertical crystal layers; the final layer to be deposited is the outer eggshell cuticle. In this thesis, mass spectrometry-based technology was used to investigate the proteome of the outer cuticle, the mammillary cones and the shell membranes in order to gain insight into biomineralization and antimicrobial functions of the avian eggshell. Proteomics analysis of the eggshell cuticle revealed multiple antimicrobial proteins, supporting the hypothesis that the outermost cuticle layer is the first barrier against invading pathogens. The two most abundant cuticle proteins identified are similar to Kunitz-like protease inhibitor (ovocalyxin-25) and ovocalyxin-32. Multiple antimicrobial proteins were also revealed to be associated with the shell membrane fibres. Among the most abundant proteins were lysozyme C, avian β-defensin-11, ovotransferrin, ovocalyxin-36 and gallin. The biomineralized shell is also an important physical barrier against invading pathogens. Proteomics analysis of the mammillary cones, the initiation sites for shell calcification, revealed several candidate proteins involved in calcitic biomineralization. Promising candidates include nucleobindin-2 and SPARC, two calcium binding proteins previously shown to modulate mineralization. In-depth analysis of the comprehensive proteomes generated by this study revealed the presence of histones in the shell

membranes, shell and cuticle compartments. Histones are cationic antimicrobial peptides, which are key molecules of the innate immune defense system of many species. This thesis reports the minimal inhibitory concentrations and minimal bactericidal concentrations of histones extracted from avian erythrocytes against Gram-positive, Gram-negative and antibiotic-resistant bacteria. Results suggest that the underlying antimicrobial mechanism is based on the interaction between histones and lipopolysaccharides / lipoteichoic acids, which are negatively charged components of bacterial cell membranes. Histones also inhibit the growth of Gram-positive biofilms; the minimal biofilm eradication concentrations were determined for *S. aureus* and methicillin-resistant *S. aureus* (MRSA). Sensitive proteomics analyses have provided great insight into the protein constituents of the eggshell matrix, with two primary roles in the innate immune defense of the egg: regulation of calcitic biomineralization and antimicrobial protection. Further research on these proteins and their functions can provide a new focus for selective breeding programs looking to enhance the egg's natural defenses, or provide inspiration for alternatives to conventional antibiotics, such as the histones.

Table of Contents

List of Figures

List of Tables

Chapter 2

Chapter 3

Chapter 4

List of Abbreviations

ABI3BP	ABI Family Member 3 (NESH) Binding Protein
ADRI	Animal Disease Research Institute
AMP	Antimicrobial Peptide
Arr	Aminoglycoside Response Regulator
ATCC	American Type Culture Collection
BCA	Bicinchoninic Acid
BLAST	Basic Local Alignment Search Tool
BPI	Bactericidal Permeability-Increasing Protein
BPPV	Benign Paroxysmal Position Vertigo
BPTI	Bovine Pancreatic Trypsin Inhibitor
CAM	Chorioallantoic Membrane
CAMA	Cecropin A-Mellitin A Amide
CAMP	Cationic Antimicrobial Peptide
CAP-11	Cationic Antibacterial Polypeptide of 11 kDa
CAP-18	Cationic Antimicrobial Peptide of 18 kDa
CD14	Cluster of Differentiation 14
CFIA	Canadian Food Inspection Agency
CFU	Colony Forming Unit
CM	Carboxymethyl
CPRC	Canadian Poultry Research Council
CREMP	Cysteine-Rich Eggshell Membrane Protein
CTL	C-Type Lectin-Like
DAVID	Database for Annotation, Visualization and Integrated Discovery

DCA	Dromaiocalcin
DEAE	Diethylaminoethyl
DEFB126	Human β-Defensin 126
DMP1	Dentin Matrix Protein 1
DTT	Dithiothreitol
EDIL3	EGF-Like Repeats and Discoidin 1-Like Domains 3
EDTA	Ethylenediaminetetraacetic Acid
EGF	Epidermal Growth Factor
EGTA	Ethyleneglycoltetraacetic Acid
EMBL-EBI	European Molecular Biology Laboratory – European Bioinformatics Institute
emPAI	exponentially modified Protein Abundance Index
EPS	Exopolysaccharide
ES MS/MS	Electrospray Tandem-Mass Spectrometry
EST	Expression Sequence Tag
FDR	False Discovery Rate
GMP	Guanosine Monophosphate
GO	Gene Ontology
GST	Glutathione S-Transferase
HAPLN3	Hyaluronan and Proteoglycan Link Protein 3
HCl	Hydrochloric acid
HIP/PAP	Hepatocarcinoma Intestine-Pancreas/Pancreatic Associated Protein
IL	Interleukin
KSPG	Keratin Sulfate Proteoglycan
LB broth	Luria-Bertani broth
LBP	Lipopolysaccharide Binding Protein

LC/MS/MS	Liquid Chromatography Tandem-Mass Spectrometry
LPS	Lipopolysaccharide
LTA	Lipoteichoic Acid
MBC	Minimum Bactericidal Concentration
MBEC	Minimum Biofilm Eradication Concentration
MEPE	Matrix Extracellular Phosphoglycoprotein
MIC	Minimum Inhibitory Concentration
MRSA	Methicillin-Resistant *Staphylococcus aureus*
MS/MS	Tandem-Mass Spectrometry
MW	Molecular Weight
NEFA	DNA Binding, EF-hand, Acidic Region Protein
NET	Neutrophil Extracellular Trap
NSERC	Natural Sciences and Engineering Research Council of Canada
NUC2B	Nucleobindin-2
OC-116	Ovocleidin-116
OC-17	Ovocleidin-17
OCX-21	Ovocalyxin-21
OCX-25	Ovocalyxin-25
OCX-32	Ovocalyxin-32
OCX-36	Ovocalyxin-36
OD	Optical Density
OVAX	Ovalbumin-Related Protein X
PAGE	Polyacrylamide Gel Electrophoresis
PAMP	Pathogen-Associated Molecular Patterns
pBLAST	protein Basic Local Alignment Search Tool

PBS	Phosphate Buffered Saline
PIC	Poultry Industry Council
PLUNC	Palate, Lung and Nasal Epithelium Clone
RARRES1	Retinoic Acid Receptor Responder (tazarotene induced) 1
RBC	Red Blood Cell
RCA	Rheacalcin
Reg	Regenerating islet-derived
RP-HPLC	Reversed Phase High-Performance Liquid Chromatography
RP-nanoLC	Reversed-Phase Nanoscale Capillary Liquid Chromatography
RT-PCR	Reverse Transcription Polymerase Chain Reaction
SCA	Struthiocalcin
SCPP	Secretory Calcium-Binding Phosphoprotein
SDS	Sodium Dodecyl Sulfate
SDS-PAGE	Sodium Dodecyl Sulfate – Polyacrylamide Gel Electrophoresis
SERPIN	Serine Protease Inhibitor
SIBLING	Small Integrin-Binding Ligand, N-Linked Glycoprotein
SLPI	Secretory Leukocyte Protease Inhibitor
SLRP	Small Leucine-Rich Proteoglycans
SNP	Single Nucleotide Polymorphism
SPARC	Secreted Protein, Acidic, Cysteine-Rich
TCA	Trichloroacetic Acid
TENP	Transiently Expressed in Neural Precursors
TNF	Tumor Necrosis Factor
WAP	Whey Acidic Protein
WHO	World Health Organization

General Introduction

The avian egg possesses multiple chemical and physical barriers that are essential in preventing bacterial growth and entry into the egg. A pathogen-free egg is critical for the propagation of avian species and for food safety of the nutritious table egg. At the time of oviposition (laying of the egg), the interior of the egg is normally free of bacterial contamination and it can remain in this state for the duration of the 21 days of incubation. The capacity to resist bacterial contamination is a very desirable trait for the unfertilized table egg intended for human consumption. The Canadian egg industry produced approximately 7 billion chicken eggs in 2013, 70% of which are designated for the table market. According to Agriculture and Agri-Food Canada, annual egg consumption in Canada has increased approximately 4 dozen eggs per person from 1995 to 2013. Eggs are a well-known functional food, meaning that they are not only a nutritive food rich in minerals and nutrients, but can also improve human health (Surai and Sparks, 2001). The nutritional content of eggs can also be manipulated to include nutrients that have been found lacking in the human diet, such as omega-3 fatty acids, vitamin E and selenium.

1. Food-borne Illnesses Associated with Contaminated Eggs

Generally, each egg compartment possesses its own physical and chemical antimicrobial defense mechanisms to prevent bacterial entry and growth. These barriers are essential since bacteria that are able to reach the nutritive yolk are able to proliferate rapidly at non-refrigerated temperatures (Board and Fuller, 1974). Bacterial contamination of the egg can occur through

vertical transmission or horizontal transmission. Vertical transmission refers to an egg that is infected by a pathogen prior to the expulsion of the egg (Keller et al., 1995). This occurs when a pathogen within an infected laying hen is transferred via the blood stream to the reproductive tissues and finally to the egg interior. This type of transmission is a huge concern in the poultry industry since infected hens do not always display visible symptoms of infection, and it is therefore difficult to detect birds laying contaminated eggs (Gast and Benson, 1995). Horizontal transmission describes the contamination of the egg after it has been expelled from the hen, possibly from bacteria within the hen's feces or the surrounding environment (Messens et al., 2005).

Food-borne illness is a major concern in the food industry. In the egg and egg product industry, the most prevalent bacteria known to cause food related diseases in humans are *Salmonella* spp., *Listeria* spp., *Staphylococcus* spp., *Bacillus* spp., *Campylobacter* spp. and *Escherichia* spp. Gram-negative bacteria are more prominent in the interior of decaying eggs while Gram-positive bacteria are typically found on the surface of the eggs due to their greater tolerance of dry conditions (Board and Tranter, 1995).

According to the American Centers for Disease Control and Prevention, *Salmonella enterica* serovar Enteritidis is the primary contaminant of eggs and egg-containing foods (Schroeder et al., 2005). Health Canada estimates that 16,600 cases of human illness are caused by *S.* Enteritidis each year in Canada (DeWinter et al., 2011). This particular bacteria poses an increased risk for egg contamination due to the lack of symptoms in the infected hens (Hogue et al., 1997). Salmonellosis can occur from 6 – 72 hours after ingesting food contaminated with *S.* Enteritidis; symptoms include fever, diarrhea, abdominal pain, nausea and vomiting.

Listeria monocytogenes is responsible for a serious food-borne disease called listeriosis. Milder infections include symptoms such as vomiting, nausea, cramps, muscle aches, diarrhea, severe headache, constipation and severe fever. More severe infections can spread to the blood stream and nervous system, which can lead to septicemia and meningitis, respectively (Hernandez-Milian and Payeras-Cifre, 2014). *L. monocytogenes* is an important concern in the food industry since it can proliferate in unfavorable conditions, including high salt concentrations and at refrigeration temperatures (Swaminathan and Gerner-Smidt, 2007). A study evaluating the occurrence of *L. monocytogenes* in the French poultry industry indicated that 15.5% of laying-hen flocks tested positive for the bacterium (Chemaly et al., 2008). *L. monocytogenes* was also found in 2% of eggshells and 8% of environmental samples collected from egg breaking plants in Western France (Rivoal et al., 2013), indicating that eggs and egg products can become contaminated during the processing phase of the industry.

Staphylococcal food poisoning is caused by ingesting food contaminated with enterotoxins produced by *Staphylococcus aureus* (Danielsson-Tham, 2013). This disease has a very short incubation period; symptoms appear 1 – 6 hours after ingestion (Rusnak et al., 2004). Initial symptoms include increased salivation and nausea followed by stomach cramps, vomiting and possibly diarrhea. *Staphylococcus* spp. has previously been identified as a major contaminant of the eggshell of table eggs (De Reu et al., 2008). A study assessing bacterial contamination of five egg grading facilities in the United States found the presence of *S. aureus* in wash water, on the conveyer as well as on washed and unwashed eggs (Moats, 1980). Between 1969 and 1990, eggs were responsible for 3.5% of reported staphylococcal food poisoning in the United Kingdom. Eggs and egg products were also responsible for 11% of reported staphylococcal food poisonings in France between 1999 and 2000 (Le Loir et al., 2003).

The ingestion of food contaminated with spore-forming *Bacillus cereus* and its toxins can lead to two types of food-borne illnesses: diarrheal and emetic illness. Diarrheal illness presents 8 – 16 hours after consumption with watery stools accompanied by abdominal pain while emetic illness involves nausea and vomiting with symptoms appearing 0.5 – 6 hours after ingestion (Logan, 2012). *B. cereus* is capable of growing at low temperatures and its spores have been shown to effectively adhere to stainless steel equipment found in food processing plants (Jan et al., 2011). A study evaluating the risk factors of *B. cereus* in the egg industry found that 13% of the eggshell surface samples tested positive for mesophilic *B. cereus* and 2.3% of samples tested positive for psychotrophic *B. cereus* (Kone et al., 2013).

The avian intestinal tract is considered to be an important reservoir for *Campylobacter jejuni*; however, the prevalence of eggs contaminated with *Campylobacter* spp. is very low. While *C. jejuni* has been identified in the oviduct of laying hens (Camarda et al., 2000), there is no evidence to support the occurrence of vertical transmission. Regarding horizontal transmission, studies have shown the presence of *Campylobacter* spp. on the surface of the egg (Jones et al., 2012; Jones and Musgrove, 2007); however, *C. jejuni* demonstrated a limited capacity to traverse the eggshell (Sahin et al., 2003). Various egg compartments inoculated with *C. jejuni* revealed low survivability of the bacteria in the air sac and albumen but viable bacteria persisted in the yolk (Sahin et al., 2003). *C. jejuni* causes campylobacteriosis, an illness lasting 2 – 5 days and characterized by diarrhea, abdominal pain, nausea, vomiting, malaise and fever.

Escherichia coli has previously been identified as a contaminant of the egg interior (De Reu et al., 2008; Mayes and Takeballi, 1983). Many studies have also identified *E. coli* as a contaminant of the egg surface as well (Jones et al., 2012; Moats, 1980; Musgrove et al., 2005; Chousalkar et al., 2010). However, a study examining the impact of commercial egg processing

on the presence of *E. coli* found a significant reduction in prevalence of *E. coli* in eggs sampled after processing compared with unwashed eggs (Musgrove et al., 2005). Like most food borne illnesses described above, symptoms include stomach cramps, vomiting and diarrhea.

2. Egg Formation

Egg formation follows a well-defined pattern of assembly as it travels the length of the oviduct (Fig. 1 and 2). The avian ovum consists primarily of yolk and a germinal disc containing the organelles and nucleus of the oocyte (Volentine et al., 1998). Once the hen ovulates, the ovum is captured by the infundibulum where fertilization occurs within 15 minutes in the germinal disc region (Birkhead et al., 1994); after which the vitelline membrane surrounding the yolk is synthesized (Nys et al., 2004). The yolk contains nutrients and minerals necessary for the proper development of the chick embryo as well as immunoglobulin Y antibodies, transferred from the hen's serum, to provide the embryo with passive immunity (Kovacs-Nolan and Mine, 2012). The vitelline membrane consists of tightly packed fibres integrated with ovomucin, vitelline membrane outer protein 1 and antimicrobial components such as lysozyme C and avian β-defensin 11 (a cationic antimicrobial peptide) (Herve-Grepinet et al., 2010). The forming egg then moves on to the magnum where it will remain for 3-4 hours while the albumen (egg white) is deposited. As a physical barrier, the albumen contains 2 - 4% ovomucin which is responsible for egg white viscosity and suggested to reduce bacterial mobility (Burley and Vadehra, 1989). The albumen also contains several varieties of antimicrobial proteins including nutrient sequestering proteins (ovotransferrin and avidin), hydrolytic antimicrobials (lysozyme C), protease inhibitors (cystatin and ovoinhibitor) and antimicrobial peptides (gallin) (Mann, 2007).

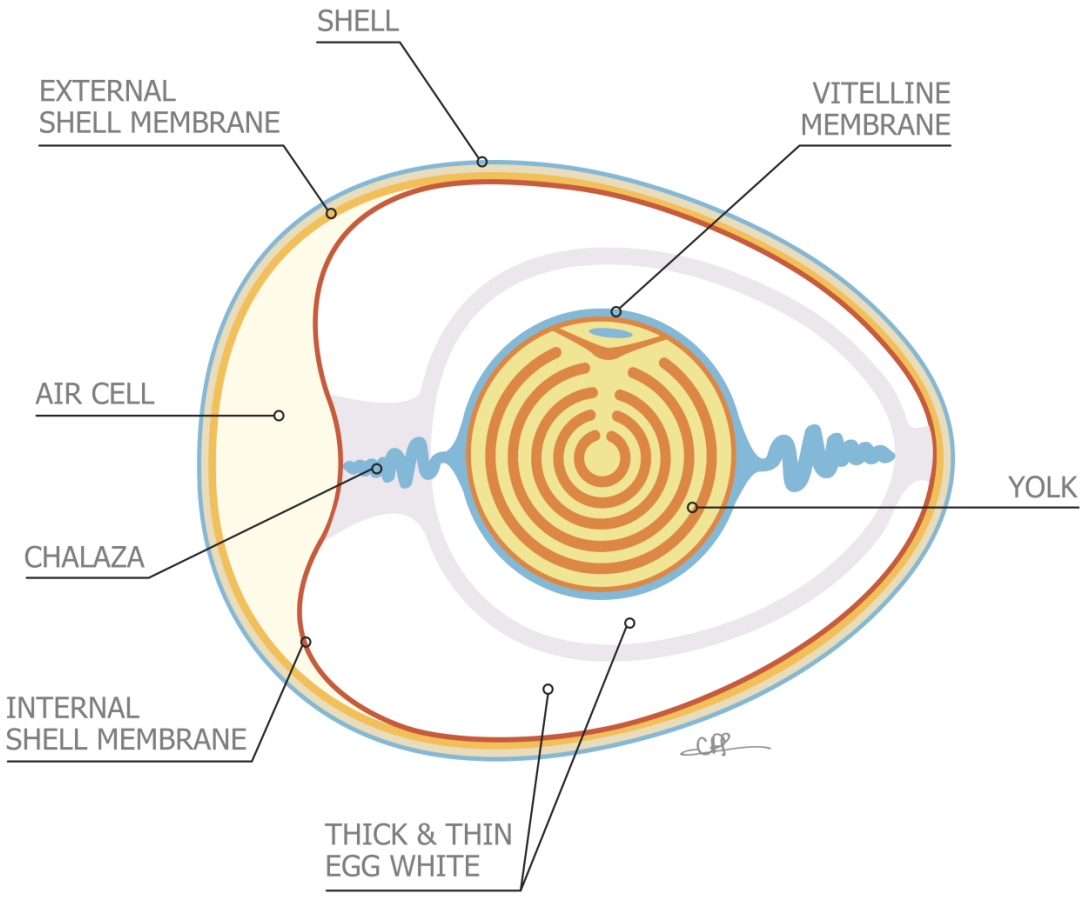

Fig. 1. Depiction of the egg interior of a fully-formed egg (longitudinal section). Source: Hincke et al., 2012. The eggshell: structure, composition and mineralization. *Frontiers in Bioscience*. 17:1266-80.

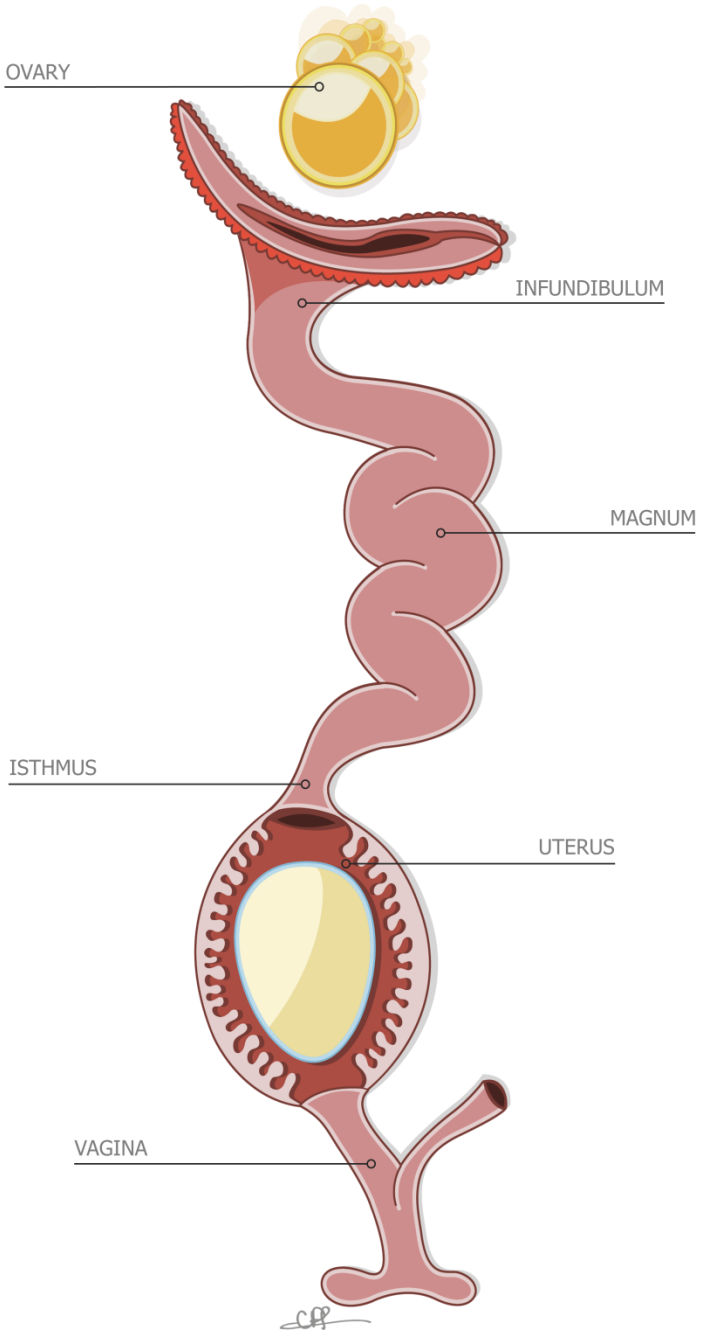

Fig. 2. Schematic of the oviduct, the reproductive system of the hen. An incomplete egg can be observed in the shell gland (uterus). Source: Hincke et al., 2012. The eggshell: structure, composition and mineralization. *Frontiers in Bioscience.* 17:1266-80.

The albumen is surrounded by the innermost layers of the avian eggshell which are a highly cross-linked meshwork known as the shell membranes (Fig. 3C). This meshwork is organized into inner and outer layers which are deposited in less than 90 minutes while the egg passes through the white isthmus (Nys et al., 2004) (Fig. 3B). Following the white isthmus, the egg enters the distal red isthmus region of the oviduct where organic aggregates deposited in a semi-periodic array on the surface of the outer shell membrane. When the egg enters the uterus, these organic aggregates become the initial sites of mineralization for shell formation and the beginning of the mammillary cones (Hincke et al., 2012). The inner shell membrane remains un-mineralized (Fig. 3D); the mechanisms involved in the inhibition of mineralization towards the egg interior are poorly understood.

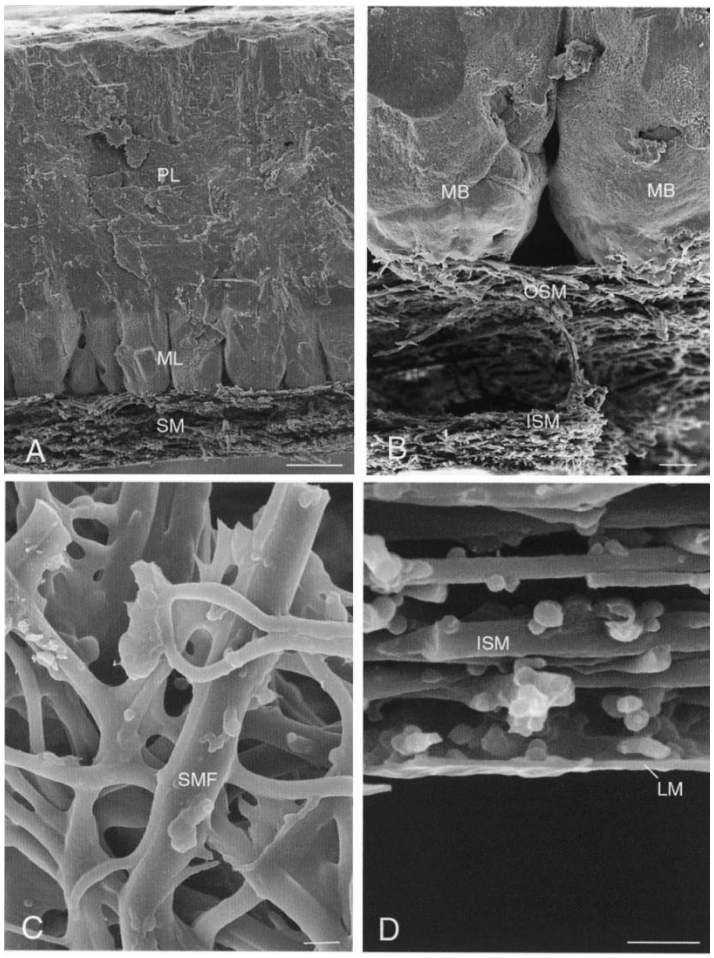

Fig. 3. Scanning electron micrographs illustrating the morphology of the eggshell and eggshell membranes. (**A**) Eggshell cross-fractured to reveal the shell membrane (SM), mammillary layer (ML) and palisade layer (PL). (**B**) Higher magnification of the membrane–mammillary body interface. Outer shell membrane fibres (OSM) insert into the tips of the mammillary bodies (MB). Inner shell membranes (ISM). (**C**) Enlargement of the shell membrane fibres (SMF) to reveal their interwoven and coalescing nature. (**D**) Inner aspect of the inner shell membrane (ISM), demonstrating the limiting membrane (LM) that surrounds the egg white (here removed during sample preparation). Scale bars (**A**) 50 µm; (**B**) 20 µm; (**C, D**) 2 µm. Source: Hincke *et al*., 2000. M*atrix Biology* 19(5), with permission from Elsevier.

The outermost barrier, and first line of defense of the egg contents, is the calcified eggshell (Fig. 4). The chicken eggshell is a biomineralized barrier of calcium carbonate with an integrated organic matrix consisting of proteins involved in calcitic biomineralization and/or antimicrobial protection (Rose and Hincke, 2009). The first calcified layer to be deposited, known as the mammillary cone layer, consists of cones of calcite crystals that eventually fuse together and grow into merged columns to form the palisade layer. This layer ends at the vertical crystal layer upon which is deposited the eggshell cuticle, a non-calcified organic coating (Nys et al., 2004).

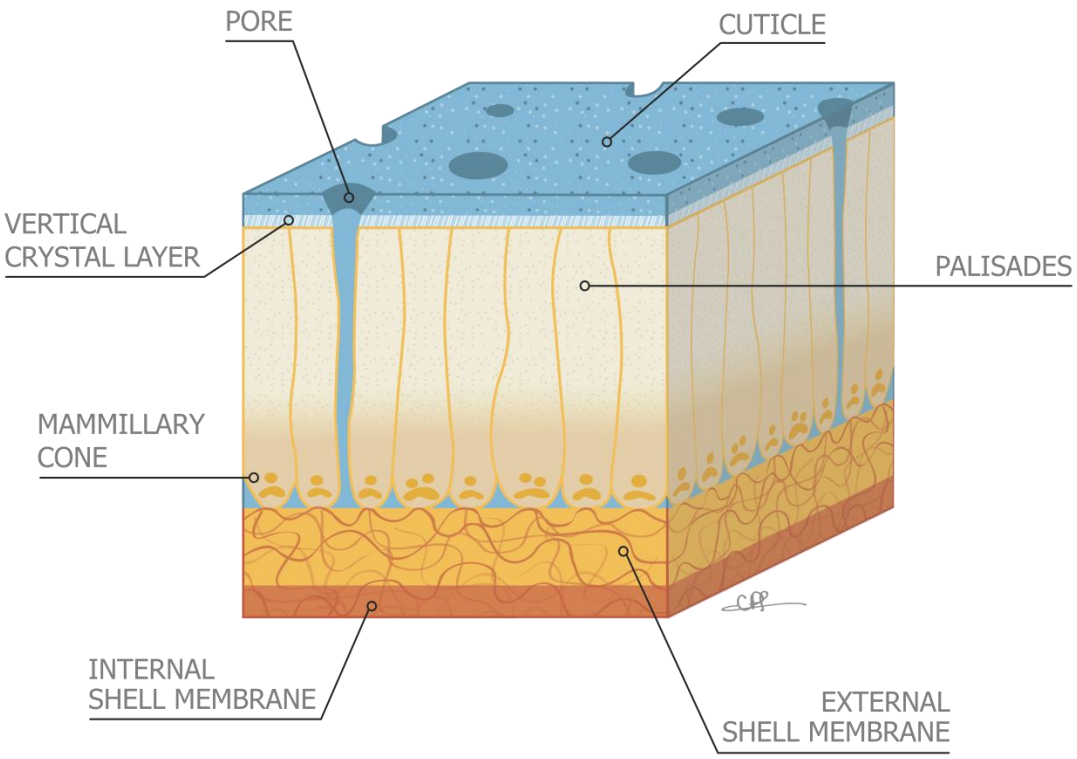

Fig. 4. Depiction of a cross-section of the avian eggshell including the shell membranes, calcified layers and outermost cuticle. Source: Hincke *et al*., 2012. The eggshell: structure, composition and mineralization. *Frontiers in Bioscience.* 17:1266-80.

3. Biomineralized Barrier

The avian eggshell is a biomineralized barrier essential for reproductive success. It has a crucial function of withstanding harsh physical and thermal conditions as well as microbial challenges originating from the external environment. It is also responsible for water and metabolic gas regulation as well as a critical source of calcium for the developing embryo (Hincke et al., 2012). Every layer of the eggshell, including shell membranes, calcified shell and cuticle layer, acts as both a physical and chemical barrier to protect the yolk and embryo.

3.1. Eggshell Membranes

Shell membrane fibres consist of collagens (type I, V and X) and cysteine-rich eggshell membrane proteins (CREMPs) (Arias et al., 1991; Kodali et al., 2011). This fibrous material is also associated with bioactive molecules that enhance the antimicrobial protection provided by this barrier. Antimicrobial proteins identified in the shell membranes include lysozyme (Hincke et al., 2000), ovotransferrin (Gautron et al., 2001) and ovocalyxin-36 (Cordeiro et al., 2013). Lysozyme and ovotransferrin are more commonly known for their antimicrobial activity in the egg white, using hydrolytic and iron-sequestering mechanisms of bacterial inhibition, respectively. Ovocalyxin-36 is an eggshell-specific matrix protein with established similarities to bactericidal permeability increasing protein and lipopolysaccharide binding protein (Cordeiro et al., 2013). A transcriptomics study assessing up-regulated genes in the white isthmus identified avian β-defensin 11 as an antimicrobial protein associated with shell membranes (Du et al.,

manuscript in preparation). Defensins are cationic antimicrobial peptides with a broad spectrum of antimicrobial activity including bacteria, fungi and viruses (Mageed et al., 2008).

The intricate meshwork and insoluble characteristics of the eggshell membrane fibres have hindered comprehensive proteomics analyses. Due to their resistance to typical protein extraction techniques, the protein constituents of the shell membrane fibres and their function remain poorly understood.

3.2. Mineralized Eggshell

One of the fastest known biomineralization process is chicken eggshell formation. Eggshell mineralization occurs in the hen uterus where the surrounding epithelial and mucosal cells secrete all the necessary components into the uterine fluid (Rose and Hincke, 2009). For 16 – 17 hours, the egg bathes in the uterine fluid, whose protein constituents change gradually as eggshell formation occurs. Shell mineralization can be separated into three distinct steps: initiation (5 hours), rapid mineralization (12 hours) and termination (1.5 hours) (Nys et al., 1999). As mentioned in the previous section, calcium carbonate mineralization is initiated at sites where organic aggregates are deposited on the surface of the outer shell membranes. These sites become the base of the mammillary cones, which are penetrated by the fibres of the outer shell membrane (Fig. 3B). The mammillary cones make up the mammillary layer of the calcified shell, which is ~100 μm in thickness, and merge into organized columns to form the palisade layer, ~300 μm thick (Arias et al., 1993). The external region of the palisade layer is responsible for absorbing external impacts; it consists of large calcite crystals and an inter-crystalline organic layer that prevents the propagation of intra-crystalline cracks (Nys et al., 2004). A high density

crystalline structure known as the vertical crystal layer marks the end of the palisade layer (Fig. 3A).

The mineralized shell represents a complex bioceramic material that can resist harsh physical assaults as well as physically block bacterial entry into the egg (Jones and Musgrove, 2005). Cracked or damaged eggshells greatly impact food safety of the table egg and reproductive success of the fertilized egg. A Canadian risk assessment evaluating the yearly consumption of eggs with cracked shells revealed that Canada produces approximately 143 million cracked eggs, believed to be responsible for an estimated 10,500 cases of salmonellosis (Todd, 1996). A high quality shell, free of microcracks, is a highly desirable trait. Studies have indicated a positive correlation between eggshell thickness and breaking strength (Ar et al., 1979); however, many other characteristics influence the overall biomechanical integrity of the shell. The size and spacing of the mammillary cones have been shown to affect the integrity of the subsequent calcified layers; also, crystal orientation in the palisade layer has been correlated with shell strength (Solomon, 1999; Rodriguez-Navarro et al., 2002). On average, older hens produce eggs with decreased eggshell integrity which leads to a higher incidence of hairline cracks and an increased probability of bacterial penetration (Messens et al., 2005). Dispersed throughout the avian eggshell are thousands of pores necessary to permit gas and water exchange required for proper embryonic development. These pores have funnel-shaped openings on the surface of the shell, with a single channel traversing the shell between the columns of the palisade layer and opening between the mammillary cones, (Chien et al., 2008). Pores have a diameter of ~49 μm, ~25 μm and ~18 μm at the exterior, middle and interior regions of the eggshell, respectively (Tyler, 1956). These pores, especially the larger ones, are all potential entry points for bacterial contamination (Ar and Rahn, 1985; Messens et al., 2005). The cuticle

layer, which will be discussed in the following section, is deposited on the surface of the egg and functions as a barrier by covering and filling the pores up to 50 μm in depth (Ruiz and Lunam, 2000).

The calcified eggshell consists of ~96% calcium carbonate with an intermingling organic matrix (~3.5%) (Hincke et al., 2008). The protein constituents of this organic matrix become incorporated into the eggshell while the forming egg bathes in the uterine fluid during the calcification process. Eggshell specific-matrix proteins have been identified using transcriptomics and proteomics approaches and two functions have been proposed, both suggesting a role in the innate defense mechanisms of the egg: biomineralization and/or antimicrobial protection. Ovocleidin-116 (OC-116), found to be abundant in the palisade layer, is the core protein of an eggshell dermatan sulfate proteoglycan and suggested to have a significant role in calcitic biomineralization (Hincke et al., 1999). Ovocleidin-17 (OC-17) was found to be abundant in the mammillary layer of the calcified eggshell; however, it was identified throughout the entire shell matrix (Hincke et al., 1995). *In vitro* studies have demonstrated the capacity of OC-17 to influence calcite crystal aggregation in a concentration-dependent method (Reyes-Grajeda et al., 2004). OC-17 also functions as an antimicrobial protein; it is a C-type lectin-like protein shown to be effective at inhibiting the growth of Gram-positive bacteria (Wellman-Labadie et al., 2008). A previous proteomics analysis of the acid-soluble matrix of the eggshell palisade layer revealed the presence of over 500 proteins which were broadly categorized as either (1) egg white proteins, (2) intracellular proteins or (3) eggshell-specific matrix proteins (Mann et al., 2006). Several egg white proteins are known antimicrobials, including lysozyme, ovotransferrin, avidin, ovomucoid, ovoinhibitor and cystatin. Intracellular proteins, including antimicrobial proteins such as histones, originate from the cells lining the oviduct of the laying

hen. They could be released by usual cellular turn-over or due to abrasion caused by the forming egg during shell calcification when the coarse egg rotates in the uterus for a period of 16 hours. Eggshell-specific matrix proteins are components of the shell matrix thought to be highly eggshell specific, including OC-116 and OC-17. The same study also identified two members of the avian β-defensin family in the shell matrix: avian β-defensin-10 and -11. All of these proteins enhance the biomineralized barrier that is the eggshell by providing antimicrobial protection.

3.3. The Cuticle

The eggshell cuticle is the final layer to be deposited onto the surface of the avian eggshell during the termination of mineralization. As the outermost layer, the cuticle is the first barrier against unfavorable environmental challenges and microbial contamination. Many functions have been attributed to the cuticle layer such as temperature control, camouflage and a suggested role in parental recognition (Sparks, 1994). It is also responsible for restricting water movement; it limits the loss of water from inside the shell as well as prevents water from the egg exterior from entering. By limiting the transfer of water across the shell, the cuticle also prevents possible bacterial contamination (Board and Halls, 1973).

The cuticle consists of two layers: an outer layer composed of proteins, polysaccharides and lipids, and an inner mineralized layer containing hydroxyapatite crystals (Whittow, 1999; Dennis et al., 1996). Cuticle coverage and thickness is irregular on the surface of the egg, varying between 0 and 10 μm (Romanoff and Romanoff, 1949). Studies have indicated that these are heritable traits that are associated with resistance to bacterial entry into the chicken egg (Bain et al., 2013). As previously mentioned, the cuticle acts as a physical barrier by forming a plug in

the eggshell pores, up to 50 μm in depth, and preventing bacterial contamination via these entry points (Ruiz and Lunam, 2000).

Previous studies have demonstrated that eggshell cuticle proteins extracted from the eggs of domestic birds, including chickens, have antimicrobial activity against Gram-positive and Gram-negative bacteria (Wellman-Labadie et al., 2008). Lysozyme and low levels of ovotransferrin were identified as cuticle-resident antimicrobials, as well as ovocalyxin-32 (OCX-32). OCX-32 is an eggshell-specific matrix protein that was identified in the uterine fluid associated with the final phase of shell calcification (Hincke et al., 2003). Studies assessing the antimicrobial potential of recombinant OCX-32 demonstrated antimicrobial activity against Gram-positive bacteria as well as carboxypeptidase inhibitory activity (Xing et al., 2007). Eggs with missing or partial cuticle layers are more vulnerable to bacterial contamination (Bain et al., 2013); possibly due to exposed eggshell pores and microcracks or a reduction in endogenous antimicrobial proteins.

The proteomes of the yolk, vitelline membrane, egg white and shell membranes have previously been characterized using mass spectrometry-based technology (Mann and Mann, 2008; Farinazzo et al., 2009; Mann, 2008; D'Ambrosio et al., 2008; Mann and Mann, 2011; Mann, 2007; Kodali et al., 2011; Kaweewong et al., 2013). The proteome of the eggshell matrix has also been investigated (Mann et al., 2006; Sun et al., 2013; Miksik et al., 2010). To date, a comprehensive proteomics analysis of the outermost organic cuticle layer and inner mammillary cones has yet to be accomplished. Knowledge of the protein constituents in both of these layers could provide insight into the antimicrobial properties of the eggshell, either by influencing the formation of this biomaterial or by identifying resident antimicrobial proteins.

4. Cationic Antimicrobial Peptides

Increased use of antibiotics in agriculture, hospitals and the community has increased the selection pressure for multi-drug resistant bacteria (Laxminarayan and Heymann, 2012). Infections due to antibiotic-resistant bacteria lead to prolonged illnesses and elevated rates of mortality. The American Centers of Disease Control and Prevention estimates that at least 23 000 deaths a year in the United States are associated with antibiotic-resistant pathogens, as well as 2 million illnesses (Laxminarayan et al., 2013). Methicillin-resistant *Staphylococcus aureus* (MRSA) incidence rates in Canadian hospitals have been steadily increasing from 0.51/1000 patient admissions in 1995 to 9.47/1000 patient admissions in 2009 (Canadian Nosocomial Infection Surveillance Program, 2011). Similarly, detection rates for vancomycin-resistant enterococci have increased from 0.37 to 1.32 per 1000 patients admitted in 1995 and 2009, respectively (Ofner-Agostini et al., 2008).

Cationic antimicrobial peptides (CAMPs) are key players in the innate immune defense system of many species and typically target components of the pathogen that cannot be easily mutated, such as lipid membrane components (Teixeira et al., 2012). This explains why few pathogens have developed resistance mechanisms to antimicrobial peptides, as opposed to antibiotics that have naturally selected for a variety of multi-drug resistant bacteria. CAMPs are suggested to use a bacteriolytic mechanism of antimicrobial activity. The positive charges of these proteins interact electrostatically with the negatively charged components located on the surface of the bacterial cell wall, such as lipopolysaccharides and lipoteichoic acids. The final step involves one of three pore forming mechanisms (barrel stave, carpet or toroidal-pore) by inserting the hydrophobic domain (likely in α-helical conformation) into the lipid bilayer

(Kawasaki and Iwamuro, 2008). This is supported by research data collected from studies on magainin 2, a CAMP isolated from the skin of *Xenopus laevis*, the African clawed frog (Matsuzaki, 1998). Other bactericidal mechanisms have also been attributed to CAMPs, including studies examining buforin II, a histone H2A-derived antimicrobial peptide from the Asian toad *Bufo bufo garagriozans*. This CAMP was found to bind tightly to DNA and RNA and its target was present in the cytoplasm of the cell rather than the cellular membrane (Park et al., 2000).

4.1. Avian β-Defensins

β-Defensins are cysteine-rich antimicrobial peptides involved in innate immune defense, found in all vertebrate species, and possessing a broad spectrum of antimicrobial activity including bacteria, fungi, and yeast. They possess a signal peptide responsible for secretion in addition to disulfide bonds between Cys(1) - Cys(5), Cys(2) - Cys(4) and Cys(3) - Cys(6) (Cuperus et al., 2013). Fourteen avian β-defensins, previously known as gallinacins, have been identified in the chicken genome (Hellgren and Ekblom, 2010) and 11 of those are found expressed in every segment of the hen's reproductive tract (Mageed et al., 2008). Even though many avian β-defensins were identified in the oviduct of the hen, proteomics analyses of the egg were only able to detect avian β-defensin-11 (eggshell, albumen, and vitelline membranes), avian β-defensin-10 (eggshell) and gallin (albumen) (Mann et al., 2006; Mann, 2008; Mann, 2007).

4.2. Histones

Histones are commonly regarded as DNA stabilization and packaging molecules that have a key role in gene expression regulation. They are the main components of the nucleosome structures. Histones H2A, H2B, H3 and H4 are termed core histones because they form the octomeric complex at the center of nucleosomes, while histones H1 and H5 are termed linker histones which hold the DNA tightly around the octomeric complex (Smith, 1991). They can also be classified in two categories according to their cationic residues: lysine-rich histones (H1, H2A and H2B) and arginine-rich histones (H3 and H4) (Parseghian and Luhrs, 2006).

Histones were first shown to possess antimicrobial activity in samples isolated from calf thymus (Hirsch, 1958). Since then many studies have indicated several histones as potent antimicrobial agents in a variety of species (Kawasaki and Iwamuro, 2008). They possess hydrophobic residues, have an overall positive charge and form amphipathic α-helical structures in a membrane-like milieu (Zasloff, 2002), which are all characteristics of cationic antimicrobial peptides (CAMPs).

Antimicrobial activity detected in the ovary and oviduct of the hen was shown to originate from histones H1 and H2B and significantly inhibited the growth of *B. subtilis* and *E. coli* (Silphaduang et al., 2006). This leads to the hypothesis that histones could participate in innate defenses protecting the egg from bacterial contamination and probably released via apoptosis of the cells lining the reproductive tract. Supporting this hypothesis is proteomics data from the acid-soluble organic matrix of the chicken eggshell confirming the presence of histones H2 and H4 in the calcified shell (Mann et al., 2006). Histones with antimicrobial activity were

also detected in acid extracts of the chicken liver that exhibited antimicrobial activity against Gram-positive and Gram-negative bacteria (Li et al., 2007).

5. Statement of Hypotheses and Objectives

Hypothesis 1: A proteomics approach to characterizing the specific proteins involved in the integrated defense strategies operating at biomineralized barriers in the avian egg can provide insight into calcitic biomineralization and antimicrobial functions of the avian eggshell by providing a protein inventory for each eggshell segment.

Objectives: (1) Characterize the protein constituents of the eggshell cuticle using a proteomics approach combined with bioinformatics analysis and identify cuticle-resident antimicrobial proteins (Chapter 2). (2) Identify mammillary cone proteins specifically involved in calcitic biomineralization using a proteomics cross-analysis approach of two eggshell models - fertilized and unfertilized (Chapter 3). (3) Characterize acid-soluble antimicrobial proteins associated with the eggshell membranes extracted from the fertilized egg and the unfertilized table egg (Chapter 3).

Hypothesis 2: Histones extracted from chicken erythrocytes possess antimicrobial properties against Gram-positive and Gram-negative bacteria.

Objectives: (1) Optimize the extraction and purification of histones from chicken erythrocytes (Chapter 5). (2) Determine the minimum inhibitory concentration (MIC) and minimum bactericidal concentrations (MBC) values of the extracted histones against a variety of planktonic Gram-positive and Gram-negative bacterial species, including MRSA (Chapter 5). (3)

Determine the minimum biofilm eradication concentration (MBEC) value of the extracted histones against Gram-positive and Gram-negative biofilms, including MRSA (Chapter 5). (4) Provide insight into the antimicrobial mechanism by assessing histone affinity for negatively charged bacterial membrane components.

6. Thesis Outline

The first part of this study, **Part 1,** examines the integrated defense strategies operating at biomineralized barriers in the avian egg. **Chapter 1** provides a literature review of proteomics and genomics analyses of eggshell-specific matrix proteins; focusing on two functions: antimicrobial protection and shell mineralization. **Chapter 2** describes the results of the comprehensive cuticle proteome obtained using a mass spectrometry-based approach, focusing on the functions of cuticle-resident antimicrobial proteins. **Chapter 3** identifies proteins associated with the mammillary cones of the mineralized shell and discusses their potential role in calcitic biomineralization. This study also examines acid-soluble proteins associated with the shell membrane fibres and reveals high levels of antimicrobial proteins.

The importance of antimicrobial defenses to protect the egg from microbial contamination is highlighted in the first part of this thesis by the numerous antimicrobial proteins present in the biomineralized barrier. The second part of this thesis, **Part 2**, focuses on histones, a family of cationic antimicrobial proteins identified in several regions of the eggshell. **Chapter 4** describes the methods used to extract histones from an alternative source (chicken erythrocytes) and reports the minimum inhibitory concentration (MIC), minimum bactericidal concentration (MBC) and minimum biofilm eradication concentration (MBEC) values for the

antimicrobial activity of the histone mixture against Gram-positive and Gram-negative bacteria, including Methicillin-Resistant *Staphylococcus aureus (*MRSA). The underlying mechanism was also examined by assessing the binding affinity between histones and negatively charged bacterial membrane components.

A general discussion, **Chapter 5**, can be found at the end of this thesis describing the importance of proteomics studies to understand the innate barriers of the eggshell, characterizing a model for calcitic biomineralization and inspiring antimicrobial agents that have potential therapeutic applications as alternatives to antibiotics.

Part 1

Proteomics Analysis Provides Insight into Integrated Defense Strategies Operating at Biomineralized Barriers

Chapter 1

“Protein Constituents of the Eggshell: Eggshell-Specific Matrix Proteins.”

Rose, MLH and Hincke MT (2009) *Cellular and Molecular Life Sciences*, 66(16):2707-19

The avian egg possesses a wide variety of physical and chemical barriers to protect the developing embryo from bacterial contamination. These barriers are critical for reproductive success of avian species and for the safe table egg intended for human consumption. The outermost barrier is the eggshell, which consists of fibrous shell membranes, the calcified shell and a proteinaceous cuticle layer. The mineralized shell consists primarily of calcium carbonate (>95%) with an integrated organic matrix. This chapter is a literature review that focuses on the eggshell-specific matrix proteins and their function in the avian eggshell.

Author contributions:

Megan LH Rose researched the literature and wrote the manuscript with contributions and revisions by Dr. Maxwell T. Hincke.

Abstract

In this article we review the results of recent proteomic and genomic analyses of eggshell matrix proteins and draw attention to the impact of these data on current understanding of eggshell formation and function. Eggshell-specific matrix proteins from avian (ovocleidins and ovocalyxins) and non-avian (paleovaterin) shells are discussed. Two possible roles for eggshell-specific matrix proteins have been proposed; both reflect the protective function of the eggshell in avian reproduction: regulation of eggshell mineralization and antimicrobial defense. An emerging concept is the dual role (mineralization / antimicrobial protection) that certain eggshell matrix proteins can play.

Introduction

The avian egg is a reproductive structure that has been shaped through evolution to resist physical, microbial and thermal challenges from the external environment, while satisfying the needs of the developing embryo. This complex structure regulates the exchange of metabolic gases and water, and provides calcium to the growing embryo. Many studies have been conducted on avian eggs and most have centered on the egg of the domestic chicken. This considerable body of work has provided insight into the function and structure of the eggshell. In this article we will review the results of recent proteomic and genomic analyses of eggshell matrix proteins and draw attention to the impact of this data on current understanding of their role in eggshell formation and function. Comparisons to the recently available genome sequence for Zebra Finch (*Taeniopygia guttata*) are made where possible (http://www.ncbi.nlm.nih.gov/projects/genome/guide/finch/). Finally, information about the non-avian turtle eggshell is presented.

Overview of Eggshell Biosynthesis

The egg is assembled as it passes through specialized regions of the oviduct. It is composed of a central yolk surrounded by the albumen, eggshell membranes, calcified eggshell and cuticle. Following ovulation, the yolk/ovum complex travels through the longest portion of the oviduct (magnum) and progressively acquires the water, ions and proteins that compose the albumen (egg white) during a 2- to 3-h period [1]. Next, the yolk and albumen complex traverse the isthmus. In the proximal (white) isthmus the inner and outer shell membranes are deposited

during a 1- to 2-h period as a highly cross-linked fibrous meshwork. These are considered to be the innermost layers of the eggshell. The inner membranes remain uncalcified, while the fibers of the outer shell membrane penetrate the mammillary cones of the calcified shell [2, 3]. The shell membranes contain type I, V and X collagens [4-6]. In the distal (red) isthmus, organic aggregates are deposited on the surface of the outer eggshell membranes in a quasi-periodic array. Calcium carbonate mineralization at these nucleation sites is the origin of the mammillary cones (Fig. 1) [3].

The incomplete egg then enters the uterus, or shell gland, where fluid is pumped into the albumen, causing it to swell to its final size. During the following 16- to 17-h period, eggshell mineralization occurs while the ovum slowly rotates within the shell gland (10-12 turns/h) [7]. Shell calcification occurs in the uterine fluid which bathes the forming egg; all ingredients of this process are secreted by the epithelial and mucosal cells that line the lumen of the uterus. The ionic and protein constituents of the uterine fluid change progressively during eggshell formation and can be subdivided into the stages of initiation (5 h), growth and rapid calcification (12 h) and termination (1.5 h) of eggshell mineralization [8].

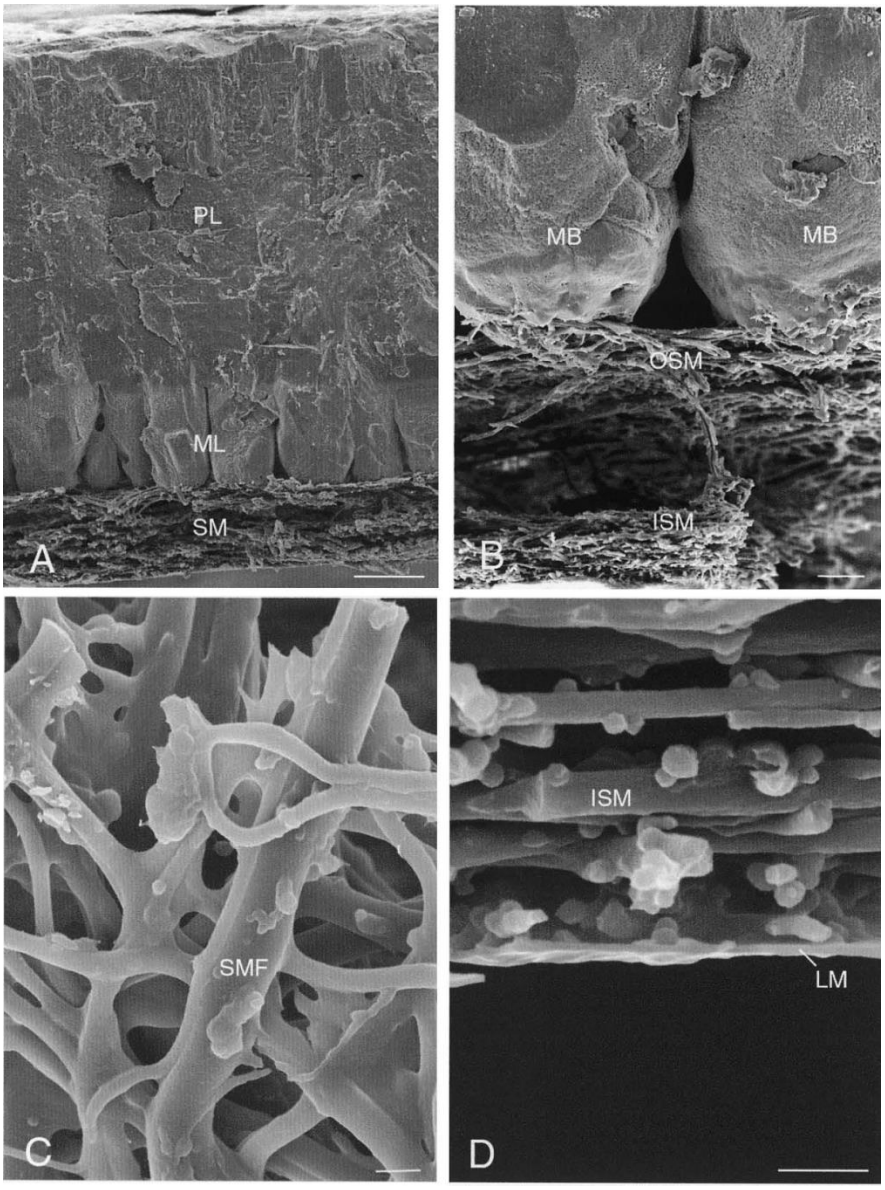

Fig. 1. Scanning electron micrographs illustrating the morphology of the eggshell and eggshell membranes. (**A**) Eggshell cross-fractured to reveal the shell membrane (SM), mammillary layer (ML) and palisade layer (PL). (**B**) Higher magnification of the membrane–mammillary body interface. Outer shell membrane fibres (OSM) insert into the tips of the mammillary bodies (MB). Inner shell membranes (ISM). (**C**) Enlargement of the shell membrane fibres (SMF) to reveal their interwoven and coalescing nature. (**D**) Inner aspect of the inner shell membrane (ISM), demonstrating the limiting membrane (LM) that surrounds the egg white (here removed during sample preparation). Scale bars (**A**) 50 µm; (**B**) 20 µm; (**C, D**) 2 µm. Reprinted from [24], with permission from Elsevier.

The mineralized shell consists primarily of calcite, the most stable polymorph of calcium carbonate, and extends from the inner mammillary cone layer, through the central palisades and the outer vertical crystal layers [3, 8] (Fig. 1). The mammillary cone layer, ~100μm thick [2], is composed of a regular array of cones or knobs, into which are embedded the individual fibers of the outer eggshell membrane. Within the mammillary cone layer, microcrystals of calcite possess spherulitic texture and are readily dissolved to mobilize calcium to meet the needs of the growing embryo [3]. The palisades region, ~300μm thick, is made up of groups of columns (crystallites) composed of elongated calcite crystals tending to a preferential orientation with either the (001) or (104) plane parallel to the shell surface [9, 10]. Variability is observed in crystal orientation which has been correlated with shell strength [10]. The outer region of the palisade layer is a tough structure made of large calcite crystals where the external impacts are absorbed by thin inter-crystalline organic layers that make intracrystalline crack propagation difficult [3]. This layer ends at the vertical single crystal layer which has a crystalline structure of higher density than that of the palisade region.

Shell pigments and eggshell cuticle are deposited on the surface of the immobilized egg during the last 1.5 h before oviposition (egg expulsion). The outermost shell layer is the eggshell cuticle, a noncalcified organic layer of variable thickness which may even be absent. A thickness range of 5-10 μm has been reported [11]. The cuticle is composed of glycoproteins, polysaccharides, lipids and inorganic phosphorus including hydroxyapatite crystals [12-14]. The cuticle is thought to play a role in controlling water exchange by repelling water or preventing its loss, and may function in limiting microbial colonization of the eggshell surface [1, 12]. This layer, as well as the outer portion of the calcified shell, contains eggshell pigments which serve as camouflage, temperature control and possibly in parental recognition [15]. Pores span the

eggshell and permit the diffusion of metabolic gases and water vapor to allow proper embryonic development [16]. As expected, eggshell thickness varies between bird species. For example, chicken eggshells are approximately 0.3-0.4 mm thick while the ostrich shell is 2.5 mm thick [17].

Biochemistry of Eggshell Matrix Proteins

The eggshell mineral is associated with an organic matrix composed of proteins, glycoproteins and proteoglycans, termed "eggshell matrix proteins", which are progressively incorporated from the precursor milieu (uterine fluid) during calcification. Their function is thought to influence the fabric of this biomaterial and/or to participate in its antimicrobial defenses. These non-mineral constituents represent about 2% by weight of the calcified eggshell, and can be released for study by demineralization of the eggshell by calcium chelation (EDTA or EGTA) or acid demineralization (acetic acid or HCl), yielding soluble and insoluble constituents. A complex array of distinct protein bands was demonstrated in the soluble intra- and extra-mineral compartments by 1D-electrophoresis (SDS-PAGE) [18, 19], and in the precursor uterine fluid, showing different patterns between the three stages of the eggshell calcification process (initial, growth and terminal) [20]. In contrast, the insoluble components which are not soluble in SDS remain relatively uncharacterized (but see [21, 22])**.** N-terminal sequencing of the electrophoretic bands allowed the egg white proteins ovalbumin, lysozyme and ovotransferrin to be identified [23-25]. N-terminal and internal amino acid sequencing of other protein bands revealed that they did not correspond to previously identified proteins and these have been subjected to more intensive investigation. Purification schemes using ion exchange

(diethylaminoethyl (DEAE) – Sepharose and carboxymethyl (CM) – Sepharose) and hydroxyapatite were developed to isolate ovocleidin-17 (OC-17) [26] and ovocalyxin-32 (OCX-32) [27] from eggshell extracts.

Other eggshell matrix proteins were characterized by a combination of molecular cloning, immunochemistry and bioinformatics. A cDNA library from pooled RNA extracted from chicken uteruses that were harvested during the mid-phase of shell calcification was successfully screened to clone novel eggshell matrix proteins [28, 29]. Expression screening of this library, using polyclonal antisera raised to partially purified eggshell matrix proteins, allowed clones with the corresponding cDNA sequences to be identified and sequenced. The conceptual amino acid sequence was compared to partial amino acid sequencing data for proteins present in uterine fluid and eggshell extracts. This method allowed the identification of two novel eggshell matrix proteins, ovocleidin-116 [28] and ovocalyxin-36 [29]. Another associated approach was to compare the available expression sequence tag (EST) sequences to partial protein or nucleotide sequences from egg components. This method was successfully used to identify a 32-kDa band abundant in uterine fluid at the terminal phase of shell calcification (OCX-32) [30].

Such studies led to the concept that eggshell matrix protein components form three characteristic groups:

i. “Egg white” proteins which are also present in the eggshell - these include ovalbumin, the most abundant egg white protein [23], lysozyme, an antimicrobial protein with hydrolytic activity against peptidoglycans on cell walls of Gram-positive bacteria [24] and ovotransferrin, which sequesters iron necessary for bacterial growth [25];

ii. Ubiquitous proteins that are found in many tissues - examples are osteopontin, a phosphorylated glycoprotein present in bone and other hard tissues [31-36], and clusterin, a widely distributed secretory glycoprotein that is also found in chicken egg white [37];

iii. Eggshell-specific matrix proteins unique to the shell calcification process that are secreted by cells in specific regions of the oviduct where eggshell mineralization is initiated (red isthmus) and continues to completion (uterus). It is these "eggshell-specific matrix proteins" which are the primary focus of this review. These matrix components are termed ovocleidins (ovo, Latin: egg; kleidoun, Greek: to lock in, implying a functional role) or ovocalyxins (ovo, Latin: egg; calyx, Latin: shell, referring to their shell location), with distinction based on apparent molecular weight by SDS-PAGE when initially characterized.

Recently, a high-throughput tandem-mass spectrometry approach (MS/MS) identified more than 500 eggshell matrix proteins [38], including the most abundant proteins that were already known (above). It is highly unlikely that all of these 520 proteins perform eggshell specific functions or are involved in eggshell assembly. The majority of them are proposed to be remnants of previous stages of egg formation occurring in proximal segments of the oviduct, or intracellular proteins released by breakdown of the cells lining the oviduct during normal turnover [38]. According to this hypothesis, all proteins that are present in the uterine fluid during the calcification process become assimilated into the eggshell, many of them in a non-specific manner. However, the "eggshell-specific" proteins that are described in this review are abundant components of the eggshell matrix and are highly likely to be relevant to eggshell function. Supportive evidence for an eggshell-specific role would be: restricted high level expression in a limited oviduct segment, up-regulation of expression in synchrony with

movement of the forming egg through the oviduct, demonstration of a secretory process (i.e. signal peptide, colloidal gold immunocytochemistry to demonstrate secretion granule localization) and secretion during eggshell formation, and finally, evidence for a role in eggshell function (i.e. calcification, antimicrobial protection). Many of these criteria have been met by the ovocleidins and ovocalyxins that are described in this review.

Two possible roles for eggshell-specific matrix proteins have been proposed; both reflect the protective function of the eggshell in avian reproduction: regulation of eggshell mineralization and antimicrobial defense. Egg calcification occurs in three distinct phases (initiation, active calcification, and termination of shell calcification), while the egg is bathed by the acellular uterine fluid containing the ionic and organic precursors of the eggshell. Each phase of shell mineralization is associated with a specific protein electrophoretic profile for the uterine fluid, suggesting that these molecules play specific roles during the calcification process [20].

Biomineralization

In general, the soluble matrix proteins of calcium carbonate biomaterials modify crystal growth, and therefore regulate the macroscopic properties of the resulting bioceramic. For example, in the mollusk shell, specific proteins control phase switching between the calcite and aragonite forms of calcium carbonate [39, 40]. A number of experimental observations support the role of the eggshell matrix proteins in determining the fabric of the eggshell and therefore influencing its resulting mechanical properties. Proteins in the uterine fluid modify the kinetics of calcium carbonate precipitation *in vitro* [41, 42]. The lag time for calcium carbonate precipitation is reduced by the uterine fluid from the initial and growth stages of eggshell mineralization, suggesting that these matrix precursors promote crystal nucleation. To a lesser

extent, the uterine fluid collected during the growth phase also enhances precipitation kinetics. In contrast, the total uterine fluid harvested at the terminal stage of calcification inhibits calcite precipitation [19]. In agreement with these observations, partially purified eggshell matrix proteins inhibit calcium carbonate precipitation and alter patterns of calcite crystal growth, leading to morphological modifications of rhombohedric calcite crystals grown *in vitro* [19, 42]. Studies to investigate the effect of purified eggshell matrix proteins on calcium carbonate crystallization and crystal growth are described in the next section.

Antimicrobial Protection

Protein extracted from the eggshell of the domestic chicken demonstrated antibacterial activity against *Pseudomonas aeruginosa, Bacillus cereus, Staphylococcus aureus, Escherichia coli,* and *Salmonella enteritidis* [43]. Ovary and oviduct tissue extracts of the domestic hen were found to show antimicrobial activity against both Gram-positive and Gram-negative bacteria [44]. Moreover, eggshell cuticle protein extracts from a number of domestic and wild bird species demonstrated antimicrobial activity against *P. aeruginosa*, *B. subtilis* and *S. aureus* [45, 46]. Therefore, antimicrobial activity has been identified in protein extracts from avian eggshell and in particular outer eggshell; however, the identity of specific proteins responsible for the activity remains to be fully elucidated (see next section: "Eggshell-specific matrix proteins").

Eggshell-Specific Matrix Proteins

Ovocleidin-17

Ovocleidin-17 (OC-17) was the first eggshell–specific matrix protein to be isolated and characterized following its chromatographic purification after eggshell decalcification [26].

Using an antibody raised to the purified protein, immunohistochemistry revealed that it is secreted by the tubular gland cells in the shell gland; within the shell it is distributed throughout the shell matrix, but concentrated in the mammillary bodies [26]. The protein sequence contains 142 amino acids including 2 phosphorylated serines, Ser-61 and -67 [47]. Moreover, the protein also occurs in the eggshell soluble organic matrix as a minor form which is glycosylated at Asn-59 (23 kDa, OC-23) [48]. Glycosylation occurs at the N-glycosylation site consensus sequence, N-A-S which contains Ser-61. In the glycosylated form of the protein, Ser-61 is not phosphorylated, indicating that these modifications are mutually exclusive. In addition, peptides without modification at Asn-59 or Ser-61, with phosphorylation of Ser-67 only, or with no phosphorylation at all, have been detected [49]. The function of these modifications remains unknown but the phosphorylation sites are preserved in closely related proteins isolated from other avian eggshells (see below) suggesting their importance.

Detailed studies have identified homologous eggshell matrix proteins in shell from a diverse number of avian species. Comparison of their primary sequences revealed that ansocalcin (goose), struthiocalcin-1 and -2 (SCA-1 and -2; ostrich), dromaiocalcin-1 and -2 (DCA-1 and -2; emu) and rheacalcin-1 and -2 (RCA-1 and -2; rhea) form two groups based on sequence identity, serine phosphorylation and conservation of cysteine residues [17, 50, 51]. Goose ansocalcin aligns reasonably well with proteins of group 1 (63-70% identity with SCA-1, DCA-1 and RCA-1), but OC-17 has much less sequence identity with group 2 where it is placed (37-39% with SCA-2, DCA-2 and RCA-2). It remains unclear why ratites differ from goose and chicken in that they possess two forms of the *"–calcin"* matrix protein as their predominant eggshell matrix proteins. It is suggested that these differences are due to loss of one gene in modern birds (goose, chicken) [51], occurring after the divergence of paleognathae (ratites and tinamous) from

neognatae (the ancestors of all other modern birds) more than 100 million years ago [52]. It can be proposed that homologous C-type lectin eggshell matrix proteins will be found in the shells of all other bird species (i.e., neoaves). One such candidate in the genome of the Zebra Finch (Accession: XP_002189493; predicted: similar to regenerating islet-derived (Reg) family, member 4, *Taeniopygia guttata*) has been identified by automated gene prediction (Fig. 2a). In contrast, sequencing of the chicken genome (May 2006, version 2.1 release, 95% complete, 7.1 x coverage) has not yet identified the OC-17 gene. Database searches with these eggshell protein sequences reveal that they belong to a heterogeneous group of proteins consisting of a single C-type lectin domain and display sequence homology to members of this family such as mammalian Reg proteins, pancreatic stone protein (lithostathine), fish Type II antifreeze proteins and anticoagulant proteins from snake venom [53]. The X-ray structure of OC-17 has been determined and reveals a mixed alpha helix/beta sheet structure and verifies the C-type lectin-like domain [54, 55]. Preliminary X-ray crystallographic studies of SCA-1 are underway [56].

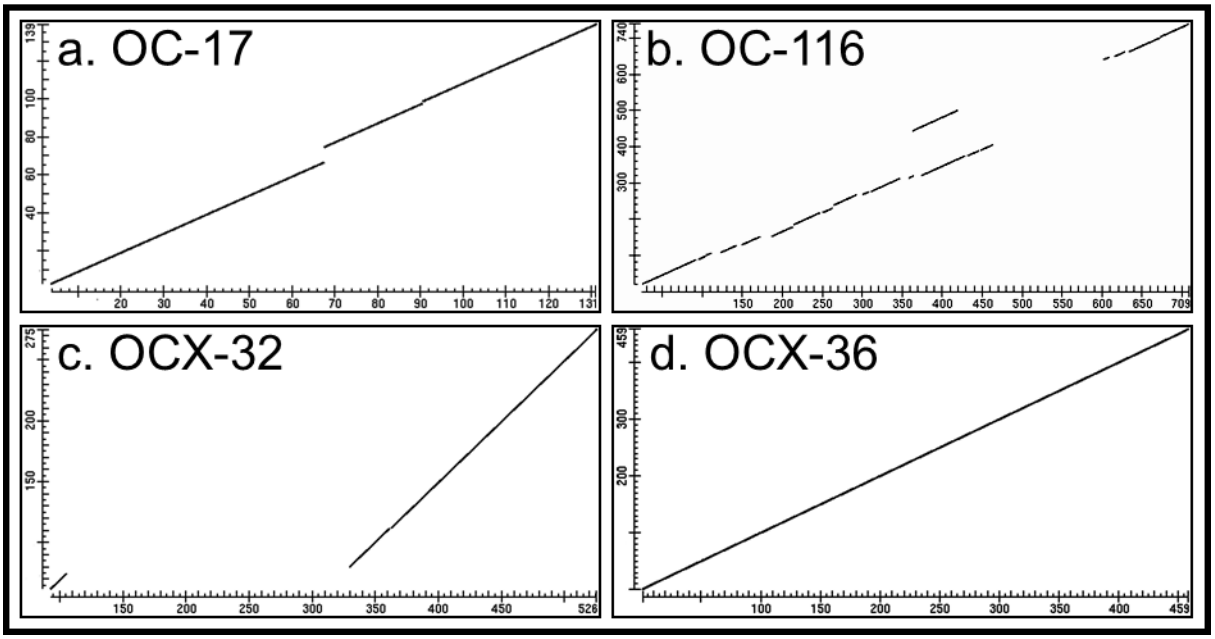

Fig. 2. Dot matrix plots to visualize regions of homology between orthologous chicken (*Gallus gallus*) and Zebra Finch (*Taeniopygia guttata*) eggshell matrix proteins. The NCBI align 2 sequences (bl2seq) tool was used. In each panel, the ordinate depicts the chicken sequence, while the Zebra Finch sequence is on the abscissa. The following accession sequences were compared (chicken, Zebra Finch): (**a**) OC-17 (Q9PRS8, XP_002189493); (**b**) OC-116 (NP_989900, XP_002190429); (**c**) OCX-32 (NP_989865, XP_002186694); (**d**) OCX-36 (Q53HW8, XP_002192664)

The properties of purified OC-17 and its goose homolog (ansocalcin), and their influence upon calcite crystallization patterns have been investigated and compared [50, 55, 57, 58]. Functionally, OC-17 and ansocalcin do not appear to be completely equivalent in their effect on calcite crystal growth *in vitro* [55, 57]. Ansocalcin showed reversible concentration-dependent aggregation in solution, and was reported to induce pits on growing calcite rhombohedral faces at lower concentrations (<50 μg/ml) and to nucleate polycrystalline aggregates of calcite crystals at higher concentrations [50]. Aggregated ansocalcin may act as a template for the nucleation of calcite crystal aggregates [57]. However, under the same conditions, OC-17 was not observed to aggregate in solution nor induce the nucleation of calcite aggregates. Nevertheless, under different experimental conditions, Reyes-Grajeda et al. [55] reported that OC-17 could modify the crystalline habit of calcium carbonate and the pattern of crystal growth at concentrations of 5-200 μg/ml. However, the observation that OC-17, but not ansocalcin, is largely destroyed by treating eggshell powder with bleach suggests a different intra-mineral location, or a different kind of interaction with mineral, for these proteins [58]. OC-17 and SCA-1, but not SCA-2, are reported to interact directly with carbonate anion, as a potential mechanism accounting for different effects upon calcite nucleation and crystal growth [59].

As previously mentioned, OC-17 shows significant similarity to the Reg family of C-type lectin proteins. Mammalian Reg III homologs (mouse Reg III gamma and human hepatocarcinoma-intestine-pancreas/pancreatic associated protein (HIP/PAP)) possess antimicrobial activity against Gram-positive bacteria [60]. OC-17 and ansocalcin were investigated to determine whether they possess antimicrobial activity [61]. A micro-broth dilution assay indicated that purified OC-17 and ansocalcin each inhibited the growth of Gram-positive bacteria, with OC-17 exhibiting greater activity. Both proteins were more active in the

presence of Ca^{2+}. A pull-down assay demonstrated that OC-17 and ansocalcin interact with bacterial cell walls and cell wall peptidoglycans [61]. Comparison of the protein structures of OC-17 and ansocalcin (modeled on the X-ray structure determined for OC-17 [55]) revealed a broad distribution of positive charges in each molecule, similar to that found in cationic antimicrobial peptides [62] (Fig. 3).

OC-17 is an abundant eggshell-matrix specific protein (40 μg/g shell) [63]. Sensitive proteomic analyses of the chicken egg yolk plasma, egg white and vitelline membrane detected low levels of OC-17 [64-66].

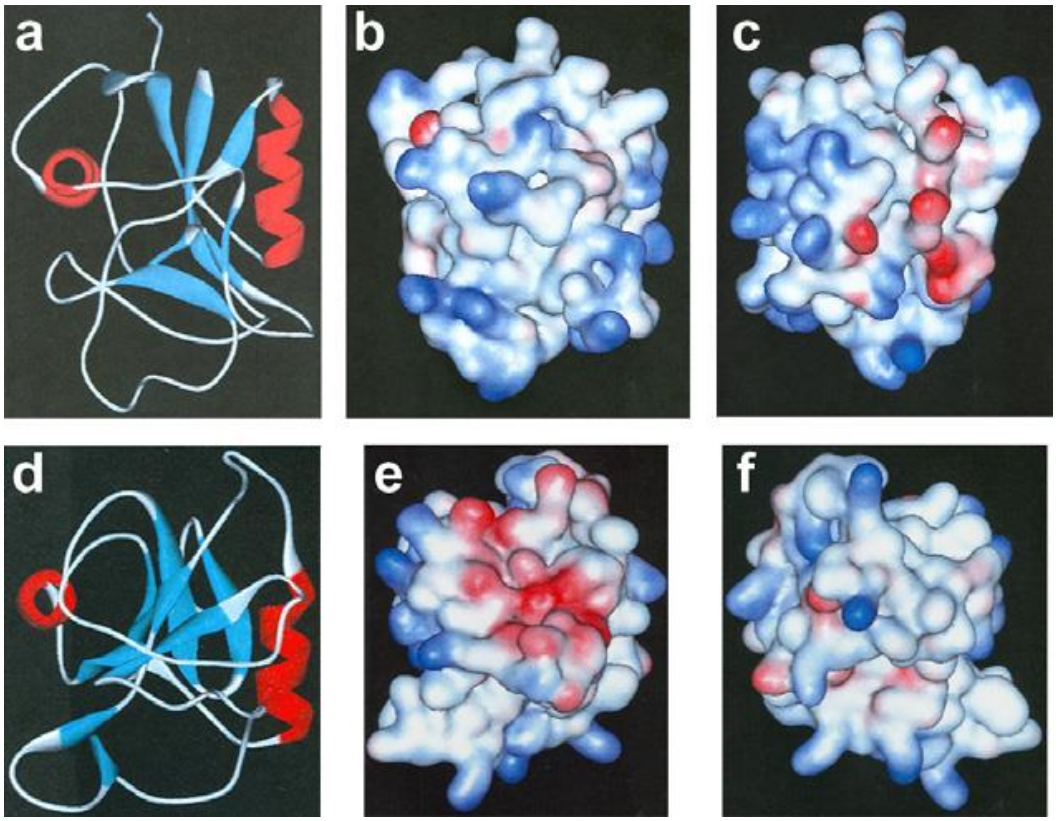

Fig. 3. Three-dimensional structures of avian eggshell C-type lectin proteins. (**a**) Crystal structure of OC-17. (**b**) Surface structure of OC-17 in the same orientation as in (a). (**c**) Surface structure of OC-17 that is rotated 180° clockwise around the Y-axis of (a). (**d**) Molecular model of ansocalcin. (**e**) Surface structure of ansocalcin model in the same orientation as in (d). (**f**) Surface structure of ansocalcin that is rotated 180° clockwise around the Y-axis of (d). In (**a**) and (**d**), protein secondary structures are indicated in blue (b-strand) and red (a-helix). The blue and red colors in the surface plot indicate the distribution of positive and negative charges, respectively. Reprinted from [61], with permission from Elsevier.

Ovocleidin-116

Ovocleidin-116 (OC-116) was the first eggshell matrix protein to be cloned, by expression screening a uterine library using an antibody raised to the abundant 116-kDa protein observed in hen uterine fluid during the active calcification phase of shell formation [28]. OC-116 is a major eggshell matrix protein, estimated at 80 μg/g eggshell powder [63]. Western blotting for OC-116 revealed that only the uterine portion of the oviduct, where shell calcification occurs, was immunopositive and that 180- and 116-kDa immunoreactive bands were detected in uterine tissue, uterine fluid and eggshell matrix. The N-terminus of the mature protein and conceptual translation product from cDNA correspond to that previously reported for a 200-kDa eggshell matrix proteoglycan that is converted to 120 kDa by chondroitinase ABC treatment [67]. Therefore, OC-116 is the core protein (predicted 75 kDa) corresponding to the doublet bands of an eggshell dermatan sulfate proteoglycan (116-120 and 180-200 kDa). It is hypothesized that the 180- to 200-kDa form of OC-116 corresponds to the N-glycosylated core protein with attached glycoaminoglycans, while the 116- to 120-kDa form corresponds to the protein without glycoaminoglycans [28]. Sequencing of peptides purified from protease-treated eggshell extract reveal that both predicted N-glycosylation sites are modified; however, while Asn-62 is entirely glycosylated, Asn-293 is only marginally occupied [63]. Detailed analysis of the carbohydrate structures attached to Asn-62 revealed 17 different oligosaccharide structures [68]. High-mannose, core-fucosylated and peripherally fucosylated structures were present. The relatively rare lacdiNAc (GalNAcbeta1-4GlcNAc) motif was detected in more than half of the structures, while the lacNAc (Galbeta1-4GlcNAc) motif, which is the more frequent motif in mammals, only occurred in 3 of the 17 glycoforms. Glycoaminoglycans associated with OC-116 have not yet been characterized.

OC-116 is phosphorylated to a variable and partial extent on at least 22 serine and threonine residues. Two sites that were frequently identified with different cleavage methods were Ser-444 and Thr-664 [49]. Ultrastructural immunocytochemistry indicates that OC-116 is synthesized and secreted from the granular cells of the uterine epithelium, and is incorporated into, and widely distributed throughout, the palisade region of the calcified eggshell [28]. Such localization studies do not distinguish between the differentially phosphorylated, N-glycosylated or glycanated forms of OC-116, nor would possible differences in eggshell distribution between the 116- and 180-kDa forms be detected by this technique. Crystal growth studies have shown that pure glycoaminoglycans affect calcite morphology, leading to crystal elongation [69], suggesting that the sulfated form of OC-116 (MW 220 kDa) would influence eggshell mineralization via electrostatic interactions.

The sequence of OC-116 is quite unlike those of other calcified tissue proteoglycans [28, 63]. Low stringency Basic Local Alignment Search Tool (BLAST) searching with the OC-116 protein sequence generated restricted and poorly significant alignments to mammalian and chicken collagens (types I, II, VII and IX), human perlecan (heparan sulfate proteoglycan), chicken aggrecan (chondroitin sulfate proteoglycan), chicken bone sialoprotein and lustrin A (component of mollusk shell extracellular matrix). No homology with avian versican was apparent by BLAST searching, although both forms of OC-116 are recognized by a monoclonal antibody that is specific for an epitope on the core protein of avian versican [67]. OC-116 does not possess common structural characteristics that are found in aggrecan, PG-M/versican, neurocan and brevican (i.e. domains that are epidermal growth factor (EGF)-like, C-type lectin-like and complement regulatory protein (CRP)-like) [70]. Proteoglycans have the potential to function in biomineralization since their glycosaminoglycan units consist of repeating

disaccharides with carboxylate and/or sulfate moieties. It remains to be determined whether the underlying mechanisms by which OC-116 acts are similar to those by which proteoglycans promote cartilage calcification and collagen mineralization in vitro [71, 72].

The release of the chicken genome sequence in 2004 revealed that the chromosomal localization of OC-116 is adjacent to that of osteopontin on chromosome 4 [73]. These 2 genes are contiguous with other mineralization–specific genes (bone sialoprotein, dentin matrix protein 1), that form the SIBLING (small integrin-binding ligand, N-linked glycoprotein) mineralization gene locus first reported in mammalian genomes (Fig. 4). This correspondence reflects synteny between avian and mammalian genomes. Moreover, investigations into the evolutionary genetics of vertebrate tissue mineralization suggest that OC-116 and other SIBLING proteins are members of the secretory calcium-binding phosphoprotein (SCPP) family that function in tetrapod mineralization [74, 75]. Based on its position within this gene locus, OC-116 is predicted to be the avian ortholog of mammalian MEPE (matrix extracellular phosphoglycoprotein) (Fig. 4). In support of this suggestion, BLAST 2-sequence testing reveals that the N-terminus of chicken OC-116 possesses about 30% identity with the *Homo sapiens* MEPE protein sequence. As expected, the SIBLING gene locus (osteopontin, OC-116, bone sialoprotein and dentin matrix protein 1) also exhibits synteny between the two avian genomes that have been sequenced to date: *Gallus gallus* and *Taeniopygia guttata* [76]. There is at best about 40% identity between the amino acid sequences of chicken and Zebra Finch OC-116; the homology is strongest between the N-terminal halves and at the C-termini (Fig. 2b). Thus, while OC-116 has evolved to fulfill a specific function in mineralization of the calcitic eggshell, there are large differences between avian forms of the protein. Further study of common features of different avian OC-116s should help to define its features that are important for mineralization.

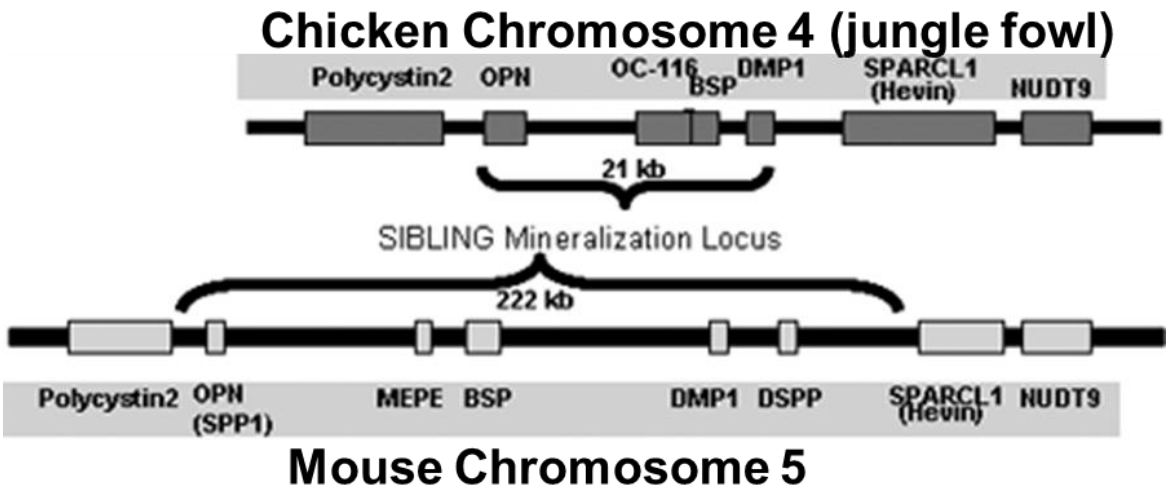

Fig. 4. Schematic depiction of the SIBLING mineralization gene loci in chicken and mouse. The Zebra Finch SIBLING locus displays an identical organization and relative placement of its OC-116 (Accession XP_002190429) as in chicken. The OC-116 gene occupies the corresponding position of the mammalian MEPE gene, suggesting that OC-116 and MEPE are orthologs. SIBLING small integrin-binding ligand, N-linked glycoprotein, OPN (SSP1) osteopontin, MEPE matrix extracellular phosphoglycoprotein, BSP bone sialoprotein, DMP1 dentin matrix protein 1, DSPP dentin sialophosphoprotein.

Proteins originating from the SCPP genes have a common characteristic; they bind calcium ions via acidic amino acids such as Glu, Asp and phospho-Ser [74]. One member, osteopontin, is also an eggshell matrix protein [31-36], and regulates calcification in vertebrate biominerals such as bone and teeth [77]. In the eggshell, osteopontin may function during mineralization by inhibiting calcium carbonate precipitation in a phosphorylation-dependent manner [32, 78]. However, OC-116 is uniquely specialized as an avian member of this mineralization-specific family, supporting the hypothesis that it has a key role in mineralization of the avian shell. A strong genetic linkage was detected between single nucleotide polymorphisms (SNPs) in the OC-116 gene during studies to investigate possible correlation between eggshell biomechanical properties and eggshell matrix protein SNPs. SNPs in the OC-116 gene are significantly associated with the eggshell elastic modulus and thickness, and with egg shape [79].

Recent studies report new possible locations for OC-116 protein. Proteomic analysis of the chicken egg yolk plasma determined its presence in the yolk [64]. OC-116 was recently detected in young chick cortical bone, laying hen medullary bone and growth plate hypertrophic chondrocytes suggesting a possible role in calcium phosphate mineralization [80].

Ovocalyxin-32

Ovocalyxin-32 (OCX-32) was originally identified as a 32-kDa uterine fluid protein that is abundant in the terminal phase of shell formation [25, 27]. Sequencing of peptides derived from the purified protein allowed ESTs to be identified that were assembled to yield a full-length composite sequence whose conceptual translation product contained the complete amino acid sequence of OCX-32. OCX-32 is expressed at high levels in the uterine and isthmus regions of

the oviduct and is secreted by the surface epithelial cells that line the lumen [25]. In the eggshell, OCX-32 localizes to the outer palisade layer, the vertical crystal layer, and the cuticle of the eggshell, in agreement with its demonstration by Western blotting at high levels in the uterine fluid during the termination phase of eggshell formation [21, 25, 27]. A study of eggshell phosphoproteins identified phosphorylation of OCX-32 at serines and threonines between position 257 and 268, but exact sites were not determined [49].

OCX-32 protein possesses limited identity (32%) to two distinct mammalian proteins, latexin, and retinoic acid receptor responder (tazarotene induced) 1 (RARRES1), that are modestly related to each other (about 30% sequence identity). Latexin is an inhibitor of carboxypeptidase A activity, and is expressed in rat cerebral cortex and mast cells [81, 82]. It plays a role in inflammation, as it is expressed at high levels and is inducible in macrophages in concert with other protease inhibitors and potential protease targets. Its structural domains share a cystatin fold architecture found in proteins that inhibit cysteine proteases [83]. RARRES1 was originally isolated from human skin. Its expression is upregulated by tazarotene as well as by retinoic acid receptors; it is downregulated in human neoplastic cells as a result of methylation of its promoter and CpG island [84]. RARRES1 has been implicated in the therapeutic effects of retinoic acid in psoriasis and in tumor suppression [85, 86]. There is conservation of corresponding exon boundaries between the aligned protein sequences of OCX-32, latexin and RARRES1, suggesting that there is an evolutionary connection between these mammalian proteins and OCX-32 (i.e. gene duplication followed by divergence) [87]. The human latexin / RARRES1 genes are located within 60 kb of each other on chromosome 3.

The timing of OCX-32 secretion into the uterine fluid has been interpreted to suggest that it plays a role in the termination of eggshell calcification [20]. This hypothesis originated from

the observations of morphological changes in calcite crystals by uterine fluid collected during the terminal phase of calcification and the location of OCX-32 in the mineral pellet after its precipitation with calcium carbonate in vitro from fresh uterine fluid [41, 42]. Studies with purified OCX-32 are necessary to investigate this possibility. A study in commercial pedigree hens for eggshell matrix candidate gene associations with eggshell quality measurements found that OCX-32 SNPs are significantly associated with mammillary layer thickness [79]; the basis for this association is unclear since OCX-32 is predominantly localized to the outer eggshell. An interesting recent observation is that the OCX-32 gene is expressed at higher levels in a low egg production strain (compared to a high production strain) of Taiwanese country chickens [88].

Another suggestion for OCX-32 function is based on OCX-32 homology to the carboxypeptidase A inhibitor latexin, and demonstration that proteinase inhibitors such as secretory leukocyte protease inhibitor (SLPI) and elafin possess antimicrobial activity through inhibition of microbial proteases [89]. OCX-32 has a predominant localization in the cuticle, the layer in direct contact with the environment and exterior pathogens, and is ideally positioned as a "first-responder" molecule against bacterial colonization of the eggshell. To obtain sufficient material for further studies of its function, recombinant OCX-32 protein was expressed in *E. coli* [90]. The protein was extracted from inclusion bodies and purified by sequential DEAE Sepharose and Ni^{2+} metal ion affinity chromatographies as a 58-kDa glutatione S-transferase (GST)-fusion protein. The refolded GST-OCX-32 significantly inhibited bovine carboxypeptidase activity and also inhibited the growth of *B. subtilis*. These results support the notion that OCX-32 provides antimicrobial protection for the egg.

Proteomic studies have recently noted low levels of OCX-32 in egg white [66] and in the vitelline membrane [65]. Using polyclonal antiserum raised to chicken OCX-32, a 32-kDa

immunoreactive band was detected by Western blotting in eggshell extracts from a variety of domestic and wild anseriform and galliform species, suggesting conservation of primary sequence across avian orders [45, 46]. This prediction is supported by a fair degree of similarity between the chicken and Zebra Finch homologous proteins (OCX-32, RARRES1, 56% identity between the respective C-terminal regions) (Fig. 2c).

Ovocalyxin-36

Ovocalyxin-36 (OCX-36) is a prominent 36-kDa protein present in the uterine fluid collected during the active calcification stage of shell mineralization. Antibodies raised to the uterine protein were used to expression-screen a hen uterine library, and a novel clone was identified which was the basis for additional rounds of hybridization-screening. The resulting consensus sequence was subsequently assembled with public database ESTs to obtain complete full-length cDNA [29]. The protein is only detected in the regions of the oviduct where eggshell formation takes place (isthmus and uterus). Moreover, the uterine OCX-36 message, quantified by real time RT-PCR, is strongly upregulated during eggshell calcification [29]. OCX-36 localizes to the calcified eggshell predominantly in the inner part of the shell, and largely to the shell membranes. OCX-36 protein sequence is 20-25% identical to mammalian proteins associated with the innate immune response, such as lipopolysaccharide-binding proteins (LBP), bactericidal permeability-increasing proteins (BPI) and palate, lung and nasal epithelium clone (Plunc) family proteins [27]. The genomic organization of LBP, BPI and OCX-36 appear to be highly conserved, suggesting an evolutionary link [27]. These observations suggest that OCX-36 is a novel and specific chicken eggshell protein related to the superfamily of LBP/BPI and Plunc proteins. These proteins are well known in mammals for their involvement in defense against

bacteria. They belong to the superfamily of proteins known to be key components of the innate immune system which act as the first line of host defense [91]. LBP proteins initiate the inflammatory host response upon the detection of a pathogen [92]. LBP binds the lipid A component of the lipopolysaccharide (LPS) layer of Gram-negative bacteria and transfers them to CD14, an LPS receptor [93]. BPI also binds LPS, followed by permeabilization of the cytoplasmic membrane and a decrease in the electrochemical gradient of the bacterial cell leading to death [94]. OCX-36 may therefore participate in natural defense mechanisms that keep the egg and oviduct free of pathogens.

OCX-36 is also detected in the vitelline membrane [65]. Chicken and Zebra Finch OCX-36 exhibit a large degree of similarity throughout the protein sequence (56% identity), as seen in Fig. 2d, indicating greater conservation between these species for this matrix protein compared to OC-17, OC-116 and OCX-32.

Other Eggshell-Specific Proteins

Recently, it was reported that 21- and 25-kDa components of the eggshell matrix/uterine fluid have been cloned [95]. Analysis of the 21-kDa protein sequence showed significant homologies with proteins containing the BRICHOS domain to which a chaperone-like function has been ascribed [96]. The 25-kDa protein contains two protease inhibitor domains. One is a whey acidic protein (WAP) type that is also present in lustrin A, a matrix protein from the nacreous layer of the shell and mother of pearl of mollusks [97].

Non-Avian Eggshell Matrix Proteins

In eggs of turtles, the eggshell consists of two parts: a fibrous shell membrane adjacent to the albumen and a calcareous layer composed of the aragonite polymorphic form of calcium carbonate. Pelovaterin is an anionic peptide present in the aragonitic eggshells of the soft-shelled turtle (*Pelodiscus sinensi*), an animal so-called because its carapace is leathery and pliable [98]. Pelovaterin was purified from the soluble organic matrix by RP-HPLC. The amino acid sequence, 42 residues in length, shows no homology to any known protein. This sequence is rich in Gly, Cys, Ser and Val with N-terminal and C-terminal sequences containing hydrophilic residues. Dynamic light scattering, fluorescence emission spectroscopy and circular dichroism indicated that pelovaterin is monomeric in lower concentrations and aggregates at high concentrations [98].

Pelovaterin seems to have a role in the biomineralization of the soft-shelled turtle eggshell. In vitro calcium carbonate crystallization tests show that pelovaterin induces the formation of the vaterite polymorph of calcium carbonate, alters crystal morphology and increases the mineral growth rate [98]. Crystal nucleation may be related to the aggregation of pelovaterin at high concentration. More recently, the same researchers have demonstrated that pelovaterin stabilizes the metastable vaterite phase of the eggshell, but under certain recrystallization conditions can induce and stabilize aragonite as the dominant polymorph [99].

NMR structural analysis indicated that pelovaterin contains a hydrophobic core and a structure similar to cationic antimicrobial peptides such as defensins [99]. Antimicrobial assays revealed that pelovaterin was very effective against the Gram-negative bacteria *P. aeruginosa* and *Proteus vulgaris*, possessed moderate activity against *Proteus mirabilis* and *S. aureus*, but showed very little activity against *E. coli* and *Enterobacter aerogenes* [99]. Scanning electron

microscopy to investigate its bactericidal activity against *P. aeruginosa* and *P. vulgaris* revealed that treatment with 10 μM pelovaterin produced pronounced wrinkling, surface roughening, and blebbing of the bacterial membrane and the majority of the cells lost their membrane integrity.

The results demonstrate the adaptability of an eggshell matrix protein to perform multiple tasks: calcium carbonate polymorph discrimination and protection of the contents of the egg against bacterial invasion.

Conclusion / Perspectives

The majority of constituents of the chicken eggshell have been identified. Future effort to compare and contrast the chicken eggshell matrix proteins with those of other avian and non-avian eggshells will pay dividends to fully determine the function of the eggshell matrix proteins. Two functional roles have been proposed: (1) regulation of eggshell mineralization, and (2) antimicrobial protection of the egg and its contents. Bioinformatic studies with nucleotide and amino acid sequences contribute to the identification of putative function of proteins; however, sensitive proteomic methods increasingly reveal the minor presence of "eggshell-specific" proteins in other egg compartments although the functional impact at these sites remains to be determined. New information from studies with purified native or recombinant proteins are necessary for *in vitro* tests to gain insight into the role of each isolated matrix component, and eventually to learn how they may function synergistically. One important goal will be to determine the impact and importance of posttranslational modification of matrix components (glycosylation, glycanation, phosphorylation, etc.), which could greatly alter their properties and interactions. An emerging concept is the dual role (mineralization/antimicrobial protection) that

certain eggshell matrix proteins can play. These investigations will continue to provide new insights into function of integrated defense strategies that operate at biomineralized barriers.

Acknowledgements. The authors work has been supported by funding from Natural Sciences and Engineering Research Council (NSERC), Ontario Ministry of Agriculture, Food and Rural affairs (OMAFRA) and Poultry Industry Council (PIC) to M.T.H.

References

1. Hincke MT, Wellman-Labadie O, McKee MD, Gautron J, Nys Y, Mann K (2008) Biosynthesis and structural assembly of eggshell components. In: Mine Y (ed) Egg bioscience and biotechnology, chapter 2. Wiley, Hoboken, pp 97–128
2. Arias JL, Fink DJ, Xiao SQ, Heuer AH, Caplan AI (1993) Biomineralization and eggshells: cell-mediated acellular compartments of mineralized extracellular matrix. Int Rev Cytol 45:217–250
3. Nys Y, Gautron J, Garcia-Ruiz JM, Hincke MT (2004) Avian eggshell mineralization: biochemical and functional characterization of matrix proteins. Comptes Rend Paleovol 3:549–562
4. Wong M, Hendrix MJC, Von der Mark K, Little C, Stern R (1984) Collagen in the egg shell membranes of the hen. Dev Biol 104:28–36
5. Arias JL, Fernandez MS, Dennis JE, Caplan AI (1991) Collagens of the chicken eggshell membranes. Connect Tissue Res 26:37–45
6. Fernandez MS, Araya M, Arias JL (1997) Eggshells are shaped by a precise spatio-temporal arrangement of sequentially deposited macromolecules. Matrix Biol 16:13–20
7. Bellairs R, Osmond M (2005) The atlas of chick development, 2nd edn. Elsevier, San Diego
8. Nys Y, Hincke MT, Arias JL, Garcia-Ruiz JM, Solomon S (1999) Avian eggshell mineralization. Poult Avian Biol Rev 10:143–166
9. Sharp RM, Silyn-Roberts H (1986) Development of preferred orientation in the eggshell of the domestic fowl. Biophys J 46:175–179

10. Rodriguez-Navarro A, Kalin O, Nys Y, Garcia-Ruiz JM (2002) Influence of the microstructure on the shell strength of eggs laid by hens of different ages. Br Poult Sci 43:395–403

11. Romanoff AL, Romanoff AJ (1949) The avian egg. Wiley, New York

12. Dennis JE, Xiao S-Q, Agarwal M, Fink DJ, Heuer AH, Caplan AI (1996) Microstructure of matrix and mineral components of eggshells from white leghorn chickens (Gallus gallus). J Morphol 228:287–306

13. Whittow GC (2000) Sturkie's avian physiology, 5th edn. Academic, San Diego

14. Fernandez MS, Moya A, Lopez L, Arias JL (2001) Secretion pattern, ultrastructural localization and function of extracellular matrix molecules involved in eggshell formation. Matrix Biol 19:793–803

15. Sparks NHC (1994) Shell accessory materials: structure and function. In: Board RG, Fuller R (eds) Microbiology of the avian egg, chapter 2. Springer, New York, pp 25–42

16. Ar A, Rahn H (1985) Pores in avian eggshells: gas conductance, gas exchange and embryonic growth rate. Resp Physiol. 61:1–20

17. Mann K, Siedler F (2004) Ostrich (Struthio camelus) eggshell matrix contains two different C-type lectin-like proteins. Isolation, amino acid sequence and posttranslational modifications. Biochim Biophys Acta 1696:41–50

18. Hincke MT, Bernard A-M, Lee ER, Tsang CPW, Narbaitz R (1992) Soluble protein constituents of the domestic fowl's eggshell. Br Poult Sci 33:505–516

19. Gautron J, Bain M, Solomon S, Nys Y (1996) Soluble matrix of hen's eggshell extracts changes in vitro the rate of calcium carbonate precipitation and crystal morphology. Br Poult Sci 37:853–866

20. Gautron J, Hincke MT, Nys Y (1997) Precursor matrix proteins in the uterine fluid change with stages of eggshell formation in hens. Connect Tissue Res 36:195–210

21. Miksik I, Eckhardt A, Sedlakova P, Mikulikova K (2007) Proteins of insoluble matrix of avian (Gallus gallus) eggshell. Connect Tissue Res 48:1–8

22. Mann K (2004) Identification of the major proteins of the organic matrix of emu (Dromaius novaehollandiae) and rhea (Rhea americana) eggshell calcified layer. Br Poult Sci 45:483–490

23. Hincke MT (1995) Ovalbumin is a component of the chicken eggshell matrix. Connect Tissue Res 31:227–233

24. Hincke MT, Gautron J, Panhéleux M, Garcia-Ruiz J, McKee MD, Nys Y (2000) Identification and localization of lysozyme as a component of eggshell membranes and eggshell matrix. Matrix Biol 19:443–453

25. Gautron J, Hincke MT, Panheleux M, Garcia-Ruiz JM, Boldicke T, Nys Y (2001) Ovotransferrin is a matrix protein of the hen eggshell membranes and basal calcified layer. Connect Tissue Res 42:255–267

26. Hincke MT, Tsang CPW, Courtney M, Hill V, Narbaitz R (1995) Purification and immunochemistry of a soluble matrix protein of the chicken eggshell (ovocleidin 17). Calcif Tissue Int 56:578–583

27. Hincke MT, Gautron J, Mann K, Panhéleux M, McKee MD, Bain M, Solomon SE, Nys Y (2003) Purification of ovocalyxin-32, a novel chicken eggshell matrix protein. Connect Tissue Res 44:16–19

28. Hincke MT, Gautron J, Tsang CPW, McKee MD, Nys Y (1999) Molecular cloning and ultrastructural localization of the core protein of an eggshell matrix proteoglycan, ovocleidin-116. J Biol Chem 274:32915–32923

29. Gautron J, Murayama E, Vignal A, Morisson M, McKee MD, Rehault S, Labas V, Belghazi M, Vidal ML, Nys Y, Hincke MT (2007) Cloning of ovocalyxin-36, a novel chicken eggshell protein related to lipopolysaccharide-binding proteins (LPB) bactericidal permeability-increasing proteins (BPI), and Plunc family proteins. J Biol Chem 282:5273–5286

30. Gautron J, Hincke MT, Panheleux M, Bain M, McKee MD, Solomon SE, Nys Y (2001) Ovocalyxin-32, a novel chicken eggshell matrix protein. Isolation, amino acid sequencing, cloning, and immunocytochemical localization. J Biol Chem 276:39243–39252

31. Pines M, Knopov V, Bar A (1994) Involvement of osteopontin in egg shell formation in the laying chicken. Matrix Biol 14:765–771

32. Hincke MT, St Maurice M (2000) Phosphorylation-dependent modulation of calcium carbonate precipitation by chicken eggshell matrix proteins. In: Goldberg M, Boskey A, Robinson C (eds) Chemistry and biology of mineralized tissues. American Academy of Orthopaedic Surgeons, Rosemont, pp 13–17

33. Fernandez MS, Escobar C, Lavelin I, Pines M, Arias JL (2003) Localization of osteopontin in oviduct tissue and eggshell during different stages of the avian egg laying cycle. J Struct Biol 143:171–180

34. Chien YC, Hincke MT, Vali H, McKee MD (2008) Ultrastructural matrix-mineral relationships in avian eggshell, and effects of osteopontin on calcite growth in vitro. J Struct Biol 163:84–99

35. Hincke MT, Chien YC, Gerstenfeld LC, McKee MD (2008) Colloidal-gold immunocytochemical localization of osteopontin in avian eggshell gland and eggshell. J Histochem Cytochem 56:467–476

36. Chien Y-C, Hincke MT, McKee MD (2009) Avian eggshell structure and osteopontin. Cells Tissue Organs 189:38–43

37. Mann K, Gautron J, Nys Y, McKee MD, Bajari T, Schneider WJ, Hincke MT (2003) Disulfide-linked heterodimeric clusterin is a component of the chicken eggshell matrix and egg white. Matrix Biol 22:397–407

38. Mann K, Maček B, Olsen JV (2006) Proteomic analysis of the acid-soluble organic matrix of the chicken calcified eggshell layer. Proteomics 6:3801–3810

39. Falini G, Albeck S, Weiner S, Addadi L (1996) Control of aragonite or calcite polymorphism by mollusk shell macromolecules. Science 271:67–69

40. Belcher AM, Wu XH, Christensen RJ, Hansma PK, Stucky GD, Morse DE (1996) Control of crystal phase-switching and orientation by soluble shell proteins. Nature 381:56–58

41. Dominguez-Vera JM, Gautron J, Garcia-Ruiz J, Nys Y (2000) The effect of avian uterine fluid on the growth behavior of calcite crystals. Poult Sci 79:901–907

42. Hernandez-Hernandez A, Gomez-Morales J, Rodriguez-Navarro AB, Gautron J, Nys Y, Garcia-Ruiz JM (2008) Identification of some active proteins in the process of hen eggshell formation. Cryst Growth Des 8:4330–4339

43. Mine Y, Oberle C, Kassaify Z (2003) Eggshell matrix proteins as defence mechanism of avian eggs. J Agric Food Chem 51:249–253

44. Silphaduang U, Hincke MT, Nys Y, Mine Y (2006) Antimicrobial proteins in chicken reproductive system. Biochem Biophys Res Commun 340:648–655

45. Wellman-Labadie O, Picman J, Hincke MT (2008) Comparative microbial toxicity of cuticle and outer eggshell protein from three species of domestic bird. Br Poult Sci 49:133–143

46. Wellman-Labadie O, Picman J, Hincke MT (2008) Antimicrobial activity of the anseriform outer eggshell and cuticle. Comp Biochem Physiol 149:640–649

47. Mann K, Siedler F (1999) The amino acid sequence of ovocleidin-17, a major protein of the avian eggshell calcified layer. Biochem Mol Biol J 47:997–1007

48. Mann K (1999) Isolation of a glycosylated form of the eggshell protein ovocleidin and determination of the glycosylation site Alternative glycosylation/phosphorylation at an N-glycosylation sequon. FEBS Lett 463:12–14

49. Mann K, Olsen JV, Macek B, Gnad F, Mann M (2007) Phosphoproteins of the chicken eggshell calcified layer. Proteomics 7:106–115

50. Lakshminarayanan R, Valiyaveettil S, Roa VS, Kini RM (2003) Purification, characterization, and in vitro mineralization studies of a novel goose eggshell matrix protein ansocalcin. J Biol Chem 278:2928–2936

51. Mann K, Siedler F (2006) Amino acid sequences and phosphorylation sites of emu and rhea eggshell C-type lectin-like proteins. Comp Biochem Physiol B 143:160–170

52. van Tuinen M, Hedges SB (2002) Calibration of avian molecular clocks. Mol Biol Evol 18:206–213

53. Zelensky AN, Gready JE (2005) The C-type lectin-like domain superfamily. FEBS J 272:6179–6217

54. Reyes-Grajeda JP, Jauregui-Zuniga D, Rodriguez-Romero A, Hernandez-Santoyo A, Bolanos-Garcia VM, Moreno A (2002) Crystallization and preliminary X-ray analysis of ovocleidin-17 a major protein of the Gallus gallus eggshell calcified layer. Protein Pept Lett 9:253–257

55. Reyes-Grajeda JP, Moreno A, Romero A (2004) Crystal structure of ovocleidin-17, a major protein of the calcified Gallus gallus eggshell: implications in the calcite mineral growth pattern. J Biol Chem 279:40876–40881

56. Reyes-Grajeda JP, Marin-Garcia L, Stojanoff V, Moreno A (2007) Purification, crystallization and preliminary X-ray analysis of struthiocalcin 1 from ostrich (Struthio camelus) eggshell. Acta Crystallogr F 63:987–989

57. Lakshminarayanan R, Kini RM, Valiyaveettil S (2002) Investigation of the role of ansocalcin in the biomineralization in goose eggshell matrix. Proc Natl Acad Sci USA 99:5155–5159

58. Lakshminarayanan R, Joseph JS, Kini RM, Valiyaveettil S (2005) Structure-function relationship of avian eggshell matrix proteins: a comparative study of two major eggshell matrix proteins, ansocalcin and OC-17. Biomacromolecules 6:741–751

59. Marin-Garcia L, Fraontana-Uribe BA, Reyes-Grajeda JP, Stojanoff V, Serrano-Posada HJ, Moreno A (2008) Chemical recognition of carbonate anions by proteins involved in biomineralization processes and their influence on calcite crystal growth. Cryst Growth Des 8:1340–1345

60. Cash HL, Whitham CV, Behrendt CL, Hooper LV (2006) Symbiotic bacteria direct expression of an intestinal bactericidal lectin. Science 313:1126–1130

61. Wellmann-Labadie O, Lakshminarayanan R, Hincke MT (2008) Antimicrobial properties of avian eggshell specific C-type lectin-like proteins. FEBS Lett 582:699–704

62. Powers JP, Hancock RE (2003) The relationship between peptide structure and antimicrobial activity. Peptides 24:1681–1691

63. Mann K, Hincke MT, Nys Y (2002) Isolation of ovocleidin-116 from chicken eggshells, correction of its amino acid sequence and identification of disulfide bonds and glycosylated Asn. Matrix Biol 21:383–387

64. Mann K, Mann M (2008) The chicken egg yolk plasma and granule proteomes. Proteomics 8:178–191

65. Mann K (2008) Proteomic analysis of the chicken egg vitelline membrane. Proteomics 8:2322–2332

66. D'Ambrosio C, Arena S, Scaloni A, Guerrier L, Boschetti E, Mendieta ME, Citterio A, Righetti PG (2008) Exploring the chicken egg white proteome with combinatorial peptide ligand libraries. J Proteome Res 7:3461–3474

67. Carrino DA, Rodriquez JP, Caplan AI (1997) Dermatan sulfate proteoglycans from the mineralized matrix of the avian eggshell. Connect Tissue Res 36:175–193

68. Nimtz M, Conradt H, Mann K (2004) LacdiNAc (GalNAcβ1–4GlcNAc) is a major motif in N-glycan structures of the chicken eggshell protein ovocleidin-116. Biochim Biophys Acta 1675:71–80

69. Arias JL, Jure C, Wiff JP, Fernandez MS, Fuenzalida V, Arias JL (2002) Effect of sulfate content of biomacromolecules on the crystallization of calcium carbonate. Mater Res Soc Symp Proc 711:243–248

70. Watanabe H, Yamada Y, Kimata K (1998) Roles of aggrecan, a large chondroitin sulfate proteoglycan, in cartilage structure and function. J Biochem 124:687–693

71. Hunter GK (1991) Role of proteoglycan in the provisional calcification of cartilage. A review and reinterpretation. Clin Orthop Relat Res 262:256–280

72. Hunter GK, Szigety SK (1992) Effects of proteoglycan on hydroxyapatite formation under non-steady-state and pseudo-steady-state conditions. Matrix 12:362–368

73. International Chicken Genome Sequencing Consortium (2004) Sequence and comparative analysis of the chicken genome provide unique perspectives on vertebrate evolution. Nature 432:695–716

74. Kawasaki K, Weiss K (2003) Mineralized tissue and vertebrate evolution: the secretory calcium-binding phosphoprotein gene cluster. Proc Natl Acad Sci USA 100:4060–4065

75. Kawasaki K, Weiss KM (2006) Evolutionary genetics of vertebrate tissue mineralization: the origin and evolution of the secretory calcium-binding phosphoprotein family. J Exp Zool B Mol Dev Evol 306:295–316

76. Stapley J, Birkhead TR, Burke T, Slate J (2008) A linkage map of the zebra finch Taeniopygia guttata provides new insights into avian genome evolution. Genetics 179:651–667

77. McKee MD, Nanci A (1996) Osteopontin: an interfacial extracellular matrix protein in mineralized tissues. Connect Tissue Res 35:197–205

78. Hincke MT, St. Maurice M, Nys Y, Gautron J, Panheleux M, Tsang CPW, Bain MM, Solomon SE, McKee MD (2000) Eggshell proteins and shell strength: molecular biology of eggshell matrix proteins and industry applications. In: Sim JS, Nakai S, Guenter W (eds) Egg nutrition and newly emerging ovo-bio technologies. CABI, New York

79. Dunn IC, Joseph NT, Bain M, Edmond A, Wilson PW, Milona P, Nys Y, Gautron J, Schmutz M, Preisinger R, Waddington D (2008) Polymorphisms in eggshell organic matrix genes are associated with eggshell quality measurements in pedigree Rhode Island Red hens. Animal Genet 40:110–114

80. Horvat-Gordon M, Yu F, Burns D, Leach RM Jr (2008) Ovocleidin (OC 116) is present in avian skeletal tissues. Poult Sci 87:1618–1623

81. Liu Q, Yu L, Gao J, Fu Q, Zhang J, Zhang P, Chen J, Zhao S (2000) Cloning, tissue expression pattern and genomic organization of latexin, a human homologue of rat carboxypeptidase A inhibitor. Mol Biol Rep 27:241–246

82. Uratani Y, Takiguchi-Hayashi K, Miyasaka N, Sato M, Jin M, Arimatsu Y (2000) Latexin, a carboxypeptidase A inhibitor, is expressed in rat peritoneal mast cells and is associated with granular structures distinct from secretory granules and lysosomes. Biochem J 346:817–826

83. Aagaard A, Listwan P, Cowieson N, Huber T, Ravasi T, Wells CA, Flanagan JU, Kellie S, Hume DA, Kobe B, Martin JL (2005) An inflammatory role for the mammalian carboxypeptidase inhibitor latexin: relationship to cystatins and the tumor suppressor TIG1. Structure 13:309–317

84. Shutoh M, Oue N, Aung PP, Noguchi T, Kuraoka K, Nakayama H, Kawahara K, Yasui W (2005) DNA methylation of genes linked with retinoid signaling in gastric carcinoma:

expression of the retinoid acid receptor beta, cellular retinol-binding protein 1, and tazarotene-induced gene 1 genes is associated with DNA methylation. Cancer 104:1609–1619

85. Nagpal S, Thacher SM, Patel S, Friant S, Malhotra M, Shafer J, Krasinski G, Asano AT, Teng M, Duvic M, Chandraratna RA (1996) Negative regulation of two hyperproliferative keratinocyte differentiation markers by a retinoic acid receptor-specific retinoid: insight into the mechanism of retinoid action in psoriasis. Cell Growth Differ 7:1783–1791

86. Jing C, El-Ghany MA, Beesley C, Foster CS, Rudland PS, Smith P, Ke Y (2002) Tazarotene-induced gene 1 (TIG1) expression in prostate carcinomas and its relationship to tumorigenicity. J Natl Cancer Inst 94:482–490

87. Hincke MT, Guest S, Gautron J, Nys Y (2003) Gene organization of ovocalyxin-32, an eggshell matrix protein. In: Proceedings of the 10th European symposium on the quality of eggs and egg products, vol 3. Saint-Brieuc, France, pp 13–19 (23–26 September 2003)

88. Yang KT, Lin CY, Liou JS, Fan YH, Chiou SH, Huand CW, Wu CP, Lin EC, Chen CF, Lee YP, Lee WC, Ding ST, Cheng WT, Huang MC (2007) Differentially expressed transcripts in shell glands from low and high egg production strains of chickens using cDNA microarrays. Anim Reprod Sci 110:113–124

89. Hagiwara K, Kikuchi T, Endo Y, Huqun, Usui K, Takahashi M, Shibata N, Kusakabe T, Xin H, Hoshi S, Miki M, Inooka N, Tokue Y, Nukiwa T (2003) Mouse SWAM1 and SWAM2 are antibacterial proteins composed of a single whey acidic protein motif. J Immunol 170:1973-1979

90. Xing J, Wellman-Labadie O, Gautron J, Hincke MT (2007) Recombinant eggshell ovocalyxin-32: Expression, purification and biological activity of the glutathione S-transferase fusion protein. Comp Biochem Physiol 147:172–177

91. Bingle CD, Craven CJ (2004) Meet the relatives: a family of BPI- and LBP-related proteins. Trends Immunol 25:53–55

92. Schumann RR, Leong SR, Flaggs GW, Gray PW, Wright SD, Mathison JC, Tobias PS, Ulevitch RJ (1990) Structure and function of lipopolysaccharide binding protein. Science 249:1429–1431

93. Hailman E, Lichenstein HS, Wurfel MM, Miller DS, Johnson DA, Kelley M, Busse LA, Zukowski MM, Wright SD (1994) Lipopolysaccharide (LPS)-binding protein accelerates the binding of LPS to CD14. J Exp Med 179:269–277

94. Dann SM, Eckmann L (2007) Innate immune defenses in the intestinal tract. Curr Opin Gastroenterol 23:115–120

95. Gautron J, Nys Y (2007) Eggshell matrix proteins. In: Huopalahti R, López-Fandiño R, Anton M, Schade R (eds) Bioactive egg compounds. Springer, Berlin, pp 103–108

96. Sánchez-Pulido L, Devos D, Valencia A (2002) BRICHOS: a conserved domain in proteins associated with dementia, respiratory distress and cancer. Tr Biochem Sci 27:329–332

97. Shen X, Belcher AM, Hansma PK, Stucky GD, Morse DE (1997) Molecular cloning and characterization of lustrin A, a matrix protein from shell and pearl nacre of Haliotis rufescens. J Biol Chem 272:32472–32481

98. Lakshminarayanan R, Chi-Jin EO, Loh XJ, Kini RM, Valiyaveettil S (2005) Purification and characterization of a vaterite-inducing peptide, pelovaterin, from the eggshells of Pelodiscus sinensi (Chinese soft-shelled turtle). Biomacromolecules 6:1429–1437

99. Lakshminarayanan R, Vivekanandan S, Samy RP, Banerjee Y, Chi-Jin EO, Teo KW, Jois SD, Kini RM, Valiyaveettil S (2008) Structure, self-assembly, and dual role of a beta-defensin-like peptide from the Chinese soft-shelled turtle eggshell matrix. J Am Chem Soc 130:4660–4668

Chapter 2

“Proteomic Analysis Provides New Insight into the Chicken Eggshell Cuticle.”

Rose-Martel M, Du J and Hincke MT (2012) *Journal of Proteomics*, 75(9):2697-706

The previous chapter demonstrates the important role that proteomics and genomics analyses have played in identifying eggshell matrix proteins. Mass spectrometry-based technology has identified over 500 proteins in the palisade layer of the calcified eggshell; however, the protein constituents of the organic cuticle layer remain uncharacterized. The cuticle is the outermost layer of the avian eggshell and it has been shown that eggs with partial or absent cuticle are more susceptible to bacterial contamination. This leads to the hypothesis that the cuticle and its components play a key role in preventing bacterial contamination of the egg contents. This chapter describes a proteomics approach to identify proteins extracted from the outermost layer of the cuticle.

Author contributions:

Eggshell cuticle protein extraction was conducted by Jingwen Du. Bioinformatics analysis, data interpretation and manuscript preparation was done by Megan Rose-Martel. Experiments, data analysis and manuscript preparation were supervised by Dr. Maxwell T. Hincke.

Abstract

The cuticle is the outermost layer of the avian eggshell, whose protein constituents remain virtually unknown. We hypothesize that cuticle components play a major role in microbial resistance, since eggs with incomplete or absent cuticle are more susceptible to bacterial contamination. In this study we extracted proteins from the outermost non-calcified layer of the cuticle of chicken eggs and subjected them to LC/MS/MS proteomic analysis. We identified 47 cuticle proteins with high confidence and reproducibility. Two proteins, similar to Kunitz-like protease inhibitor and ovocalyxin-32 (a carboxypeptidase A inhibitor), were the most abundant of the cuticle proteins. A number of proteins known to have antimicrobial activity in the egg were detected (lysozyme C, ovotransferrin, ovocalyxin-32, cystatin, ovoinhibitor) as well as possible new candidates (myeloperoxidase, ovocalyxin-36 and members of the SERPIN family). This is the first comprehensive report of cuticle proteome, a starting point to determine cuticle function and the molecular basis of its antimicrobial properties.

1. Introduction

Integrated defense strategies that operate at biomineralized barriers are a hallmark of sophisticated biological structures. One example, although not well understood, is the calcified eggshell that is essential for reproduction in birds and reptiles. The avian calcified shell is a complex structure that is deposited while the forming egg is retained in the distal oviduct (uterus / shell gland) during an extended period. Genetics controls the shell permeability for metabolic gases and water, which depends on the characteristics of its pores - number, density, branching pattern and caliber. Ultimately, a cuticle is deposited onto the eggshell surface during the final phase of egg formation [1]. The cuticle mainly consists of proteins (> 85%) and possesses two layers: the innermost is mineralized and contains hydroxyapatite-containing vesicles deposited during the final phase of eggshell calcification (termination); the outermost remains non-mineralized [2] and [3]. The cuticle is distributed unevenly over the surface of the egg; its thickness ranges from 5 to 10 μm [4]. The cuticle covers the calcified shell and fills the entry to its pores (up to 50 μm in depth), creating a barrier which inhibits water movement across the shell and prevents dehydration of the egg interior [5]. Moreover, the cuticle physically excludes bacterial penetration of pores and limits microbial colonization on the egg's surface [6] and [7]. Eggs with absent or incomplete cuticle are more susceptible to bacterial contamination [8]. Cuticle desiccation during egg storage or incubation leads to cracks that expose eggshell pores and leave the egg vulnerable to contamination by pathogens [9]. A pathogen-free egg is extremely important for avian reproduction and survival of the developing embryo, in addition to food safety of the nutritious unfertilized egg intended for human consumption. Eggs and egg-containing foods are the main vehicles for *Salmonella enteritidis* intoxication (poisoning) [10], in

addition to potential contamination by *E. coli, Pseudomonas* sp., *Micrococcus* sp. and various other bacterial strains [7]. In order to understand the molecular basis for the antimicrobial function of the eggshell cuticle and gain further overall insight into cuticle function, we performed a comprehensive proteomic analysis of the outermost (non-calcified) layer of the cuticle.

2. Materials and Methods

2.1. Cuticle Protein Extraction

Unwashed freshly laid eggs from Lohmann LSL-Lite chickens were obtained from Laviolette Poultry Farm, St-Isidore, Ontario. In two independent trials, intact eggs (n = 5) were individually extracted in sterile plastic bags containing 2 mL of extraction solution: 1% SDS or 1% SDS, 2 mM DTT. The egg surface was manually massaged for 5 minutes with extraction solution to solubilize the cuticle layer. An empty plastic bag was treated with extraction solution to assess possible contamination arising from the extraction method (none was detected). The individual extraction samples were transferred to Amicon Ultra-4 Centrifugal Filter Devices (molecular weight cutoff of 3000 Da, Millipore Corporation, Billerica, MA) and centrifuged at 4000 rpm to concentrate the dilute cuticle extracts. The protein concentration of each concentrated extract was measured with the bicinchoninic acid (BCA) assay (Thermo Scientific, Hampton, NH) before pooling for electrophoresis. Pooled extracts were resolved by SDS-PAGE using a precast 4-12% BisTris gel (Invitrogen, Carlsbad, CA). The gels were sectioned and sent to the Proteomics Platform of the Eastern Quebec Genomics Centre (Laval, QC) for LC/MS/MS

analysis (services include in-gel digestion, mass spectrometry and Mascot database searching, 2.2, 2.3, 2.4 and 2.5).

2.2. Protein In-Gel Digestion

Gel sections were placed in 96-well microplates, washed with water and digested with trypsin on a MassPrep liquid handling robot (Waters, Milford, MA) [11] and [12]. Proteins were reduced with 10 mM DTT, alkylated with 55 mM iodoacetamide and digested with 126nM of modified, sequencing grade, porcine trypsin (Promega, Madison, WI) at 58 °C for 1 h. The digestion products were extracted using 1% formic acid, 2% acetonitrile followed by 1% formic acid, 50% acetonitrile, pooled, vacuum centrifuged dried and then resuspended into 7 μL of 0.1% formic acid. Only 2 μL of the resuspended extracts were analyzed by mass spectrometry.

2.3. Mass Spectrometry

Online reversed-phase nanoscale capillary liquid chromatography and electrospray mass spectrometry (ES MS/MS) were used to separate and analyze peptide samples. The experiments were performed with a Thermo Surveyor MS pump connected to a LTQ linear ion source (ThermoFisher, San Jose, CA). Peptide separation occurred on a Self-Pack PicoFrit column (New Objective, Woburn, MA) containing Jupiter packing material (Phenomenex, Torrence, CA) 5u, 300A, C18, 10 cm × 0.075 mm internal diameter. Peptides were eluted by a 2–50% solvent B (acetonitrile, 0.1% formic acid) linear gradient in 30 minutes, at 200 nL/min (obtained by flow-splitting) while the mass spectra were obtained using Xcalibur software version 2.0 and a data dependent acquisition mode. Collision-induced dissociation of the seven most intense ions followed each full scan mass spectrum (400 to 2000 m/z). Other parameters include an enabled

dynamic exclusion (30 second exclusion duration) function and a relative collisional fragmentation energy set to 35%.

2.4. Database Searching

The MS/MS results were analyzed with Mascot (Matrix Science, London, UK; version 2.2.0), searching the uniref-100.2010.06.Gallus.gallus.9031database (37461 entries), with trypsin digestion. Search parameters included a fragment ion mass tolerance of 0.50 Da and a parent ion tolerance of 2.0 Da. The iodoacetamide derivative of cysteine was specified in Mascot as a fixed modification, while oxidation of methionine was specified as a variable modification. Two missed cleavages were allowed. The same procedure was repeated with Mascot set up to search uniref-100_2010_06_Bacteria_2 database (5093156 entries) to assess possible bacterial contamination of the unwashed egg surface by bacteria from the farm environment or chicken feces. No peptides of bacterial origin were detected.

2.5. Criteria for Protein Identification

Validation of MS/MS based peptide and protein identifications were performed using Scaffold (version Scaffold-3_00_08, Proteome Software Inc., Portland, OR) and were accepted if they were identified at $p \leq 0.05$ probability, specified by the Protein Prophet algorithm [13] and [14]. Protein identifications also required at least 2 unique peptides to be accepted. The principles of parsimony were utilized to group proteins that contained similar peptides and could not be differentiated based on MS/MS analysis alone.

2.6. Bioinformatic Analysis

The relative quantification of the identified proteins were calculated using the exponentially modified protein abundance index (emPAI) = 10^($N_{observed}$ / $N_{observable}$) − 1, where $N_{observed}$ is the amount of unique parent ions obtained and $N_{observable}$ corresponds to the amount of peptides expected after digestion with trypsin [15]. The protein Basic Local Alignment Search Tool (pBLAST) was used to align proteins identified by Scaffold against the non-redundant protein sequence database for the species *Gallus gallus* (9031). Potential signal peptides in the predicted full-length protein were assessed using the SignalP 4.0 Server (www.cbs.dtu.dk/services/SignalP) and were only accepted as valid if both the neural network and hidden Markov models identified a signal peptide ($p \leq 0.05$). Gene Ontology (GO) term enrichment analysis using the Database for Annotation, Visualization and Integrated Discovery (DAVID) Functional Annotation Tool (DAVID Bioinformatics Resources 6.7, NIAID/NIH) was used to highlight the more relevant GO terms associated to biological processes and molecular functions [16].

3. Results

3.1. Cuticle Extraction

The amount of cuticle extracted from each egg was variable; an average of 123 (± 59) μg of protein / egg was extracted with 1% SDS, 2 mM DTT [range 74–215 μg/egg]. However, significantly less cuticle protein was extracted with SDS alone, revealing an average of 62 (± 14) μg/egg [range 42 – 78 μg]. The same 1% SDS, 2 mM DTT protocol repeated with grocery store eggs revealed only 39 (± 4) μg/egg of extracted cuticle. The lower cuticle protein of the grocery

store eggs is likely a consequence of the commercial washing process (cleaning with brushes and alkaline detergents) before eggs are sold for consumption [17]. Individual extraction samples were pooled together for electrophoresis in order to obtain proteomic results representative of multiple eggs. SDS-PAGE revealed intense Coomassie Blue-stained bands at 32 kDa and 10 kDa as well as less intensely stained bands at 27, 20, 14 and 8 kDa (Fig. 1). The entire extraction process and proteomic analysis was repeated twice to confirm reproducibility.

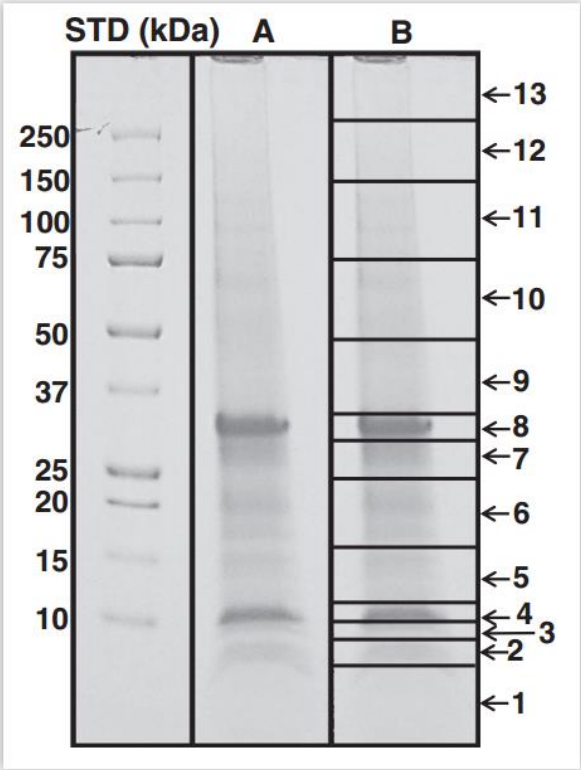

Fig. 1 – SDS-PAGE analysis of 30 µg of cuticle proteins from 5 pooled fractions, all extracted with 1% SDS, 2 mM DTT. Bars and numbers indicate where the gel was sectioned and the fragments that were sent for LC/MS/MS sequencing analysis (lane B).

3.2. Cuticle Proteome

Each gel was sectioned as depicted in Fig. 1 and subjected to LC/MS/MS analysis. Two independent proteomic analyses were merged by combining the entire dataset of spectra, in order to increase the threshold for significance to detect the less abundant proteins. Table 1 lists the 47 proteins that were confirmed in the cuticle extract by at least 2 unique peptides ($p \leq 0.05$). The most abundant cuticle proteins were predicted: similar to Kunitz-like protease inhibitor and ovocalyxin-32 (OCX-32) with emPAI values of 14.08 and 112.62, respectively. Ovalbumin also had an elevated emPAI of 35.79, however this value was quite variable between individual extracts (2.44 and 35.79). We hypothesize that this is caused by the inconsistent contamination of the egg surface by egg white. The protein sequence of predicted: similar to Kunitz-like protease inhibitor in the NCBI protein database, (REFSEQ ID: XP_001235178.2), has recently been updated and confirmed by the EST database. However, 3 unique peptides identified during proteomic analysis are only present in the predicted C-terminal sequence of the original protein sequence (REFSEQ ID: XP_001235178.1), suggesting that it also is a valid sequence (Table 2). Alternative splicing to produce both versions of the protein is a possible explanation for this discrepancy. Each gene product has a different predicted molecular weight: XP_001235178.1: 36 kDa; XP_001235178.2: 23 kDa (Fig. 2). Protein migration in the gel was quite disperse, possibly due to breakdown products; but the majority of the assigned spectra were present in gel slice 6 (15–23 kDa) (Fig. 1).

Table 1 – Merged results for cuticle proteins extracted with 1% SDS, 2 mM DTT identified in two independent analyses.

Identified proteins	MW (kDa)	UniProt ID	No. of unique peptides	Coverage (%)	emPAI [a]	Signal peptide [b]	Also present in [c]	Gel section [d]
Ovocalyxin-32 [e]	31	C7G541	34	85	112.62 (54.46,16.61)	Yes	vm, w, s, c	1–13
Ovalbumin	43	P01012	18	56	35.79 (2.44,35.79)	No	y, vm, w, s	1–13
Similar to Kunitz-like protease inhibitor	23	N/A (REFSEQ ID: XP_001235178)	23	50	14.08 (8.41,14.78)	Yes	w, s, c	1–13
Lysozyme C	16	P00698	9	50	9.53 (6.96,6.84)	Yes	y, vm, w, s	2, 4
Glutathione peroxidase 3	25	F1NPJ8	7	36	4.89 (1.43,1.90)	Yes	y, vm, w, s	5–6
Ovoinhibitor	52	P10184	18	48	4.15 (4.15,0.64)	Yes	y, vm, w, s	4–8, 10
Ovotransferrin	78	P02789	24	41	2.56 (0.48,2.17)	No	y, vm, w, s	8, 10
Similar to prostate stem cell antigen	13	F1NXM7	2	24	1.61 (0.90,0.90)	Yes	y, s	5
Serum albumin	70	P19121	16	28	1.54 (0.75, 0.86)	Yes	y, vm, w, s	10
gastrokine-2 (OCX-21)	21	E1C2G7	4	33	1.26 (0.5, 0.84)	Yes	s	2, 4
Hemoglobin subunit β	16	P02112	3	30	1.19 (1.19, 1.19)	No	s	4, 13
Ovocalyxin-36	49	Q53HW8	6	23	0.88 (0.88, 0.72)	Yes	vm, s, c	5, 8–9
predicted: selenium-binding protein 1-like	78	N/A (REFSEQ ID: XP_003642728)	14	23	0.75 (0.65, 0.25)	No		8–13
Cystatin	15	P01038	3	27	0.75 (0.75, 0.75)	Yes	y, vm, w, s	4
Hemoglobin subunit α-A	15	P01994	2	15	0.75 (0,0.75)	No		7
β-hexosaminidase subunit α precursor	59	F1NEX5	11	18	0.69 (0.69, 0.16)	Yes	s	10
Chain A, structure of an avian Igy-Fc 3–4 fragment	25	N/A (PDB ID: 2W59_A)	5	35	0.67 (0.67, 0.67)	No	y	4, 10
predicted: similar to SDF3	47	E1C7H6	7	20	0.61 (0.47, 0.10)	Yes	y, vm, s	9
Vitellogenin-2	203	E1BYN6	17	11	0.47 (0, 0.47)	Yes	y, vm, w, s	2, 6–13
Epithelial cell adhesion molecule	34	Q5F381	4	10	0.46 (0.46, 0)	Yes		8
Nucleobindin-2	54	F1NGB1	4	11	0.44 (0.44, 0)	Yes	w, s	10
Similar to FKSG18	39	F1NWW1	3	10	0.41 (0.26, 0.12)	No	s	8
Clusterin	49	F1NGP2	4	10	0.31 (0.20, 0.09)	Yes	y, vm, w, s, c	8
Leucine-rich repeat-containing protein 19	43	F1P096	4	12	0.28 (0.13, 0.13)	No	vm, w, s	8
predicted: annexin A8	37	E1C8K3	2	5	0.27 (0, 0.27)	No	s	9
Similar to myeloperoxidase precursor	81	F1P3V5	5	9	0.25 (0.18, 0.12)	No		10–11
Tubulin α-1 chain	46	P02552	2	7	0.25 (0, 0.25)	No	vm, s	
Actin, cytoplasmic 1/2/5	42	P53478, P60706, Q5ZMQ2	4	20	0.24 (0.24, 0.24)	No	y, vm, w, s	8
Apolipoprotein A-IV	41	O93601	4	14	0.24 (0.24, 0)	Yes	s	8
Ovalbumin-related protein Y	44	P01014	3	10	0.22 (0.11, 0.22)	No	y, vm, w, s	10
Tubulin β-3 chain	50	P09206	3	11	0.22 (0, 0.22)	No	vm, s	6
Similar to neuronal pentraxin-2	48	E1C7S1	2	6	0.18 (0.18, 0)	No	s	10
Similar to α-2-plasmin inhibitor	51	F1NAR5	3	4	0.17 (0.17, 0.08)	Yes	y, s	10
Proactivator polypeptide (saposin A-D precursor)	58	O13035	2	5	0.16 (0.16, 0)	Yes	y, s	10
Polymeric immunoglobulin receptor precursor	69	N/A (REFSEQ ID: NP_001038109)	2	4	0.13 (0.13, 0.05)	Yes	vm, w, s	10
Aminopeptidase N	109	O57579	3	4	0.13 (0.09, 0.15)	No	y, w, s	11
Ovocleidin-116	77	F1NSM7	3	6	0.12 (0.12, 0)	Yes	y, vm, w, s, c	8, 10
predicted: mucin-5B	322	N/A (REFSEQ ID: XP_421033)	5	2	0.11	No	s	12–13
Neuroserpin	47	Q90935	2	6	0.10 (0, 0.10)	Yes	s	4–5
predicted: hyaluronidase-1	49	N/A (REFSEQ ID: XP_424356)	2	6	0.09 (0.09, 0)	Yes	s	9
Similar to ovomacroglobulin, ovostatin, partial	166	F1NEW8	3	2	0.05 (0.05, 0.06)	No	s	10–11
predicted: similar to Mesothelin	88	N/A (REFSEQ ID: XP_414835)	2	4	0.05 (0.05, 0.05)	Yes	s	11
Apolipoprotein B	484	F1NV02	11	3	0.04 (0, 0.04)	Yes	y, vm, w	10–13
predicted: thrombospondin type-1 domain-containing protein 4	114	N/A (REFSEQ ID: XP_413780)	2	2	0.04 (0.04, 0)	No		11
Similar to basement membrane-specific heparan sulfate proteoglycan core protein, partial	129	F1NAT6	2	2	0.03 (0.03, 0)	No	s	9, 11
Vitellogenin-1	211	P87498	4	2	0.02 (0, 0.02)	Yes	y, vm, w, s	10

Table 1 *(continued)*

Identified proteins	MW (kDa)	UniProt ID	No. of unique peptides	Coverage (%)	emPAI [a]	Signal peptide [b]	Also present in [c]	Gel section [d]
predicted: ovalbumin-related protein Y	45	N/A (REFSEQ ID: XP_418984)	2	5	N/A	No	y, vm, w, s	5, 9, 11

a. The relative quantification of the identified proteins were calculated using the exponentially modified protein abundance index (emPAI)= 10^($N_{observed}/N_{observable}$)−1, see Materials and Methods Section 2.6. For each identified protein, the emPAI value of the merged analyses is given, with the individual values in parentheses (Cuticle Extract: CE-1, CE-2).

b. Signal peptides were predicted using SignalP 3.0 server.

c. Egg compartment where previously detected: y, yolk; vm, vitelline membrane; w, egg white; s, eggshell; c, cuticle.

d. Gel section in which peptides corresponding to the identified proteins were identified, see Fig. 1.

e. Several isoforms of this protein were identified in the sample. This table lists the isoform with the highest emPAI value. See Table 3 for a list of the identified peptides of all isoforms.

Table 2 – Identified peptides corresponding to two versions of the predicted: similar to Kunitz-like protease inhibitor sequence.[a]

	REFSEQ ID	
Unique peptide sequences	XP_001235178.1	XP_001235178.2
APAEETAR	x	x
CPFRCPQPVPARPDTYPK	x	x
CPQPVPARPDTYPK	x	x
CPQPVPARPDTYPKK	x	x
GLEAFLLGDSNQR	**x**	
KKVPHIIGCCNSTCSSDTDFPNHLR	x	x
KRTYCYACIPALR	x	x
KVPHIIGCCNSTCSSDTDFPNHLR	x	x
QPVLLGLPLSGLPGALPHR	**x**	
RTYCYACIPALR	x	x
SCRVFVHSSCGGNANNFR	x	x
SSCGGNANNFR	x	x
SVLPEKDDFHPR	x	x
SVLPEKDDFHPRTDTDPTTNCVNNCR	x	x
TDGRSVLPEKDDFHPR	x	x
TDTDPTTNCVNNCR	x	x
TDTDPTTNCVNNCRDDGNCR	x	x
TLAECQQVCQ	x	x
TLAECQQVCQHGESWAR	**x**	
TYCYACIPALR	x	x
VFVHSSCGGNANNF	x	x
VFVHSSCGGNANNFR	x	x
VPHIIGCCNSTCSSDTDFPNHLR	x	x

[a] Peptides that do not correspond to the updated version REFSEQ ID: XP_001235178.2 are indicated by gaps.

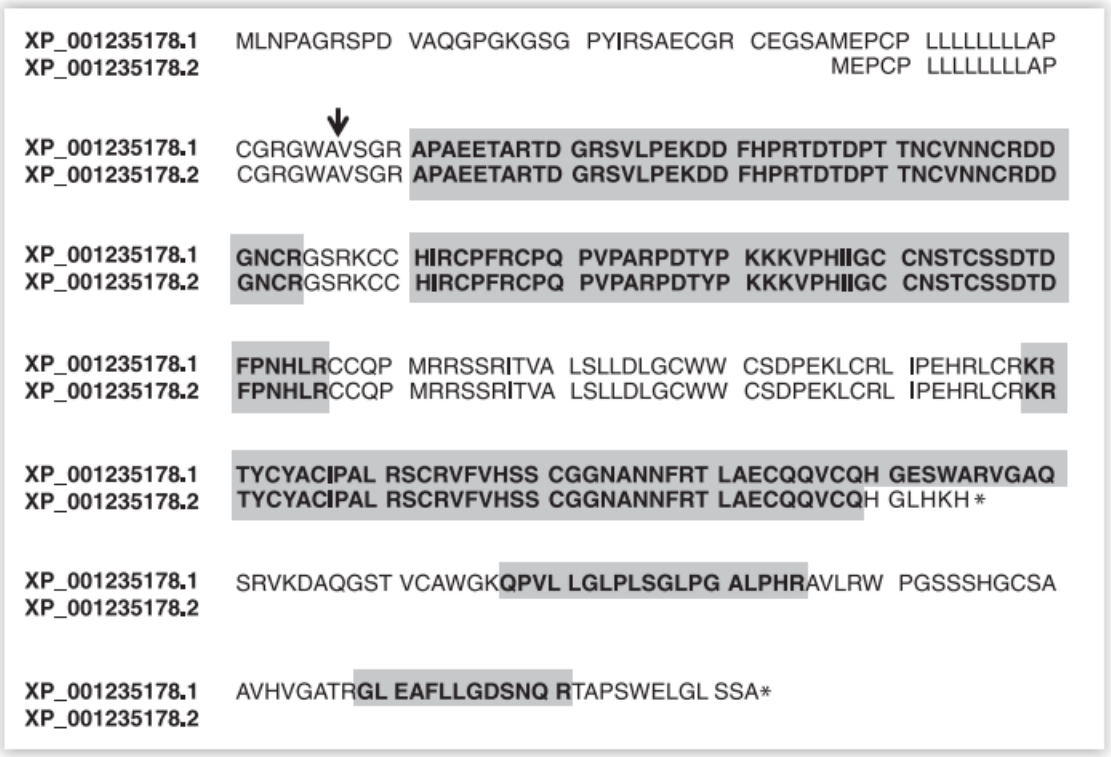

Fig. 2 – Protein sequence alignment of the two versions of predicted: similar to Kunitz-like protease inhibitor. REFSEQ ID: XP_001235178.1 represents a previous version of the protein while REFSEQ ID: XP_001235178.2 corresponds to the newly updated sequence. The identified peptides corresponding to each sequence are highlighted in grey. Asterisks (*) indicate the location of the STOP codons predicted in conceptual translation product, and an arrow designates the cleavage site of the signal peptide, predicted by SignalP 4.0.

The other most abundant protein, OCX-32, was found to reflect 4 different isoforms of the same protein (Table 3, Fig. S1). We were able to obtain the emPAI value of three isoforms: 112.62 for UNIPROT ID: C7G541, 71.78 for D3KYT5 and 52.92 for C7G542.

Table 3 – Identified peptides corresponding to four isoforms of ovocalyxin-32.[a]

Identified peptide sequences	UNIPROT ID			
	D3KYT5	C7G540	C7G541	C7G542
AQVSSVKQQIR	x	x	x	x
CVHAQNKK	x	x	x	x
DNAVAFK	x	x	x	x
EASPSRPLALHK	x	x	x	x
EAVWAAWTALHYINSHEASPSR	x	x	x	x
EAVWAAWTALHYINSHEASPSRPLAL	x	x	x	x
EAVWAAWTALHYINSHEASPSRPLALHK	x	x	x	x
EAVWAAWTALHYINSHEASPSRPLALHKVVK	x	x	x	x
ERLPWPQVPGVMHPLNPSHR		x	x	
ERLPWPQVPGVMRPLNPSHR	x			x
FIVLLHEIPTQQLNV	x		x	
FIVLLHEIPTQQLNVCHMYLVWTLGHPIR	x		x	
FIVLLHEIPTQQMNVCHMYLVWR				*
FIVLLHEIPTQQMNVCHMYLVWTLGHPIR		*		
FYEYLQHQK	x	x	x	x
FYEYLQHQKK	x	x	x	x
GSSHIMWKQSTEHTGYLLAQVSSVK			*	
KDNAVAFK	x	x	x	x
KDNAVAFKFIVLLHEIPTQQLNVCHMYLVWTLGHPIR	x		x	
KPITANYIPDSH	x		x	
KPITANYIPDSHGNIAHD	x		x	
KPITANYIPDSHGNIAHDHLQLWGLAIVGSSHIMWK			*	
KQIQEEDHR	x	x	x	x
KQIQEEDHRFYEYLQHQK	x	x	x	x
KSPPVVHAK	*			
KSPPVVHGK		x	x	x
LPWPQVPGVMHPLNPSHR		x	x	
PLNPSHR	x			x
PQVPGVMHPLNPSHR		x	x	
QIQEEDHR	x	x	x	x
QIQEEDHRFYEYLQHQK	x	x	x	x
QQIRKDNAVAFK	x	x	x	x
QSTEHTGYLLAQVSSVK	x	x	x	x
QSTEHTGYLLAQVSSVKQQIR	x	x	x	x
QSTEHTGYLLAQVSSVKQQIRK	x	x	x	x
SPPVVHAK	*			
SPPVVHAKCVHAQNK	*			
SPPVVHGK		x	x	x
YSCAPDNHGLEDGSGQDSGSAAGTSHETK	x	x	x	x
YYVHCTTEGYIHGENAGSCFATVLYLK	x	x	x	x
YYVHCTTEGYIHGENAGSCFATVLYLKK	x	x	x	x

[a] Peptides that are exclusive to a single isoform are indicated by asterisk and their spectra depicted in Fig. S1. More information on peptides exclusive to a single isoform can be found in Table S2.

3.3. Classification of Cuticle Proteins

Using the DAVID Functional Annotation Tool, we were able to identify the more relevant GO terms corresponding to the molecular functions and biological processes of our 47 proteins (Table 4). The software was able to identify two clusters. The first group consists of 10 proteins involved in enzyme regulator activity, 7 of which are predicted to possess serine-type endopeptidase inhibitor activity, also known as serine protease inhibitors (SERPINs). These include predicted: similar to α-2-plasmin inhibitor, ovalbumin, ovoinhibitor, ovalbumin-related protein Y, predicted: similar to Kunitz-like protease inhibitor, neuroserpin and predicted: ovalbumin-related protein Y. The second cluster consists of proteins involved in lipid metabolism and transport such as apolipoprotein A-IV, vitellogenin-1 and vitellogenin-2. Although not detected by the DAVID software, another cluster can be made with proteins possessing known antimicrobial activity such as lysozyme C, ovotransferrin, OCX-32, cystatin and ovoinhibitor.

Table 4 – GO term clusters corresponding to the biological processes and molecular functions of the cuticle proteins.

Clusters	GO Terms		P-Value [a]	Proteins [b]
Enzyme regulator activity				
E-score [c] 8.71	GO:0004866	Endopeptidase inhibitor activity	6.57E−11	F1NAR5; P01012; P10184; XP_418984; XP_001235178; Q90935; P01038; P01014; F1NEW8
	GO:0030414	Peptidase inhibitor activity	1.13E−10	F1NAR5; P01012; P10184; XP_418984; XP_001235178; Q90935; P01038; P01014; F1NEW8
	GO:0004857	Enzyme inhibitor activity	9.75E−10	F1NAR5; P01012; P10184; XP_418984; XP_001235178; Q90935; P01038; P01014; F1NEW8
	GO:0004867	Serine-type endopeptidase inhibitor activity	7.59E−09	F1NAR5; P01012; P10184; XP_418984; XP_001235178; Q90935; P01014
	GO:0030234	Enzyme regulator activity	5.00E−07	F1NAR5; O93601; P01012; P10184; XP_418984; XP_001235178; Q90935; P01038; P01014; F1NEW8
Lipid metabolism and transport				
E-score 2.54	GO:0010876	Lipid localization	1.67E−04	O93601; P87498; E1BYN6; F1NEX5
	GO:0005319	Lipid transporter activity	0.002178	O93601; P87498; E1BYN6
	GO:0006869	Lipid transport	0.004484	O93601; P87498; E1BYN6
	GO:0033036	Macromolecule localization	0.006045	O93601; P87498; E1BYN6; F1NAT6; F1NEX5
	GO:0051179	Localization	0.019084	P19121; O93601; P01994; P87498; E1BYN6; F1NAT6; P02112; F1NEX5

[a] P-value corresponds to the EASE score determined by the DAVID software.
[b] Corresponds to DATABASE ID # utilized in Table 1.
[c] E-score represents the enrichment score determined by the DAVID software.

4. Discussion

The chicken eggshell cuticle is in direct contact with the outside environment and therefore represents the first line of defense against a harsh external environment. Eggs with absent or incomplete cuticle layers are more susceptible to microbial contamination [8]. The cuticle provides a physical barrier to restrict bacterial entry through pores [6]; however, this does not explain the observation that the cuticle limits microbial colonization of the egg surface [7]. In order to gain more insight into cuticle function, a comprehensive proteomic study was undertaken.

A novel and successful feature of our study was the minimalistic processing approach to concentrate the dilute cuticle extract, which allowed us to identify for the first time a large number of cuticle constituents. Extended dialysis of dilute solutions, which can lead to protein losses and/or degradation, was avoided. Cuticle protein extraction with 1% SDS, 2 mM DTT, followed by LC/MS/MS proteomic analysis, produced a comprehensive catalog of the most abundant proteins situated in the outermost (non-calcified) layer of the avian egg. A previous proteomic study of the calcified eggshell started with shell that had been first treated to remove the cuticle; over 520 protein constituents of the mineralized eggshell matrix were identified [18]. Another proteomic study identified only seven cuticle proteins after scraping the EDTA insoluble proteins off the surface of the intact egg [19]. Our data shows limited overlap with their results. We confirmed the cuticle presence of ovocleidin-116 (OC-116), OCX-32, similar to Kunitz-like protease inhibitor, OCX-36 and clusterin, but not OC-17 or collagen I chain, all of which were previously identified in both the cuticle (mixture of mineralized and non-mineralized layers) and eggshell matrix [18] and [19]. Compared to other proteomic studies of the various

egg compartments (yolk, vitelline membrane, egg white, mineralized shell [18], [19], [20], [21], [22], [23], [24], [25] and [26]), several novel identifications were made in our study: predicted: selenium-binding protein 1-like, similar to myeloperoxidase precursor, hemoglobin subunit α-A, epithelial cell adhesion molecule and predicted: thrombospondin type-1 containing protein 4.

A previous study of the egg white proteome identified a selenium binding protein-1-A-like (REFSEQ ID: XP_003642729.1) [23], which is not the same protein detected in this study. The function of the selenium-binding protein in cuticle is not clear. Selenium and its binding proteins are being investigated in cancer cell growth inhibition; these are reported to interact with glutathione peroxidase [27], a protein important in oxidative stress which we also identify in the cuticle. A few studies also observed the inhibitory effects of selenium on *E. coli* and *S. aureus* growth [28] and [29]. Another previously unidentified constituent, myeloperoxidase, exerts an antibacterial effect by generating reactive oxidizing products. It is a resident antimicrobial in mammalian neutrophil leukocytes and a key player in host defense mechanisms, showing inhibitory activity towards a variety of bacteria including *S. aureus, E. coli* and *P. aeruginosa* [30]. Little information is available for predicted: thrombospondin type-1 containing protein 4. This protein is known to be part of the protease and lacunin superfamily and possesses metalloendopeptidase activity according to GO term annotation. The thrombospondin type-1 domain is present in many extracellular proteins involved in cell-matrix binding and signaling [31].

Eggshell matrix proteins have previously been organized into 3 broad groups: eggshell matrix-specific proteins, egg white proteins and ubiquitous / miscellaneous proteins [1] and [18]. This is also a convenient manner to catalog the cuticle proteins identified in this study.

4.1. Eggshell-Specific Proteins

One of the most abundant cuticle protein, similar to Kunitz-like protease inhibitor (also annotated as ovocalyxin-25, [Gautron, Hincke *et al.*, manuscript in preparation, 32]), possesses a motif placing it in the Bovine Pancreatic Trypsin Inhibitor (BPTI)/kunitz family of SERPINs, which is categorized as an enzyme regulator (Table 4). This family of protease inhibitors is basic in nature and characterized by a disulfide rich α-β fold structure with three highly conserved disulfide bonds and small molecular mass [33]. A highly studied member of this family, BPTI, possesses antimicrobial activity and inhibits the growth of a variety of both Gram-positive and Gram-negative strains of bacteria [34]. A wide range of opportunistic pathogens possess membrane-bound proteases, or release extracellular proteases, which increases their pathogenicity; these proteases are an excellent target for antimicrobials [35]. Our study documents two forms of this protein, which may represent alternative splicing, and reflect distinct biological activities (Fig. 2). Since extracts from multiple eggs were pooled before analysis, it is not clear whether different versions of this protein co-exist in the same animal.

The other abundant cuticle constituent was found to be OCX-32, previously described as an eggshell-specific protein that is highly expressed in the isthmus and uterine regions of the hen reproductive tract [1] and [36]. Immunofluorescence revealed that it is enriched in the cuticle layer, but also found in the outer calcified layer [36]. It is enriched in the uterine fluid associated with the terminal phase of calcification, the components of which modify calcite crystal growth *in vitro*: the calcite crystals are decreased in size and the lag time for their nucleation is much shorter [37]. OCX-32 is categorized by the biomineral tissue development GO term due to the hypothesis that this protein regulates the arrest of eggshell calcification. However, the OCX-32 protein sequence possesses 30% identity to a carboxypeptidase A inhibitor, leading to the

alternative hypothesis that it is an antimicrobial protein that targets microbial proteases [1]. In support of this prediction, purified recombinant OCX-32 inhibits carboxypeptidase A activity and inhibits the growth of Gram-positive bacteria *B. subtilis* [38]. The impact of non-synonymous single nucleotide polymorphisms (SNPs) on the activity of different version of the protein, as verified in this study, is not yet clear.

OCX-36 is an eggshell-specific matrix protein that previous proteomic analyses have detected in vitelline membrane, egg white and eggshell, in addition to the eggshell membranes where it is particularly abundant. It is a member of the Bactericidal/Permeability-Increasing (BPI) family of innate immune proteins that bind bacterial lipopolysaccharides (LPS) [39]. Thus GO terms associated with OCX-36 involve lipid binding functions.

OC-116 is a major eggshell-specific matrix protein which is classified with biomineral tissue development due to its proposed role in shell calcification [1]. OCX-21 (gastrokine-2), the most recently identified OCX protein, possesses a BRICHOS domain and is proposed to function as a chaperone to promote correct protein folding and stability during eggshell mineralization [32].

4.2. Egg White Proteins

Ovalbumin, ovotransferrin, lysozyme C, ovoinhibitor and cystatin are well-known egg white proteins that this study identified in the cuticle layer. This is consistent with previous reports of lysozyme and ovotransferrin on the shell surface [40], [41] and [42]. It is possible that internal egg constituents derived from broken / cracked eggs during automated collection and processing may contaminate the shell surface. The cuticle presence of chain A, structure of an avian Igy-Fc 3–4 fragment, vitellogenin-1 and − 2, which are abundant yolk proteins, also

supports this hypothesis. GO term associations identify lysozyme C and ovotransferrin as antimicrobial proteins, which are grouped with proteins involved in the response to stress and biotic stimuli. Lysozyme C is expressed in all segments of the hen oviduct and possesses hydrolytic activity against cell wall polysaccharides of Gram-positive bacteria. Ovotransferrin stunts bacterial growth by sequestering iron, a necessary growth factor for pathogens, and is classified in the iron binding and iron transport GO term categories. Ovalbumin, the most abundant egg white protein, is a non-functional member of the SERPIN family and possesses no antimicrobial activity; however, digestion with trypsin generates several peptides which inhibit *B. subtilis* growth [43]. Ovoinhibitor is also a SERPIN proteinase inhibitor and possesses trypsin, chymotrypsin and elastase inhibitory activity as well as inhibitory activity against bacterial and fungal proteases [44]. Cystatin is an inhibitor of cysteine proteinases which are present in certain viruses; it also inhibits growth of Gram-positive and -negative bacteria [45]. GO terms place ovalbumin, ovoinhibitor and cystatin in the enzyme regulator activity category (Table 4).

4.3. Ubiquitous/Miscellaneous Proteins

A variety of low abundance proteins were significantly identified in our extracts (Table 1). Proteins such as serum albumin, clusterin, nucleobindin-2 and apolipoproteins are detected in many different tissues and cellular compartments. A previous study identified clusterin in the chicken eggshell matrix and egg white, and suggested a chaperone role during egg formation [46]. A number of proteins are typically described as cellular constituents and lack a predicted signal peptide for secretion: predicted: mucin-5B, hemoglobin subunits α-A and β, actin, saposin, tubulin and annexin. These are all described as cytoplasmic proteins by the cellular component GO terms. This is similar to the vast majority of the proteins detected in the mineralized eggshell

proteome [1]. It has been proposed that abrasion of the luminal wall by the eggshell during calcification (a process lasting over 17 hours), in addition to normal turnover of the uterine epithelial cells, leads to release of cellular contents into the lumen and their incorporation into the calcifying shell and cuticle as a non-specific background phenomenon [18].

4.4. Function of the Cuticle Constituents

Previous studies examining the antimicrobial activity of the cuticle noted an inhibitory effect on the growth of Gram-positive (*B. subtilis, S. aureus*) and Gram-negative (*P. aeruginosa*) bacteria [47] and [48]. The results of this study reinforce the notion of an antimicrobial role; proteins with known antimicrobial activity were identified that could reduce microbial colonization of the egg surface. In addition to OCX-32, lysozyme and ovotransferrin, our analysis revealed other proteins with known antimicrobial activity, as well as some promising new candidates. Cystatin has bactericidal activity against both Gram-positive (*S. aureus, S. gallinarum*) and Gram-negative (*P. aeruginosa, P. gingivalis, E. coli*) bacteria [45] while ovoinhibitor inhibits fungal and bacterial proteases [44]. One of the most abundant proteins in our cuticle extract is a protein predicted to be similar to Kunitz-like protease inhibitor; we hypothesize that this protein, along with the other members of the SERPIN family of proteins (Table 4), also inhibit bacterial and fungal proteases. Other potential antimicrobial proteins are OCX-36 based on its similarities to well-known innate immune proteins, and myeloperoxidase by generating reactive oxidizing products.

The benefits of a protective barrier surrounding the egg to promote food safety are evident. Gram-positive bacteria frequently contaminate the eggshell surface since they are capable of withstanding desiccating conditions, while Gram-negative bacteria more frequently

contaminate the interior of the egg [49]. Our results demonstrate that washed grocery eggs have less cuticle protein compared to the farm eggs. One industrial strategy is to coat eggs with edible material such as mineral oil, chitosan-lysozyme, soy proteins or whey proteins [50] and [51]. These coatings act as a physical barrier only or do not possess the wide range of antimicrobials that the natural cuticle possesses. Additional manipulations during egg processing result in an increased incidence of microcracks [52] and elevated opportunities for bacterial contamination.

In summary, we have currently identified at least 47 proteins localized in the outer cuticle layer of the chicken eggshell. Only two of these proteins (similar to Kunitz-like protease inhibitor and OCX-32) comprise the vast majority of the cuticle proteins. This study is the first step towards understanding the role of the cuticle and its individual constituents. Since eggs with incomplete or absent cuticles are more susceptible to bacterial contamination, identification of cuticle-resident antimicrobials could provide new targets for selective breeding programs (i.e. marker assisted selection) to enhance the innate immune defenses of the egg for enhanced food safety.

Conflict of interest statement

The authors have no financial or commercial conflicts of interests to declare.

Acknowledgments

This work was supported by the Natural Sciences and Engineering Research Council of Canada (NSERC) and the Poultry Industry Council (PIC). We would like to thank Hamed Esmaili for excellent technical assistance and Marcel Laviolette Jr. from Laviolette Poultry Farm (St-Isidore,

Ontario) for providing us with fresh farm eggs. We would also like to thank the Proteomics platform of the Eastern Quebec Genomics Centre (Laval, QC) for their proteomic services.

References

[1] Rose ML, Hincke MH. Protein constituents of the eggshell: eggshell-specific matrix proteins. Cell Mol Life Sci 2009;66:2707–19.

[2] Dennis JM, Xiao SQ, Agarwal M, Fink DJ, Heuer AH, Caplan AI. Microstructure of matrix and mineral components of eggshells from White Leghorn Chickens (Gallus gallus). J Morphol 1996;228:287–306.

[3] Hincke MT, Chien Y-C, Gerstenfeld LC, McKee MD. Colloidal-gold immunocytochemical localization of osteopontin in avian eggshell gland and eggshell. J Histochem Cytochem 2008;56:467–76.

[4] Romanoff AL, Romanoff AJ. The avian egg. New York: John Wiley and Sons Inc.; 1949.

[5] Ruiz J, Lunam CA. Ultra structural analysis of the eggshell: contribution of the individual calcified layers and the cuticle to hatchability and egg viability in broiler breeders. Br Poult Sci 2000;41:584–92.

[6] Board RG, Halls NA. The cuticle: a barrier to liquid and particle penetration of the shell of the hen's egg. Br Poult Sci 1973;14: 69–97

[7] Board RG, Tranter HS. The Microbiology of eggs. In: Stadelman WJ, Cotterill OJ, editors. Egg Science and Technology. 3rd edition. Westport: AVI Publishing Company, Inc.;1986.

[8] Sparks NHC, Board RG. Cuticle, shell porosity and water intake through hen's eggshells. Br Poult Sci 1984;25:267–76.

[9] Mayes FJ, Takeballi MA. Microbial contamination of the hen's egg: a review. J Food Prot 1983;46:1092–8.

[10] Schroeder CM, Naugle AL, Schlosser WD, Hogue AT, Angulo FJ, Rose JS, et al. Estimate of illnesses from Salmonella enteritidis in eggs, United States, 2000. Emerg Infect Dis 2005;11:113–5.

[11] Shevchenko A, Jensen ON, Podtelejnikov AV, Sagliocco F, Wilm M, Vorm O, et al. Linking genome and proteome by mass spectrometry: large-scale identification of yeast proteins from two dimensional gels. Proc Natl Acad Sci U S A 1996;93:14440–5.

[12] Havlis J, Thomas H, Sebela M, Shevchenko A. Fast-response proteomics by accelerated in-gel digestion of proteins. Anal Chem 2003;75:1300–6.

[13] Keller A, Nesvizhskii AI, Kolker E, Aebersold R. Empirical statistical model to estimate the accuracy of peptide identifications made by MS/MS and database search. Anal Chem 2002;74:5383–92.

[14] Nesvizhskii AI, Keller A, Kolker E, Aebersold R. A statistical model for identifying proteins by tandem mass spectrometry. Anal Chem 2003;75:4646–58.

[15] Ishihama Y, Oda Y, Tabata T, Sato T, Nagasu T, Rappsilber J, et al. Exponentially modified protein abundance index (emPAI) for estimation of absolute protein amount in proteomics by the number of sequenced peptides per protein. Mol Cell Proteomics 2005;4:1265–72.

[16] Huang DW, Sherman BT, Lempicki RA. Systematic and integrative analysis of large gene lists using DAVID Bioinformatics Resources. Nat Protoc 2009;4:44–57.

[17] Knape KD, Chavez C, Burgess RP, Coufal CD, Carey JB. Comparison of Eggshell Surface Microbial Populations for In-Line and Off-Line Commercial Egg Processing Facilities. Poult Sci 2002;81:695–8.

[18] Mann K, Macek B, Olsen JV. Proteomic analysis of the acid-soluble organic matrix of the chicken calcified eggshell layer. Proteomics 2006;6:3801–10.

[19] Miksik I, Sedlakova P, Lacinova K, Pataridsi S, Eckhardt A. Determination of insoluble avian eggshell matrix proteins. Anal Bioanal Chem 2010;397:205–14.

[20] Farinazzo A, Restuccia U, Bachi A, Guerrier L, Fortis F, Boschetti E, et al. Chicken egg yolk cytoplasmic proteome, mined via combinatorial peptide ligand libraries. J Chromatogr A 2009;1216:1241–52.

[21] Mann K, Mann M. The chicken egg yolk plasma and granules proteome. Proteomics 2008;8:178–91.

[22] Mann K. Proteomic analysis of the chicken egg vitelline membrane. Proteomics 2008;8:2322–32.

[23] D'Ambrosio C, Arena S, Scaloni A, Guerrier L, Boschetti E, Mendieta ME, et al. Exploring the chicken egg white proteome with combinatorial peptide ligand libraries. J Proteome Res 2008;7:3461-74

[24] Mann K, Mann M. In-depth analysis of the chicken egg white proteome using an LTQ Orbitrap Velos. Proteome Sci 2011;9:7.

[25] Mann K. The chicken egg white proteome. Proteomics 2007;7:3558–68.

[26] Guerin-Dubiard C, Pasco M, Molle D, Desert C, Croquennec T, Nau F. Proteomic analysis of hen egg white. J Agric Food Chem 2006;54:3901–10.

[27] Stammer K, Edassery SL, Barua A, Bitterman P, Bahr JM, Hales DB, et al. Selenium-Binding Protein 1 expression in ovaries and ovarian tumors in the laying hen, a spontaneous model of human ovarian cancer. Gynecol Oncol 2008;109:115-21.

[28] Yang J, Huang K, Qin S, Wu X, Zhao Z, Chen F. Antibacterial action of selenium-enriched probiotics against pathogenic Escherichia coli. Dig Dis Sci 2009;54:246–54.

[29] Tran PA, Webster TJ. Selenium nanoparticles inhibit Staphylococcus aureus growth. Int J Nanomedicine 2011;6:1553–8.

[30] Allen RC, Stephens Jr JT. Myeloperoxidase selectively binds and selectively kills microbes. Infect Immun 2011;79:474–85.

[31] Adams JC, Tucker RP. The thrombospondin type 1 repeat (TSR) superfamily: diverse proteins with related roles in neuronal development. Dev Dyn 2000;218:280–99.

[32] Gautron J, Nys Y. Eggshell matrix proteins. Bioactive egg compounds. Germany: Springer-Verlag; 2007.

[33] Lima CA, Torquato RJ, Sasaki SD, Justo GZ, Tanaka AL. Biochemical characterization of a Kunitz type inhibitor similar to dendrotoxins produced by Rhipicephalus (Boophilus) microplus (Acari: Ixodidae) hematocytes. Vet Parasitol 2010;167:279–87.

[34] Pellegrini A, Thomas U, von-Fellenberg R, Wild P. Bactericidial activities of lysozyme and aprotinin against gram-negative and gram positive bacteria related to their basic character. J Appl Bacteriol 1992;72:180-7.

[35] Travis J, Potempa J. Bacterial proteinases as targets for the development of second-generation antibiotics. Biochim Biophys Acta 2000;1477:35–50.

[36] Gautron J, Hincke MT, Mann K, Panheleux M, Bain M, McKee MD, et al. Ovocalyxin-32, a novel chicken eggshell matrix protein. Isolation, amino acid sequencing, cloning, and immunocytochemical localization. J Biol Chem 2001;276: 39243–52.

[37] Dominguez-Vera JM, Gautron J, Garcia-Ruiz J, Nys Y. The effect of avian uterine fluid on the growth behavior of calcite crystals. Poult Sci 2000;79:901–7.

[38] Xing J,Wellman-Labadie O, Gautron J, Hincke MT. Recombinant eggshell ovocalyxin-32: expression, purification and biological activity of the glutathione S-transferase fusion protein. Comp Biochem Physiol B Biochem Mol Biol 2007;147:172–7.

[39] Gautron J, Murayama E, Vignal A, Morisson M, McKee MD, Rehault S, et al. Cloning of ovocalyxin-36, a novel chicken eggshell protein related to lipopolysaccharide-binding proteins, and plunc family proteins. J Biol Chem 2007;282:5273-86.

[40] Hincke MT, Gautron J, Panheleux M, Garcia-Ruiz MD, McKee MD, Nys Y. Identification and localization of lysozyme as a component of the eggshell membranes and shell matrix. Matrix Biol 2000;19:443–53.

[41] Gautron J, Hincke MT, Dominguez-Vera JM, Garcia-Ruiz MD, Nys Y. Ovotransferrin is a matrix protein of the hen eggshell membranes and basal calcified layer. Connect Tissue Res 2001;42:255–67.

[42] Vadehra DV, Baker RC, Naylor HB. Distribution of lysozyme activity in the exteriors of eggs from Gallus gallus. Comp Biochem Physiol B 1972;43:503–8.

[43] Pellegrini A, Hulsmeier AJ, Hunziker P, Thomas U. Proteolytic fragments of ovalbumin display antimicrobial activity. Biochim Biophys Acta 2004;1672:76–85

[44] Begum S, Saito A, Xu X, Kato A. Improved functional properties of the ovoinhibitor by conjugating with galactomannan. Biosci Biotechnol Biochem 2003;67:1897–902.

[45] Kolaczkowska A, Kolaczkowska M, Sokolowska A, Miecznikowska H, Kubiak A, Rolka K, et al. The antifungal properties of chicken egg cystatin against Candida yeast isolates showing different levels of azole resistance. Mycoses 2010;53:314–20.

[46] Mann K, Gautron J, Nys Y, Mckee MD, Bajari T, Schneider WJ, et al. Disulfide-linked heterodimeric clusterin is a component of the chicken eggshell matrix and egg white. Matrix Biol 2003;22:397–407.

[47] Wellman-Labadie O, Picman J, Hincke MT. Antimicrobial activity of the Anseriform outer eggshell and cuticle. Comp Biochem Physiol B Biochem Mol Biol 2008;149:640–9.

[48] Wellman-Labadie O, Lemaire S, Mann K, Picman J, Hincke MT. Antimicrobial activity of lipophilic avian eggshell surface extracts. J Agric Food Chem 2010;58:10156–61.

[49] Stadelman WJ, Cotterill OJ. Egg science and technology. New York: Food Products Press; 1995.

[50] Kim KW, Daeschel M, Zhao Y. Edible coatings for enhancing microbial safety and extending shelf life of hard-boiled eggs. J Food Sci 2008;73:M227–35.

[51] Biladeau AM, Keener KM. The effects of edible coatings on chicken egg quality under refrigerated storage. Poult Sci 2009;88:1266–74.

[52] Bain MM, MacLeod N, Thomson R, Hancock JW. Microcracks in eggs. Poult Sci 2006;85:2001–8.

Supplementary Data

Fig S1 Spectra corresponding to the peptides that are exclusive to a single ovocalyxin-32 isoform (Table 3).

A) UNIPROT ID: D3KYT5

Peptide sequence KSPPVVHAK:

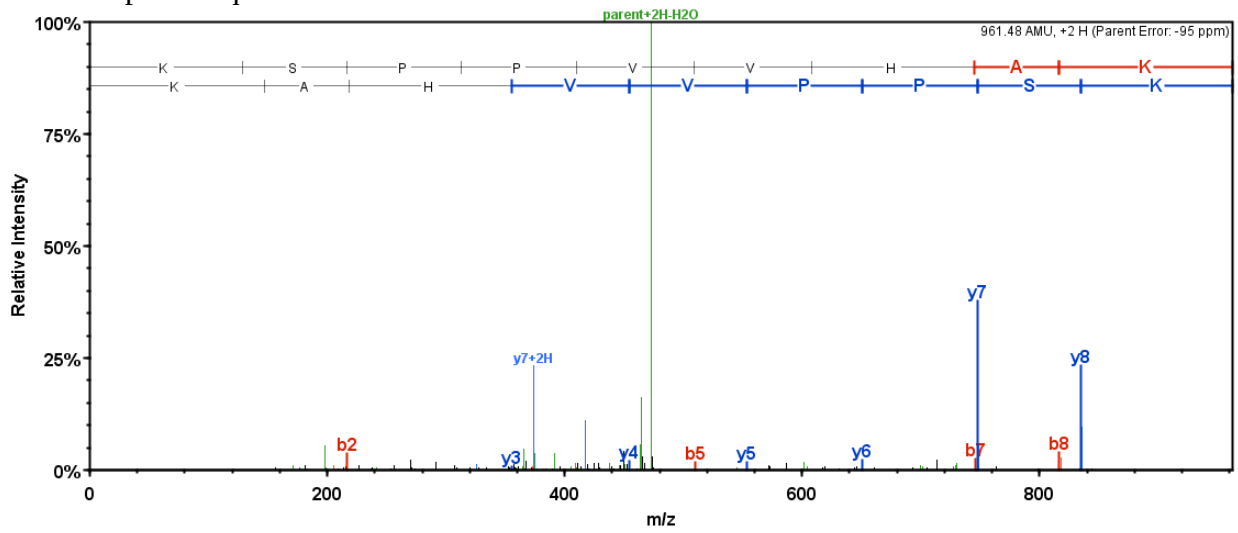

Peptide sequence SPPVVHAK:

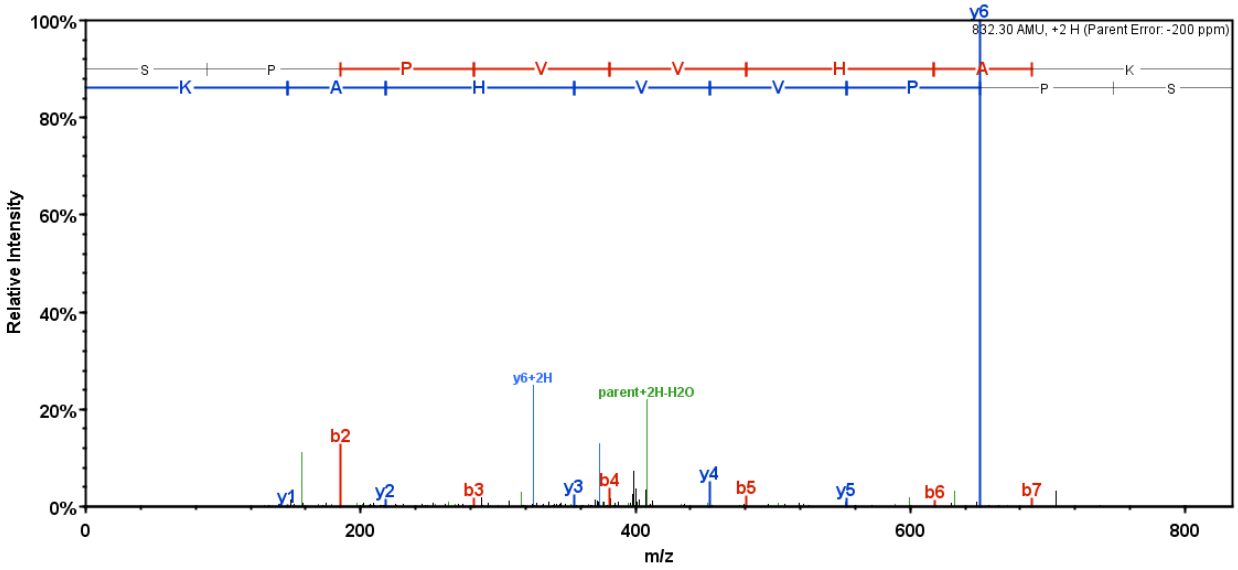

Peptide sequence SPPVVHAKCVHAQNK:

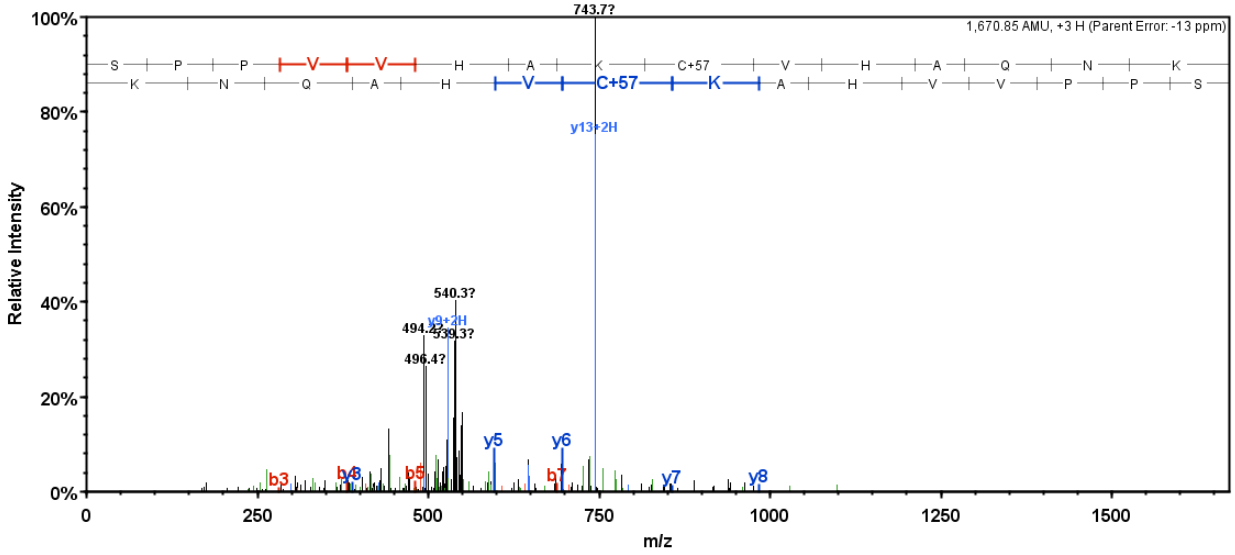

B) UNIPROT ID: C7G540

Peptide sequence FIVLLHEIPTQQMNVCHMYLVWTLGHPIR:

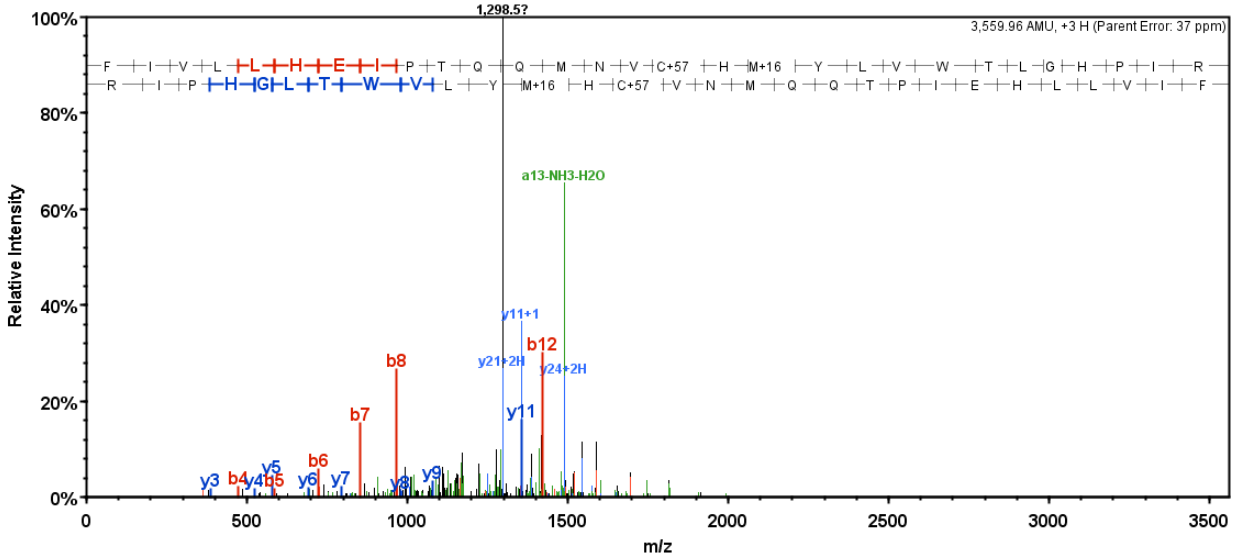

C) UNIPROT ID: C7G541

Peptide sequence GSSHIMWKQSTEHTGYLLAQVSSVK:

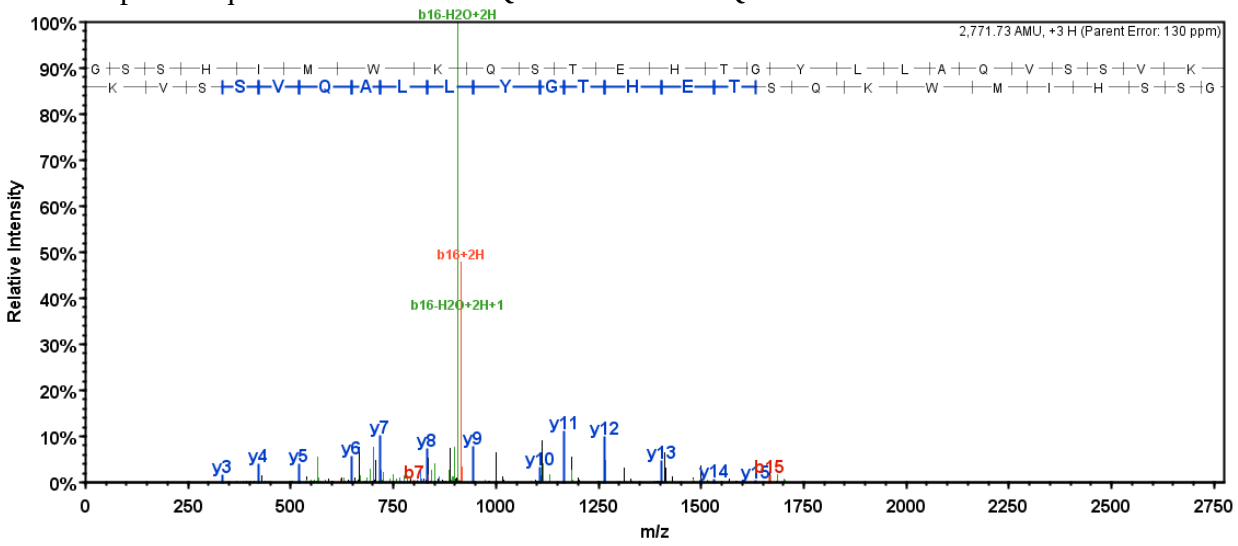

Peptide sequence KPITANYIPDSHGNIAHDHLQLWGLAIVGSSHIMWK:

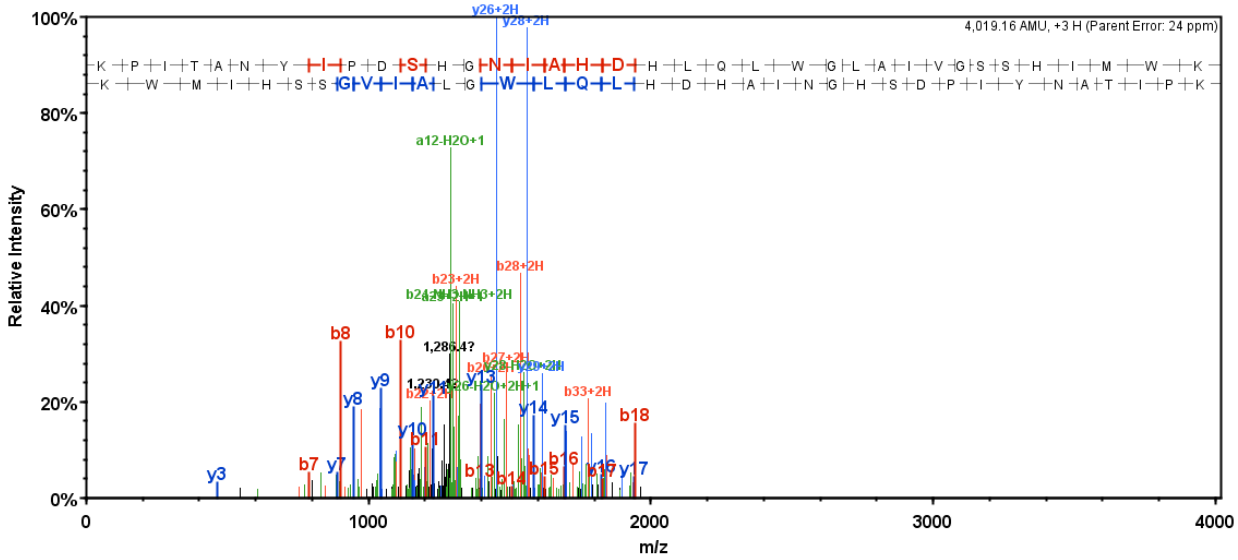

D) UNIPROT ID: C7G542

Peptide sequence FIVLLHEIPTQQMNVCHMYLVWR:

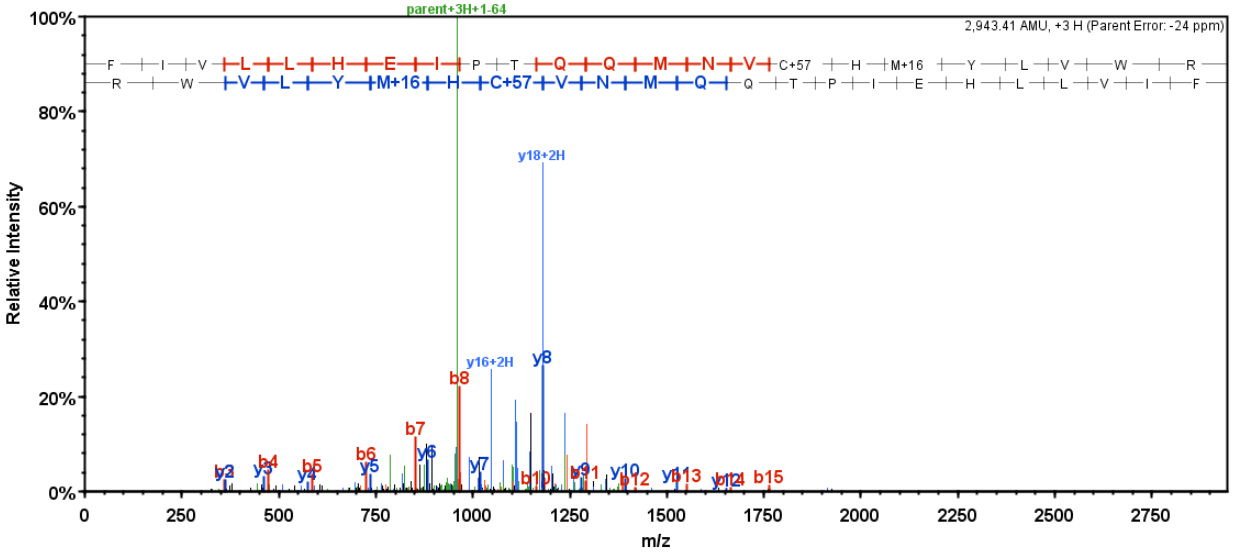

Table S1: Peptide sequences corresponding to the 47 identified peptides in the cuticle extract and the charge state of the corresponding spectra.

Identified Proteins[a]	NCBI or UniProt ID	Peptide Sequence[b]	# of +1H spectra	# of +2H spectra	# of +3H spectra
predicted: similar to Kunitz-like protease inhibitor	XP_001235178.2	APAEETAR	119	451	0
		CPFRCPQPVPARPDTYPK	0	1	14
		CPQPVPARPDTYPK	2	364	177
		CPQPVPARPDTYPKK	0	15	0
		GLEAFLLGDSNQR	0	1	0
		KKVPHIIGCCNSTCSSDTDFPNHLR	0	0	3
		KRTYCYACIPALR	0	5	2
		KVPHIIGCCNSTCSSDTDFPNHLR	0	0	1
		QPVLLGLPLSGLPGALPHR	0	1	1
		RTYCYACIPALR	0	21	2
		SCRVFVHSSCGGNANNFR	0	2	32
		SSCGGNANNFR	0	1	0
		SVLPEKDDFHPR	5	291	246
		SVLPEKDDFHPRTDTDPTTNCVNNCR	0	0	1
		TDGRSVLPEKDDFHPR	0	0	2
		TDTDPTTNCVNNCR	0	85	0
		TDTDPTTNCVNNCRDDGNCR	0	0	165
		TLAECQQVCQ	0	1	0
		TLAECQQVCQHGESWAR	0	0	1
		TYCYACIPALR	10	104	0
		VFVHSSCGGNANNF	0	1	0
		VFVHSSCGGNANNFR	6	1285	1258
		VPHIIGCCNSTCSSDTDFPNHLR	0	1	5
Ovocalyxin-32	BAI77469.1	AQVSSVKQQIR	0	1	0
		CVHAQNKK	0	33	0
		DNAVAFK	310	0	0
		EASPSRPLALHK	0	1	0
		EAVWAAWTALHYINSHEASPSR	0	0	11
		EAVWAAWTALHYINSHEASPSRPLAL	0	0	1
		EAVWAAWTALHYINSHEASPSRPLALHK	0	3	38
		EAVWAAWTALHYINSHEASPSRPLALHKVVK	0	0	1
		ERLPWPQVPGVMRPLNPSHR	0	0	1
		FIVLLHEIPTQQLNV	0	1	0
		FIVLLHEIPTQQLNVCHMYLVWTLGHPIR	0	0	7
		FYEYLQHQK	18	718	44
		FYEYLQHQKK	0	2	0
		KDNAVAFK	5	496	0
		KDNAVAFKFIVLLHEIPTQQLNVCHMYLVWTLGHPIR	0	0	1
		KPITANYIPDSH	0	3	0
		KPITANYIPDSHGNIAHD	0	0	3
		KQIQEEDHR	0	17	0
		KQIQEEDHRFYEYLQHQK	0	3	8
		KSPPVVHAK	0	64	0
		PLNPSHR	0	1	0
		QIQEEDHR	0	118	0
		QIQEEDHRFYEYLQHQK	0	22	30
		QQIRKDNAVAFK	0	3	0
		QSTEHTGYLLAQVSSVK	11	213	257
		QSTEHTGYLLAQVSSVKQQIR	0	10	39
		QSTEHTGYLLAQVSSVKQQIRK	0	1	8
		SPPVVHAK	21	521	0
		SPPVVHAKCVHAQNK	0	0	1
		YSCAPDNHGLEDGSGQDSGSAAGTSHETK	0	0	2
		YYVHCTTEGYIHGENAGSCFATVLYLK	0	0	5
		YYVHCTTEGYIHGENAGSCFATVLYLKK	0	0	6

	BAI23347.1	AQVSSVKQQIR	0	1	0
		CVHAQNKK	0	33	0
		DNAVAFK	310	0	0
		EASPSRPLALHK	0	1	0
		EAVWAAWTALHYINSHEASPSR	0	0	11
		EAVWAAWTALHYINSHEASPSRPLAL	0	0	1
		EAVWAAWTALHYINSHEASPSRPLALHK	0	3	38
		EAVWAAWTALHYINSHEASPSRPLALHKVVK	0	0	1
		ERLPWPQVPGVMHPLNPSHR	0	0	2
		FIVLLHEIPTQQLNV	0	1	0
		FIVLLHEIPTQQLNVCHMYLVWTLGHPIR	0	0	7
		FYEYLQHQK	18	718	44
		FYEYLQHQKK	0	2	0
		GSSHIMWKQSTEHTGYLLAQVSSVK	0	0	1
		KDNAVAFK	5	496	0
		KDNAVAFKFIVLLHEIPTQQLNVCHMYLVWTL GHPIR	0	0	1
		KPITANYIPDSH	0	3	0
		KPITANYIPDSHGNIAHD	0	0	3
		KPITANYIPDSHGNIAHDHLQLWGLAIVGSSHI MWK	0	0	3
		KQIQEEDHR	0	17	0
		KQIQEEDHRFYEYLQHQK	0	3	8
		KSPPVVHGK	0	1	0
		LPWPQVPGVMHPLNPSHR	0	5	30
		PQVPGVMHPLNPSHR	0	1	0
		QIQEEDHR	0	118	0
		QIQEEDHRFYEYLQHQK	0	22	30
		QQIRKDNAVAFK	0	3	0
		QSTEHTGYLLAQVSSVK	11	213	257
		QSTEHTGYLLAQVSSVKQQIR	0	10	39
		QSTEHTGYLLAQVSSVKQQIRK	0	1	8
		SPPVVHGK	0	21	0
		YSCAPDNHGLEDGSGQDSGSAAGTSHETK	0	0	2
		YYVHCTTEGYIHGENAGSCFATVLYLK	0	0	5
		YYVHCTTEGYIHGENAGSCFATVLYLKK	0	0	6
Ovalbumin	P01012.2	ADHPFLFCIK	0	9	2
		AFKDEDTQAMPFR	0	35	18
		DILNQITKPNDVYSFSLASR	0	4	7
		ELINSWVESQTNGIIR	0	14	1
		ELYRGGLEPINFQTAADQAR	0	7	12
		GGLEPINFQTAADQAR	4	92	6
		HIATNAVLFFGR	1	49	6
		IKVYLPR	0	2	0
		ISQAVHAAHAEINEAGR	0	63	77
		LTEWTSSNVMEER	0	39	0
		LTEWTSSNVMEERK	0	3	0
		LYAEERYPILPEYLQCVK	0	19	25
		LYAEERYPILPEYLQCVKELYR	0	0	4
		NVLQPSSVDSQTAMVLVNAIVFK	0	19	13
		TAMVLVNAIVFK	0	1	0
		VHHANENIFYCPIAIMSALAMVYLGAK	0	0	1
		VTEQESKPVQMMYQIGLFR	0	13	27
		YPILPEYLQCVK	0	12	0

Ovotransferrin	P02789	AIANNEADAISLDGGQVFEAGLAPYK	0	1	0
		DDNKVEDIWSFLSK	0	3	0
		DLLFKDLTK	0	2	0
		DLLFKDSAIMLK	0	3	0
		DPVLKDLLFK	0	3	0
		DPVLKDLLFKDSAIMLK	0	0	2
		ECNLAEVPTHAVVVRPEK	0	1	0
		EFLGDKFYTVISSLK	0	2	0
		EGTTYKEFLGDKFYTVISSLK	0	1	4
		FFSASCVPGATIEQK	0	10	0
		GAIEWEGIESGSVEQAVAK	0	4	0
		GTEFTVNDLQGK	0	10	0
		KDPVLKDLLFK	0	0	2
		KDSNVNWNNLK	0	2	0
		KGTEFTVNDLQGK	0	9	1
		LKPIAAEVYEHTEGSTTSYYAVAVVK	0	0	1
		NAPYSGYSGAFHCLK	0	3	0
		SAGWNIPIGTLIHR	0	6	1
		SDFHLFGPPGK	0	1	0
		TCNPSDILQMCSFLEGK	0	2	0
		TDERPASYFAVAVAR	0	5	3
		VAAHAVVAR	0	11	0
		VAAHAVVARDDNKVEDIWSFLSK	0	0	3
		YFGYTGALR	0	1	0
Ovoinhibitor precursor	NP_001025783.1	CFFCNAYVQSNR	0	5	0
		CREEVPELDCSK	0	4	0
		CRQEIPEIDCDQYPTR	0	1	0
		CRQEIPEIDCDQYPTRK	0	1	3
		DGNTMVACPR	0	20	0
		DGTSWVACPR	0	3	0
		EHGANVEKEYDGECRPK	0	2	1
		HVMIDCSPYLQVVR	0	15	1
		ILLPVCGTDGFTYDNECGICAHNAQHGTEVKK	0	0	1
		ILSPVCGTDGFTYDNECGICAHNAEQR	0	0	5
		LEIGSVDCSKYPSTVSK	0	3	0
		LEIGSVDCSKYPSTVSKDGR	0	0	1
		LHDGECKLEIGSVDCSK	0	1	0
		LHDGECKLEIGSVDCSKYPSTVSK	0	0	2
		NLKPVCGTDGSTYSNECGICLYNR	0	0	1
		QEIPEIDCDQYPTR	0	3	0
		QEIPEIDCDQYPTRK	0	1	0
		VSPICTMEYVPHCGSDGVTYSNR	0	0	13
Lysozyme C	P00698	CKGTDVQAWIR	0	9	0
		FESNFNTQATNR	0	25	0
		GTDVQAWIR	0	10	0
		GYSLGNWVCAAK	0	8	0
		HGLDNYR	0	1	0
		HGLDNYRGYSLGNWVCAAK	0	0	1
		IVSDGNGMNAWVAWR	0	7	0
		KIVSDGNGMNAWVAWR	0	2	0
		NTDGSTDYGILQINSR	0	18	0
Serum albumin precursor	NP_990592.1	AVAMITFAQYLQR	0	4	0
		CVANEDAPECSKPLPSIILDEICQVEK	0	0	2
		KMPQVPTDLLLETGK	0	1	0
		KMPQVPTDLLLETGKK	0	0	4
		LLINLIK	0	5	0
		LLINLIKR	0	3	0
		LVKDVVDLAQK	0	11	0
		MMSNLCSQQDVFSGK	0	1	0
		MPQVPTDLLLETGKK	0	0	1
		QLIYLSQKYPK	0	17	0
		RHPEFSIQLIMR	0	0	7
		RPCFTAMGVDTK	0	2	0
		TIADGFTAMVDK	0	1	0
		VSFLGHFIYSVAR	0	3	0
		VSQPDFVQPYQR	0	2	0
		YNDLKEETFK	0	1	0

predicted: selenium-binding protein 1-like	XP_423396.3	DVSGWILPK	0	1	0
		ETGIDQPDFLATIDLNPR	0	2	0
		GFNPDDLKK	0	3	0
		GGPVTVCRDEELK	0	1	0
		HNVLISTAGMVPR	0	16	2
		IQLSVDGKR	0	2	0
		IYVVDVGTQCR	0	9	0
		IYVVDVGTQCRAPTVCK	0	0	2
		LILPCLISSR	0	2	0
		LILPGLISSR	0	4	0
		LVGQVFVGGSILR	0	7	0
		MIEPVDVFWK	0	4	0
		RLNVWNLSCR	0	2	0
		TLTQCFDLGEDSLPLSVK	0	2	0
Vitellogenin-2 precursor	NP_001026447.1	AVRLPLSLPVGPR	0	6	0
		DASFIQNTYLHK	0	1	0
		ELPTETPLVSAYLK	0	1	0
		FLEVVQLCR	0	3	0
		IANADNLESIWR	0	5	0
		ILGQEVAFININK	0	2	0
		ILGQEVAFININKELLQQVMK	0	0	1
		IQKNPVLQQVACLGYSSVVNR	0	0	2
		LPLSLPVGPR	0	6	0
		LSQLLESTMQIR	0	6	0
		QQLTLVEVR	0	1	0
		QSDSGTLITDVSSR	0	3	0
		TMFPSAIISK	0	2	0
		VEGLADVIMK	0	1	0
		VGATGEIFVVNSPR	0	5	0
		WLLSAVSASGTTETLK	0	3	0
		YRFPAVLPQMPLQLIK	0	1	1
Ovocalyxin-36 precursor	NP_001026032.1	AMQQVLSDAIIQTGLLEK	0	15	8
		DSITDLYPTGCTSCPAASPLSIR	0	2	0
		GLLSSPTIITGLHLER	0	7	0
		HLQGMALPNIMSDR	0	2	0
		LLVEIYLPR	0	3	0
Glutathione peroxidase 3 precursor	NP_001156704.1	ANIATVKNDIIAYMR	0	2	2
		FLVGTDGVPVMR	0	5	0
		NDIIAYMR	0	1	0
		NSCPPVAEEFGNPK	0	3	0
		QEPGQNSEILPALK	0	6	0
		YVRPGGGFVPNFQLFQK	0	4	4
		YVRPGGGFVPNFQLFQKGDVNGAK	0	0	1
predicted: prostate stem cell antigen	XP_418414.2	GCEASCQEDYQDFKVGNR	0	0	1
		VIGFFSIISK	3	18	0
predicted: myeloperoxidase	XP_415716.2	FGHTSVQPFVSR	0	1	0
		IIMEGGIDPLIR	0	4	0
		LYNAFPLPLVR	0	2	0
		VGPLLACIIGTQFR	0	12	0
		WLPAAYEDGVSVPR	0	2	0
β-hexosaminidase subunit alpha precursor	NP_001025561.1	ALIFSAAR	1	0	0
		ALIFSAARPAENK	0	1	0
		ALIFSAARPAENKQPWR	0	1	1
		ALLSAPWYLNR	0	3	0
		GLETFSQLVGR	0	1	0
		GYMVWQEVFDNGVK	0	2	0
		LLDIVSSLGK	1	2	0
		NLQDAYVR	0	1	0
		SNPEILAFMK	0	1	0
		SNPEILAFMKK	0	1	0
		VRPDTIIHVWK	0	1	0
Chain A, structure of an avian IgY-Fc 3-4 fragment	2W59_A	AVPATEFVTTAVLPEER	0	5	0
		FTCTVQHEELPLPLSK	0	1	0
		NTGPTTPPLIYPFAPHPEELSLSR	0	0	1
		TANGAGGDGDTFFVYSK	0	3	0
		VTLSCLVR	0	6	0

predicted: gastrokine-2	XP_417666.1	IDEASIPELQEIGR	0	2	0
		SGLYSSDTIFDYQHGYIATR	0	0	6
		VMWVQFQSGNAMFGSIR	0	2	0
		YGRPIEQLCK	0	5	0
Ovalbumin-related protein Y	NP_001026172.1	KFYTGGVEEVNFK	0	1	1
		TFSVLPEYLSCAR	0	1	0
		YNPTNAILFFGR	0	10	0
Apolipoprotein B precursor	NP_001038098.1	FALSGIVTPGAK	0	1	0
		FTTPEFTVLNSFK	0	1	0
		GAILSTLQAVQNYLK	0	1	0
		GFEPTLEALFGEK	0	1	0
		IPEIIAQAISK	0	2	0
		IQIQNIDIR	0	1	0
		ISEVTLTGQIR	0	1	0
		LSGLQELNIQK	0	1	0
		NSFLINIPLPFGGR	0	1	0
		TEEIPPLIENR	0	1	0
		TPDFIVPLTDLK	0	1	0
predicted: mucin-5B	XP_421033.3	AAGYDLCSQPQDIR	0	6	0
		CSLDVGLECR	0	1	0
		GQDGEVPFTVR	0	1	0
		LKCSLDVGLECR	0	1	0
		SLQSLDQKLK	0	3	0
Hemoglobin subunit β	NP_990820.1	FFASFGNLSSPTAILGNPMVR	0	3	0
		LLIVYPWTQR	0	5	0
		VNVAECGAEALAR	0	4	0
Similar to ovomacroglobulin, ovostatin, partial	XP_423478.3	AVDQSVFLLQPER	0	1	0
		GTTVSEPVLLSLPR	0	4	0
		ITAAGVVNTVR	0	5	0
Cystatin precursor	NP_990831.2	ALQFAMAEYNR	0	5	0
		LLGAPVPVDENDEGLQR	0	3	0
		YILQVEIGR	0	1	0
predicted: similar to SDF3	XP_001234865.1	IAQLPLTEGVSAMFFLPTK	0	1	0
		LAAAVSNFGYDLYR	0	1	0
		LKLNYEEALGNTVK	0	1	0
		LNYEEALGNTVKETR	0	1	0
		LQSLFTSPDFTK	0	2	0
		TVHAVLSLPK	0	1	0
Actin, cytoplasmic 1/2/5	P53478, P60706, Q5ZMQ2	GYSFTTTAER	0	1	0
		SYELPDGQVITIGNER	0	3	0
		TTGIVMDSGDGVTHTVPIYEGYALPHAILR	0	0	1
		VAPEEHPVLLTEAPLNPK	0	3	0
Nucleobindin-2 precursor	NP_001006468.1	ELDLVSHHVR	0	2	0
		KLQQANPPAGPAGELK	0	1	0
		LQTADIEEIKSGK	0	1	0
		LVTLEEFLR	0	4	0
Polymeric immunoglobulin receptor precursor	NP_001038109.1	IIDNTGFLPGPYEGR	0	6	0
		SCLTVVSTSGYR	0	2	0
predicted: similar to α-2-plasmin	XP_415807.2	EVPTTVKIPK	0	1	0
		LAGATLSLASR	0	5	0
		RLAGATLSLASR	0	1	0
Hemoglobin subunit subunit α-A	NP_001004376.1	KVVAALIEAANHIDDIAGTLSK	0	1	1
		VVAALIEAANHIDDIAGTLSK	0	1	3
Vitellogenin-1	NP_001004408.1	ACADAVILPLK	0	1	0
		ALLLSEIR	0	1	0
		SNIEEVLLALK	0	2	0
		YLLDLLPAAASHR	0	1	1

Clusterin precursor	NP_990231.1	ELHPFLQHPVHGFHR	0	1	1
		EQFEDALR	0	1	0
		RFEDLEER	0	1	0
		YIDTEVENAINGVK	0	1	0
predicted: leucine-rich repeat-containing protein 19	XP_422399.1	GLENLQTLLLR	0	1	0
		GTLLTHFPSLR	0	1	0
		SLLHAPSSLPR	0	1	0
		SNSLQELEVPFFLPLR	0	2	0
Tubulin β-3 chain	P09206.1	AVLVDLEPGTMDSVR	0	1	0
		GHYTEGAELVDSVLDVVR	0	1	0
		LHFFMPGFAPLTSR	0	3	0
Aminopeptidase N	NP_990192.1	AQIIDDAFNLAR	0	1	0
		FLEAPVVSEADKLR	0	2	0
		TGPILSFFER	0	2	0
proactivator polypeptide precursor (saposin A-D precursor)	NP_990142.1	LVTDVQEAVR	0	2	0
		SVPLQTLVPAQVVHEVK	0	2	0
Apolipoprotein A-IV precursor	NP_990269.1	ALEPFATELREK	0	1	0
		ETVDQLQQAEITK	0	1	0
		GLSPYAQEVQDGLNR	0	1	0
		LAPLAQQLDER	0	1	0
Ovocleidin-116	AAF00982.3	GNCPGQHQILLK	0	1	0
		GVVGGMVVPEGHR	0	1	0
		LGQAARPEVAPAPSTGGR	0	2	0
Epithelial cell adhesion molecule precursor	NP_001012582.1	DVKDDSIFLNNK	0	1	0
		KTPLNAESLTR	0	1	0
		TPLNAESLTR	0	1	0
		YLKDTITSR	0	1	0
predicted: torsin-1B	XP_415473.2	AVTGFSNNPSPK	0	1	0
		NFLSQLLAR	0	1	0
		VPLYQEQLQNWIR	0	1	0
predicted: ovalbumin-related protein Y	XP_418984.3	SRPILPIYLK	0	2	0
		SVNIHLLFK	0	1	0
specific heparan sulfate proteoglycan core protein, partial	XP_427362.2	APDGLLLFSAGK	0	2	0
		VEGTALMLPAVR	0	1	0
Neuroserpin precursor	NP_001004411.1	GLGITEVFSR	0	2	0
		QEVPLVTLEPLVK	0	1	0
predicted: similar to Mesothelin	XP_414835.2	GAPSSLTTEELQVVSSLVR	0	2	0
		LLLEALACLK	0	1	0
predicted: neuronal pentraxin-2	XP_414750.3	ETVLQQKETIGSQR	0	1	0
		QKTETALNALLER	0	1	0
predicted: annexin A8	XP_421646.1	GLGTDEQAIIEVLTK	0	1	0
		GLGTDEQAIIEVLTKR	0	1	0
Tubulin α-1 chain	P02552.1	AVFVDLEPTVIDEVR	0	1	0
		LIGQIVSSITASLR	0	1	0
predicted: thrombospondin type-1 domain- containing protein 4	XP_413780.3	FYEWEPFAEVK	0	1	0
		TLTVQQYR	0	1	0
predicted: hyaluronidase-1	XP_424356.1	ALYPSIYLPQQLQGTDK	0	1	0
		VAFLQLDPNR	0	1	0

[a)] Protein identification probability was 100% for all 47 proteins.
[b)] The best peptide identification probability is 95% for all listed peptides.

Table S2: Peptides exclusive to one of four identified ovocalyxin-32 isoforms and associated Mascot and Tandem –log(e) scores.

Excl. to NCBI acc. #	Peptide Sequence	Best Peptide Iden. Prob. (%)	Best Mascot Ion Score	Best Mascot Identity Score	Best X! Tandem – log(e) Score	NTT[a]	Peptide Charge
BAI77469.1	(K)KSPPVVHAK(C)	95	52.07	40.73	1.85	2	2
	(K)SPPVVHAK(C)	95	57.59	40.99	2.92	2	2
	(K)SPPVVHAKcVHAQNK(K)	95	8.19	39.45	1.92	2	3
BAI23347.1	(V)GSSHIMWKQSTEHTGYLLAQVSSVK(Q)	95			2.96	1	3
	(K)KPITANYIPDSHGNIAHDHLQLWGLAIVGSSHIMWK(Q)	95	87.59	35.16	8.89	2	3
BAI23346.1	(-)IVLLHEIPTQQMNVcHMYLVWTLGHPIR(-)	95	24.97	36.06	4.40	2	3
BAI23348.1	(-)FIVLLHEIPTQQMNVcHMYLVWR(-)	95	71.75	37.31	8.60	2	3

[a] NTT: number of expected enzymatic termini

Chapter 3

“Novel Identification of Matrix Proteins Involved in Calcitic Biomineralization.”

Rose-Martel M, Smiley S and Hincke MT (2015) *Journal of Proteomics*, 116:81-96

The literature review in Chapter 1 emphasizes the role of eggshell-specific matrix proteins in biomineralization. The key proteins and their precise roles in the initial stages of shell formation is currently unknown. This chapter presents results from a cross-analysis of proteomics data derived from two mineralized models: fertilized and unfertilized chicken eggshells, which identified proteins associated with the mammillary cones that are the sites of initiation of eggshell formation. The biomechanical integrity of the entire eggshell is influenced by the size and spacing of these mammillary cones. Shell integrity is essential for food safety since cracked eggs are more susceptible to bacterial contamination.

Avian eggshell formation is an excellent model to study calcitic biomineralization since it is the fastest known biomineralization process. We hypothesize that proteins localized in the mammillary cones regulate the earliest stages of eggshell formation. Calcitic biomineralization by calcium carbonate is an important process in the formation of otoconia, which are gravity receptor organs located in the inner ear and are responsible for balance and for sensing linear acceleration. Deficiencies in the regulation of their biomineralization can lead to otoconia degeneration and eventually benign paroxysmal position vertigo (BPPV), which is the main cause of vertigo in humans. The human homologs of the proteins identified in this study are therefore potential candidates to play a role in otoconia formation.

Author contributions:

Proteins from shell membranes and mammillary cones were extracted by Sandy Smiley with the help of Megan Rose-Martel. Bioinformatics analysis, data interpretation and manuscript preparation were done by Megan Rose-Martel. Dr. Maxwell T. Hincke conceived the experimental approach and design, and supervised experiments, data analysis and manuscript preparation and revision.

Abstract

Calcitic biomineralization is essential for otoconia formation in vertebrates. This process is characterized by protein-crystal interactions that modulate crystal growth on an extracellular matrix. An excellent model for the study of calcitic biomineralization is the avian eggshell, the fastest known biomineralization process. The objective of this study is to identify and characterize matrix proteins associated with the eggshell mammillary cones, which are hypothesized to regulate the earliest stage of eggshell calcification. Mammillary cones were isolated from 2 models, fertilized and unfertilized, and the released proteins were identified by RP-nanoLC and ES-MS/MS proteomics. Proteomics analysis identified 49 proteins associated with the eggshell membrane fibres and, importantly, 18 mammillary cone-specific proteins with an additional 18 proteins identified as enriched in the mammillary cones. Among the most promising candidates for modulating protein-crystal interactions were extracellular matrix proteins, including ABI family member 3 (NESH) binding protein (ABI3BP), tiarin-like, hyaluronan and proteoglycan link protein 3 (HAPLN3), collagen alpha-1(X), collagen alpha-1(II) and fibronectin, in addition to the calcium binding proteins calumenin, EGF-like repeats and discoidin 1-like domains 3 (EDIL3), nucleobindin-2 and SPARC. In conclusion, we identified several cone-resident proteins that are candidates to regulate initiation of eggshell calcification. Further study of these proteins will determine their roles in modulating calcitic biomineralization and lead to insight into the process of otoconia formation / regeneration.

1. Introduction

Biomineralization is the process of directed mineral formation from supersaturated ion solutions, and is critical for the formation of biological hard tissues such as bone, teeth and calcified shells [1]. Calcitic biomineralization is essential for the formation of otoconia in vertebrates; these are calcium carbonate crystals located in the gravity receptor organs in the inner ear and are responsible for sensing linear acceleration and maintaining balance [2]. The formation of each otoconium is modulated by precise protein-crystal interactions between calcium carbonate and the otoconial membrane, which consists of Otolin-1, a member of the collagen X family, and five non-collagenous glycoproteins as well as keratan sulfate proteoglycan (KSPG) [2,3]. The most common cause of vertigo in humans is benign paroxysmal position vertigo (BPPV), a disease caused by the detachment of otoconia from the otolith organs [4]. This is especially common in elderly people who are prone to otoconia degeneration [5], which features mass reduction and structural damage [4]. Further studies are necessary to characterize the protein-crystal interactions that form and maintain the otoconia in order to develop strategies to slow or reverse degeneration.

Similar to otoconia formation, calcitic biomineralization leading to eggshell formation in birds occurs on the eggshell membranes, a highly cross-linked extracellular matrix containing cysteine-rich eggshell membrane proteins (CREMPs) and collagens type I, V and X [1,6,7] (Fig. 1B). Eggshell formation is one of the fastest known biomineralization processes; in chickens, complete formation represents deposition of approximately 6g of calcium carbonate over a 17-hour period within the uterus [1]. The chicken calcified eggshell is an accessible model for the study of calcitic biomineralization.

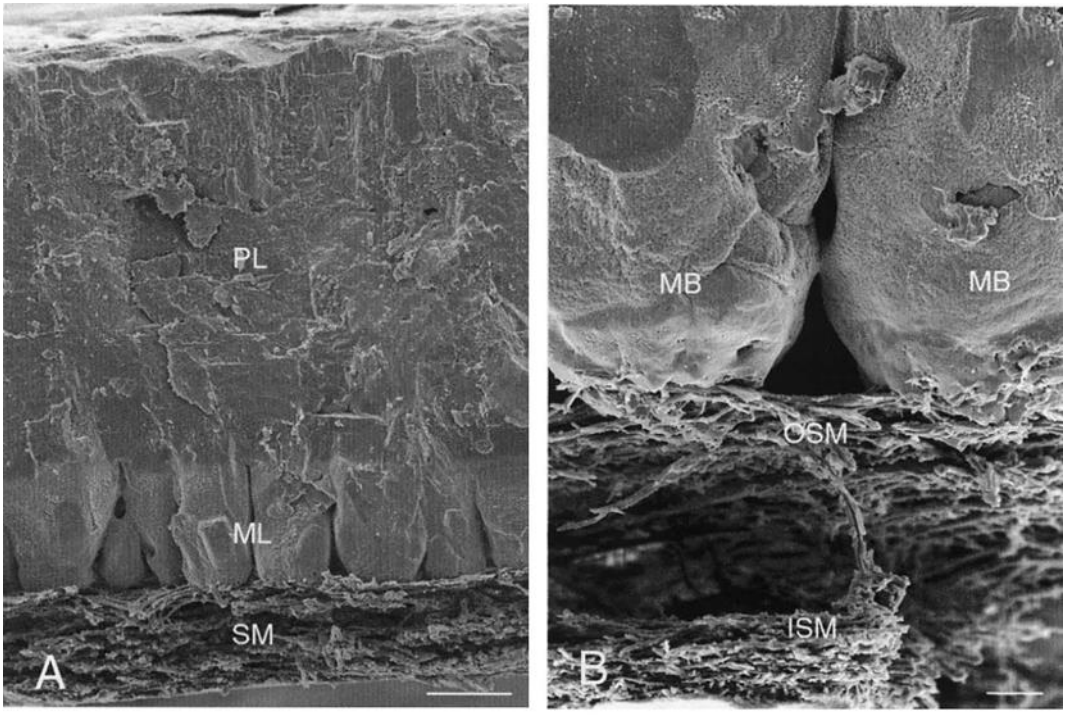

Fig. 1. Scanning electron micrographs illustrating the morphology of the eggshell and eggshell membranes. (A) Eggshell cross-fractured to reveal the shell membrane (SM), mammillary layer (ML) and palisade layer (PL). (B) Higher magnification of the membrane/mammillary body interface. Outer shell membrane fibres (OSM) insert into the tips of the mammillary bodies (MB). Inner shell membranes (ISM). Scale bars: A, 50 µm and B, 20 µm. *Reprinted from "Matrix Biology 19(5), Hincke, M.T., Gautron, J., Panheleux, M., Garcia-Ruiz, J., McKee, M.D., Nys, Y., pp. 443-53, Copyright (2000)", with permission from Elsevier.*

Egg formation occurs with highly regulated temporal and spatial control; the beginning of eggshell deposition occurs with eggshell membrane fabrication while the forming egg passes through the white isthmus segment of the oviduct. Subsequently, the incomplete egg enters the distal red isthmus region where organic aggregates are deposited in a semi-periodic array on the surface of the outer eggshell membranes. Calcium carbonate deposition begins at these nucleation sites once the forming egg moves into the uterine portion of the oviduct, where it remains for approximately 17 hours while the calcified mammillary cone (~100µm) and palisade (~300µm) layers are deposited; finally, the proteinaceous cuticle (~5-10µm) is laid down [8-10] (Fig. 1A, B). The size and spacing of the mammillary cones influence the overall strength and biomechanical properties of the completed eggshell [11].

The mammillary cones are particularly relevant to embryonic development in the fertilized egg; the calcium reserve body located at the base of each cone contains reactive microcrystals of calcite which are more susceptible to dissolution and the calcium mobilization which is necessary for embryonic growth [10,12,13].

Previous proteomics analysis has produced abundant information concerning the protein composition of the palisade and cuticle layers of the chicken eggshell, as well as preliminary data on the protein composition of the shell membranes [6,9,14-17]. However, little is known about proteins that are specifically associated with the mammillary cones; in particular, the proteins that are involved at the earliest stages of eggshell mineralization and therefore regulate calcification of the eggshell are poorly understood. In this study we specifically focussed on the protein constituents of the mammillary cones, and examined mammillary cone proteins isolated with 2 different approaches: fertilized incubated eggs and unfertilized table eggs. In the fertilized egg model, calcium resorption occurring during embryonic development results in the

dissolution of the calcium reserve body at the base of the mammillary cones, which leaves the cone tips attached to the membrane fibres. In the unfertilized egg model, cone dissolution was mimicked using acidic solutions. In each case, following dissolution of the cone base, application of mechanical traction to the membranes pulls off the adhering mammillary cones for subsequent analysis of cone-resident proteins [10]. Using a proteomics approach, we identified proteins associated with both the eggshell membranes and the mammillary cones. Eighteen proteins were identified exclusively in the mammillary cones, while another 18 proteins were enriched in the mammillary cones. Understanding the processes that initiate eggshell mineralization will lead to improved understanding of calcitic mineralization in other hard tissue models, and could lead to insight into the process of otoconia formation / regeneration in vertebrates.

2. Materials and Methods

2.1. Shell Membrane Removal from Fertilized Eggs

Freshly laid fertilized eggs from White Leghorn hens were obtained from the Animal Disease Research Institute (ADRI, Canada) and incubated obtuse end up in a humidified, rocking Petersime Incubator Model 1 (Petersime Incubator Co., Ohio, USA) at 37°C. Fertilized eggs at 15 or 19 days of development were carefully cut open using a rotary tool. The egg contents were removed and embryos were sacrificed by decapitation according to the University of Ottawa Animal Care Ethics Committee Guidelines (Animal Care Committee protocol number: CMM-129). Each half shell was washed multiple times with demineralized water, once with 1M NaCl for 5 minutes and then rinsed again with water before carefully removing the membranes by manual traction.

2.2. Shell Membrane Removal from Unfertilized Eggs

Experiments using unfertilized eggs were performed with Burnbrae Farms Super Bon-EE eggs purchased from a local grocery store. Eggs were cut in half using a rotary tool with a cutting saw attachment. Egg contents were discarded and the half shells were washed multiple times with running demineralized water, followed by washing with 1M NaCl (5 min) and then further rinsing in demineralized water. The bases of mammillary cones were selectively dissolved by incubating 20mL of 0.1N HCl in the egg halves for 0 minutes (<5 sec, quick rinse) or for 30 minutes at room temperature. Following the incubation, the egg halves were rinsed with distilled water and the membranes were carefully pulled from the shell interior.

2.3. Harvesting Mammillary Cone Proteins from Eggshell Membranes

Eggshell membranes were washed with 1M NaCl for 1 hour at room temperature followed by an overnight wash in demineralized water at 4°C, both with agitation. For each experiment, washed membranes from 3 eggs were cut into strips, pooled in equal masses and incubated in 45mL of 0.01N HCl for 20 minutes at room temperature with agitation. Water was used in lieu of 0.01N HCl for the negative control for cone dissolution. Samples were concentrated to a final volume of 500µL using Amicon Ultra Centrifugal Filter Units with a molecular weight cut-off of 3000Da (Millipore Canada Ltd., Ontario, Canada). Solutions were neutralized by adding 500µL of 1M Tris HCl, pH 8, and further concentrated to a final volume of 250µL.

2.4. Light Microscopy

The presence or absence of mammillary cones associated with the extracted shell membranes was confirmed using light microscopy. Pieces of eggshell membranes, approximately $1cm^2$, were stained with 0.1% toluidine blue for 90 seconds and then rinsed with water to remove excess stain. Membranes were observed using the Olympus CX41 System Microscope (Olympus America Inc., New York, USA) at 10X magnification and images were captured with a Q-color 3 digital camera and Q-capture software (Olympus America Inc., New York, USA). The same procedure was used to confirm whether the mammillary cones on membranes treated with 0.01N HCl were completely dissolved.

2.5. Sample Preparation

Protein concentration of each sample was determined using a bicinchoninic acid (BCA) assay (Thermo Scientific, Illinois, USA). Samples were resolved by SDS-PAGE using a NuPAGE 4-12% BisTris gel (Life technologies, California, USA) and protein bands were visualized by staining with 0.25% Coomassie Brilliant Blue R-250 (Amresco, Ohio, USA). Bands were sectioned and sent to the Proteomics Platform of the Quebec Genomics Center (Quebec, Canada) for proteomics analysis.

2.6. Protein Identification by Proteomics

Protein in-gel digestion with trypsin, separation of peptides and analysis were completed following a previously described protocol [9], with a few modifications. Briefly, following digestion with trypsin, peptides were separated by reversed-phase (RP) nanoscale capillary liquid chromatography (nanoLC) performed using an Agilent 1200 nano pump connected to a 5600

mass spectrometer (AB Sciex, Framingham, Massachusetts, USA) with a nanoelectrospray ion source and mass spectra were obtained using Analyst software (Version 1.6, AB Sciex, Framingham, Massachusetts, USA) (ES-MS/MS). MS/MS peak lists were created using ProteinPilot (Version 4.5, AB Sciex, Framingham, Massachusetts, USA) and analysed using Mascot (Version 2.4.0, Matrix Science, London, UK) and X! Tandem (CYCLONE version, 2010.12.01.1), both programmed to search the TAX_GallusGallus_9031_20141114 database (unknown version, 222250 entries) with carbamidomethyl (C) as a fixed modification and deamidation (NQ), Gln pyro-Glu (N-term Q), phospho (STY) and oxidation (MP) as variable modifications.

2.7. Criteria for Protein Identification

Peptide and Protein identifications based on MS/MS data was validated using Scaffold (version 4.3.4, Proteome Software Inc., Oregon, USA). These identifications were only accepted if they were detected with >95.0% probability. Additionally, peptide identification had a 1.0% FDR threshold and protein identification required at least 2 unique peptides. Proteins comprised of similar peptides were clustered according to the principals of parsimony when they could not be differentiated solely by MS/MS analysis.

2.8. Bioinformatics Analysis

Proteins identified as “unknown” or “uncharacterized” by Scaffold were identified using the protein Basic Local Alignment Search Tool (pBLAST) to search the *Gallus gallus* non-redundant protein sequence database (9031). Gene ontology terms were obtained from several sources including the Database for Annotation, Visualization and Integrated Discovery

(DAVID) bioinformatics Functional Annotation Tool (DAVID Bioinformatics Resources 6.7, NIAID/NIH), the EMBL-EBI QuickGO browser (European Molecular Biology Laboratory – European Bioinformatics Institute) and e!Ensembl (www.ensembl.org). The DAVID bioinformatics software was also used for functional annotation clustering. Finally, signal peptides were detected by analyzing the predicted full length sequences using the SignalP 4.1 Server (http://www.cbs.dtu.dk/services/SignalP).

3. Results

3.1. Optimization of Protein Extraction

The calcium reserve body, located at the base of the mammillary cones, consists of reactive microcrystals of calcite that are more susceptible to dissolution compared with the bulk mammillary cone mineral [12]. The objective of our experimental approach was to selectively dissolve the calcium reserve body, while leaving the tips of the mammillary cones still attached to the eggshell membrane fibres.

In the **fertilized** egg model, beginning at day 11 of embryonic development, the eggshell represents the major supply of calcium for skeletal development of the chick embryo [10]. The cone bases dissolve within a milieu acidified by protons secreted by the cells of the chorionic layer of the chorioallantoic membrane (CAM) [18]. The process of calcium mobilization from the shell is dependent on the physiological stage of embryonic development. Pilot experiments determined that cones were not present on shell membranes stripped from eggs during day 0 to 15 of embryonic development. However, cones were present on the detached membranes obtained from eggs corresponding to days 16-19 of embryonic development. For this study with

the fertilized model, membranes from eggs at day 19 of embryonic development were used to study the protein composition of the mammillary cones; eggs from day 15 were a source of the negative control membranes (Fig. 2E and G).

In the **unfertilized** egg model, we aimed to mimic the physiological process. Pilot experiments were conducted to optimize the selective dissolution of mammillary cone bases with acid solutions. Various concentrations of hydrochloric acid (0.01, 0.1 and 1N) with several incubation times (0, 30, 60, 120, 180 minutes) were tested in order to achieve sufficient dissolution to break off mammillary cones that remained associated with the shell membrane fibres, without completely dissolving them. Fig. 2A and C illustrate the effects of 0.1N HCl on cone base dissolution. In the absence of acid (incubation of 0 minutes) the base of the mammillary cones stay firmly attached to the calcified shell and the membranes are stripped off the shell without attached cones. Light microscopy images of membranes stained with 0.1% toluidine blue confirmed the absence of mammillary cones (Fig. 2A). However, after incubating the shell interior for 30 minutes with 0.1N HCl, the membranes begin to detach from the shell, indicating dissolution of the inner calcified shell. The mammillary cones remain associated with the stripped shell membranes. This is clearly visible using light microscopy, where a quasi-periodic array of toluidine blue-stained structures can be observed (Fig. 2C).

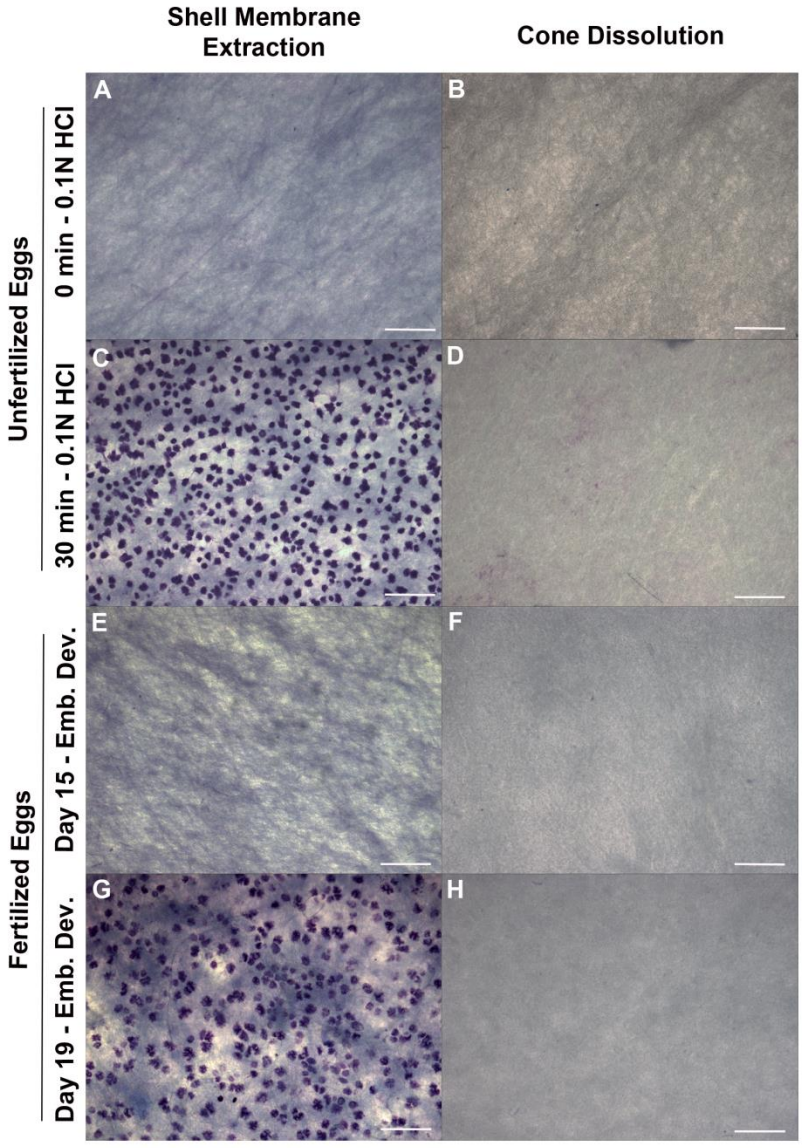

Fig. 2. Light microscopy analysis of extracted shell membranes from two experimental models. (A and C) Shell halves from unfertilized eggs were treated with 0.1N HCl for 0 or 30 minutes and shell membranes were stripped off the shell and stained with toluidine blue. (E and G) Shell membranes from fertilized eggs were stripped off the shell after 15 or 19 days of embryonic development. After the shell membranes were extracted cones were dissolved in 0.01N HCl. Shell membranes were stained after cone extraction to confirm cone dissolution for both the unfertilized eggs (B and D) and fertilized eggs (F and H).

3.2. Harvesting Mammillary Cone Proteins

Membranes with attached cones were washed with sterile water and then incubated with dilute acid to completely dissolve the mineralized cones. Treated membranes were analyzed using light microscopy to confirm complete cone dissolution. Fig. 2D and H clearly demonstrate the complete removal of cones from experimental samples. Control membranes lacking cones (unfertilized model – 0 minute, 0.1N HCl; and fertilized model – day 15 of embryonic development) were also treated with dilute acid as negative controls (Fig. 2B and F). The extracted proteins were then concentrated and resolved by SDS-PAGE for visualization of proteins with Coomassie Blue staining. An intense band migrated at 14kDa in all four samples (Fig. 3A and B). A small number of bands were seen in the samples from the fertilized eggs; only one additional faint band was seen at 41kDa in the sample corresponding to day 19 of embryonic development, with two additional bands (5 and 41kDa) observed in the control (day 15 of embryonic development) (Fig. 3B). For the unfertilized egg model, faint bands were detected at 5, 10, 17, 32 and 41kDa in the experimental sample, while bands at 5, 10 and 41kDa were detected from the control membranes (Fig. 3A). The polyacrylamide gels were sectioned as shown in Fig. 3A and B, and the slices were subjected to proteomics analysis by RP-nanoLC and ES MS/MS.

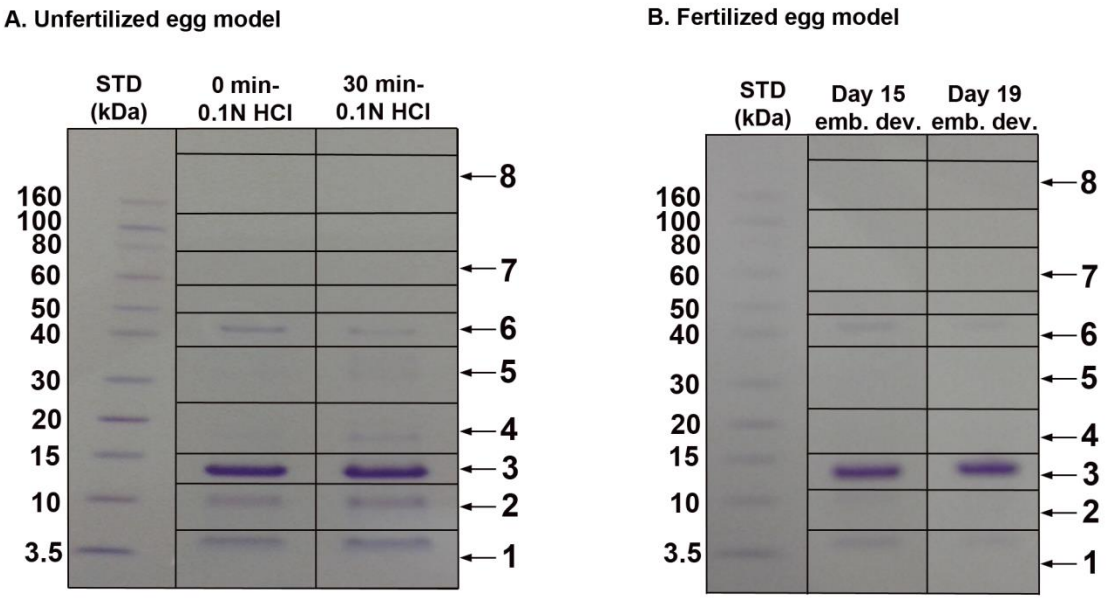

Fig. 3. SDS-PAGE analysis of extracted cone proteins from both experimental models. Proteins extracted from the shell membranes with 0.01N HCl were concentrated and separated on a 4-12% gradient gel. (A) Protein profile corresponding to 0 and 30 minute incubation with 0.1N HCl as well as (B) 15 and 19 days of embryonic development. Gels were sectioned and bands labelled 1-8 from each lane were sent for RP-nanoLC and ES MS/MS proteomic analysis.

3.3. Proteomics Analysis

3.3.1. Membrane Fibre Proteome

Light microscopy confirmed the absence of mammillary cones on unfertilized (time 0) and fertilized (day 15) membranes (Fig. 2A and E); hence extracted proteins from these control situations were associated solely with the eggshell membrane fibres and correspond to proteins soluble in dilute acid. In the unfertilized egg model, 80 unique proteins were identified in the 0 minute 0.1N HCl eggs (control), while 317 proteins were identified in the sample from fertilized eggs incubated 15 days (control) (Table S2). Proteins from both independent models were compared and 49 proteins were identified as being common to both models (Fig. 4A) (Table S1). Among the 49 proteins identified in the eggshell membranes were 10 previously identified as "egg white" proteins. These include ovalbumin, lysozyme C, ovotransferrin, ovomucoid, riboflavin-binding protein, ovoinhibitor, cystatin, ovostatin, avidin and TENP. The 14 kDa band seen in all samples was predominately lysozyme. There were also five proteins classified as "eggshell-specific matrix proteins": ovocleidin-116 (OC-116), ovocleidin-17 (OC-17), ovocalyxin-36 (OCX-36), ovocalyxin-21 (OCX-21, also known as gastrokine-2) and ovocalyxin-25 (OCX-25, LOC771972). GO term enrichment analysis and functional annotation clustering of the eggshell membrane proteins revealed three clusters of functions significantly enriched: enzyme inhibitor activity (E-score 9.11), defense response / response to bacterium (E-score 4.38) and cell adhesion (E-score 1.26) (Table 1). Included in the "response to bacterium" cluster were antimicrobial peptides known as avian β-defensins -9, -10 and -11 (previously known as gallinacins). Further analysis of the control and experimental samples revealed the presence of many avian β-defensins, especially in the fertilized egg model (Table 2).

Table 1. Functional annotation clustering analysis for the 49 proteins associated with the eggshell membranes (Table S1).

	GO Terms	P-Value[a]	Identified Proteins[b]
Two Identified Clusters			
Enzyme Inhibitor Activity **E-score[c] 9.11**	GO:0004866~endopeptidase inhibitor activity	3.14E-10	Ovocalyxin-25, Ovomucoid, Ovoinhibitor, Ovalbumin-related protein X, Ovalbumin, Ovalbumin-related protein Y, Cystatin, Ovostatin, Plasminogen activator inhibitor type 1 member 2 precursor
	GO:0004867~serine-type endopeptidase inhibitor activity	4.61E-10	Ovocalyxin-25, Ovomucoid, Ovoinhibitor, Ovalbumin-related protein X, Ovalbumin, Ovalbumin-related protein Y, Ovostatin, Plasminogen activator inhibitor type 1 member 2 precursor
	GO:0030414~peptidase inhibitor activity	5.36E-10	Ovocalyxin-25, Ovomucoid, Ovoinhibitor, Ovalbumin-related protein X, Ovalbumin, Ovalbumin-related protein Y, Cystatin, Ovostatin, Plasminogen activator inhibitor type 1 member 2 precursor
	GO:0004857~enzyme inhibitor activity	4.59E-09	Ovocalyxin-25, Ovomucoid, Ovoinhibitor, Ovalbumin-related protein X, Ovalbumin, Ovalbumin-related protein Y, Cystatin, Ovostatin, Plasminogen activator inhibitor type 1 member 2 precursor
Defense response **E-score 4.38**	GO:0009617~response to bacterium	8.17E-06	Beta-2-microglobulin, Avian β-defensin-10, Lysozyme C, Avian β-defensin-9, Avian β-defensin-11, Ovocleidin-17, Cochlin
	GO:0042742~defense response to bacterium	6.25E-05	Avian β-defensin-10, Lysozyme C, Avian β-defensin-9, Avian β-defensin-11, Ovocleidin-17, Cochlin
	GO:0006952~defense response	1.41E-04	Fibronectin, Avian β-defensin-10, Lysozyme C, Avian β-defensin-9, Avian β-defensin-11, Ovocleidin-17, Cochlin
Cell adhesion **E-score 1.26**	GO:0007155~cell adhesion	4.42E-02	Fibronectin, Lactadherin isoform 2, PREDICTED: EGF-like repeats and discoidin I-like domains 3 isoform X2, Cadherin-1
	GO:0022610~biological adhesion	4.42E-02	Fibronectin, Lactadherin isoform 2, PREDICTED: EGF-like repeats and discoidin I-like domains 3 isoform X2, Cadherin-1
Enriched GO Term			
	GO:0008289~lipid binding	1.57E-02	Serum albumin, Ovoglobulin G2 type AA (TENP protein), Apolipoprotein A-I, Ovocalyxin-36, Ovocleidin-17

a. P-value corresponds to the EASE score determined by the DAVID software.
b. Correspond to proteins associated with the eggshell membranes (Table S1)
c. E-score: enrichment score determined by the DAVID software.

Table 2. List of avian β-defensins identified in membranes / mammillary cones in four different experimental conditions.

Identified Proteins	UniProt Accession Number	Unique Peptides[a]			
		UF[b]-0	UF[b]-30	FE[c]-15	FE[c]-19
Avian β-defensin 1α	P46157			2	2
Avian β-defensin 2	E1AFU7			3	2
Avian β-defensin 6	Q6QLR3			2	
Avian β-defensin 7	E1AFV0		2	5	2
Avian β-defensin 9	Q6QLR1	2		3	3
Avian β-defensin 10	Q6QLQ9	4	7	9	7
Avian β-defensin 11	Q6IV20	23	27	24	19

a. Information obtained from Scaffold software, version 4.3.4
b. UF-0/30; Unfertilized Egg – 0/30 min incubation with 0.1N HCl
c. FE-15/19; Fertilized Egg – day 15/19 of embryonic development

3.3.2. Mammillary Cone Proteome

A large number of proteins (168) were identified in the sample from 19 day fertilized eggs (experimental) (Table S2), which corresponds to extraction from proteins of both membrane fibres and mammillary cones. Only 57 proteins of these 168 were unique to day 19 eggs, by comparison to proteins extracted from the day 15 control membranes (317), and therefore likely to be from the interior of the mammillary cones. In the unfertilized egg model, 144 proteins were identified in the 30 minute 0.1N HCl sample (experimental), while 80 were identified in the 0 minute 0.1N HCl eggs (control) (Table S2). Only 70 identified proteins were unique to the experimental sample and were not found in the 0 minute control. These represent the proteins specifically associated with the mammillary cones in the unfertilized model. The power of having two independent models for biological replication was exploited by cross-comparison of proteins extracted from the mammillary cones in each experimental data set (Fig. 4B). Eighteen proteins were common to both models (Table 3).

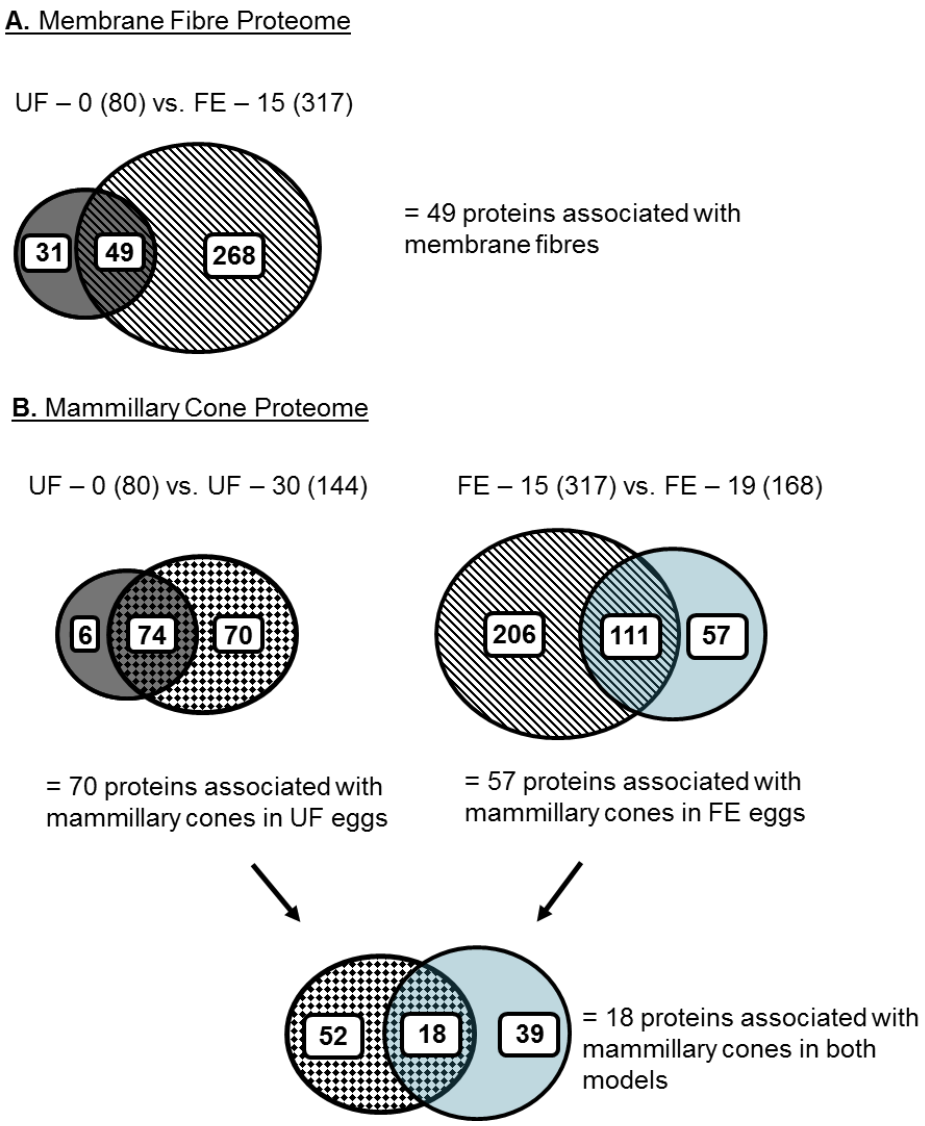

Fig. 4. Summary of proteomics cross-analysis of data from two eggshell membrane models. (A) Proteins corresponding to the eggshell membrane fibres were obtained by comparing the proteins identified in the control samples of the unfertilized egg model (UF – 0) and fertilized egg model (FE – 15). (B) Proteins corresponding to the mammillary cones were obtained by subtracting the proteins identified in the control samples (UF – 0 and FE – 15) from the corresponding experimental sample (UF – 30 and FE – 19) and selecting the proteins associated to mammillary cones that are common in both models.

Table 3. List of 18 proteins identified as being associated with the mammillary cones.

Identified proteins	UniProt Accession Number	Molecular Weight[a]	Unique peptides[a]		Normalized Spectra[a]		Signal Peptide[d]	Also present in[e]
			UF-30[b]	FE-19[c]	UF-30[b]	FE-19[c]		
VH1 protein	A2N883	12 kDa	4	2	48	38	Yes	
Immunoglobulin heavy chain variable region	UPI000044ACDE	26 kDa	2	4	40	37	No	
Immunoglobulin heavy chain variable region	UPI000011B1F0	13 kDa	2	2	36	32	No	
PREDICTED: prostatic acid phosphatase-like	UPI000240B515	44 kDa	8	12	24	31	No	s, w
ABI family, member 3 (NESH) binding protein (ABI3BP)	E1C0S4	167 kDa	12	9	20	29	Yes	s
PIT54 protein precursor	UPI0000611E49	80 kDa	3	6	28	13	Yes	s, w, vw, y
Nucleobindin-2	F1NGB1	54 kDa	9	5	24	10	Yes	c, s, w
Alpha 1 type II procollagen	Q7T2Z7	120 kDa	8	4	16	6	No	s
Tiarin-like	Q25C35	56 kDa	3	8	5	17	Yes	w, vm
SPARC	F1P291	34 kDa	5	2	17	5	Yes	s
PREDICTED: hyaluronan and proteoglycan link protein 3	E1BUN0	41 kDa	2	7	4	17	Yes	s
Golgi apparatus protein 1	Q02391	130 kDa	6	4	10	5	Yes	s, w
PREDICTED: uncharacterized protein LOC419301	UPI00035045B0	42 kDa	4	2	7	5	No	
Calumenin	UPI0000E8211C	8 kDa	2	2	4	6	Yes	
Moesin	E1BV34	69 kDa	2	3	4	4	No	vm
Out at first protein homolog	Q71SY6	31 kDa	2	2	4	3	Yes	s
Transthyretin	P27731	16 kDa	2	3	3	4	Yes	s, y
Coagulation factor VIII	F1NPT2	230 kDa	2	2	3	3	Yes	s

a. Information obtained from Scaffold software, version 4.3.4
b. UF-30; Unfertilized Egg – 30 min incubation with 0.1N HCl
c. FE-19; Fertilized Egg – day 19 of embryonic development
d. Signal peptides were predicted using SignalP 4.1 server
e. Egg compartment where previously detected: y, yolk; vm, vitelline membrane; w, egg white; s, eggshell; c, cuticle [6, 9, 14-17, 34, 38, 58-61]

GO term analysis revealed that certain mammillary cone-specific proteins had characteristics that were relevant to calcitic biomineralization. The ABI family, member 3 (NESH) binding protein (ABI3BP) is involved in extracellular matrix organization, positive regulation of cell-substrate adhesion and collagen binding, and possesses a fibronectin type 3 protein domain. Nucleobindin-2, SPARC and calumenin are involved in calcium ion binding and possess the EF hand calcium binding domain. SPARC is also involved in extracellular matrix binding and bone development, and contains a follistatin/osteonectin EGF protein domain. The GO terms associated to collagen alpha-1(II) indicates a function in ossification, cell adhesion and extracellular matrix organization. The uncharacterized protein, LOC419301, possesses three WAP (whey acidic protein) domains and is classified as a serine-type endopeptidase inhibitor. GO term analysis yielded no obvious indication of the potential function of the other proteins in avian eggshell formation.

Further analysis focused on proteins that were enriched in experimental samples containing mammillary cones, compared to the controls. Analysis of the normalized spectral abundance demonstrated that 86 proteins were > 2.00-fold enriched in the 30 minute 0.1N HCl experimental sample compared to the 0 minute 0.1N HCl control for the unfertilized egg model. Furthermore, 84 proteins were > 2-fold more abundant in samples from the eggs at 19 days of embryonic development compared to eggs at 15 days of embryonic development. Cross-analysis of both list revealed 18 proteins common to both the unfertilized and fertilized egg models, increasing the likelihood that they play a role in the initiation of calcium mineralization (Table 4).

Table 4. List of 18 proteins at least twice as abundant in UF-30 and FE-19 compared to controls UF-0 and FE-15.

Identified proteins	UniProt Accession Number	Molecular Weight[a]	Unique peptides[a]				-Fold Increase in Normalized Spectra[d]		Signal Peptide[e]	Also present in[f]
			UF-0[b]	UF-30[b]	FE-15[c]	FE-19[c]	UF-30[b]	FE-19[c]		
PREDICTED: EGF-like repeats and discoidin I-like domains 3 isoform X2	F1NCN3	54 kDa	22	52	25	44	5.72	5.72	Yes	s, sm
Clusterin	Q9YGP0	51 kDa	19	36	21	35	3.47	4.47	Yes	c, s, sm, w, vm, y
Serum albumin	F2Z4L6	64 kDa	16	41	2	36	3.69	35.03	No	c, s, w, y
Ovostatin	P20740	166 kDa	9	28	11	37	2.78	6.56	Yes	s, sm, w, vm, y
Collagen alpha-1(X) chain	P08125	66 kDa	7	23	10	19	4.22	2.87	Yes	s, sm
polymeric immunoglobulin receptor precursor	UPI00004C9AD9	71 kDa	6	15	0	10	2.60	N/A	No	c, s, w, vm
Apolipoprotein D	Q5G8Y9	22 kDa	5	8	0	3	2.08	N/A	Yes	s, ew, vm, y
Fibronectin	F1NJT4	259 kDa	5	35	22	25	9.07	2.03	Yes	s, y
Sulfhydryl oxidase 1	Q8JGM4	83 kDa	4	16	9	11	6.93	4.17	Yes	c, s, w vm
Ig mu chain C region	P01875	48 kDa	2	5	0	9	2.72	N/A	No	s, ew, y
PREDICTED: mucin-5AC	E1C037	453 kDa	2	14	2	7	5.51	9.52	No	s
Ovostatin-like	F1NEW8	165 kDa	2	10	0	10	4.82	N/A	Yes	c, s
Mucin-5B	Q98UI9	234 kDa	2	17	0	23	9.89	N/A	Yes	c, s, vm, ew
Tsukushin	F1NDH7	39 kDa	2	3	0	2	2.23	N/A	Yes	s
Proactivator polypeptide	E1BSP1	58 kDa	0	13	2	3	N/A	2.34	Yes	c, s, y
Hemopexin	H9L385	45 kDa	0	7	5	7	N/A	2.44	No	s, w, vm, y
Ovocalyxin-32	C7G540	31 kDa	0	4	4	7	N/A	3.82	Yes	c, s, sm, w, vm
Carbonic anhydrase IV	E1C004	38 kDa	0	3	2	4	N/A	6.42	No	s

a. Information obtained from Scaffold software, version 4.3.4
b. UF-0 / -30; Unfertilized Egg – 0 min incubation with 0.1N HCl / -30 min incubation with 0.1N HCl
c. FE-15 / -19; Fertilized Egg – day 15 of embryonic development / -day 19 of embryonic development

d. Normalized Spectra obtained from Scaffold software, version 4.3.4; In analyses where proteins were absent in the control, the –fold increase is unavailable.
e. Signal peptides were predicted using SignalP 4.1 server
f. Egg compartment where previously detected: y, yolk; vm, vitelline membrane; w, egg white; s, eggshell; c, cuticle [6, 9, 14-17, 34, 38, 58-61]

Potential candidates associated with the initial phase of shell mineralization include EGF-like repeats and discoidin I-like domains 3 (EDIL3), clusterin, serum albumin, collagen alpha-1(X), fibronectin, ovocalyxin-32 (OCX-32) and carbonic anhydrase IV (Table 4). EDIL3 is 5.72-fold enriched in both the unfertilized and fertilized egg models. GO analysis indicates a function in calcium ion binding as well as cell adhesion. GO term analysis of clusterin revealed that it is involved in multiple biological processes and molecular functions. Previous studies have suggested that clusterin has a chaperone function that might promote proper folding of matrix proteins during eggshell mineralization (Mann et al., 2003). Our study indicates that it is 3.47-fold and 4.47-fold increased in abundance in the unfertilized and fertilized models, respectively, when compared to the appropriate controls; this suggests that it is enriched in the mammillary cones. Serum albumin, a major blood protein, is capable of binding a variety of ligands including DNA, drugs, fatty acids, metal ions, lipids, toxic substances and oxygen. Its protein abundance was 35.03-fold higher in the fertilized egg model compared to 3.69-fold higher in the unfertilized egg model. GO term analysis for collagen alpha-1(X) identifies this protein as a constituent of proteinaceous extracellular matrices. Normalized spectral abundance revealed that collagen alpha-1(X) was 4.22-fold and 2.87-fold enriched in the unfertilized and fertilized egg models, respectively. Fibronectin was found to be 9.07-fold more abundant in the unfertilized model compared with a 2.03-fold enrichement in the fertilized egg model. Fibronectin is involved with cell, cell-matrix and cell-substrate adhesion and has a fibronectin, type II, collagen-binding domain. OCX-32 was detected solely in the sample with mammillary cones in the unfertilized egg model and was 3.82-fold more abundant in the sample with mammillary cones in the fertilized model when compared to the shell membrane control (Table 4). OCX-32 is involved in biomineral formation and is a member of the proteinase inhibitor latexin family of proteins. GO

terms for carbonic anhydrase IV include bicarbonate transport as well as carbonate dehydratase activity. Normalized spectral abundance revealed a 6.42-fold enrichment in the fertilized eggs; however, this protein was only detected in the sample with mammillary cones in the unfertilized egg model (Table 4).

4. Discussion

During eggshell mineralization, the initial calcification events that give rise to the mammillary cones occur on the surface of the outer shell membrane fibres. As mineralization of the cones proceeds, fusion at their bases produces a continuous layer of mineral (Fig. 1). Further deposition of calcite produces the main eggshell thickness, the palisade layer [12]. The mammillary cone layer is thus an array of protrusions on the inner eggshell surface, possessing protein-rich centers, whose formation is a seminal event in eggshell mineralization; in fact, spacing and height of the mammillary cones are ultimately responsible for important biomechanical properties of the complete shell. In this study we tested the hypothesis that proteins related to the initial cone mineralization events could be liberated and identified from the mammillary cone interior following their selective detachment from the eggshell interior.

In unfertilized eggs, the proteins of the mammillary cones were successfully extracted by selectively dissolving the cone bases by incubation with 0.1N HCl for 30 minutes. Cone tips remained attached to the membranes since the membrane fibres penetrate the cone apices. Acid treatment for 0 minutes served as a control; in this case, cones resisted removal when the membranes were pulled from the shell interior, and were absent from the detached membranes. In the case of the fertilized eggs, natural eggshell resorption occurs at the cone bases to provide

the embryo with calcium; therefore, membranes with attached cones can be mechanically detached from the shell [10]. Up to embryonic day 11, the developing embryo obtains the necessary calcium from the egg yolk; at later times, the eggshell becomes the main source of calcium up to hatching [10]. The chorioallantoic membrane (CAM) begins to form around days 5 and 6 of embryonic development, and progressively develops to line the eggshell membranes [20]. By day 11, the chorioallantoic membrane is fully adherent to the inner shell membrane; however, the cells responsible for proton secretion do not become fully differentiated until day 12 – 14 [21]. This observation correlates with studies demonstrating that the calcium content of fertilized eggs increases rapidly from day 14 until hatching [21]. Our experiments showed that shell dissolution did not significantly degrade the mammillary cone bases until after day 15, which provided us with a control for the fertilized egg model. However, cone base dissolution occurred progressively after day 16; this process was optimal by day 19. Cross-analyzing the proteins released from cone interiors by decalcification in the two models, and their respective controls, allowed us to identify mammillary cone - specific proteins.

Cross-analysis of proteomics data from eggshell membrane control samples revealed 49 proteins soluble in dilute acid that were solely associated with the eggshell membrane fibres (Table S1). Analysis of the protein constituents indicates a potential role for the eggshell membrane fibres in antimicrobial defense of the egg. Three identified proteins inhibit bacterial growth by sequestering nutrients necessary for their survival; ovotransferrin (iron), avidin (biotin) and riboflavin-binding protein (vitamin B2) [22]. We also identified three proteins similar to Bactericidal Permeability Increasing (BPI) protein and Lipopolysaccharide binding protein (LBP): OCX-36, ovoglobulin G2 type AA (TENP) and BPI-fold containing family C protein. BPI and LBP both bind bacterial lipopolysaccharides; however, BPI has a direct

antibacterial activity against bacteria while LBP upregulates the inflammatory response [23]. OCX-36 isolated from chicken eggshell membranes inhibits the growth of Gram-positive *S. aureus* while TENP contributes to the antimicrobial activity of emu egg white against Gram-positive *B. subtilis* and *M. luteus* [23,24]. OCX-32 is also an eggshell-specific matrix protein and is identified in this study as a mammillary cone protein (Table 4). Recombinant GST-OCX-32 fusion protein significantly inhibits the growth of *B. subtilis* [25]. Enrichment analysis and functional clustering annotation revealed nine proteins possessing endopeptidase inhibitor activity (Table 1). Among them is cystatin, a cysteine protease inhibitor with bactericidal activity towards both Gram-positive and Gram-negative bacteria [26]. The remaining eight proteins are classified as serine protease inhibitors (SERPINs). Ovalbumin is a non-functional member of this protein family; however, ovoinhibitor possesses inhibitory activity towards both bacterial and fungal proteases [27,28]. It is possible that other SERPINs participate in the antimicrobial defense of the egg via a similar mechanism. OCX-25 (LOC771972) is an eggshell-specific matrix protein and is part of the Bovine Pancreatic Trypsin Inhibitor (BPTI)/Kunitz family of serine protease inhibitors. Similar to BPTI, it is hypothesized to possess antimicrobial activity against both Gram-positive and Gram–negative bacteria [9]. Interestingly, ovalbumin-related protein X (OVAX), also a non-inhibitory member of the SERPIN family of protease inhibitors, inhibits both Gram-positive and Gram-negative bacterial growth via poorly understood mechanisms [29]. Antimicrobial peptides (AMPs) are effective against a wide range of pathogens, including Gram-positive and Gram-negative bacteria, fungus and yeast; avian β-defensins and gallin were identified in the eggshell membrane fibers. Defensins from a variety of species are antimicrobial peptides involved in innate immune defense with a broad spectrum of antimicrobial activity. Fourteen avian β-defensins have been identified, of which 11 are

expressed in every segment of the hen reproductive tract [30,31]. Our study reveals the presence of avian β-defensins -9, -10 and -11 in the eggshell membrane fibres of both fertilized and unfertilized egg. It is noteworthy that avian β-defensins -1α, -2, and -6 were only detected in the samples from fertilized eggs, suggesting that they are synthesized by the developing chick embryo and play a role in its innate immunity (Table 2). Avian β-defensin-7 was identified in fertilized egg samples as well as the unfertilized sample corresponding to membrane fibres and mammillary cones. Our proteomics analysis also identified gallin in the eggshell membrane fibres. Gallin is an antimicrobial peptide related to the avian β-defensin family of peptides which was initially observed in chicken egg white [32]. Recombinant gallin significantly inhibits *E. coli* bacterial growth [32]. In summary, the protein constituents of the eggshell membrane fibres that we have identified in this study support the notion that the membrane fibres function as a bacteriostatic and bactericidal meshwork to resist microbial contamination of the egg interior [33].

Proteomics cross-analysis revealed 18 proteins uniquely associated with the mammillary cones, as well as 18 proteins that were >2.00-fold enriched in mammillary cone extracts. We believe that these proteins are authentic cone proteins and are excellent candidates for playing a specific role in the initial phases of mineralization in eggshell formation.

One of the most abundant cone-specific proteins is ABI family, member 3 (NESH) binding protein (ABI3PB). Also known as Target of NESH-SH3, this 102kDa protein has previously been identified in the eggshell matrix and uterine fluid of laying hens [17,34]. Studies in mice revealed that ABI3PB, also known as eratin, is an extracellular matrix protein capable of binding collagen type VI as well as heparin. In humans, the ABI3BP gene was shown to be highly expressed in the perichondrium, tendons and ligaments, primarily at the site of attachment

[35]. There are also several studies indicating that a change in ABI3BP gene expression may play a critical role in Kashin-Beck disease, a chronic osteochondropathy [36,37].

Nubleobindin-2, also known as NEFA, is a 54kDa noncollagenous bone protein identified in this study as a moderately abundant protein associated with the mammillary cones. Previously identified in the eggshell palisades, egg white and the cuticle, nucleobindin-2 has an EF-hand calcium ion binding domain [9,17,38]. Previous *in vitro* studies have identified NEFA as an eggshell matrix protein capable of inhibiting the precipitation of calcium carbonate in a phosphorylation-dependant manner [39]. An *in vivo* study examining the function of NUCB21-83, also known as nefastatin-1, in a rat model for postmenapausal osteoporosis, showed increased bone mass density in rats injected with NUCB21-83 [40]. Further *in vitro* studies revealed that NUCB21-83 also promoted osteoblast differentiation and inhibited osteoclast differentiation [40]. These studies suggest that nucleobindin-2 exhibits a regulatory role in calcium mineralization, and should be further explored in the context of calcitic biomineralization.

Collagens type I, V and X have previously been identified in the highly cross-linked matrix of the eggshell membranes [41]. Collagen type X was also recently identified in hen uterine fluid during the initial stage of shell formation [34]. Our study identified collagens type II and X as proteins associated with the mammillary cones. Previous studies examining the role of collagens type II and X in matrix-vesicle mediated mineralization suggest that both types of collagens aid in calcium uptake to promote mineralization [42]. Interestingly, the increase in calcium uptake was found to be linked to the binding between types II and X collagens and annexin V, a protein also identified in our study [42]. Annexin V, present in the fertilized egg model (control and experimental samples) and the unfertilized egg model (experimental sample

only), is a calcium-binding protein strongly expressed in bone and calcifying connective tissue [43] (Table S2). The interaction between these collagens and annexin V could be a key step in the early stages of mineralization.

Tiarin-like protein, better known as olfactomedin-4, is a secreted extracellular matrix protein. This 56kDa glycoprotein was previously identified in the eggshell matrix and is thought to be an adhesive matrix component, since it binds to lectins and cadherins, that are both calcium-dependant cell adhesion proteins [17,44]. It is noteworthy that cadherin-1 is present in eggshell membrane fibres (Table S2). Therefore, it is possible that tiarin-like protein and is an effective substrate for cell adhesion and possibly an anchor between mineralized shell and shell membranes. Hyaluronan and proteoglycan link protein 3 (HAPLN3) is also an extracellular matrix protein that is widely expressed in many vertebrate tissues. It is suggested to be involved in the organization and integrity of the extracellular matrix by stabilizing hyaluronan and chondroitin sulfate proteoglycan aggregates [45].

Another moderately abundant protein found to be associated with the mammillary cones is SPARC (secreted protein, acidic, cysteine-rich), a 34kDa glycoprotein considered to be a matricellular protein. Matricellular proteins regulate cell-matrix interactions and cell functions rather than participate directly in the organization of structural elements [46]. SPARC possesses two calcium-binding regions: an N-terminal glutamic acid-rich domain that binds 5-8 calcium ions with a low affinity and a C-terminal containing an EF-hand domain pair each capable of binding one calcium ion with a high affinity [47]. SPARC was initially identified as osteonectin, a major component in bone extracellular matrix located in every region where bone mineral was freshly deposited [48]. This study demonstrated that osteonectin binds hydroxyapatite calcium crystals as well as collagen type I, *in vitro*, and suggested that osteonectin could be responsible

for initiating mineral formation and promote crystal attachment to a collagenous matrix [48]. Additional studies have confirmed that SPARC can bind to collagen types I-V and inhibit hydroxyapatite crystal growth [49-51]. There is decreased RNA expression and lower levels of osteonectin protein in osteogenesis imperfect, and osteonectin-null mice exhibit a decrease in bone remodeling and bone mass [52,53]. SPARC was identified in murine otoconia, and is necessary for zebrafish otolith formation (the fish equivalent of otoconia), with a proposed biomineralization function [54,55]. All of these studies indicate the potential role of SPARC in the initiation of calcium mineralization and/or a link between collagenous extracellular membranes and mineralized calcium.

Proteomics cross-analysis revealed an uncharacterized mammillary cone protein, LOC419301, which possesses 3 four-disulfide core WAP (whey acidic protein) domains. A similar protein identified in abalone shell, named perlwapin, also possesses three consecutive WAP domains and was shown to inhibit the growth of calcium carbonate crystals within the nacreous layer [56]. This suggests that the uncharacterized protein identified in this study could have a dual protease inhibitor / regulation of calcification function.

An uncharacterized protein with the UniParc accession number UPI0000E8211C was identified as a mammillary cone protein. BLAST analysis of the identified peptide sequences in the UniProt database revealed this protein has 93% identity with calumenin from domestic duck, and likely corresponds to chicken calumenin. Calumenin is characterized as a calcium ion binding protein with multiple EF-hand domains and suggested to be involved in calcium homeostasis in mouse heart [57]. Similar to nucleobindin-2 and SPARC, chicken calumenin could play a regulatory role in calcium mineralization.

The most abundant protein enriched in the mammillary cones is EGF-like repeats and discoidin I-like domains 3 (EDIL3). This protein has been previously identified in the shell matrix and the shell membranes, as well as in the hen uterine fluid at the initial stage of shell calcification [14,16,34]. EDIL3 is an extracellular matrix protein that possesses three calcium-binding EGF-like domains and two coagulation factor 5/8 C-terminal domains (discoidin domains) involved in cell adhesion. The localization of EDIL3 in the mammillary cones, its elevated levels in uterine fluid during initial shell formation and the presence of calcium ion binding domains, strongly suggest that EDIL3 could play a significant role in the early stages of shell formation.

Clusterin is a component of the eggshell matrix [19] and has been identified in every compartment of the avian egg: the cuticle, palisade layer, shell membranes, egg white, vitelline membrane and yolk [9,14-17,38,58-61]. Here we have detected higher levels of cone-resident clusterin in both the fertilized and unfertilized egg models, which is consistent with the hypothesis that clusterin functions as a chaperone to inhibit premature aggregation and precipitation of proteins during shell calcification [19]. This is consistent with higher levels of clusterin identified in the hen uterine fluid during the initial stage of shell calcification [34].

Serum albumin is an abundant plasma protein capable of binding a variety of ligands, including calcium ions [62], and is one of the 18 proteins enriched in samples containing mammillary cones, in both egg models. Several studies have revealed opposing roles for serum albumin in crystal mineralization and nucleation and found that these processes were concentration-dependent. Low levels of serum albumin have previously been shown to promote octacalcium phosphate and calcium oxalate crystal growth [63,64]. These effects were inhibited when higher levels of serum albumin were tested, suggesting that serum albumin covers the

surface of the crystals, potentially blocking sites necessary for crystal growth or preventing ions from reaching the crystals [65]. All of these results combined indicate a potential regulatory function for serum albumin in the nucleation of calcium carbonate crystals for eggshell formation.

Polymeric immunoglobulin receptor is a calmodulin-binding, integral membrane glycoprotein involved in mucosal defense via IgA binding [66]. However its function might not be limited to mucosal immunity. It is noteworthy that calmodulin, which possesses a calcium binding EF-hand domain pair, was also identified as a low abundance membrane component in this study with at least two unique peptides (Table S2). Polymeric immunoglobulin receptor could be involved in the initiation of mineralization by binding and localizing calcium-binding proteins to the nucleation sites.

Fibronectin is a 273kDa glycoprotein found in the extracellular matrices of connective tissues. It consists of multiple repeats of three domains: type I, II and III which bind collagen, integrins, heparin and other extracellular molecules [67]. Several studies have identified fibronectin as a strong candidate for nucleation in early calcification after observing the formation of apatite crystals when fibronectin was incubated with calcium phosphate crystals [68,69]. This is supported by *in vivo* studies observing fibronectin in early bone formation, and a strong association between fibronectin and collagen type I in the bone matrix, using a rat model [70]. *In vitro* studies suggest that fibronectin functions as an anchor for extracellular matrix proteins that cannot bind collagen, including osteopontin [71]. The presence of fibronectin in both the shell membranes and mammillary cones for both models of this study further support a role in collagen fibril organization and calcitic mineralization.

Tsukushin is a member of the small leucine-rich proteoglycans (SLRP) family of proteins known for regulating collagen fibril assembly [72]. It has been previously identified in the eggshell matrix, hen uterine fluid during active calcification and termination, and the gene is over-expressed in hen uterine cells during active calcification [34,73].

Proactivator polypeptide was previously identified in the egg yolk, shell matrix and cuticle and is better known as prosaposin, the precursor to four sphingolipid activator proteins: saposins A, B, C and D [9,15,17,61]. A study evaluating the gene expression of an osteoblast-like cell line demonstrated the up-regulation of the prosaposin gene when the cells were treated with retinoic acid, a treatment that inhibits the development of the mineralized matrix [74]. Another study identified the human prosaposin gene as being up-regulated in osteoporosis [75]. Saposins are commonly known for their role in lysosomal sphingolipid metabolism; however, there has been no demonstration of a potential function in the regulation of mineralization.

Ovocalyxin-32 is an eggshell-specific matrix protein identified in many egg compartments including the cuticle, eggshell, eggshell membranes, egg white and the vitelline membranes [9,14-17,38,58,59]. However, it is particularly abundant in the cuticle and outer calcified layer of the chicken eggshell [76]. The abundance of OCX-32 in the outer eggshell layers, as well as increased concentration in uterine fluid corresponding to the terminal phase of calcification, have suggested a function in the termination of calcification [77]. Additionally, recent studies have detected elevated levels of OCX-32 in uterine fluid during the initial phase of shell calcification [34]. Proteomic analysis revealed the presence of OCX-32 in the shell membranes [16]; and it could be involved in the inhibition of calcification towards the egg white.

Calcitic mineralization of the chicken eggshell occurs in an acellular uterine fluid which is supersaturated with respect to calcium and bicarbonate. Carbonic anhydrase activity hydrates

carbon dioxide to produce bicarbonate [78], which is then transported across the basolateral membrane into the uterine lumen where shell mineralization occurs. The current study identified carbonic anhydrase IV, a membrane associated carbonic anhydrase, to be more abundant in samples with mammillary cones when compared with shell membrane control samples. Its elevated abundance in mammillary cones of fertilized eggs, compared with the unfertilized model, may be due to the presence of carbonic anhydrase in the villus cavity cells of the chorioallantoic membrane [20]. Carbonic anhydrase is also expressed in the mammalian inner ear, likely providing the bicarbonate necessary for otoconia formation and maintenance as well as pH regulation [2].

Ovocleidin-17 (OC-17) and Ovocleidin-116 (OC-116) are eggshell-specific matrix proteins that have previously been shown to modulate shell calcification [8]. Immunohistochemistry of decalcified eggshell reveals that OC-17 is present across the shell matrix but concentrated in the mammillary bodies [79]. Proteomics data from this study supports immunohistochemistry findings; OC-17 is 5.3-fold enriched in the mammillary cones of the unfertilized model and 1.6-fold enriched in fertilized eggs. Colloidal gold immunocytochemistry demonstrates that OC-116 is dispersed throughout the eggshell palisade layer and is the most abundant matrix protein in this zone [15,80]. In this study, we observed that OC-116 is 1.5-fold enriched in the mammillary cones (unfertilized model), but present at equivalent levels in both membranes and cones of the fertilized model. This data suggests that OC-116 is more directly involved in the active calcification stage of shell formation (palisades mineralization) rather than crystal nucleation.

Calcitic mineralization is essential not only for eggshell formation but also for otoconia formation in vertebrates. Similar characteristics can be observed in the spectrum of proteins

identified in both eggshell and otoconia (Table 5). Currently, nine murine proteins have been identified in mammalian otoconia. These proteins are referred to as otoconins and include otoconin-90, otolin-1, keratan sulfate proteoglycan (KSPG), α-tectorin, fetuin-A, osteopontin, SPARC-like protein 1, SPARC and dentin matrix protein 1 (DMP1) [2]. Moreover, the otoconial membrane consists of otolin-1, otogelin, otogelin-like, α-tectorin, β-tectorin and otoancorin [2]. Otoconin-90 is the most abundant protein found in otoconia [2]. It is a calcium-binding protein and is one of the phospholipase A2 family of proteins. Similarly, PREDICTED: group 10 secretory phospholipase A2 is a calcium-binding protein that was shown to be associated to the mammillary cones in the fertilized eggs of this study (Table S2). Otolin-1 is a member of the collagen X family of proteins and functions as a fibrous scaffold tissue for otoconia formation [3], which is a similar function as proposed for collagen X, the most abundant collagen constituent of the highly cross-linked eggshell membrane fibres [41]. KSPGs are the major class of proteoglycan in mouse and chicken otoconia [54,81]. Their negative charges attract calcium ions and they form large complexes with collagens and other proteoglycans [2]. In the chicken egg, keratan sulfate has been detected in the shell membranes, mammillary cones and shell matrix with a proposed function in the regulation of crystal nucleation [82,83]. Otoconial membrane proteins otogelin and α-tectorin are structurally similar to mucin-5B and mucin-5AC identified as enriched in the mammillary cones of this study (Table 4). All four proteins are rich in von Willebrand factor type D domains, C8 (8 conserved cysteine residues) domains and trypsin inhibitor like cysteine rich domains. Fetuin-A, also known as α-2-HS-glycoprotein, is an abundant non-collagenous protein found in bone with an inhibitory function on calcium phosphate biomineralization [84]. It is noteworthy that α-2-HS-glycoprotein was also identified as a mammillary cone associated protein in the unfertilized egg sample of this study, suggesting

a possible role in the inhibition of mineralization towards the interior of the egg. Osteopontin (SPP1) and dentin matrix protein 1 (DMP1) were not detected in this cone-specific study; they are well characterized proteins involved in ossification and biomineral tissue development that have previously been identified in the chicken eggshell matrix [15,17,85]. A likely explanation for the absence of osteopontin from our proteomics data is its predominant localization within the palisade region of the calcified shell [86]. Finally, SPARC, identified in otoconia and in mammillary cones in this study, is a protein rich in cysteine residues, which possesses both calcium-binding EF-hand and collagen-binding domains [87,88]. While carbonic anhydrase, enriched in the mammillary cones, has not been identified in the otoconia structure, it is expressed in the endolymphatic sac of the inner ear and is essential for normal otoconia formation [2].

Table 5. Similarities between proteins involved in eggshell and otoconia formation.

Otoconia/Otoconial membrane	Eggshell/Eggshell membranes	Function
Otoconin-90	group 10 secretory phospholipase A2	Calcium ion binding
Otolin-1	Collagen-X	Fibrous scaffold tissue for biomineralization
Keratan sulfate proteoglycan (KSPG)	Keratan sulfate proteoglycan (KSPG)	Regulation of crystal nucleation
α-tectorin	Mucin-5B and Mucin-5AC	Unknown: rich in von Willebrand type D, C8 (8 conserved cysteines) and Trypsin inhibitor like cysteine rich domains
Otogelin	Mucin-5B and Mucin-5AC	Unknown: rich in von Willebrand type D, C8 (8 conserved cysteines) and Trypsin inhibitor like cysteine rich domains
Fetuin-A (α-2-HS-glycoprotein)	α-2-HS-glycoprotein	Negative regulation of mineralization
Osteopontin	Osteopontin	Calcitic biomineralization
SPARC	SPARC	Calcium ion and collagen binding
Dentin matrix protein 1 (DMP-1)	Dentin matrix protein 1 (DMP-1)	Ossification and biomineral tissue development
Carbonic anhydrase	Carbonic anhydrase	Bicarbonate transport

Our results demonstrate many similarities between the proteins involved in calcitic mineralization and those associated with calcium phosphate mineralization in bone formation. However, there are key differences between these biomineralization processes with respect to the cellular role. The eggshell is formed while the egg bathes in the uterine fluid within the lumen of the shell gland; the epithelial and glandular cells that secrete these protein and ionic fluid constituents are not intrinsic components of the mineralized layer, as is however the case with bone formation [41]. In a process similar to that of eggshell formation, otoconia mineralization occurs on the surface of the sensory epithelium in the inner ear while the surrounding epithelial cells synthesize and secrete the necessary protein and ionic components [2]. Our study demonstrates that the regulation of calcitic biomineralization in chicken eggshell formation is a model that could provide insight to understand otoconia mineralization.

5. Conclusions

This study describes a novel approach to isolate and identify mammillary cone proteins in the calcified egg. By cross-analyzing the proteins found in two linked, yet independent, biomineralization models, we have identified 18 proteins uniquely associated with calcification, and an additional 18 proteins enriched in the mineralized cones, as compared to the control extracellular matrix. Most of the promising candidates are divided into two categories; the first are extracellular matrix proteins: ABI family member 3 (NESH) binding protein, tiarin-like, hyaluronan and proteoglycan link protein 3 (HAPLN3), collagen alpha-1(X), collagen alpha-1(II) and fibronectin. The second category corresponds to calcium ion binding proteins, including calumenin, EGF-like repeats and discoidin 1-like domains 3 (EDIL3), nucleobindin-2

and SPARC; the latter two which have been previously identified as potential modulators of calcification. Further study is required to determine their precise roles in the early stages of eggshell mineralization, and in the formation of other hard tissues. Eventually, we anticipate that this approach will lead to new strategies to modulate the calcitic biomineralization involved in human diseases such as otoconial degeneration.

Conflict of Interest

The authors have no conflicts of interest to declare.

Acknowledgments

This work was supported by the discovery program of the Natural Sciences and Engineering Research Council of Canada (NSERC) (155449-2011). The authors would like to thank Dr. Sylvie Bourassa and Daniel Defoy from the Proteomics Platform of the Quebec Genomics Center (Laval, QC) for their proteomics services and their expertise. We acknowledge useful insight and discussions with Drs. Yves Nys and Joel Gautron of INRA, Tours, France, in the context of the IMPACT project (Agence Nationale de la Recherche: ANR-13-BSV6-0007-01). The authors would also like to thank an anonymous reviewer for providing valuable insight.

References

[1] Arias JL, Fernandez MS, Laraia VJ, Janicki J, Heuer AH, Caplan AI. The Avian Eggshell as a Model of Biomineralization. MRS Online Proceedings Library 1990;218.

[2] Lundberg YW, Xu Y, Thiessen KD, Kramer KL. Mechanisms of otoconia and otolith development. Developmental Dynamics 2014.

[3] Moreland KT, Hong M, Lu W, Rowley CW, Ornitz DM, De Yoreo JJ, Thalmann R. In vitro calcite crystal morphology is modulated by otoconial proteins otolin-1 and otoconin-90. PLoS One 2014;9:e95333.

[4] Walther LE, Blödow A, Buder J, Kniep R. Principles of Calcite Dissolution in Human and Artificial Otoconia. PloS one 2014;9:e102516.

[5] Igarashi M, Saito R, Mizukoshi K, Alford BR. Otoconia in young and elderly persons: a temporal bone study. Acta Otolaryngol 1993;113:26-9.

[6] Kodali VK, Gannon SA, Paramasivam S, Raje S, Polenova T, Thorpe C. A novel disulfide-rich protein motif from avian eggshell membranes. PLoS One 2011;6:e18187.

[7] Arias JL, Fernandez MS, Dennis JE, Caplan AI. Collagens of the chicken eggshell membranes. Connect Tissue Res 1991;26:37-45.

[8] Rose ML, Hincke MT. Protein constituents of the eggshell: eggshell-specific matrix proteins. Cell Mol Life Sci 2009;66:2707-19.

[9] Rose-Martel M, Du J, Hincke MT. Proteomic analysis provides new insight into the chicken eggshell cuticle. J Proteomics 2012;75:2697-706.

[10] Chien YC, Hincke MT, McKee MD. Ultrastructure of avian eggshell during resorption following egg fertilization. J Struct Biol 2009;168:527-38.

[11] Solomon SE. Gordon Memorial Lecture. An egg ist ein ei, es un huevo, est un oeuf. Br Poult Sci 1999;40:5-11.

[12] Hincke MT, Nys Y, Gautron J, Mann K, Rodriguez-Navarro AB, McKee MD. The eggshell: structure, composition and mineralization. Front Biosci (Landmark Ed) 2012;17:1266-80.

[13] Nys Y, Gautron J, Garcia-Ruiz JM, Hincke MT. Avian eggshell mineralization: biochemical and functional characterization of matrix proteins. Comptes Rendus Palevol 2004;3:549-62.

[14] Miksik I, Sedlakova P, Lacinova K, Pataridis S, Eckhardt A. Determination of insoluble avian eggshell matrix proteins. Anal Bioanal Chem 2010;397:205-14.

[15] Mann K, Macek B, Olsen JV. Proteomic analysis of the acid-soluble organic matrix of the chicken calcified eggshell layer. Proteomics 2006;6:3801-10.

[16] Kaweewong K, Garnjanagoonchorn W, Jirapakkul W, Roytrakul S. Solubilization and identification of hen eggshell membrane proteins during different times of chicken embryo development using the proteomic approach. Protein J 2013;32:297-308.

[17] Sun C, Xu G, Yang N. Differential label-free quantitative proteomic analysis of avian eggshell matrix and uterine fluid proteins associated with eggshell mechanical property. Proteomics 2013;13:3523-36.

[18] Narbaitz R, Bastani B, Galvin NJ, Kapal VK, Levine DZ. Ultrastructural and immunocytochemical evidence for the presence of polarised plasma membrane H(+)-ATPase in two specialised cell types in the chick embryo chorioallantoic membrane. J Anat 1995;186 (Pt 2):245-52.

[19] Mann K, Gautron J, Nys Y, McKee MD, Bajari T, Schneider WJ, Hincke MT. Disulfide-linked heterodimeric clusterin is a component of the chicken eggshell matrix and egg white. Matrix Biology 2003;22:397-407.

[20] Gabrielli MG, Accili D. The chick chorioallantoic membrane: a model of molecular, structural, and functional adaptation to transepithelial ion transport and barrier function during embryonic development. J Biomed Biotechnol 2010;2010:940741.

[21] Crooks RJ, Simkiss K. Respiratory acidosis and eggshell resorption by the chick embryo. J Exp Biol 1974;61:197-202.

[22] Wellman-Labadie O, Picman J, Hincke MT. Avian antimicrobial proteins: structure, distribution and activity. Worlds Poult Sci J 2007;63:421-38.

[23] Cordeiro CM, Esmaili H, Ansah G, Hincke MT. Ovocalyxin-36 is a pattern recognition protein in chicken eggshell membranes. PloS one 2013;8:e84112.

[24] Maehashi K, Ueda M, Matano M, Takeuchi J, Uchino M, Kashiwagi Y, Watanabe T. Biochemical and Functional Characterization of Transiently Expressed in Neural Precursor (TENP) Protein in Emu Egg White. J Agric Food Chem 2014;62:5156-62.

[25] Xing J, Wellman-Labadie O, Gautron J, Hincke MT. Recombinant eggshell ovocalyxin-32: Expression, purification and biological
activity of the glutathione S-transferase fusion protein. comp biochem phys B 2007;147:172.

[26] Kolaczkowska A, Kolaczkowski M, Sokolowska A, Miecznikowska H, Kubiak A, Rolka K, Polanowski A. The antifungal properties of chicken egg cystatin against Candida yeast isolates showing different levels of azole resistance. Mycoses 2010;53:314-20.

[27] Pellegrini A, Hülsmeier AJ, Hunziker P, Thomas U. Proteolytic fragments of ovalbumin display antimicrobial activity. Biochimica et Biophysica Acta (BBA)-General Subjects 2004;1672:76-85.

[28] Begum S, Saito A, Xu X, Kato A. Improved functional properties of the ovoinhibitor by conjugating with galactomannan. Biosci Biotechnol Biochem 2003;67:1897-902.

[29] Rehault-Godbert S, Labas V, Helloin E, Herve-Grepinet V, Slugocki C, Berges M, Bourin MC, Brionne A, Poirier JC, Gautron J, Coste F, Nys Y. Ovalbumin-related protein X is a heparin-binding ov-serpin exhibiting antimicrobial activities. J Biol Chem 2013;288:17285-95.

[30] Mageed AA, Isobe N, Yoshimura Y. Expression of avian β-defensins in the oviduct and effects of lipopolysaccharide on their expression in the vagina of hens. Poult Sci 2008;87:979-84.

[31] Herve-Grepinet V, Rehault-Godbert S, Labas V, Magallon T, Derache C, Lavergne M, Gautron J, Lalmanach AC, Nys Y. Purification and characterization of avian beta-defensin 11, an antimicrobial peptide of the hen egg. Antimicrob Agents Chemother 2010;54:4401-9.

[32] Gong D, Wilson PW, Bain MM, McDade K, Kalina J, Herve-Grepinet V, Nys Y, Dunn IC. Gallin; an antimicrobial peptide member of a new avian defensin family, the ovodefensins, has been subject to recent gene duplication. BMC Immunol 2010;11:12,2172-11-12.

[33] Gautron J, Hincke M, Panheleux M, Garcia-Ruiz J, Boldicke T, Nys Y. Ovotransferrin is a matrix protein of the hen eggshell membranes and basal calcified layer. Connect Tissue Res 2001;42:255-67.

[34] Marie P, Labas V, Brionne A, Harichaux G, Hennequet-Antier C, Nys Y, Gautron J. Quantitative proteomics and bioinformatic analysis provide new insight into protein function during avian eggshell biomineralization. Journal of Proteomics 2015;113:178-93.

[35] Bandyopadhyay A, Kubilus JK, Crochiere ML, Linsenmayer TF, Tabin CJ. Identification of unique molecular subdomains in the perichondrium and periosteum and their role in regulating gene expression in the underlying chondrocytes. Dev Biol 2008;321:162-74.

[36] Zhang F, Guo X, Zhang Y, Wen Y, Wang W, Wang S, Yang T, Shen H, Chen X, Tian Q, Tan L, Deng HW. Genome-wide copy number variation study and gene expression analysis identify ABI3BP as a susceptibility gene for Kashin-Beck disease. Hum Genet 2014;133:793-9.

[37] Wang WZ, Guo X, Duan C, Ma WJ, Zhang YG, Xu P, Gao ZQ, Wang ZF, Yan H, Zhang YF, Yu YX, Chen JC, Lammi MJ. Comparative analysis of gene expression profiles between the normal human cartilage and the one with endemic osteoarthritis. Osteoarthritis and Cartilage 2009;17:83-90.

[38] D'Ambrosio C, Arena S, Scaloni A, Guerrier L, Boschetti E, Mendieta ME, Citterio A, Righetti PG. Exploring the chicken egg white proteome with combinatorial peptide ligand libraries. J Proteome Res 2008;7:3461-74.

[39] Hincke MT, St-Maurice M. Eggshell proteins inhibit calcium carbonate precipitation. Canadian Federation of Biological Societies 2000.

[40] Li R, Wu Q, Zhao Y, Jin W, Yuan X, Wu X, Tang Y, Zhang J, Tan X, Bi F, Liu JN. The novel pro-osteogenic activity of NUCB2(1-83.). PLoS One 2013;8:e61619.

[41] Arias JL, Nakamura O, Fernandez MS, Wu JJ, Knigge P, Eyre DR, Caplan AI. Role of type X collagen on experimental mineralization of eggshell membranes. Connect Tissue Res 1997;36:21-33.

[42] Kirsch T, Harrison G, Golub EE, Nah HD. The roles of annexins and types II and X collagen in matrix vesicle-mediated mineralization of growth plate cartilage. J Biol Chem 2000;275:35577-83.

[43] Kirsch T, Nah H, Shapiro IM, Pacifici M. Regulated Production of Mineralization-competent Matrix Vesicles in Hypertrophic Chondrocytes. J Cell Biol 1997;137:1149-60.

[44] Liu W, Chen L, Zhu J, Rodgers GP. The glycoprotein hGC-1 binds to cadherin and lectins. Exp Cell Res 2006;312:1785-97.

[45] Spicer AP, Joo A, Bowling RA,Jr. A hyaluronan binding link protein gene family whose members are physically linked adjacent to chondroitin sulfate proteoglycan core protein genes: the missing links. J Biol Chem 2003;278:21083-91.

[46] Bornstein P, Sage EH. Matricellular proteins: extracellular modulators of cell function. Curr Opin Cell Biol 2002;14:608-16.

[47] Sodek J, Zhu B, Huynh MH, Brown TJ, Ringuette M. Novel functions of the matricellular proteins osteopontin and osteonectin/SPARC. Connect Tissue Res 2002;43:308-19.

[48] Termine JD, Kleinman HK, Whitson SW, Conn KM, McGarvey ML, Martin GR. Osteonectin, a bone-specific protein linking mineral to collagen. Cell 1981;26:99-105.

[49] Giudici C, Raynal N, Wiedemann H, Cabral WA, Marini JC, Timpl R, Bachinger HP, Farndale RW, Sasaki T, Tenni R. Mapping of SPARC/BM-40/osteonectin-binding sites on fibrillar collagens. J Biol Chem 2008;283:19551-60.

[50] Sasaki T, Göhring W, Mann K, Maurer P, Hohenester E, Knäuper V, Murphy G, Timpl R. Limited cleavage of extracellular matrix protein BM-40 by matrix metalloproteinases increases its affinity for collagens. J Biol Chem 1997;272:9237-43.

[51] Romberg RW, Werness PG, Riggs BL, Mann KG. Inhibition of hydroxyapatite crystal growth by bone-specific and other calcium-binding proteins. Biochemistry 1986;25:1176-80.

[52] Muriel MP, Bonaventure J, Stanescu R, Maroteaux P, Guenet JL, Stanescu V. Morphological and biochemical studies of a mouse mutant (fro/fro) with bone fragility. Bone 1991;12:241-8.

[53] Fedarko NS, Robey PG, Vetter UK. Extracellular matrix stoichiometry in osteoblasts from patients with osteogenesis imperfecta. J Bone Miner Res 1995;10:1122-9.

[54] Xu Y, Zhang H, Yang H, Zhao X, Lovas S, Lundberg YYW. Expression, functional, and structural analysis of proteins critical for otoconia development. Developmental Dynamics 2010;239:2659-73.

[55] Kang Y, Stevenson AK, Yau PM, Kollmar R. Sparc protein is required for normal growth of zebrafish otoliths. Journal of the Association for Research in Otolaryngology 2008;9:436-51.

[56] Treccani L, Mann K, Heinemann F, Fritz M. Perlwapin, an Abalone Nacre Protein with Three Four-Disulfide Core (Whey Acidic Protein) Domains, Inhibits the Growth of Calcium Carbonate Crystals. Biophys J 2006;91:2601-8.

[57] Sahoo SK, Kim do H. Characterization of calumenin in mouse heart. BMB Rep 2010;43:158-63.

[58] Mann K, Mann M. In-depth analysis of the chicken egg white proteome using an LTQ Orbitrap Velos. Proteome Sci 2011;9:7,5956-9-7.

[59] Mann K. Proteomic analysis of the chicken egg vitelline membrane. Proteomics 2008;8:2322-32.

[60] Mann K. The chicken egg white proteome. Proteomics 2007;7:3558-68.

[61] Mann K, Mann M. The chicken egg yolk plasma and granule proteomes. Proteomics 2008;8:178-91.

[62] Majorek KA, Porebski PJ, Dayal A, Zimmerman MD, Jablonska K, Stewart AJ, Chruszcz M, Minor W. Structural and immunologic characterization of bovine, horse, and rabbit serum albumins. Mol Immunol 2012;52:174-82.

[63] Ebrahimpour A, Perez L, Nancollas GH. Induced crystal growth of calcium oxalate monohydrate at hydroxyapatite surfaces. The influence of human serum albumin, citrate, and magnesium. Langmuir 1991;7:577-83.

[64] Combes C, Rey C, Freche M. In vitro crystallization of octacalcium phosphate on type I collagen: influence of serum albumin. J Mater Sci Mater Med 1999;10:153-60.

[65] Combes C, Rey C. Adsorption of proteins and calcium phosphate materials bioactivity. Biomaterials 2002;23:2817-23.

[66] Wieland WH, Orzaez D, Lammers A, Parmentier HK, Verstegen MW, Schots A. A functional polymeric immunoglobulin receptor in chicken (Gallus gallus) indicates ancient role of secretory IgA in mucosal immunity. Biochem J 2004;380:669-76.

[67] Halper J, Kjaer M. Basic components of connective tissues and extracellular matrix: elastin, fibrillin, fibulins, fibrinogen, fibronectin, laminin, tenascins and thrombospondins. Adv Exp Med Biol 2014;802:31-47.

[68] Daculsi G, Pilet P, Cottrel M, Guicheux G. Role of fibronectin during biological apatite crystal nucleation: ultrastructural characterization. J Biomed Mater Res 1999;47:228-33.

[69] Couchourel D, Escoffier C, Rohanizadeh R, Bohic S, Daculsi G, Fortun Y, Padrines M. Effects of fibronectin on hydroxyapatite formation. J Inorg Biochem 1999;73:129-36.

[70] Weiss RE, Reddi AH. Synthesis and localization of fibronectin during collagenous matrix-mesenchymal cell interaction and differentiation of cartilage and bone in vivo. Proc Natl Acad Sci U S A 1980;77:2074-8.

[71] Beninati S, Senger DR, Cordella-Miele E, Mukherjee AB, Chackalaparampil I, Shanmugam V, Singh K, Mukherjee BB. Osteopontin: Its Transglutaminase-Catalyzed Posttranslational Modifications and Cross-Linking to Fibronectin. J Biochem 1994;115:675-82.

[72] Kalamajski S, Oldberg Å. The role of small leucine-rich proteoglycans in collagen fibrillogenesis. Matrix Biology 2010;29:248-53.

[73] Brionne A, Nys Y, Hennequet-Antier C, Gautron J. Hen uterine gene expression profiling during eggshell formation reveals putative proteins involved in the supply of minerals or in the shell mineralization process. BMC Genomics 2014;15:220.

[74] Kitching R, Qi S, Li V, Raouf A, Vary CP, Seth A. Coordinate gene expression patterns during osteoblast maturation and retinoic acid treatment of MC3T3-E1 cells. J Bone Miner Metab 2002;20:269-80.

[75] Hopwood B, Tsykin A, Findlay DM, Fazzalari NL. Gene expression profile of the bone microenvironment in human fragility fracture bone. Bone 2009;44:87-101.

[76] Gautron J, Hincke MT, Mann K, Panhéleux M, Bain MM, McKee MD, Solomon SE, Nys Y. Ovocalyxin-32, a novel chicken eggshell matrix protein: isolation, amino acid sequencing, cloning and immunochemical localization. J Biol Chem 2001;276:39243.

[77] Dominguez-Vera JM, Gautron J, Garcia-Ruiz JM, Nys Y. The effect of avian uterine fluid on the growth behavior of calcite crystals. Poult Sci 2000;79:901-7.

[78] Gay CV, Faleski EJ, Schraer H, Schraer R. Localization of carbonic anhydrase in avian gastric mucosa, shell gland and bone by immunohistochemistry. J Histochem Cytochem 1974;22:819-25.

[79] Hincke M, Tsang C, Courtney M, Hill V, Narbaitz R. Purification and immunochemistry of a soluble matrix protein of the chicken eggshell (ovocleidin 17). Calcif Tissue Int 1995;56:578-83.

[80] Hincke MT, Gautron J, Tsang CP, McKee MD, Nys Y. Molecular cloning and ultrastructural localization of the core protein of an eggshell matrix proteoglycan, ovocleidin-116. J Biol Chem 1999;274:32915-23.

[81] Fermin CD, Lovett AE, Igarashi M, Dunner K,Jr. Immunohistochemistry and histochemistry of the inner ear gelatinous membranes and statoconia of the chick (Gallus domesticus). Acta Anat (Basel) 1990;138:75-83.

[82] Arias JL, Carrino DA, Fernandez MS, Rodriguez JP, Dennis JE, Caplan AI. Partial biochemical and immunochemical characterization of avian eggshell extracellular matrices. Arch Biochem Biophys 1992;298:293-302.

[83] Fernandez MS, Araya M, Arias JL. Eggshells are shaped by a precise spatio-temporal arrangement of sequentially deposited macromolecules. Matrix Biol 1997;16:13-20.

[84] Brylka L, Jahnen-Dechent W. The role of fetuin-A in physiological and pathological mineralization. Calcif Tissue Int 2013;93:355-64.

[85] Mann K, Olsen JV, Maček B, Gnad F, Mann M. Phosphoproteins of the chicken eggshell calcified layer. Proteomics 2007;7:106-15.

[86] Hincke MT, Chien YC, Gerstenfeld LC, McKee MD. Colloidal-gold immunocytochemical localization of osteopontin in avian eggshell gland and eggshell. J Histochem Cytochem 2008;56:467-76.

[87] Xu Y, Zhang H, Yang H, Zhao X, Lovas S, Lundberg YW. Expression, functional, and structural analysis of proteins critical for otoconia development. Dev Dyn 2010;239:2659-73.

[88] Maurer P, Hohenadl C, Hohenester E, Gohring W, Timpl R, Engel J. The C-terminal portion of BM-40 (SPARC/osteonectin) is an autonomously folding and crystallisable domain that binds calcium and collagen IV. J Mol Biol 1995;253:347-57.

Supplementary Data

Table S1. List of 49 proteins identified as being associated with the eggshell membrane (common to UF-0 and FE-15).

Identified Proteins[a]	UniProt Accession Number	Unique Peptides[b]		Normalized Total Spectra[b]		Coverage[b]	
		UF - 0	FE - 15	UF - 0	FE - 15	UF - 0	FE - 15
Lysozyme C	P00698	47	64	3573	3565	86%	86%
Ovalbumin	P01012	55	63	1204	815	91%	82%
Gallinacin-11	Q6IV20	23	24	924	426	74%	74%
Ovotransferrin	E1BQC2	73	43	587	171	78%	58%
Ovocleidin-116	F1NSM7	33	37	383	322	45%	43%
Ovocalyxin-36	Q53HW8	24	16	364	254	36%	33%
Gallin	D5GR55	15	17	318	201	71%	62%
Ovomucoid	P01005	16	12	157	112	58%	47%
PREDICTED: beta-microseminoprotein-like	UPI000350608B	9	12	125	138	66%	70%
Ovocleidin-17	Q9PRS8	8	19	51	199	68%	68%
Clusterin	Q9YGP0	19	21	135	84	35%	36%
Glutathione peroxidase	F1NPJ8	14	11	103	115	53%	46%
Riboflavin-binding protein	P02752	15	8	174	41	35%	27%
PREDICTED: EGF-like repeats and discoidin I-like domains 3 isoform X2	F1NCN3	22	25	115	97	43%	47%
Lactadherin isoform 2	E1C0K5	20	15	138	56	30%	24%
Vitelline membrane outer layer protein 1 (VMO-1)	P41366	16	15	83	101	71%	70%
Cystatin	P01038	6	7	45	89	41%	54%
Ovocalyxin-21 (gastrokine-2)	E1C2G7	9	8	62	71	61%	56%
Hep21 protein	Q8AV77	11	15	54	78	67%	69%
Alpha 1-acid glycoprotein	Q8JIG5	9	8	81	44	39%	39%
Ovalbumin-related protein X	R9TNA6	11	9	89	31	28%	22%
Extracellular fatty acid-binding protein	E1C0K1	10	12	57	59	38%	35%
Ovocalyxin-25 (LOC771972)	UPI000240C407	6	6	65	43	34%	36%

Gallinacin-10	Q6QLQ9	4	9	34	74	62%	62%
Lysyl oxidase homolog 2	E1C3U7	12	16	35	59	18%	24%
Ovoinhibitor	P10184	19	10	59	28	25%	27%
Ig lambda chain V-1 region	R9PXM5	5	2	68	10	32%	16%
Collagen alpha-1(X) chain	P08125	7	10	26	40	14%	14%
Ovoglobulin G2 type AA (TENP protein)	I0J172	10	6	36	24	39%	19%
PREDICTED: similar to spore coat protein sp45, partial	UPI000044A8C0	3	4	16	42	13%	14%
Fibronectin	F1NJT4	5	22	11	46	2%	12%
Cadherin-1	P08641	4	6	23	29	6%	6%
Ovostatin	P20740	9	11	24	26	6%	7%
Serum albumin	F2Z4L6	16	2	45	4	29%	3%
Avidin	P02701	6	4	32	16	44%	24%
Cochlin	O42163	3	10	14	34	9%	25%
Ovalbumin-related protein Y	E1BTF4	4	2	26	13	16%	8%
Cathepsin B	F1N9D8	7	9	20	15	24%	31%
PREDICTED: BPI fold-containing family C protein	UPI00035060A4	7	4	24	6	6%	4%
Apolipoprotein A-I	P08250	4	9	10	18	18%	29%
Calmodulin	P62149	2	6	5	20	7%	38%
Prostaglandin-H2 D-isomerase precursor	E1BTX1	3	4	8	15	17%	23%
Sulfhydryl oxidase 1	Q8JGM4	4	9	7	13	6%	11%
PREDICTED: somatomedin-B and thrombospondin type-1 domain-containing protein-like	F1NHA7	3	5	5	14	18%	31%
Programmed cell death protein 6	F1NHD8	2	6	5	10	11%	23%
Gallinacin-9	Q6QLR1	2	3	4	10	33%	48%
Plasminogen activator inhibitor type 1, member 2 precursor	E1BWU2	4	3	10	3	11%	13%
PREDICTED: mucin-5AC	E1C037	2	2	6	3	0%	0%
Beta-2-microglobulin	P21611	2	2	5	3	26%	26%

a. Proteins extracted with 0.01N HCl (see Materials and Methods, section 2.3)

b. Information obtained from Scaffold software, version 4.3.4

Table S2. List of 423 proteins identified in the eggshell membrane and/or mammillary cones of fertilized (FE) and unfertilized (UF) eggs.

Identified Proteins	UniProt Accession Number	Molecular Weight[a]	Unique peptides[a]				Normalized Total Spectra[a]				Percent coverage[a]			
			UF - 0[b]	UF - 30[b]	FE – 15[c]	FE – 19[c]	UF - 0	UF - 30	FE - 15	FE - 19	UF - 0	UF - 30	FE - 15	FE - 19
Lysozyme C	P00698	16 kDa	47	64	66	49	3573	3565	3718	3178	86%	86%	86%	88%
Ovalbumin	P01012	43 kDa	55	63	53	40	1204	815	698	866	91%	82%	84%	84%
Gallinacin-11	Q6IV20	12 kDa	23	24	19	27	924	426	275	770	74%	74%	76%	76%
Ovotransferrin	E1BQC2	78 kDa	73	43	65	82	587	171	454	677	78%	58%	77%	84%
Ovotransferrin CC type	Q4ADJ6	78 kDa	2	0	2	2	587	0	443	660	77%	0%	72%	77%
Ovocleidin-116	F1NSM7	77 kDa	33	37	28	51	383	322	307	592	45%	43%	40%	54%
PREDICTED: EGF-like repeats and discoidin I-like domains 3 isoform X2	F1NCN3	54 kDa	22	25	44	52	115	97	552	657	43%	47%	60%	71%
Ovocalyxin-36	Q53HW8	49 kDa	24	16	22	31	364	254	247	438	36%	33%	38%	42%
Clusterin	Q9YGP0	51 kDa	19	21	35	36	135	84	374	470	35%	36%	50%	48%
Gallin	D5GR55	7 kDa	15	17	10	13	318	201	150	190	71%	62%	64%	62%
Ovocleidin-17	V5NUE7	17 kDa	8	19	21	20	51	199	313	273	68%	68%	79%	70%
Lactadherin isoform 2	E1C0K5	59 kDa	20	15	32	30	138	56	239	260	30%	24%	44%	46%
Ovocalyxin-36	F1P1Y2	58 kDa	2	0	0	3	335	0	0	355	30%	0%	0%	35%
Ovomucoid	P01005	23 kDa	16	12	10	11	157	112	83	110	58%	47%	55%	69%
PREDICTED: beta-microseminoprotein-like	UPI0003506 08B	12 kDa	9	12	10	10	125	138	72	111	66%	70%	70%	70%
Riboflavin-binding protein	P02752	27 kDa	15	8	11	12	174	41	91	116	35%	27%	29%	29%
Glutathione peroxidase	F1NPJ8	25 kDa	14	11	8	14	103	115	58	97	53%	46%	40%	58%
Immunoglobulin alpha heavy chain	UPI0000117 60E	62 kDa	17	0	16	17	125	0	112	135	32%	0%	28%	31%
Serum albumin	F2Z4L6	64 kDa	16	2	36	41	45	4	128	168	29%	3%	59%	72%
Collagen alpha-1(X) chain	P08125	66 kDa	7	10	19	23	26	40	115	111	14%	14%	37%	37%
Ovostatin	P20740	166 kDa	9	11	37	28	24	26	173	67	6%	7%	25%	20%
Keratin, type II cytoskeletal cochleal	O93532	54 kDa	0	58	31	2	0	199	74	14	0%	80%	49%	10%

Cystatin	P01038	15 kDa	6	7	9	8	45	89	96	46	41%	54%	54%	59%
Ovalbumin-related protein X	R9TNA6	45 kDa	11	9	9	12	89	31	60	93	28%	22%	24%	30%
Vitelline membrane outer layer protein 1 (VMO-1)	P41366	20 kDa	16	15	6	18	83	101	32	55	71%	70%	34%	71%
Zona pellucida sperm-binding protein 3	P79762	47 kDa	0	15	22	0	0	101	169	0	0%	30%	36%	0%
Ovoinhibitor	P10184	52 kDa	19	10	12	23	59	28	47	128	25%	27%	32%	27%
Ovocalyxin-21 (gastrokine-2)	E1C2G7	21 kDa	9	8	5	11	62	71	28	94	61%	56%	28%	63%
Ovocalyxin-25 (LOC771972)	UPI000240C407	24 kDa	6	6	6	7	65	43	65	76	34%	36%	36%	41%
Fibronectin	F1NJT4	259 kDa	5	22	25	35	11	46	92	98	2%	12%	14%	18%
Hep21 protein	Q8AV77	12 kDa	11	15	12	13	54	78	53	56	67%	69%	69%	67%
Zona pellucida protein 1	Q9DER4	100 kDa	0	15	21	0	0	73	164	0	0%	20%	23%	0%
Alpha 1-acid glycoprotein	Q8JIG5	22 kDa	9	8	8	7	81	44	50	48	39%	39%	34%	37%
Lysyl oxidase homolog 2	E1C3U7	87 kDa	12	16	11	18	35	59	49	54	18%	24%	19%	25%
Gallinacin-10	Q6QLQ9	7 kDa	4	9	7	7	34	74	55	25	62%	62%	62%	68%
Extracellular fatty acid-binding protein	E1C0K1	20 kDa	10	12	4	13	57	59	15	46	38%	35%	21%	51%
polymeric immunoglobulin receptor precursor	UPI00004C9AD9	71 kDa	6	0	10	15	31	0	48	81	10%	0%	18%	24%
Keratin, type I cytoskeletal 19	F1NDN9	46 kDa	0	33	17	2	0	99	38	12	0%	60%	35%	7%
immunoglobulin Y heavy chain constant region, partial	UPI0000D6CA6F	61 kDa	10	0	0	10	86	0	0	60	27%	0%	0%	24%
Actin, cytoplasmic type 1, 2, 5	P53478	42 kDa	0	22	13	0	0	93	52	0	0%	57%	40%	0%
Hemoglobin subunit beta	P02112	16 kDa	0	4	8	0	0	76	68	0	0%	70%	57%	0%
Beta-H globin	Q90864	16 kDa	0	9	3	0	0	78	60	0	0%	64%	50%	0%
Ig lambda chain V-1 region	R9PXM5	24 kDa	5	2	4	4	68	10	21	36	32%	16%	26%	26%
Ovoglobulin G2 type AA	I0J172	47 kDa	10	6	7	10	36	24	32	44	39%	19%	18%	35%
PREDICTED: keratin, type II cytoskeletal 8	H9KZP2	42 kDa	0	27	15	0	0	89	45	0	0%	60%	42%	0%

Cadherin-1	P08641	98 kDa	4	6	9	9	23	29	50	32	6%	6%	9%	10%
Sulfhydryl oxidase 1	Q8JGM4	83 kDa	4	9	11	16	7	13	53	50	6%	11%	11%	26%
Immunoglobulin heavy chain variable region	UPI000044ACDE	26 kDa	0	0	4	2	45	0	37	40	13%	0%	22%	19%
Serine peptidase inhibitor, Kazal type 7 (SPINK7)	F1NMN2	44 kDa	0	0	0	4	0	0	0	122	0%	0%	0%	50%
Mucin-5B	Q98UI9	234 kDa	2	0	23	17	4	0	82	36	1%	0%	12%	9%
PREDICTED: keratin, type II cytoskeletal 8	UPI0000E82530	51 kDa	0	2	2	0	0	81	38	0	0%	42%	32%	0%
PREDICTED: BPI fold-containing family C protein	UPI00035060A4	103 kDa	7	4	7	6	24	6	44	33	6%	4%	7%	6%
Cochlin	O42163	59 kDa	3	10	11	8	14	34	41	14	9%	25%	26%	19%
Keratin, type I cytoskeletal 14	Q6PVZ1	51 kDa	0	22	13	0	0	69	31	0	0%	44%	29%	0%
Ovalbumin-related protein X	E1BTF4	44 kDa	4	2	4	5	26	13	31	28	16%	8%	11%	22%
PREDICTED: histone H3.2-like	UPI0000447264	82 kDa	0	3	7	0	0	61	37	0	0%	10%	8%	0%
Avidin	P02701	17 kDa	6	4	3	9	32	16	13	33	44%	24%	15%	57%
Apolipoprotein A-I	P08250	31 kDa	4	9	12	13	10	18	35	30	18%	29%	39%	47%
Histone H2B 1/2/3/4/6	P0C1H3	14 kDa	0	4	0	0	0	87	0	0	0%	64%	0%	0%
PREDICTED: keratin, type I cytoskeletal 12	UPI00004499EE	83 kDa	5	0	0	6	49	0	0	38	4%	0%	0%	4%
Malate dehydrogenase	E1BVT3	36 kDa	0	21	5	0	0	76	11	0	0%	61%	18%	0%
VH1 protein	A2N883	12 kDa	0	0	2	4	0	0	38	48	0%	0%	43%	48%
Ig gamma chain	UPI0000115DA8	54 kDa	3	0	2	3	51	0	7	27	30%	0%	10%	27%
PREDICTED: protein S100-A9-like	UPI000350548E	28 kDa	0	8	12	0	0	25	60	0	0%	27%	40%	0%
Ig mu chain C region	P01875	48 kDa	2	0	9	5	7	0	56	20	6%	0%	26%	18%
Keratin 6A	H9KZ27	57 kDa	7	0	2	8	29	0	28	27	9%	0%	12%	11%
Alpha-2-macroglobulin-like 1	F1NTK2	168 kDa	0	0	23	0	0	0	83	0	0%	0%	15%	0%
Ovocalyxin-32	C7G540	31 kDa	0	4	7	4	0	10	38	28	0%	14%	26%	19%
Cathepsin B	F1N9D8	38 kDa	7	9	10	13	20	15	21	20	24%	31%	33%	37%

PREDICTED: similar to spore coat protein sp45, partial	UPI000044A8C0	34 kDa	3	4	4	0	16	42	19	0	13%	14%	14%	0%
Vitellogenin-2	F1NFL6	205 kDa	0	9	26	0	0	15	62	0	0%	5%	15%	0%
Heat shock protein 10	O42283	12 kDa	0	18	4	0	0	68	7	0	0%	86%	29%	0%
EW135	U6C3W5	104 kDa	4	0	0	13	7	0	0	68	5%	0%	0%	18%
Hemoglobin subunit alpha-A	P01994	15 kDa	0	6	7	0	0	36	34	0	0%	53%	51%	0%
Immunoglobulin heavy chain variable region	UPI000011B1F0	13 kDa	0	0	2	2	0	0	32	36	0%	0%	27%	27%
PREDICTED: mucin-5AC	E1C037	453 kDa	2	2	7	14	6	3	26	33	0%	0%	2%	5%
Annexin A2	P17785	39 kDa	0	20	5	2	0	53	9	3	0%	49%	15%	6%
ATP synthase subunit alpha	F1NI22	60 kDa	0	14	0	0	0	64	0	0	0%	26%	0%	0%
PREDICTED: prostate stem cell antigen	F1NXM7	13 kDa	0	7	4	8	0	17	14	31	0%	44%	32%	44%
Actin, alpha cardiac muscle 1	P68034	42 kDa	0	2	0	0	0	62	0	0	0%	34%	0%	0%
Protein S100-A11	P24479	11 kDa	0	7	2	0	0	51	5	0	0%	55%	23%	0%
Histone H4 type VIII	P70081	12 kDa	0	9	4	0	0	38	17	0	0	56%	42%	0
Immunoglobulin heavy chain	H9KZ23	13 kDa	3	0	0	0	55	0	0	0	43%	0%	0%	0%
PREDICTED: prostatic acid phosphatase-like	UPI000240B515	44 kDa	0	0	12	8	0	0	31	24	0%	0%	40%	28%
myeloid protein 1 precursor	F1NEF7	35 kDa	0	13	0	0	0	55	0	0	0%	39%	0%	0%
ATP synthase subunit beta, mitochondrial	Q5ZLC5	57 kDa	0	12	7	0	0	39	13	0	0%	28%	18%	0%
VH1 protein	A2N884	12 kDa	0	0	0	2	0	0	0	52	0%	0%	0%	47%
Hemopexin	H9L385	45 kDa	0	5	7	7	0	10	24	17	0%	16%	22%	22%
Apolipoprotein B	Q197X2	523 kDa	0	0	30	0	0	0	51	0	0%	0%	7%	0%
ABI family, member 3 (NESH) binding protein (ABI3BP)	E1C0S4	167 kDa	0	0	9	12	0	0	29	20	0%	0%	7%	10%
ATP synthase, H+ transporting, mitochondrial F1 complex, O subunit	F1P304	25 kDa	0	12	0	0	0	47	0	0	0%	54%	0%	0%
Plasminogen activator inhibitor type 1, member 2	E1BWU2	49 kDa	4	3	6	12	10	3	17	17	11%	13%	18%	37%

precursor														
EW135 (88% identity)	UPI00003AF026	79 kDa	0	0	0	2	0	0	0	46	0%	0%	0%	15%
Keratin, type I cytoskeletal 10	UPI00003AC98B	60 kDa	2	0	0	2	28	0	0	19	4%	0%	0%	3%
Ovostatin-like	F1NEW8	165 kDa	2	0	10	10	5	0	18	23	2%	0%	8%	8%
Gallinacin-7	E1AFV0	7 kDa	0	5	2	2	0	32	9	5	0%	71%	20%	48%
Hemoglobin subunit rho (97% identity)	P02127	16 kDa	0	4	0	0	0	45	0	0	0%	56%	0%	0%
L-lactate dehydrogenase B chain	P00337	36 kDa	0	9	8	2	0	25	18	2	0%	31%	26%	6%
PREDICTED: alpha-2-antiplasmin isoform X1	UPI0000E81365	57 kDa	0	0	0	11	0	0	0	44	0%	0%	0%	24%
Annexin A5	P17153	36 kDa	0	12	7	3	0	27	12	4	0%	33%	22%	10%
Immunoglobulin heavy chain variable region	UPI000044A215	26 kDa	0	0	5	0	0	0	43	0	0%	0%	23%	0%
Apolipoprotein D	Q5G8Y9	22 kDa	5	0	3	8	12	0	5	25	25%	0%	16%	38%
60 kDa heat shock protein, mitochondrial	Q5ZL72	61 kDa	0	14	0	0	0	42	0	0	0%	31%	0%	0%
PIT54 protein precursor	UPI0000611E49	80 kDa	0	0	6	3	0	0	13	28	0%	0%	11%	11%
Hemoglobin subunit alpha-D	P02001	16 kDa	0	7	5	0	0	27	14	0	0%	55%	55%	0%
Vimentin	F1NJ08	53 kDa	0	21	0	0	0	41	0	0	0%	46%	0%	0%
PREDICTED: protein S100-A9-like	UPI0003504D25	14 kDa	0	5	7	0	0	5	33	0	0%	66%	68%	0%
PREDICTED: beta-microseminoprotein A1-like	E1BXW5	13 kDa	0	4	0	3	0	25	0	13	0%	28%	0%	32%
Proactivator polypeptide	E1BSP1	58 kDa	0	2	3	13	0	3	6	28	0%	3%	7%	31%
PREDICTED: uncharacterized protein LOC771972	F1NPR2	14 kDa	2	0	0	0	37	0	0	0	28%	0%	0%	0%
PREDICTED: similar to keratin 18, partial	UPI000044ACE9	27 kDa	0	10	4	0	0	26	11	0	0%	27%	14%	0%
Carbonic anhydrase IV	E1C004	38 kDa	0	2	4	3	0	4	23	9	0%	5%	10%	8%
PREDICTED: somatomedin-B and thrombospondin type-1	F1NHA7	27 kDa	3	5	4	2	5	14	14	3	18%	31%	31%	8%

domain-containing protein-like														
Nucleobindin-2	F1NGB1	54 kDa	0	0	5	9	0	0	10	24	0%	0%	13%	23%
Prostaglandin-H2 D-isomerase precursor	E1BTX1	21 kDa	3	4	2	2	8	15	5	3	17%	23%	11%	10%
Carboxypeptidase A2	E1C2B2	47 kDa	0	5	7	0	0	17	14	0	0%	12%	15%	0%
Trypsin inhibitor ClTI-1	P85000	6 kDa	2	0	0	2	17	0	0	14	40%	0%	0%	40%
Cytochrome c oxidase subunit 5A, mitochondrial isoform 1, 2 (predicted)	E1C043	17 kDa	0	8	2	0	0	27	3	0	0%	42%	19%	0%
Aminopeptidase N	O57579	109 kDa	3	0	0	11	7	0	0	23	3%	0%	0%	12%
Immunoglobulin J polypeptide	E1BY93	18 kDa	4	0	0	5	13	0	0	17	29%	0%	0%	29%
Astacin-like metalloendopeptidase	P0DJJ2	46 kDa	0	3	6	0	0	8	20	0	0%	10%	18%	0%
Keratin, type I cytoskeletal 12	F1NDN6	54 kDa	0	2	2	0	0	15	12	0	0%	7%	6%	0%
Histone H1.11R	F1NME1	22 kDa	0	6	0	0	0	25	0	0	0%	22%	0%	0%
Calmodulin	P62149	17 kDa	2	6	0	0	5	20	0	0	7%	38%	0%	0%
Peroxiredoxin 3	E1BR10	28 kDa	0	8	0	0	0	25	0	0	0%	33%	0%	0%
Peptidyl-prolyl cis-trans isomerase B	P24367	24 kDa	0	6	3	0	0	14	11	0	0%	31%	14%	0%
Serpin peptidase inhibitor, clade F, member 1	E1C7H6	110 kDa	3	0	6	0	6	0	18	0	3%	0%	5%	0%
zona pellucida protein D	Q766V2	47 kDa	0	2	9	0	0	3	21	0	0%	5%	13%	0%
Glyceraldehyde-3-phosphate dehydrogenase	P00356	36 kDa	0	9	0	0	0	24	0	0	0%	39%	0%	0%
NADH dehydrogenase [ubiquinone] 1 alpha subcomplex subunit 2	F1NDF3	11 kDa	0	4	2	0	0	20	3	0	0%	39%	25%	0%
Polyadenylate-binding protein 1	Q5ZL53	71 kDa	0	10	0	0	0	23	0	0	0%	16%	0%	0%
Serpin H1	P13731	46 kDa	0	10	0	0	0	23	0	0	0%	24%	0%	0%
Alpha 1 type II procollagen	Q7T2Z7	120 kDa	0	0	4	8	0	0	6	16	0%	0%	5%	8%
Tiarin-like	Q25C35	56 kDa	0	0	8	3	0	0	17	5	0%	0%	19%	7%

SPARC	F1P291	34 kDa	0	0	2	5	0	0	5	17	0%	0%	8%	17%
Prohibitin transcript variant 2	D5M8S3	30 kDa	0	7	5	0	0	15	7	0	0%	28%	20%	0%
Cytochrome c	P67881	12 kDa	0	6	0	0	0	22	0	0	0%	46%	0%	0%
Neuroserpin	Q90935	47 kDa	0	3	3	6	0	5	7	10	0%	10%	10%	15%
Sciellin	R4GG61	44 kDa	0	3	6	0	0	5	16	0	0%	8%	13%	0%
PREDICTED: keratin, type I cytoskeletal 18-like	R4GKA1	19 kDa	0	4	3	0	0	13	9	0	0%	37%	30%	0%
Hydroxyacyl-coenzyme A dehydrogenase, mitochondrial	E1BZH9	34 kDa	0	12	0	0	0	21	0	0	0%	34%	0%	0%
PREDICTED: cytokine-like 1	F1NSV3	15 kDa	0	8	3	0	0	16	4	0	0%	55%	26%	0%
Histone H5	P02259	21 kDa	0	6	2	0	0	16	4	0	0%	26%	16%	0%
PREDICTED: hyaluronan and proteoglycan link protein 3	E1BUN0	41 kDa	0	0	7	2	0	0	17	4	0%	0%	20%	6%
similar to immunoglobulin lambda chain	F1NSC8	12 kDa	2	0	0	0	20	0	0	0	35%	0%	0%	0%
Antimicrobial peptide CHP1	P80389	4 kDa	0	3	2	0	0	13	7	0	0%	64%	46%	0%
PREDICTED: mesothelin-like protein-like	UPI0003503633	82 kDa	0	2	5	0	0	7	13	0	0%	2%	7%	0%
Annexin A8	E1C8K3	37 kDa	0	12	0	0	0	20	0	0	0%	39%	0%	0%
Elongation factor 1-alpha 1	Q90835	50 kDa	0	7	0	0	0	20	0	0	0%	17%	0%	0%
Myosin light polypeptide 6	P02607	17 kDa	0	6	0	0	0	20	0	0	0%	56%	0%	0%
Gallinacin-9	Q6QLR1	7 kDa	2	3	3	0	4	10	6	0	33%	48%	48%	0%
78 kDa glucose-regulated protein	Q90593	72 kDa	0	6	7	0	0	9	11	0	0%	12%	15%	0%
Programmed cell death protein 6	F1NHD8	22 kDa	2	6	0	2	5	10	0	4	11%	23%	0%	11%
Secretory trypsin inhibitor	UPI00003AAAEA	8 kDa	0	2	4	0	0	9	10	0	0%	42%	46%	0%
immunoglobulin heavy chain variable region	UPI000011B1F7	11 kDa	4	0	2	0	14	0	4	0	51%	0%	39%	0%
PREDICTED: tumor necrosis factor receptor superfamily member 6B	F1NCY6	34 kDa	2	0	0	3	10	0	0	9	8%	0%	0%	12%

PREDICTED: EGF containing fibulin-like extracellular matrix protein 1	E1C6M8	66 kDa	4	0	3	6	6	0	5	7	9%	0%	5%	11%
Peptidyl-prolyl cis-trans isomerase	D0EKR3	18 kDa	0	8	0	0	0	18	0	0	0%	40%	0%	0%
Galactosylceramidase	F1NJ89	77 kDa	4	0	4	0	10	0	9	0	7%	0%	7%	0%
PREDICTED: protein disulfide-isomerase A6 isoform 2	F1NK96	49 kDa	0	8	0	0	0	17	0	0	0%	22%	0%	0%
Gelsolin	F1NKF3	86 kDa	0	4	2	0	0	12	5	0	0%	6%	3%	0%
ADP/ATP translocase 3	F1NJ10	35 kDa	0	4	5	0	0	6	11	0	0%	11%	15%	0%
Receptor protein tyrosine phosphatase LAR	A3FB57	201 kDa	0	0	0	11	0	0	0	17	0%	0%	0%	7%
Elongation factor Tu, mitochondrial	P84172	38 kDa	0	7	2	0	0	14	3	0	0%	25%	7%	0%
Aspartate aminotransferase, mitochondrial	P00508	47 kDa	0	10	0	0	0	16	0	0	0%	31%	0%	0%
PREDICTED: ES1 protein homolog, mitochondrial isoform X2	E1C2F4	24 kDa	0	8	0	0	0	16	0	0	0%	44%	0%	0%
60S ribosomal protein L27	P61355	16 kDa	0	6	0	0	0	16	0	0	0%	49%	0%	0%
Dynein, light chain, LC8-type 1	F6UQS5	11 kDa	0	6	0	0	0	16	0	0	0%	52%	0%	0%
Heterogeneous nuclear ribonucleoprotein H3	Q5F3D2	37 kDa	0	5	0	0	0	16	0	0	0%	23%	0%	0%
45 kDa calcium-binding protein	Q5ZKE5	42 kDa	0	0	0	7	0	0	0	16	0%	0%	0%	22%
Mesencephalic astrocyte-derived neurotrophic factor (99% identity)	UPI0000ECAE4A	20 kDa	0	9	0	0	0	15	0	0	0%	49%	0%	0%
Nucleoside diphosphate kinase	O57535	17 kDa	0	7	0	0	0	15	0	0	0%	52%	0%	0%
Mitochondrial ubiquinol-cytochrome-c reductase complex core protein 2	D0VX29	47 kDa	0	6	0	0	0	15	0	0	0%	15%	0%	0%
Type I alpha-keratin 15	Q6PVZ2	48 kDa	0	2	0	0	0	15	0	0	0%	12%	0%	0%

Charged multivesicular body protein 4b	Q5ZHP5	25 kDa	0	4	3	2	0	6	6	3	0%	17%	12%	12%
Beta-2-microglobulin	P21611	13 kDa	2	2	2	2	5	3	4	4	26%	26%	26%	26%
Golgi apparatus protein 1	Q02391	130 kDa	0	0	4	6	0	0	5	10	0%	0%	3%	6%
Vitellogenin-1	P87498	211 kDa	0	5	6	0	0	6	9	0	0%	3%	4%	0%
PREDICTED: 2,4-dienoyl-CoA reductase, mitochondrial	E1BXS5	36 kDa	0	9	0	0	0	15	0	0	0%	25%	0%	0%
Stress-70 protein, mitochondrial	F1NZ86	73 kDa	0	8	0	0	0	15	0	0	0%	16%	0%	0%
40S ribosomal protein S10	E1C4N0	19 kDa	0	6	0	0	0	15	0	0	0%	33%	0%	0%
Gallinacin-2	E1AFU7	4 kDa	0	3	2	0	0	9	5	0	0%	91%	49%	0%
Pro-neuropeptide Y	P28673	11 kDa	2	0	0	4	4	0	0	11	22%	0%	0%	39%
Tsukushin	F1NDH7	39 kDa	2	0	2	3	4	0	2	8	7%	0%	7%	12%
Fructose-1,6-bisphosphatase	F6QGI8	45 kDa	0	8	0	0	0	14	0	0	0%	23%	0%	0%
Transcription factor A, mitochondrial	F1NG46	30 kDa	0	8	0	0	0	14	0	0	0%	31%	0%	0%
PREDICTED: aminoacyl tRNA synthase complex-interacting multifunctional protein 1 (92% identity)	UPI0000610D6B	39 kDa	0	7	0	0	0	14	0	0	0%	20%	0%	0%
Ribosomal protein S18	UPI00000FBFC1	18 kDa	0	6	0	0	0	14	0	0	0%	33%	0%	0%
Tubulin beta-7 chain	P09244	50 kDa	0	6	0	0	0	14	0	0	0%	16%	0%	0%
Lamin-A	P13648	73 kDa	0	5	0	0	0	14	0	0	0%	11%	0%	0%
Myosin regulatory light chain 2, smooth muscle minor isoform	UPI0000ECCE36	20 kDa	0	5	0	0	0	14	0	0	0%	24%	0%	0%
Amyloid beta A4 protein precursor	E1C440	83 kDa	0	4	0	0	0	14	0	0	0%	6%	0%	0%
Stathmin-3	F1N9N4	16 kDa	0	3	0	6	0	5	0	9	0%	14%	0%	39%
Annexin A1	F1N9S7	39 kDa	0	6	3	0	0	9	4	0	0%	20%	9%	0%
PREDICTED: galactocerebrosidase isoform	F1NJ89	77 kDa	0	0	0	6	0	0	0	13	0%	0%	0%	10%

Dickkopf-related protein 3	Q90839	39 kDa	0	0	0	5	0	0	0	13	0%	0%	0%	20%
Cysteine-rich secretory protein 2	F1NFI1	27 kDa	0	5	2	0	0	10	3	0	0%	23%	5%	0%
Annexin A6	E1BWX1	87 kDa	0	3	6	0	0	5	9	0	0%	5%	11%	0%
PREDICTED: teneurin-4	F1NVT4	301 kDa	0	2	5	0	0	5	9	0	0%	1%	2%	0%
3-ketoacyl-CoA thiolase, mitochondrial	F1N8J0	42 kDa	0	7	0	0	0	13	0	0	0%	29%	0%	0%
Actin-related protein 2/3 complex, subunit 3	E1C8Y3	21 kDa	0	7	0	0	0	13	0	0	0%	43%	0%	0%
Serine/arginine-rich splicing factor 1	Q5ZML3	28 kDa	0	7	0	0	0	13	0	0	0%	23%	0%	0%
Cathepsin Z	E1C4M3	34 kDa	0	5	0	0	0	13	0	0	0%	14%	0%	0%
40S ribosomal protein S15	F2Z4M3	17 kDa	0	2	0	0	0	13	0	0	0%	9%	0%	0%
Histone H2A.V	P02272	14 kDa	0	2	0	0	0	13	0	0	0%	26%	0%	0%
Metalloproteinase inhibitor 3-like	R4GFR4	20 kDa	0	5	0	3	0	8	0	4	0%	26%	0%	22%
Beta-defensin 1 antimicrobial peptide	E5KV53	7 kDa	0	2	2	0	0	8	4	0	0%	28%	28%	0%
PREDICTED: uncharacterized protein LOC419301	UPI0003504 5B0	42 kDa	0	0	2	4	0	0	5	7	0%	0%	4%	9%
PREDICTED: aldehyde dehydrogenase, mitochondrial	E1BT93	57 kDa	0	8	0	0	0	12	0	0	0%	17%	0%	0%
ATP synthase, H+ transporting, mitochondrial Fo complex, subunit d	E1C658	18 kDa	0	6	0	0	0	12	0	0	0%	37%	0%	0%
Lamin B2	F1NP51	68 kDa	0	6	0	0	0	12	0	0	0%	10%	0%	0%
Hemoglobin subunit pi	P02007	16 kDa	0	4	0	0	0	12	0	0	0%	42%	0%	0%
Tenascin	F1N8F4	199 kDa	0	0	0	7	0	0	0	12	0%	0%	0%	5%
PREDICTED: similar to spore coat protein sp45, partial (84% identity)	UPI0000ECB EAB	35 kDa	0	0	0	3	0	0	0	12	0%	0%	0%	12%
RAE1 RNA export 1 homolog	E1C7F8	47 kDa	0	7	0	0	0	11	0	0	0%	26%	0%	0%
Tropomyosin alpha-3 chain	Q5ZLJ7	29 kDa	0	7	0	0	0	11	0	0	0%	32%	0%	0%
40S ribosomal protein S13	Q6ITC7	17 kDa	0	6	0	0	0	11	0	0	0%	25%	0%	0%

PREDICTED: putative phospholipase B 81b isoform X2	E1BZF7	62 kDa	0	6	0	0	0	11	0	0	0%	11%	0%	0%
14-3-3 protein zeta	Q5ZKC9	28 kDa	0	5	0	0	0	11	0	0	0%	25%	0%	0%
Actin-related protein 2/3 complex, subunit 4	F1P010	20 kDa	0	5	0	0	0	11	0	0	0%	24%	0%	0%
Cytochrome b-c1 complex subunit 6	F1NHW5	10 kDa	0	3	0	0	0	11	0	0	0%	51%	0%	0%
Histone H2A.J	P70082	15 kDa	0	3	0	0	0	11	0	0	0%	34%	0%	0%
PREDICTED: gamma-glutamyltranspeptidase 1	F1NVY4	62 kDa	0	2	0	2	0	2	0	9	0%	4%	0%	4%
PREDICTED: polyubiquitin-C isoformX2	UPI0000449214	43 kDa	2	0	2	2	2	0	3	4	7%	0%	7%	7%
40S ribosomal protein S3	F1NPA9	27 kDa	0	7	0	0	0	10	0	0	0%	37%	0%	0%
PREDICTED: hydroxysteroid dehydrogenase-like protein 2-like isoform 1	E1C7S2	44 kDa	0	7	0	0	0	10	0	0	0%	20%	0%	0%
40S ribosomal protein S3a	F2Z4K7	30 kDa	0	6	0	0	0	10	0	0	0%	25%	0%	0%
Destrin	P18359	19 kDa	0	5	0	0	0	10	0	0	0%	32%	0%	0%
PREDICTED: eukaryotic translation elongation factor 1 epsilon-1	F1P4I1	20 kDa	0	5	0	0	0	10	0	0	0%	25%	0%	0%
Calumenin	UPI0000E8211C	8 kDa	0	0	2	2	0	0	6	4	0%	0%	18%	61%
GM2 ganglioside activator	R4GJV6	18 kDa	0	3	0	2	0	6	0	4	0%	18%	0%	10%
MAp19	Q6Q1Q7	76 kDa	0	2	2	0	0	5	5	0	0%	4%	4%	0%
PREDICTED: group 10 secretory phospholipase A2	E1C202	18 kDa	0	0	4	0	0	0	10	0	0%	0%	40%	0%
Endoplasmic reticulum resident protein 29	F1NRM8	29 kDa	0	6	0	0	0	9	0	0	0%	22%	0%	0%
PREDICTED: keratin, type I cytoskeletal 18-like	UPI0003506809	15 kDa	0	5	0	0	0	9	0	0	0%	31%	0%	0%
PREDICTED: similar to heteroproteinous nuclear ribonucleoprotein C	UPI0000E81CCD	8 kDa	0	5	0	0	0	9	0	0	0%	35%	0%	0%
V-type proton ATPase	Q5ZKJ9	26 kDa	0	5	0	0	0	9	0	0	0%	22%	0%	0%

subunit E 1														
Desmin	P02542	53 kDa	0	4	0	0	0	9	0	0	0%	13%	0%	0%
Cytochrome c oxidase subunit 6C	E1BW78	9 kDa	0	3	0	0	0	9	0	0	0%	39%	0%	0%
Lymphocyte antigen 86	F1P4F3	18 kDa	0	2	0	2	0	5	0	4	0%	15%	0%	15%
Epithelial cell adhesion molecule	Q5F381	34 kDa	0	2	3	0	0	4	5	0	0%	4%	7%	0%
Collagen, type V, alpha 2	R4GM21	124 kDa	0	0	0	5	0	0	0	9	0%	0%	0%	6%
Moesin	E1BV34	69 kDa	0	0	3	2	0	0	4	4	0%	0%	5%	3%
PREDICTED: exostoses (multiple)-like 2	R4GMG4	38 kDa	0	3	2	0	0	5	3	0	0%	10%	8%	0%
Fibrinogen alpha chain	P14448	82 kDa	0	0	5	0	0	0	9	0	0%	0%	12%	0%
Integrin beta	F1N8N7	89 kDa	0	0	5	0	0	0	9	0	0%	0%	6%	0%
PREDICTED: transmembrane protease serine 9	F1NP62	117 kDa	0	0	4	0	0	0	9	0	0%	0%	4%	0%
Enoyl-CoA hydratase, mitochondrial precursor	F1NR44	32 kDa	0	6	0	0	0	8	0	0	0%	24%	0%	0%
PREDICTED: splicing factor, proline- and glutamine-rich isoform X5	F1P555	70 kDa	0	6	0	0	0	8	0	0	0%	10%	0%	0%
Sorcin	F1NUE0	80 kDa	0	6	0	0	0	8	0	0	0%	8%	0%	0%
ATP synthase subunit gamma	H9KZF8	33 kDa	0	5	0	0	0	8	0	0	0%	17%	0%	0%
Eukaryotic translation initiation factor 3 subunit F	E1C050	35 kDa	0	5	0	0	0	8	0	0	0%	18%	0%	0%
Guanine nucleotide-binding protein subunit beta-2-like 1	P63247	35 kDa	0	5	0	0	0	8	0	0	0%	18%	0%	0%
PREDICTED: cytochrome b-c1 complex subunit 1, mitochondrial	F1NAC6	56 kDa	0	4	0	0	0	8	0	0	0%	7%	0%	0%
12K serum protein, beta-2-m cross-reactive	Q7LZS1	12 kDa	0	2	0	2	0	5	0	4	0%	23%	0%	23%
Leucine zipper protein 2	E1BVD3	39 kDa	0	0	0	5	0	0	0	8	0%	0%	0%	15%
Out at first protein homolog	Q71SY6	31 kDa	0	0	2	2	0	0	3	4	0%	0%	8%	8%
Electron-transfer-	F1N9U8	37 kDa	0	5	0	0	0	7	0	0	0%	22%	0%	0%

flavoprotein, alpha polypeptide														
Heat shock cognate 71 kDa protein	F1NWP3	71 kDa	0	5	0	0	0	7	0	0	0%	11%	0%	0%
Nucleolin	P15771	76 kDa	0	5	0	0	0	7	0	0	0%	7%	0%	0%
PREDICTED: dnaJ homolog subfamily B member 11	F1NVY5	41 kDa	0	5	0	0	0	7	0	0	0%	12%	0%	0%
Translocase of inner mitochondrial membrane 8 homolog A	F1NIC5	12 kDa	0	5	0	0	0	7	0	0	0%	52%	0%	0%
Fructose-bisphosphate aldolase B	P07341	39 kDa	0	4	0	0	0	7	0	0	0%	15%	0%	0%
PREDICTED: 40S ribosomal protein S16 isoform X3	R4GGJ0	16 kDa	0	4	0	0	0	7	0	0	0%	21%	0%	0%
serine/arginine-rich splicing factor 7	UPI0000612 5B9	29 kDa	0	4	0	0	0	7	0	0	0%	21%	0%	0%
SWI/SNF related, matrix associated, actin dependent regulator of chromatin, subfamily e, member 1	F1NCC9	47 kDa	0	4	0	0	0	7	0	0	0%	12%	0%	0%
Phosphoglycerate kinase	F1NU17	45 kDa	0	3	0	0	0	7	0	0	0%	9%	0%	0%
PREDICTED: tubulin alpha-3 chain	F1N9J7	50 kDa	0	3	0	0	0	7	0	0	0%	10%	0%	0%
Protein S100-A10	P27003	11 kDa	0	3	0	0	0	7	0	0	0%	32%	0%	0%
Serine/arginine-rich splicing factor 6	E1C270	40 kDa	0	3	0	0	0	7	0	0	0%	10%	0%	0%
PREDICTED: leucine zipper protein 1 isoform X4	R4GHN9	123 kDa	2	0	0	0	7	0	0	0	2%	0%	0%	0%
Hydroxyacyl-CoA dehydrogenase/3-ketoacyl-CoA thiolase/enoyl-CoA hydratase (trifunctional protein), alpha subunit (HADHA), nuclear gene encoding mitochondrial protein	F1NI29	86 kDa	0	2	4	0	0	2	5	0	0%	2%	6%	0%
Transthyretin	P27731	16 kDa	0	0	3	2	0	0	4	3	0%	0%	39%	24%

Voltage-dependent anion-selective channel protein 2	Q9I9D1	30 kDa	0	0	4	0	0	0	6	0	0%	0%	18%	0%
39S ribosomal protein L12, mitochondrial	UPI000240C392	21 kDa	0	5	0	0	0	6	0	0	0%	30%	0%	0%
NADH dehydrogenase [ubiquinone] 1 alpha subcomplex subunit 8 isoform 1	UPI0000449363	127 kDa	0	5	0	0	0	6	0	0	0%	3%	0%	0%
Pyruvate dehydrogenase E1 component subunit beta, mitochondrial	F1N823	40 kDa	0	5	0	0	0	6	0	0	0%	17%	0%	0%
Serine protease	O42417	43 kDa	0	5	0	0	0	6	0	0	0%	12%	0%	0%
14-3-3 protein epsilon	Q5ZMT0	29 kDa	0	4	0	0	0	6	0	0	0%	17%	0%	0%
39S ribosomal protein L44, mitochondrial precursor	E1C5L8	36 kDa	0	4	0	0	0	6	0	0	0%	12%	0%	0%
Eukaryotic translation initiation factor 3 subunit I	E1C6T8	36 kDa	0	4	0	0	0	6	0	0	0%	14%	0%	0%
Citrate synthase	R4GLP7	43 kDa	0	3	0	0	0	6	0	0	0%	7%	0%	0%
Small nuclear ribonucleoprotein-associated protein B	R9PXM6	47 kDa	0	3	0	0	0	6	0	0	0%	5%	0%	0%
40S ribosomal protein S7 isoformX6	F1NN16	42 kDa	0	2	0	0	0	6	0	0	0%	4%	0%	0%
Immunoglobulin heavy chain variable region	UPI00003AF500	12 kDa	0	0	0	3	0	0	0	6	0%	0%	0%	35%
Glutathione S-transferase	Q08392	20 kDa	3	0	0	0	6	0	0	0	14%	0%	0%	0%
Coagulation factor VIII	F1NPT2	230 kDa	0	0	2	2	0	0	3	3	0%	0%	1%	2%
Acetyltransferase component of pyruvate dehydrogenase complex	E1C6N5	67 kDa	0	4	0	0	0	5	0	0	0%	6%	0%	0%
Calpain small subunit	O42134	24 kDa	0	4	0	0	0	5	0	0	0%	19%	0%	0%
Coatomer subunit epsilon	Q5ZIK9	34 kDa	0	4	0	0	0	5	0	0	0%	16%	0%	0%
PREDICTED: ATP synthase subunit b, mitochondrial	F1NSC1	29 kDa	0	4	0	0	0	5	0	0	0%	19%	0%	0%
Annexin A4	H9KZI4	36 kDa	0	3	0	0	0	5	0	0	0%	11%	0%	0%
DNA-directed RNA	E1BSD8	17 kDa	0	3	0	0	0	5	0	0	0%	21%	0%	0%

polymerases I, II, and III subunit RPABC3 isoform 1														
EGF containing fibulin-like extracellular matrix protein 1	E1C6M8	51 kDa	0	3	0	0	0	5	0	0	0%	6%	0%	0%
NADH dehydrogenase [ubiquinone] 1 alpha subcomplex subunit 5	E1BRT9	13 kDa	0	3	0	0	0	5	0	0	0%	31%	0%	0%
Palmitoyl-protein thioesterase 1 precursor	F1NYK1	34 kDa	0	3	0	0	0	5	0	0	0%	12%	0%	0%
PREDICTED: 3-hydroxyacyl-CoA dehydrogenase type-2, partial	H9L135	24 kDa	0	3	0	0	0	5	0	0	0%	15%	0%	0%
PREDICTED: adenylate kinase 2, mitochondrial	F1NJ73	27 kDa	0	3	0	0	0	5	0	0	0%	13%	0%	0%
PREDICTED: anterior gradient protein 2 homolog isoformX2	E1C937	20 kDa	0	3	0	0	0	5	0	0	0%	16%	0%	0%
PREDICTED: enoyl-CoA hydratase domain-containing protein 2, mitochondrial	F1NSS6	31 kDa	0	3	0	0	0	5	0	0	0%	11%	0%	0%
PREDICTED: hydroxyacyl-CoA dehydrogenase/3-ketoacyl-CoA thiolase/enoyl-CoA hydratase (trifunctional protein), beta subunit (HADHB), transcript variant X5	E1BTT4	51 kDa	0	3	0	0	0	5	0	0	0%	6%	0%	0%
Prohibitin-2	F1N833	31 kDa	0	3	0	0	0	5	0	0	0%	9%	0%	0%
stomatin (EPB72)-like 2	F1P0P3	39 kDa	0	3	0	0	0	5	0	0	0%	11%	0%	0%
ATP synthase, H+ transporting, mitochondrial F1 complex, delta subunit	R4GKB8	7 kDa	0	2	0	0	0	5	0	0	0%	33%	0%	0%
Gallinacin-6	Q6QLR3	8 kDa	0	2	0	0	0	5	0	0	0%	34%	0%	0%
KIAA0319-like	E1C633	123 kDa	0	2	0	0	0	5	0	0	0%	1%	0%	0%

Basement membrane-specific heparan sulfate proteoglycan core protein	Q6KDZ1	433 kDa	0	2	0	2	0	2	0	4	0%	1%	0%	1%
Actin, cytoplasmic 2-like (99% identity)	Q5ZMQ2	45 kDa	0	0	0	3	0	0	0	5	0%	0%	0%	8%
Alpha-2-HS-glycoprotein	E1BZE1	37 kDa	0	0	0	3	0	0	0	5	0%	0%	0%	8%
Procollagen-lysine,2-oxoglutarate 5-dioxygenase 1	F1NMF6	84 kDa	0	0	2	0	0	0	5	0	0%	0%	3%	0%
PREDICTED: AP-1 complex subunit beta-1 isoform	E1BY12	106 kDa	0	4	0	0	0	5	0	0	0%	3%	0%	0%
PREDICTED: phosphatidylinositide phosphatase SAC1	F1NK59	87 kDa	0	4	0	0	0	5	0	0	0%	7%	0%	0%
Thioredoxin	P08629	12 kDa	0	4	0	0	0	5	0	0	0%	42%	0%	0%
40S ribosomal protein S14	Q5ZHW8	16 kDa	0	3	0	0	0	5	0	0	0%	24%	0%	0%
Cell surface glycoprotein MUC18 precursor	F1NXW9	69 kDa	0	3	0	0	0	5	0	0	0%	6%	0%	0%
Heterogeneous nuclear ribonucleoprotein A/B	F1NIB4	25 kDa	0	3	0	0	0	5	0	0	0%	18%	0%	0%
Heterogeneous nuclear ribonucleoprotein M	Q5ZL80	76 kDa	0	3	0	0	0	5	0	0	0%	5%	0%	0%
High mobility group protein B1	Q9YH06	25 kDa	0	3	0	0	0	5	0	0	0%	7%	0%	0%
PREDICTED: poly(rC)-binding protein 2-like	H9L011	48 kDa	0	3	0	0	0	5	0	0	0%	8%	0%	0%
Protein NipSnap homolog 2	F1NZ68	33 kDa	0	3	0	0	0	5	0	0	0%	10%	0%	0%
Protein syndesmos	Q9IAY5	33 kDa	0	3	0	0	0	5	0	0	0%	11%	0%	0%
3,2-trans-enoyl-CoA isomerase, mitochondrial	E1C3T6	33 kDa	0	2	0	0	0	5	0	0	0%	9%	0%	0%
Glutathione S-transferase kappa 1	F1N9G6	25 kDa	0	2	0	0	0	5	0	0	0%	10%	0%	0%
PREDICTED: ATP synthase subunit epsilon-like protein, mitochondrial-like	UPI00003AC300	6 kDa	0	2	0	0	0	5	0	0	0%	35%	0%	0%
PREDICTED: peptidyl-tRNA hydrolase ICT1,	F1NND9	19 kDa	0	2	0	0	0	5	0	0	0%	12%	0%	0%

mitochondrial (99% identity)														
UPF0568 protein C14orf166 homolog	F1NA45	27 kDa	0	2	0	0	0	5	0	0	0%	12%	0%	0%
PREDICTED: cadherin-related family member 4	R4GFT8	77 kDa	0	0	0	3	0	0	0	4	0%	0%	0%	5%
Tenascin Y variant	Q91008	207 kDa	0	0	0	3	0	0	0	4	0%	0%	0%	2%
PREDICTED: inter-alpha-trypsin inhibitor heavy chain H5 isoform X2	E1BTM0	107 kDa	0	0	3	0	0	0	4	0	0%	0%	4%	0%
Immunoglobulin light-chain VJ region	UPI0000115 1E3	11 kDa	0	0	2	0	0	0	4	0	0%	0%	29%	0%
Integrin alpha-6	F1P0B0	115 kDa	0	0	2	0	0	0	4	0	0%	0%	2%	0%
Sclerostin domain-containing protein 1	Q6VYA3	23 kDa	0	0	2	0	0	0	4	0	0%	0%	9%	0%
LYR motif-containing protein 4	R4GGF7	10 kDa	0	4	0	0	0	4	0	0	0%	40%	0%	0%
17-beta-hydroxysteroid dehydrogenase type IV	O42484	80 kDa	0	3	0	0	0	4	0	0	0%	5%	0%	0%
Collagen, type XVIII, alpha 1	F1NW38	144 kDa	0	3	0	0	0	4	0	0	0%	2%	0%	0%
Hypothetical protein RCJMB04_33h2	Q5ZHT5	16 kDa	0	3	0	0	0	4	0	0	0%	23%	0%	0%
Mitochondrial cytochrome c1, heme protein	D0VX26	27 kDa	0	3	0	0	0	4	0	0	0%	20%	0%	0%
Phosphate carrier protein, mitochondrial	F1NZ24	40 kDa	0	3	0	0	0	4	0	0	0%	12%	0%	0%
Succinate dehydrogenase [ubiquinone] iron-sulfur subunit, mitochondrial	F1NNF7	33 kDa	0	3	0	0	0	4	0	0	0%	11%	0%	0%
60S ribosomal protein L30	P67883	13 kDa	0	2	0	0	0	4	0	0	0%	30%	0%	0%
Carboxypeptidase	F1NIN2	53 kDa	0	2	0	0	0	4	0	0	0%	6%	0%	0%
Clathrin light chain B	F1NUW5	28 kDa	0	2	0	0	0	4	0	0	0%	9%	0%	0%
Endoplasmic reticulum lectin 1	F1NCV8	55 kDa	0	2	0	0	0	4	0	0	0%	6%	0%	0%
Heterogeneous nuclear ribonucleoprotein D0	Q5ZIH1	29 kDa	0	2	0	0	0	4	0	0	0%	9%	0%	0%

NADH dehydrogenase [ubiquinone] 1 alpha subcomplex subunit 6	UPI0000E7F8AA	14 kDa	0	2	0	0	0	4	0	0	0%	20%	0%	0%
NADH dehydrogenase [ubiquinone] iron-sulfur protein 3, mitochondrial	F1ND23	29 kDa	0	2	0	0	0	4	0	0	0%	10%	0%	0%
Peroxiredoxin-1	P0CB50	22 kDa	0	2	0	0	0	4	0	0	0%	10%	0%	0%
PREDICTED: 60S ribosomal protein L23a (95% identity)	E1BS06	17 kDa	0	2	0	0	0	4	0	0	0%	14%	0%	0%
PREDICTED: coiled-coil-helix-coiled-coil-helix domain-containing protein 3, mitochondrial	UPI000044745B	30 kDa	0	2	0	0	0	4	0	0	0%	11%	0%	0%
PREDICTED: coiled-coil-helix-coiled-coil-helix domain-containing protein 6A, mitochondrial	E1C4D9	19 kDa	0	2	0	0	0	4	0	0	0%	16%	0%	0%
PREDICTED: transgelin-2-like	UPI000240CC5B	22 kDa	0	2	0	0	0	4	0	0	0%	10%	0%	0%
PREDICTED: U2 small nuclear ribonucleoprotein B'' isoform 2	R4GH36	26 kDa	0	2	0	0	0	4	0	0	0%	9%	0%	0%
Prefoldin subunit 2	R4GME1	18 kDa	0	2	0	0	0	4	0	0	0%	12%	0%	0%
Protein SEC13 homolog	E1BVC4	47 kDa	0	2	0	0	0	4	0	0	0%	5%	0%	0%
Ras-related protein Rab-1A	F6UGI5	22 kDa	0	2	0	0	0	4	0	0	0%	11%	0%	0%
Ubiquitin-40S ribosomal protein S27a	P79781	20 kDa	0	2	0	0	0	4	0	0	0%	16%	0%	0%
Adenomatous polyposis coli	E1BZS9	312 kDa	0	0	0	3	0	0	0	4	0%	0%	0%	1%
Apolipoprotein AIV	O93601	41 kDa	0	0	0	3	0	0	0	4	0%	0%	0%	14%
Mucin 6, oligomeric mucus/gel-forming	R9PXQ5	294 kDa	0	0	0	3	0	0	0	4	0%	0%	0%	1%
Corticotropin-releasing factor-binding protein isoform 1	E1C1R3	38 kDa	0	0	0	2	0	0	0	4	0%	0%	0%	6%
PREDICTED: carbohydrate sulfotransferase 12	UPI00004490B7	157 kDa	0	0	0	2	0	0	0	4	0%	0%	0%	2%

Receptor-type tyrosine-protein phosphatase delta precursor	UPI0000610489	218 kDa	0	0	0	2	0	0	0	4	0%	0%	0%	2%
Tenascin-R	Q00546	148 kDa	0	0	0	2	0	0	0	4	0%	0%	0%	2%
Plakoglobin	E1C1V3	82 kDa	0	0	3	0	0	0	3	0	0%	0%	5%	0%
Spectrin alpha chain, non-erythrocytic 1	F1NHT3	285 kDa	0	0	3	0	0	0	3	0	0%	0%	1%	0%
ATPase, H+ transporting, lysosomal accessory protein 2 (ATP6AP2)	F1NB42	39 kDa	0	0	2	0	0	0	3	0	0%	0%	5%	0%
Carboxypeptidase M precursor	E1C041	50 kDa	0	0	2	0	0	0	3	0	0%	0%	5%	0%
Cortactin-binding protein 2	A0M8U5	178 kDa	0	0	2	0	0	0	3	0	0%	0%	1%	0%
Interleukin 1 receptor accessory protein	E1C117	42 kDa	0	0	2	0	0	0	3	0	0%	0%	5%	0%
Syntenin-1	Q5ZHM8	32 kDa	0	0	2	0	0	0	3	0	0%	0%	7%	0%
Uroplakin 3B	F1P4N7	26 kDa	0	0	2	0	0	0	3	0	0%	0%	5%	0%
Succinyl-CoA ligase [ADP-forming] subunit beta, mitochondrial	Q5F3B9	50 kDa	0	3	0	0	0	3	0	0	0%	7%	0%	0%
Uncharacterized protein	E1BYN5	196 kDa	0	3	0	0	0	3	0	0	0%	2%	0%	0%
ADP-ribosylation factor 5	Q5ZKR9	21 kDa	0	2	0	0	0	3	0	0	0%	8%	0%	0%
ATP synthase subunit f, mitochondrial	F1NIF9	84 kDa	0	2	0	0	0	3	0	0	0%	3%	0%	0%
Calpastatin	A4ZZ64	79 kDa	0	2	0	0	0	3	0	0	0%	4%	0%	0%
Collagen alpha-1(III) chain	P12105	121 kDa	0	2	0	0	0	3	0	0	0%	3%	0%	0%
Desmocollin-2	F1NJD7	98 kDa	0	2	0	0	0	3	0	0	0%	3%	0%	0%
Eukaryotic translation initiation factor 3 subunit E	Q5ZLA5	52 kDa	0	2	0	0	0	3	0	0	0%	5%	0%	0%
Eukaryotic translation initiation factor 4E	R4GGL4	26 kDa	0	2	0	0	0	3	0	0	0%	10%	0%	0%
Exosome component 7	E1BXI2	32 kDa	0	2	0	0	0	3	0	0	0%	8%	0%	0%
Glutathione peroxidase	Q8QG67	19 kDa	0	2	0	0	0	3	0	0	0%	13%	0%	0%
Isocitrate dehydrogenase [NADP]	F1NPG2	47 kDa	0	2	0	0	0	3	0	0	0%	6%	0%	0%

Lectin, mannose-binding 2	R4GG92	64 kDa	0	2	0	0	0	3	0	0	0%	4%	0%	0%
Mitochondrial inner membrane protein	Q5ZMI2	79 kDa	0	2	0	0	0	3	0	0	0%	6%	0%	0%
Peptidyl-prolyl cis-trans isomerase	R4GLM6	16 kDa	0	2	0	0	0	3	0	0	0%	18%	0%	0%
PREDICTED: 26S proteasome non-ATPase regulatory subunit 11	F1NPA2	48 kDa	0	2	0	0	0	3	0	0	0%	4%	0%	0%
PREDICTED: 28S ribosomal protein S23, mitochondrial	E1C2E9	22 kDa	0	2	0	0	0	3	0	0	0%	15%	0%	0%
PREDICTED: 40S ribosomal protein S25	F1NU56	15 kDa	0	2	0	0	0	3	0	0	0%	14%	0%	0%
PREDICTED: endonuclease G, mitochondrial isoform X3	UPI0000449 3C9	130 kDa	0	2	0	0	0	3	0	0	0%	2%	0%	0%
PREDICTED: tubulointerstitial nephritis antigen-like 1	F1N8G6	52 kDa	0	2	0	0	0	3	0	0	0%	6%	0%	0%
Ras-related C3 botulinum toxin substrate 1	F1N8D9	20 kDa	0	2	0	0	0	3	0	0	0%	10%	0%	0%
Retinoic acid receptor responder protein 2 precursor	F1NIP4	19 kDa	0	2	0	0	0	3	0	0	0%	11%	0%	0%
Succinyl-CoA ligase [GDP-forming] subunit beta, mitochondrial	UPI00003AA 96E	41 kDa	0	2	0	0	0	3	0	0	0%	5%	0%	0%
Tetraspanin	E1C992	29 kDa	0	2	0	0	0	3	0	0	0%	8%	0%	0%
Follistatin	Q90844	38 kDa	0	0	0	2	0	0	0	3	0%	0%	0%	7%
Glutathione S-transferase	Q9W6J3	21 kDa	0	0	0	2	0	0	0	3	0%	0%	0%	12%
Insulin-like growth factor-binding protein 3	A6N8N6	31 kDa	0	0	0	2	0	0	0	3	0%	0%	0%	7%
Pantetheinase precursor	E1BUA6	58 kDa	0	0	0	2	0	0	0	3	0%	0%	0%	5%
Serpin peptidase inhibitor, clade G (C1 inhibitor), member 1	F1NA58	52 kDa	0	0	0	2	0	0	0	3	0%	0%	0%	5%
PREDICTED: dynein heavy chain 1, axonemal	F1NWW4	480 kDa	0	0	2	0	0	0	2	0	0%	0%	1%	0%

PREDICTED: NAD(P) transhydrogenase, mitochondrial	E1C6A1	114 kDa	0	0	2	0	0	0	2	0	0%	0%	2%	0%
Trefoil factor 2	E1BZ37	14 kDa	0	0	2	0	0	0	2	0	0%	0%	11%	0%
Acetyl-CoA acetyltransferase, cytosolic	F1NT20	41 kDa	0	2	0	0	0	2	0	0	0%	5%	0%	0%
Filamin	Q90WF1	273 kDa	0	2	0	0	0	2	0	0	0%	1%	0%	0%
G protein-coupled receptor 98	F1NAC4	685 kDa	0	2	0	0	0	2	0	0	0%	1%	0%	0%
Heterogeneous nuclear ribonucleoprotein H	F1NEG6	57 kDa	0	2	0	0	0	2	0	0	0%	5%	0%	0%
Macrophage migration inhibitory factor	Q02960	12 kDa	0	2	0	0	0	2	0	0	0%	22%	0%	0%
Mitochondrial import inner membrane translocase subunit Tim10	E1BXY8	10 kDa	0	2	0	0	0	2	0	0	0%	31%	0%	0%
PDZ domain-containing protein 11	Q5ZIK2	16 kDa	0	2	0	0	0	2	0	0	0%	16%	0%	0%
PREDICTED: tight junction protein ZO-1	UPI0003504919	197 kDa	0	2	0	0	0	2	0	0	0%	1%	0%	0%
Serine peptidase inhibitor, Kunitz type 1	F1P2Y9	61 kDa	0	2	0	0	0	2	0	0	0%	4%	0%	0%
Small nuclear ribonucleoprotein Sm D3	Q5ZL58	14 kDa	0	2	0	0	0	2	0	0	0%	15%	0%	0%
Splicing factor 3B subunit 5	UPI00006106F8	10 kDa	0	2	0	0	0	2	0	0	0%	41%	0%	0%
Tight junction protein ZO-2	F1NK34	131 kDa	0	2	0	0	0	2	0	0	0%	2%	0%	0%
U2 small nuclear ribonucleoprotein A	F1NAC8	28 kDa	0	2	0	0	0	2	0	0	0%	8%	0%	0%
WD repeat-containing protein 61	F1NFT8	33 kDa	0	2	0	0	0	2	0	0	0%	6%	0%	0%
Collagen alpha-2(VI) chain	R4GKA6	102 kDa	0	0	0	2	0	0	0	2	0%	0%	0%	4%
Dystroglycan	A4VAR9	98 kDa	0	0	0	2	0	0	0	2	0%	0%	0%	3%
PREDICTED: interleukin-1 receptor accessory protein isoform X2	UPI000240BECB	89 kDa	0	0	0	2	0	0	0	2	0%	0%	0%	2%

PREDICTED: matrilin-2	F1NG76	105 kDa	0	0	0	2	0	0	0	2	0%	0%	0%	2%
PREDICTED: thrombospondin type-1 domain-containing protein 7A (96% identity)	F1NPY9	164 kDa	0	0	0	2	0	0	0	2	0%	0%	0%	2%
Similar to PREDICTED: nephronectin (92% identity)	UPI0000ECC 4C1	62 kDa	0	0	0	2	0	0	0	2	0%	0%	0%	4%

a. Information obtained from Scaffold software, version 4.3.4
b. UF- 0/30; Unfertilized Egg – 0/30 min incubation with 0.1N HCl
c. FE- 15/19; Fertilized Egg – day 15/19 of embryonic development

Additional supplementary data to this article can be found online at http://dx.doi.org/10.1016/j.jprot.2015.01.002

Table S3. Peptide sequences, charge state of spectra and Mascot scores corresponding to the proteins identified in the unfertilized egg model after 0 minute incubation with 0.1 N HCl (UF-0).

Table S4. Peptide sequences, charge state of spectra and Mascot scores corresponding to the proteins identified in the unfertilized egg model after 30 minute incubation with 0.1 N HCl (UF-30).

Table S5. Peptide sequences, charge state of spectra and Mascot scores corresponding to the proteins identified in the fertilized egg model after 15 days of embryonic development (FE-15).

Table S6. Peptide sequences, charge state of spectra and Mascot scores corresponding to the proteins identified in the fertilized egg model after 19 days of embryonic development (FE-19).

Part 2

Eggshell Inspired Antimicrobials – Antimicrobial Properties of Avian Histones

Chapter 4

“Inhibition of Gram-Positive and Gram-Negative Planktonic and Biofilm Cultures by Antimicrobial Histones Extracted from Chicken Erythrocytes.”

Rose-Martel M, Berhane NA and Hincke MT (2015) Manuscript in preparation for submission to the *International Journal of Antimicrobial Agents*

Results regarding the inhibition of planktonic bacterial cultures were published as a peer-reviewed Letter to the Editor which can be found at the end of this chapter:

“Antimicrobial Histones from Chicken Erythrocytes Bind Bacterial Cell Wall Lipopolysaccharides and Lipoteichoic Acids.”

Rose-Martel M and Hincke MT (2014) *International Journal of Antimicrobial Agents*, 44(5):470-472

Comprehensive proteomics analyses have revealed the presence of histones throughout the calcified shell and the shell membranes (Chapter 3; Mann et al., 2006). These analyses are the first step towards understanding the role of eggshell protein constituents in the innate defense of the egg. Histones were identified in a lipophilic cuticle extract with antimicrobial activity against Gram-positive and Gram-negative bacteria (Wellman-Labadie et al., 2010); however, the dose-response and concentration of histones in different chicken eggshell compartments is currently unknown. The egg industry generates large quantities of eggshell waste; however, the extraction and purification of histone proteins from this material would be costly and time consuming with poor yield of pure sample which would complicate interpretation. Interestingly, avian erythrocytes, unlike mammalian, are nucleated and are therefore an ideal and abundant source of histones due to their ease of harvest from blood which is a significant waste product of the poultry industry. This alternative source for histone extraction and purification allowed us to extract large amounts of highly purified histones and to characterize their antimicrobial properties.

Author contributions:

Letter to the Editor: experiments, data analysis and manuscript preparation were all conducted by Megan Rose-Martel under the supervision of Dr. Maxwell T. Hincke.

Manuscript in preparation: Protein extraction and characterization were done by Megan Rose-Martel. MBEC assays were executed by Nahom A. Berhane and Megan Rose-Martel. The data analysis and manuscript preparation were all completed by Megan Rose-Martel under the supervision of Dr. Maxwell T. Hincke.

Abstract

Extensive use of antibiotics has selected for a variety of multi-drug resistant bacteria, which is a pressing concern due to the increasing prevalence of nosocomial and community-acquired infections. Another equally serious concern is bacterial biofilms - surface-attached colonies encased in an exopolysaccharide matrix that possess increased resistance to antimicrobial compounds. Biofilms are associated with numerous human diseases including cystic fibrosis, endocarditis, and infections caused by contaminated medical devices. Promising alternatives to antibiotics are cationic antimicrobial peptides (CAMPs), which are key players in the innate immune defense system of many living organisms that target pathogen components that cannot be easily mutated. Histones are an archetypal CAMP. This study characterizes the antimicrobial activity of histones extracted from chicken erythrocytes against Gram-negative and Gram-positive planktonic bacteria, including *E. faecalis* and methicillin-resistant *S. aureus*. Antimicrobial activity against biofilms of *S. aureus*, MRSA and *P. aeruginosa* were also studied. A mobility shift assay was used to determine the affinity of histones for *E. coli*, *S. typhimurium* and *P. aeruginosa* lipopolysaccharides (LPS), as well as *S. aureus*, *E. faecalis* and *B. subtilis* lipoteichoic acids (LTA); overall, these results suggested that histones target pathogens via conserved negatively charged components imbedded in their cellular membranes. A correlation between the antimicrobial activity of histones towards Gram-positive bacteria and LTA-histone binding affinity was observed. These results demonstrate that histone-derived molecules have the possibility for development of novel antibiotics for the treatment of both planktonic and biofilm-forming bacteria.

1. Introduction

Extensive use of antibiotics has selected for multiple multi-drug resistant bacteria, which is a pressing concern due to their increasing prevalence. From 1995 to 2007, Canadian hospitals experienced a 17-fold increase in MRSA incidence, of which >75% were thought to be acquired in a hospital or health-care setting [1]. The gravity of the situation was recently highlighted by the World Health Organization (WHO) [2].

Following environmental triggers, planktonic bacteria can form cell-surface interaction and join together to form a surface-attached colony encased in an exopolysaccharide (EPS) matrix [3]. These surface-attached colonies, known as a biofilms, are an important concern in hospitals due to their attachment and proliferation on medical devices, such as catheters, prosthetic joints, mechanical heart valves and other indwelling devices, as well as on living tissue, including heart valves (infective endocarditis) and lungs (cystic fibrosis) [4, 5]. Biofilms are known to possess increased resistance to antimicrobial compounds when compared to planktonic cells, possibly due to the inability of the antimicrobial compound to diffuse into the biofilm due to interactions with the EPS or due to a decrease in bacterial metabolic and growth rates [3].

Histones, more commonly known for their role in DNA stabilization and packaging, were first shown to possess antimicrobial activity in samples isolated from calf thymus [6]. Since then many studies have identified histones in a variety of species as potent antimicrobial agents [7]. They possess hydrophobic residues, have an overall positive charge and form amphipathic α-helical structures in a membrane-like milieu [8]; all of these are characteristics of cationic antimicrobial peptides (CAMPs). CAMPs are key players in the innate immune defense system

of many species and typically target components of the pathogen that cannot be easily mutated, such as lipid membrane components [9]. This explains why few pathogens have developed resistance mechanisms to antimicrobial peptides, as opposed to antibiotics, that have, through extensive use, selected for a variety of multi-drug resistant bacteria.

Avian blood, in contrast to that of mammals, contains nucleated erythrocytes with DNA packaged by histones. Thus chicken blood is a potential source for purification of histones [10]. In this study, we examine the antimicrobial activity of a histone mixture (H1, H2A, H2B, H3, H4 and H5) extracted from chicken erythrocytes against a variety of Gram-negative and Gram-positive planktonic bacteria, including *E. faecalis* and Methicillin-Resistant *Staphylococcus aureus* (MRSA). We also examine the anti-biofilm properties of the histone mixture on *S. aureus*, MRSA and *P. aeruginosa* biofilms using the minimal biofilm eradication concentration (MBEC) assay.

In order to explore the mechanism underlying the antimicrobial activity, we investigated histone interaction with LPS and LTA isolated from a variety of different pathogens. We demonstrate the potential of histones isolated from chicken erythrocytes to provide protection against both planktonic bacteria and biofilms, which will inspire identification of novel antimicrobial peptides.

2. Materials and Methods

2.1. Acid Extraction of Histones

White Rock chickens were euthanized by decapitation at local slaughterhouses in accordance with Canadian Food Inspection Agency (CFIA) regulations. Blood was collected

immediately after decapitation (~37.5ml of blood/bird with 1.5mg EDTA/ml). Erythrocytes were pelleted at 300 x g for 10 minutes and washed with PBS. Histones were extracted using a modified protocol for mammalian cell cultures based on Shechter *et al*., 2007 [11]. Briefly, erythrocytes corresponding to 100ml of blood were lysed with 1000ml of 10mM Tris-Cl pH 8.0, 1mM KCl, 1.5mM $MgCl_2$ and 1mM DTT for 1 hour at 4°C with light agitation. The extracted nuclei were pelleted at 10,000 x g for 10 minutes at 4°C and washed with PBS. The presence of hemoglobins in the PBS supernatant after each wash was detected by a spectral scan (absorbance from 300-500nm) using the EON microplate spectrophotometer (BioTek, Winooski, VT, USA). When no discernable peak was detected at 400nm, the nuclei were treated with 400ml of 0.4N H_2SO_4 for 1 hour at 4°C with light agitation. The nuclear debris was pelleted at 16,000 x g for 10 minutes at 4°C and discarded. Histones were purified from the supernatant by TCA-precipitation; 133ml of 100% TCA was added to the supernatant in small increments and the suspension was incubated on ice for 1 hour. Histones were pelleted at 16,000 x g for 10 minutes at 4°C and washed twice with acetone, without disturbing the pellet, at 16,000 x g for 5 minutes at 4°C. The histone pellet was dissolved in 100ml of sterile ddH_2O and passed through an Amicon Ultra centrifugal filter unit with a 3,000Da molecular weight cut off (Millipore Corporation, Billerica, MA, USA) at 750 x g for 30 minutes. The retained histones were flash frozen and freeze dried overnight. The same procedure was used to extract histones from Orlopp Bronze turkey erythrocytes.

2.2. SDS-PAGE and LC/MS/MS Analysis

Samples were analyzed by SDS-PAGE on 15% polyacrylamide gels using the mini-PROTEAN 3 electrophoresis system (Bio-Rad Laboratories, Hercules, CA, USA). Bands were

analyzed by densitometry using ImageJ densitometry software (version 1.6, NIH, Bethesda, MD) and excised for shipping to the Proteomics Platform of the Eastern Quebec Genomics Centre (Laval, QC) for LC/MS/MS proteomics analysis, as previously described [12]. Results were analyzed using Scaffold (version Scaffold-3.00.08, Proteome Software Inc., Portland, OR). Identification of proteins was only deemed significant if two peptides were identified at $p \leq 0.05$ probability.

2.3. Preparation of Bacterial Inocula

The tested strains include Gram-positive bacteria: *B. subtilis* (ATCC 19659), *S. aureus* (ATCC 6538) and *E. faecalis* (clinical isolate) as well as Gram-negative bacteria: *E. coli* (K12), *P. aeruginosa* (ATCC 15442) and *S. typhimurium* (ATCC 1535). We also tested Gram-positive MRSA, a clinical isolate confirmed to be methicillin resistant by a cefoxitin disk screen test (data not shown). Bacterial colonies from glycerol stocks were plated on LB agar and incubated overnight at 37°C. Single colonies from LB agar plates were grown in 3ml of LB broth overnight at 37°C, shaken at 250rpm. The inocula were diluted 1:50 in fresh LB broth, incubated with the previous conditions until the optical density at 600nm reached 0.2 (~10^8 CFUs/ml). The bacterial suspension was pelleted at 3000 x g, 4°C for 10 minutes, washed with PBS and adjusted to 10^5 CFUs/ml in PBS for the microbroth dilution assay. For the MBEC assay, the bacterial suspension was adjusted to 10^5 CFUs/ml in LB broth.

2.4. Microbroth Dilution Assay

The antimicrobial activity against planktonic bacterial cells was evaluated using a microbroth dilution assay based on a previously described protocol [13]. Histones were dissolved

in sterile water, pH 7.4, serially two-fold diluted and aliquoted in a 1:1 ratio with bacteria in a 96-well microplate. Kanamycin and sterile water, pH 7.4, replaced the histones for positive and negative controls for inhibition of growth, respectively. Microplates were incubated 1 hour at 37°C and 250rpm, after which 200µl of LB broth was added to each well. The EON microplate spectrophotometer and Gen5 data analysis software (BioTek, Winooski, VT, USA) was used to monitor the growth of bacteria by measuring the optical density at 600nm every 15 minutes for 18 hours with continuous shaking at 37°C. The lowest histone concentration without visible bacterial growth was designated the minimum inhibitory concentration (MIC). Wells containing bacteria at MIC, MIC x 2 and MIC x 3 concentrations of histones were plated on LB agar and incubated at 37°C for 18 hours. The lowest concentration of histones without a single colony was designated the minimum bactericidal concentration (MBC). Each microplate contained serially ten-fold diluted bacterial cultures in order to generate a standard curve for the number of viable bacteria versus bacterial lag time to calculate the corresponding bacterial growth inhibition for each histone concentration tested.

2.5. Minimum Biofilm Eradication Concentration (MBEC) Assay

The effect of the histone mixture on biofilm growth was assessed using the MBEC Assay according to the manufacturer instructions (Innovotech Inc., Alberta, Canada). Briefly, wells of a 96-well microplate were inoculated with 150µl of bacterial inoculum and covered with a lid possessing 96 identical pegs. The device was incubated for 24 hours at 37°C and 100rpm. Following incubation, planktonic cells were rinsed away by immersing the 96-peg lid in a sterile 96-well microplate with 200µl of sterile PBS. Biofilms were then challenged with 200µl of histones that were dissolved in sterile water, pH 7.4, and serially two-fold diluted in a sterile 96-

well microplate. Positive and negative controls for inhibition of growth were assessed by replacing histones with kanamycin and sterile water, pH 7.4. The device was incubated for 2 hours at 37°C and 100rpm, and the 96-peg lid was rinsed twice as described above and placed in a sterile 96-well microplate with 200µl of LB broth. The device was sonicated for 10 minutes in order to dislodge the biofilms from the pegs, after which the peg-lid was replaced with a sterile, clear lid. Bacterial growth was monitored using the EON microplate spectrophotometer and Gen5 data analysis software (BioTek, Winooski, VT, USA) with the optical density at 600nm measured every 30 minutes for 24 hours with continuous shaking at 37°C. The lowest histone concentration without visible bacterial growth was designated the minimum biofilm eradication concentration (MBEC). Each microplate contained serially ten-fold diluted bacterial cultures obtained from the uninhibited biofilm control sample in order to generate a standard curve for the number of viable bacteria in the inoculum versus bacterial growth lag time. Bacterial growth inhibition for each histone concentration tested can be determined from the standard curve. Biofilm colony counts were obtained by breaking off pegs with sterile pliers prior to the antimicrobial challenge. Pegs were immersed in 1ml sterile PBS, sonicated for 10 minutes and plated on LB agar for colony counting.

2.6. Mobility Shift Assay

LPS and LTA binding activity was assessed with *S. typhimurium* ATCC 7823 LPS, *P. aeruginosa* 10 ATCC 27316 LPS, *B. subtilis* LTA and *E. faecalis* LTA from Sigma (St-Louis, MO, USA) as well as ultrapure *E. coli* O111:B4 LPS and *S. aureus* LTA from InvivoGen (San Diego, CA, USA). Binding activity was evaluated using a mobility shift assay modified from Stinson et al. 1998 [14]. Purified histones dissolved in PBS, pH 7.4, were incubated with

increasing concentrations of purified LPS or LTA for 15 minutes at room temperature. Samples were loaded onto a non-denaturing 7% polyacrylamide gel, run for 60 minutes at 200V and stained with 0.25% Coomassie Brilliant Blue. Histone-LPS or LTA binding activity was determined by observing the shift in electrophoretic mobility of histones towards the anode.

2.7. Hemolytic Assay

The potential for hemolytic activity was assessed using rat red blood cells (RBCs) and based on a previously described protocol [15]. A Crl:CD (SD) IGS rat was euthanized with carbon dioxide; blood was collected via cardiac puncture in a BD vacutainer containing 5.4mg of K_2EDTA (BD Canada, Mississauga, Ontario). All procedures were carried out in accordance with the University of Ottawa Animal Care Committee guidelines. RBCs were pelleted from 1ml of blood by centrifugation at 1000 x g for 10 minutes. The serum was removed and the RBCs were washed three times with PBS, pH 7.4. RBCs were resuspended in PBS to a final volume of 1ml and diluted 1:10 in PBS. The resuspended RBCs were incubated in a 1:1 (v/v) ratio with different concentrations of histones and incubated at 37°C with shaking at 200rpm for 1 hour. Controls include PBS and 0.05% Triton-X, representing no hemolysis and 100% hemolysis, respectively. To monitor hemoglobin release, samples were centrifuged at 1000 x g for 5 minutes and the absorbance of the supernatant measured at 405nm. The percent hemolysis was calculated according to the following equation: hemolysis (%) = ((OD405nm sample - OD405nm no hemolysis)/(OD405nm 100% hemolysis - OD405nm no hemolysis)) x 100.

2.8. Statistical Analyses

The Student's T-test was used to determine the statistical significance of bacterial growth inhibition between the MIC, MBC and MBEC value of each tested strain in the microbroth dilution assay and MBEC assay. It was also utilized to determine significant variations in bacterial growth when calculating dose-dependent logarithmic inhibition. The Student's T-test was also used to determine significant hemolytic activity of the histone mixture compared to the PBS (no hemolysis) control. A P value ≤ 0.05 was necessary for statistical significance.

3. Results

3.1. Assessment of Purified Histones by Proteomics

Histones were extracted and purified from chicken erythrocytes by sulfuric acid extraction and TCA precipitation. This method yielded 2.3 ± 0.6 mg of histones/ml of whole blood. SDS-PAGE analysis revealed 7 distinct bands which were analyzed by densitometry and cut out for proteomics analysis (Fig. 1A). The identified bands correspond to H1 (9.7% ± 1), H2A (15% ± 1), H2B (19% ± 1), H3 (24% ± 1), H4 (14.6% ± 0.4) and H5 (18% ± 1) (Table 1, Fig. 1A). The H1 band was composed of both H1.11L and H1.11R; there is a 93% identity between the histone H1 variants, with the H1.11R sequence being 6 amino acids shorter (Fig. 1B). Every histone possessed an exponentially modified protein abundance index (emPAI) > 700. Lower abundant contaminants include SAP domain containing ribonucleoprotein, 60S ribosomal protein L7a, THO complex subunit 4, peptidyl-prolyl cis-trans isomerase, high mobility group proteins, adenylate kinase 2, myosin light polypeptide 6, small nuclear ribonucleoprotein Sm D3, hemoglobin subunits α-A and α-D, with emPAI values ranging from 1

– 5. Using spectral counting, we determined that these contaminants correspond to < 5% of the histone mixture in total.

A similar SDS-PAGE profile was obtained from histones extracted from turkey erythrocytes using the same methodology as for chicken histones (Fig. S1). Currently, the turkey proteomics database does not have distinct accession numbers for the two histone H1 variants corresponding to histones H1.11L and histones H1.11R in the chicken database. One notable difference between the two avian extracts, confirmed using densitometry analysis, was the increased level of the higher molecular weight histone H1in the turkey extract when compared with H1.11L in the chicken extract (Table S1). Identity scores were obtained from sequence alignments comparing the chicken histones versus the turkey histones using the UniProt alignment software. The identity scores revealed that all corresponding protein sequences were at least 90% identical, with the exception of histones H1 which were ~80% identical (Table S2). Due to the high level of similarity between the histones from both species, further experiments were conducted using histones extracted from chicken erythrocytes with the assumption that the results can be extended to histones extracted from turkey erythrocytes.

Table 1. Densitometry and LC/MS/MS proteomics analysis results of sequenced chicken histone bands.

Bands[a]	Identified proteins[b]	# of unique peptides[b]	UniProt ID[b]	% of total histone sample (± SD)[c]	Coverage (%)[b]
Band 1	Histone H1.11L	41	**P08287**	3.7 ± 0.6	49
	Histone H1.01	32	**P08284**		47
	Histone H1.03	36	**P08285**		44
Band 2	Histone H1.11R	26	**P08288**	6 ± 1	51
	Histone H1.01	25	**P08284**		46
	Histone H1.11L	23	**P08287**		43
Band 3	Histone H5	25	**P02259**	18 ± 1	50
Band 4	Histone H3.2	19	**P84229**	24 ± 1	62
Band 5	Histone H2B 1/2/3/4/6	27	**P0C1H3**	19 ± 1	75
	Histone H2B 8	26	**Q9PSW9**		75
	Histone H2B 7	25	**P0C1H5**		69
Band 6	Histone H2A (fragment)	18	**F1NDS3**	15 ± 1	72
	Histone H2A.V	6	**P02272**		54
	Histone H2A (fragment)	3	**F1P5G5**		16
Band 7	Histone H4	29	**P62801**	14.6 ± 0.4	73

a. Bands are depicted in Fig. 1.
b. Data obtained from Scaffold version Scaffold-3.00.08, Proteome Software Inc
c. Results obtained from densitometry analysis using ImageJ densitometry software version 1.6; SD, standard deviation

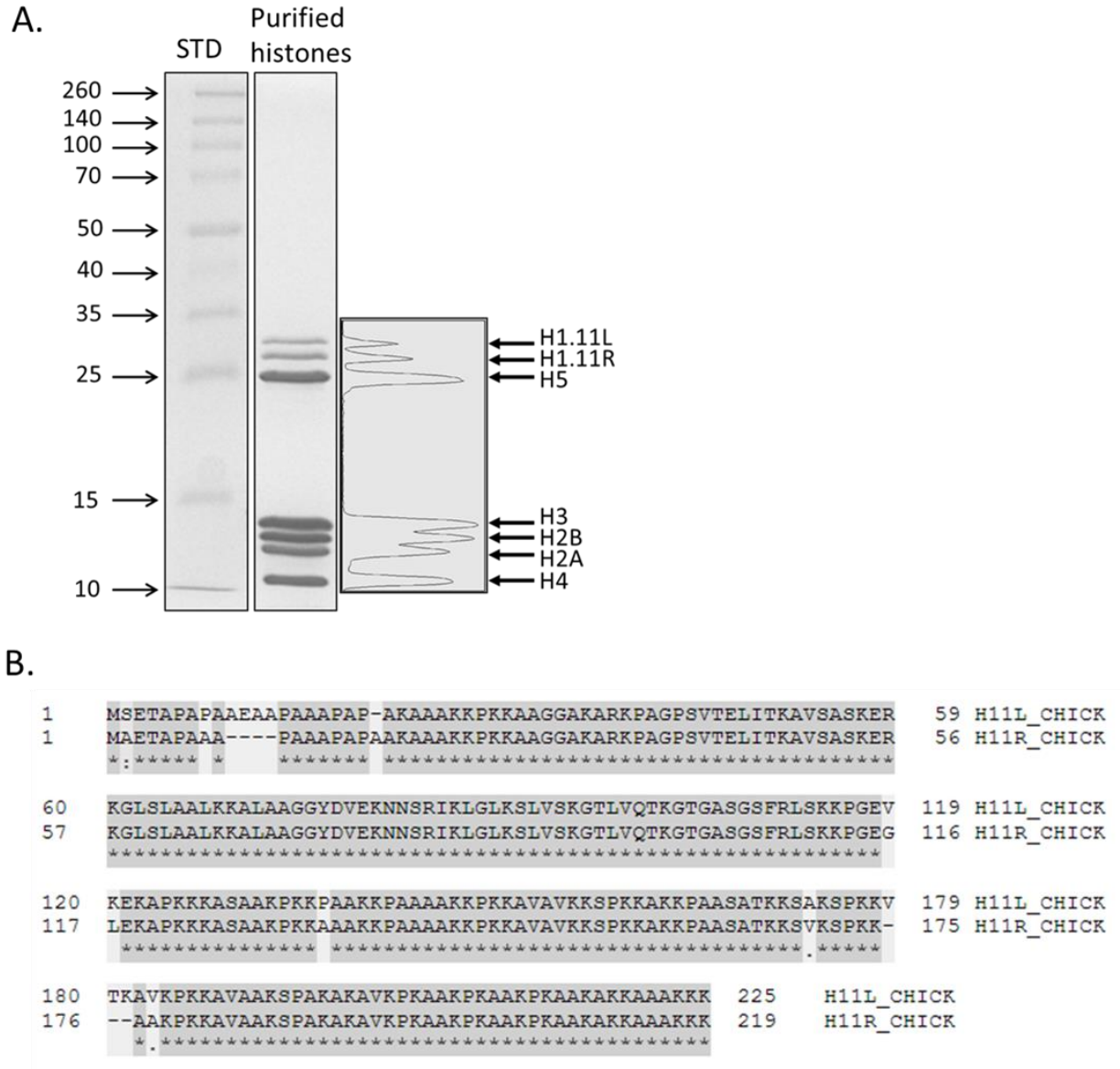

Fig. 1. SDS-PAGE analysis of TCA-precipitated histone mixture extracted from chicken erythrocytes. (A) A 15% acrylamide gel revealed 7 distinct bands which were analyzed using densitometry as well as cut out and sent for proteomics LC/MS/MS analysis. Results allowed us to distinguish a band for histones H1.11L, H1.11R, H2A, H2B, H3, H4 and H5 (see Table 1 for proteomics and densitometry results). STD: molecular weight standards (kDa). (B) Alignment of chicken histone H1.11L and H1.11R sequences. Dark grey: similarities.

3.2. Antimicrobial Activity

A microbroth dilution assay was used to determine the MIC and MBC of histones versus Gram-positive and Gram-negative planktonic bacteria (Table 2). The histone mixture was significantly more potent in inhibiting the growth of Gram-negative *S. typhimurium* and *P. aeruginosa* when compared to *E. coli*. *E. coli*, *S. typhimurium* and *P. aeruginosa* have MICs of 21 ± 3 μg/ml, 4 ± 0 μg/ml and 5 ± 1 μg/ml, respectively, which are not statistically different from their MBCs. The most susceptible Gram-positive bacterial species was *B. subtilis*, with a MIC of 3 ± 1 μg/ml; the least susceptible was *E. faecalis*, requiring 700 ± 100 μg/ml to inhibit bacterial growth (MIC) and 1100 ± 200 μg/ml to cause bacterial cell death (MBC). The MICs of *S. aureus* and MRSA were not significantly different from each other, demonstrating similar susceptibilities at 6 ± 1 μg/ml and 8 ± 2 μg/ml, respectively. Therefore histones exert potent antimicrobial activity towards both Gram-negative and Gram-positive planktonic bacteria, with *E. faecalis* demonstrating markedly less susceptibility.

Table 2. MIC, MBC and MBEC values of the purified extracted histone mixture for Gram-positive and Gram-negative bacteria determined by a microbroth dilution assay and MBEC assay

Bacteria	MIC (µg/ml)[a]	MBC (µg/ml)[b]	MBEC (µg/ml)[c]
Gram-positive			
B. subtilis	3 ± 1	3.9 ± 0.4	-
E. faecalis	700 ± 100	1100 ± 200	-
S. aureus	6 ± 1	6 ± 1	27 ± 8
MRSA	8 ± 2	8 ± 2	25 ± 8
Gram-negative			
E. coli	21 ± 3	21 ± 3	-
S. typhimurium	3.6 ± 0.4	5 ± 1	-
P. aeruginosa	5 ± 1	5 ± 1	>512

a. MIC – minimum inhibitory concentration (mean ± SD) determined by a microbroth dilution assay
b. MBC – minimum bactericidal concentration (mean ± SD) determined by a microbroth dilution assay
c. MBEC – minimum biofilm eradication concentration (mean ± SD) determined by an MBEC assay

Antimicrobial activity was also assessed by monitoring the increase in lag time for detection of bacterial growth when treated with increasing histone concentrations. Bacterial growth curves of serially ten-fold diluted cultures served as standard curves to determine the correlation between bacterial growth lag time and initial concentration of viable bacteria. We determined that histone inhibition of each bacterial species was dose-dependent. Fig. 2 and 3 demonstrate the progressive bacterial growth inhibition for each bacterial species. The growth of Gram-negative bacteria was shown to be significantly inhibited (>2 logs) at concentrations of 0.5 µg/ml histones for *P. aeruginosa* and *S. typhimurium,* while 1 µg/ml of histones was needed for the same effect in *E. coli* (Fig. 5). Gram-positive *E. faecalis* was less susceptible to inhibition by histones, requiring 64 µg/ml to inhibit bacterial growth by 4 logs. However, 2 – 4 µg/ml histones produced the same effect in *B. subtilis*, *S. aureus* and MRSA (Fig. 4), which only require 1 µg/ml for a 2-log reduction.

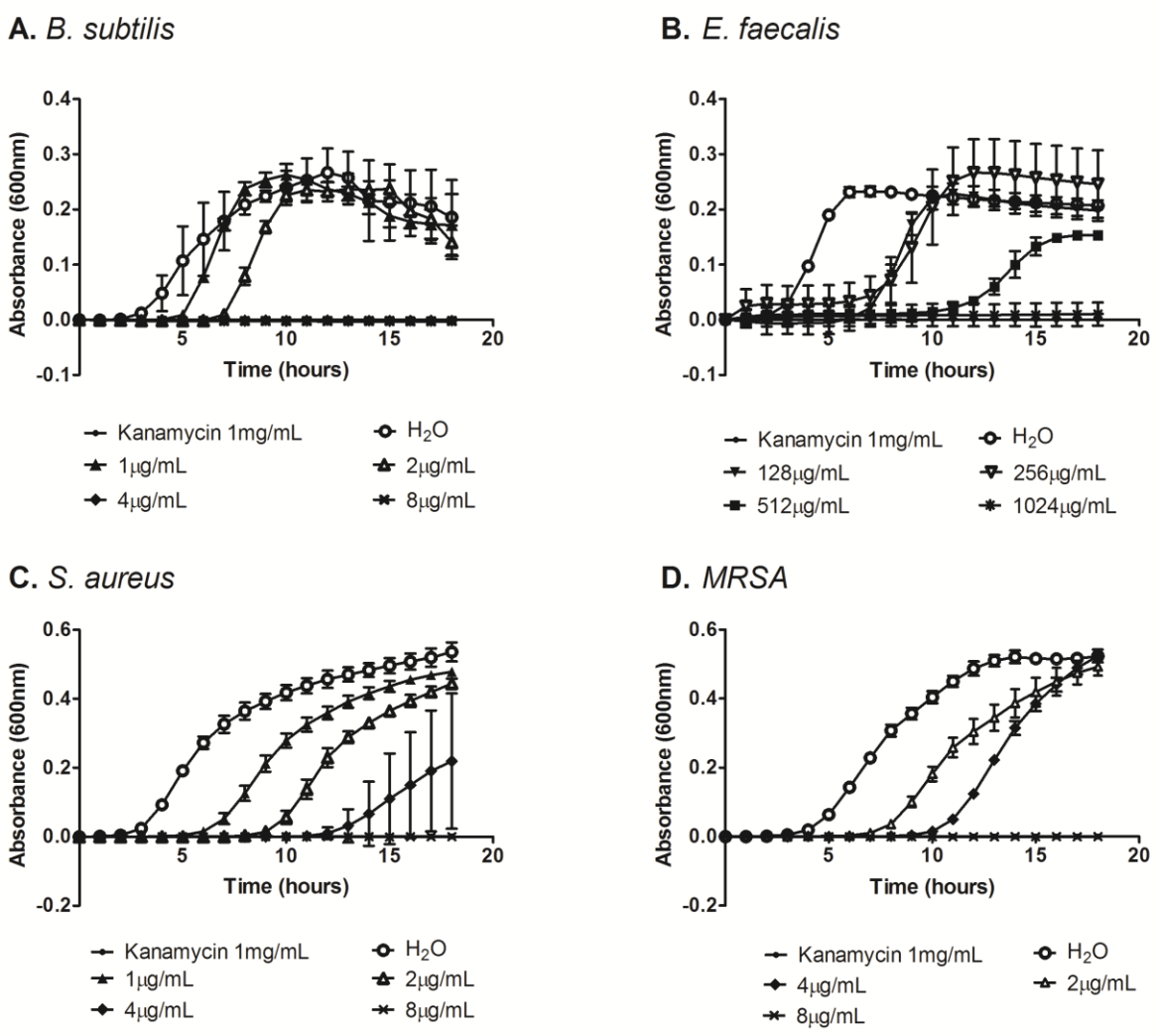

Fig. 2. Dose-dependent growth inhibition of Gram-positive bacteria treated with histone mixture from chicken erythrocytes determined by a microbroth dilution assay. Four Gram-positive bacterial strains were tested with sterile H_2O, pH 7.4, and kanamycin as negative and positive controls for inhibition, respectively. Results are representative of three independent trials, each in triplicate.

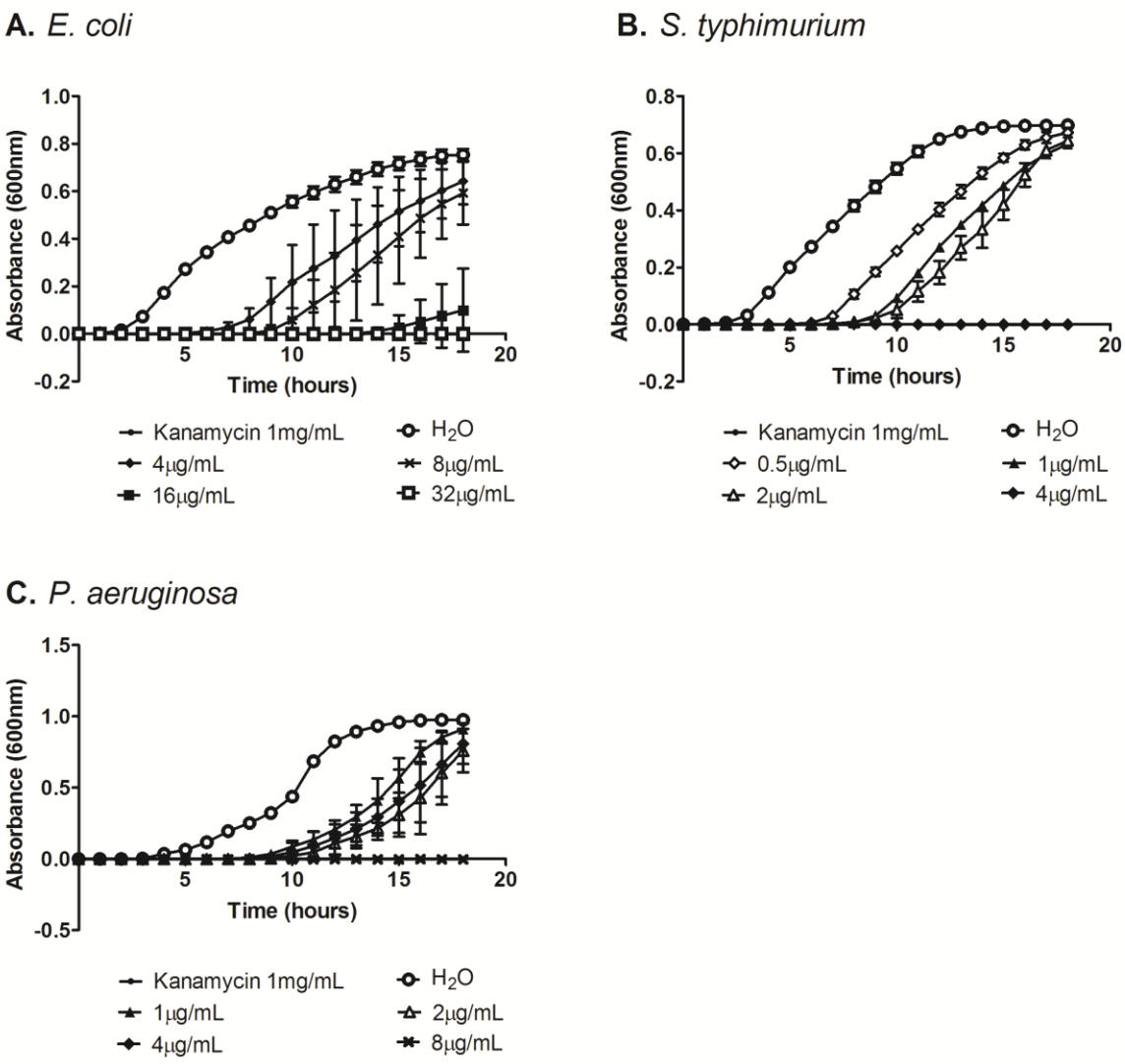

Fig. 3. Dose-dependent growth inhibition of Gram-negative bacteria treated with histone mixture from chicken erythrocytes determined by a microbroth dilution assay. Three Gram-negative bacterial strains were tested with sterile H_2O, pH 7.4, and kanamycin as negative and positive controls for inhibition, respectively. Results are representative of three independent trials, each in triplicate.

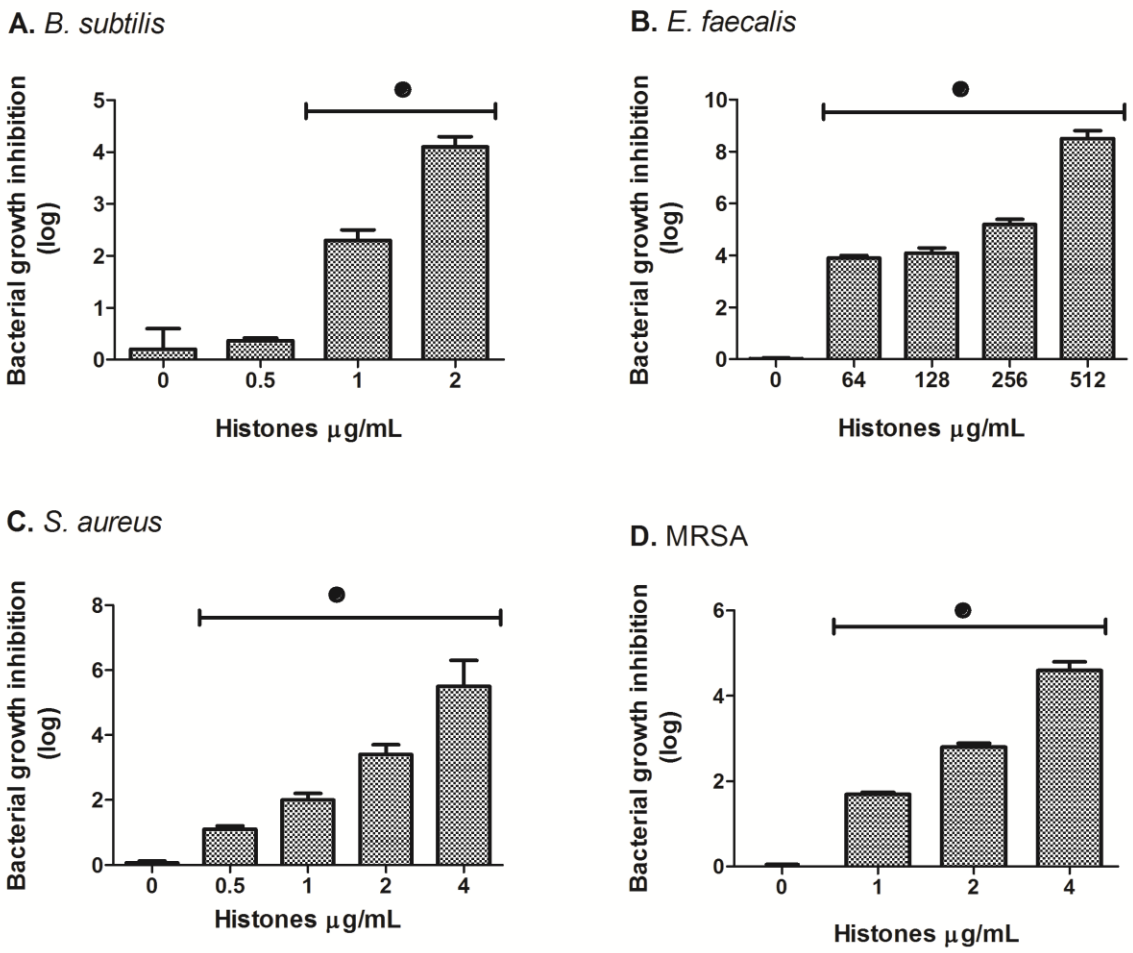

Fig. 4. Dose-dependent logarithmic bacterial growth inhibition of Gram-positive bacteria treated with histone mixture from chicken erythrocytes determined by a microbroth dilution assay. Statistical analysis was done by Student's T-Test, (•) indicates $p \leq 0.001$ compared with the 0 µg/ml histones. Results are of three independent trials, each in triplicate.

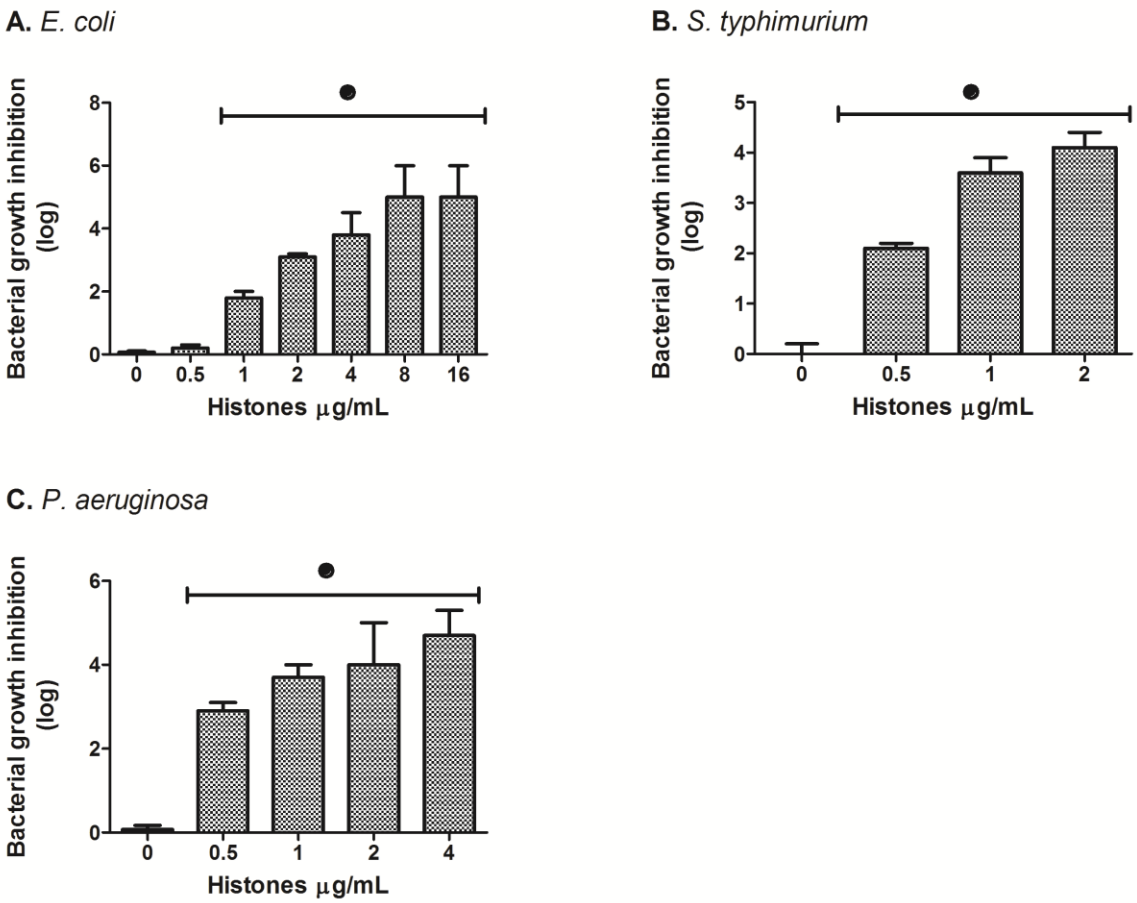

Fig. 5. Dose-dependent logarithmic bacterial growth inhibition of Gram-negative bacteria treated with histone mixture from chicken erythrocytes determined by a microbroth dilution assay. Statistical analysis was done by Student's T-Test, (•) indicates $p \leq 0.01$ compared with the 0 μg/ml histones. Results are of three independent trials, each in triplicate.

3.3. MBEC Assay

The anti-biofilm properties of the histone mixture were assessed using a device that allowed us to grow biofilms on pegs projecting from a 96-well microplate lid. After 24 hours of incubation with the MBEC device, *S. aureus* and MRSA biofilms reach ~10^5 CFUs/peg while *P. aeruginosa* biofilms reach ~10^7 CFUs/peg. The histone mixture was effective in eradicating both Gram-positive *S. aureus* and MRSA biofilms but has no significant inhibitory effect on Gram-negative *P. aeruginosa* biofilms (Fig. 6). The MBEC values for *S. aureus* and MRSA were determined to be 27 ± 8 μg/ml and 25 ± 8 μg/ml, respectively; not significantly different from each other, demonstrating similar susceptibilities between the two biofilms. These values are statistically greater (~ 4-fold) than the MIC and MBC values determined for some bacterial cells (planktonic) in the previous microbroth dilution assay (Table 2). The least susceptible biofilm was *P. aeruginosa* with an unknown MBEC value >512 μg/ml.

For both the *S. aureus* and MRSA biofilms we were able to detect significant growth inhibition with 8 and 16 μg/ml histones (Fig. 7A). However, a significant dose-dependent response to the increasing histone concentrations was only observed with MRSA biofilms, which is also reflected in the bacterial growth curves (Fig. 6A and B). Interestingly, MRSA was significantly more resistant to 8 μg/ml of histones with 0.8 ± 0.4 logs of inhibition when compared to *S. aureus* with 1.9 ± 0.4 logs of inhibition. No significant inhibition of *P. aeruginosa* biofilm growth was detected for any of the tested histone concentrations (Fig. 7B). However, when treated with 16, 64 and 256 μg/ml histones, *P. aeruginosa* biofilms showed significant increase in growth compared to the uninhibited control.

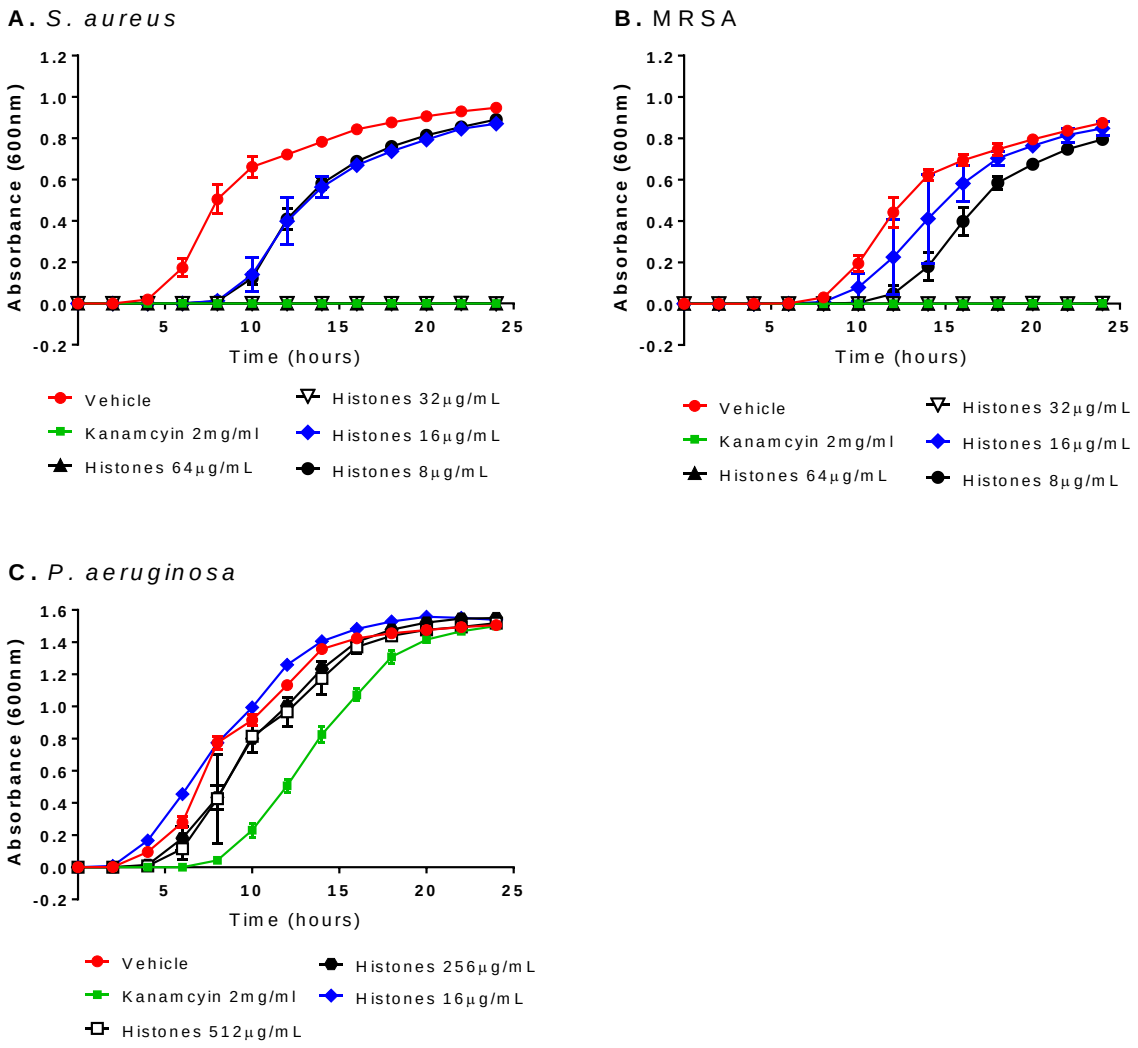

Fig. 6. Dose-dependent growth inhibition of biofilms treated with histone mixture from chicken erythrocytes determined by an MBEC assay. Gram-positive biofilms (*S. aureus* and MRSA) consist of ~10^5 CFUs/peg and Gram-negative biofilm (*P. aeruginosa*) consists of ~10^7 CFUs/peg. Growth curves are representative of three independent trials, each in triplicate.

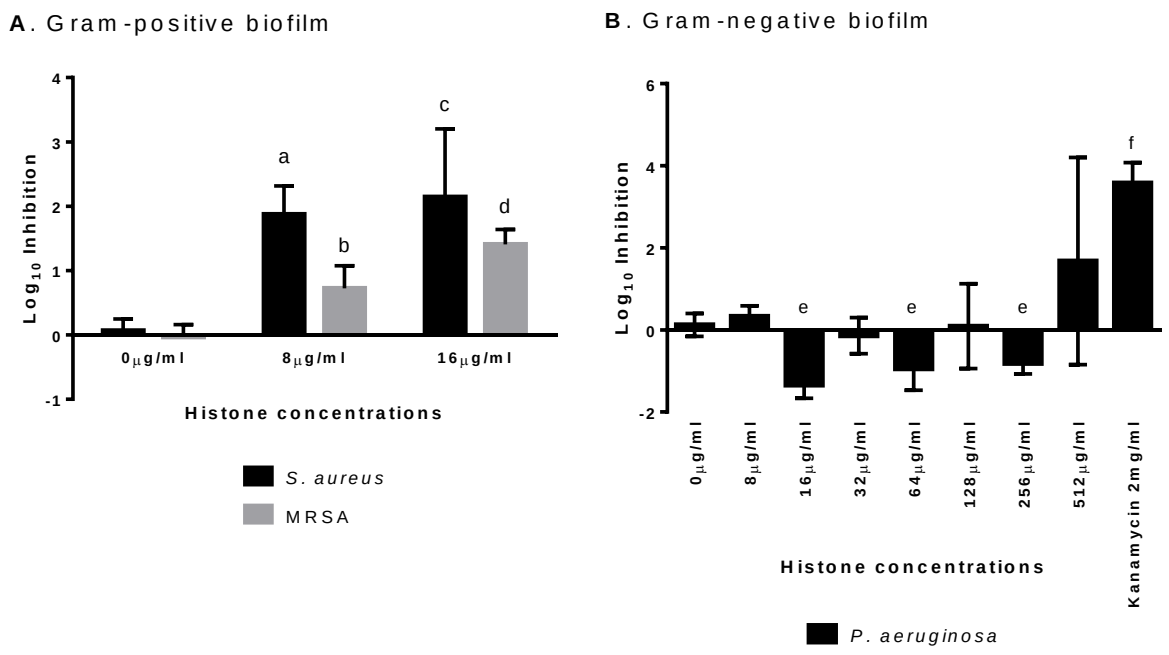

Fig. 7. Dose-dependent logarithmic bacterial growth inhibition of biofilms treated with histone mixture from chicken erythrocytes determined by an MBEC assay. Gram-positive biofilms consist of ~10^5 CFUs/peg and Gram-negative biofilm consists of ~10^7 CFUs/peg. Statistical analysis was done by Student's T-Test, (a) $p \leq 0.003$ vs. 0 µg/ml *S. aureus* and $p \leq 0.02$ vs. 8 µg/ml MRSA; (b) $p \leq 0.05$ vs. 0 and 16 µg/ml MRSA and $p \leq 0.02$ vs. 8 µg/ml *S. aureus*; (c) $p \leq 0.03$ vs. 0 µg/ml *S. aureus*; (d) $p \leq 0.001$ vs. 0 µg/ml MRSA and $p \leq 0.05$ vs. 8 µg/ml MRSA; (e) $p \leq 0.04$ vs. 0 µg/ml *P. aeruginosa* (biofilm growth); (f) $p \leq 0.0005$ vs. 0 µg/ml *P. aeruginosa* (biofilm inhibition). Results are of three independent trials, each in triplicate.

3.4. LPS and LTA Mobility Shift Assay

The first step in the antimicrobial mechanism of CAMPs is the electrostatic interaction between the positive charges of the antimicrobial and the negatively charged molecules located on the surface of the bacterial cell wall. Gram-negative bacteria possess lipopolysaccharides (LPS) and glycolipids on the outer membrane providing an overall negative charge to the bacteria [16]. On the other hand, Gram-positive bacteria possess lipoteichoic acids (LTA), which are anionic polymers anchored to the peptidoglycan layer [17]. Histones have an elevated isoelectric point and therefore migrate towards the anode during native-PAGE, confirmed by loading 5µg of histones as a positive control for cationic mobility (Fig. 8). Since LPS and LTA are negatively charged, they do not enter the gel. When histone-LPS/LTA complexes are formed, the negative charges of these bacterial cell wall components decrease the cationic mobility of the histones in a dose-dependent trend until the positive charges of the histones are neutralized and the proteins no longer migrate towards the anode. Fig. 8A, B and C demonstrate that histones bind strongly to *B. subtilis* and *S.aureus* LTA, with saturated binding at 5µg of LTA, compared with *E. faecalis* LTA which required 7.5µg of LTA. Similarly, 5µg of *P. aeruginosa* LPS completely bound to and neutralized the positive charges of the histone molecules (Fig. 8F). However, the lowest histone-LPS binding affinities observed were for *S. typhimurium* LPS, requiring 10µg of LPS to saturate the charge on histone molecules; while more than 10µg of *E. coli* LPS is necessary (Fig. 8D and E). Binding variability between bacterial strains could be attributed to the differences in endotoxin purity from different manufacturers, to the difference in molecular weight between the different LPS and LTA species and to variations in the exact composition of LPS and LTA between bacteria.

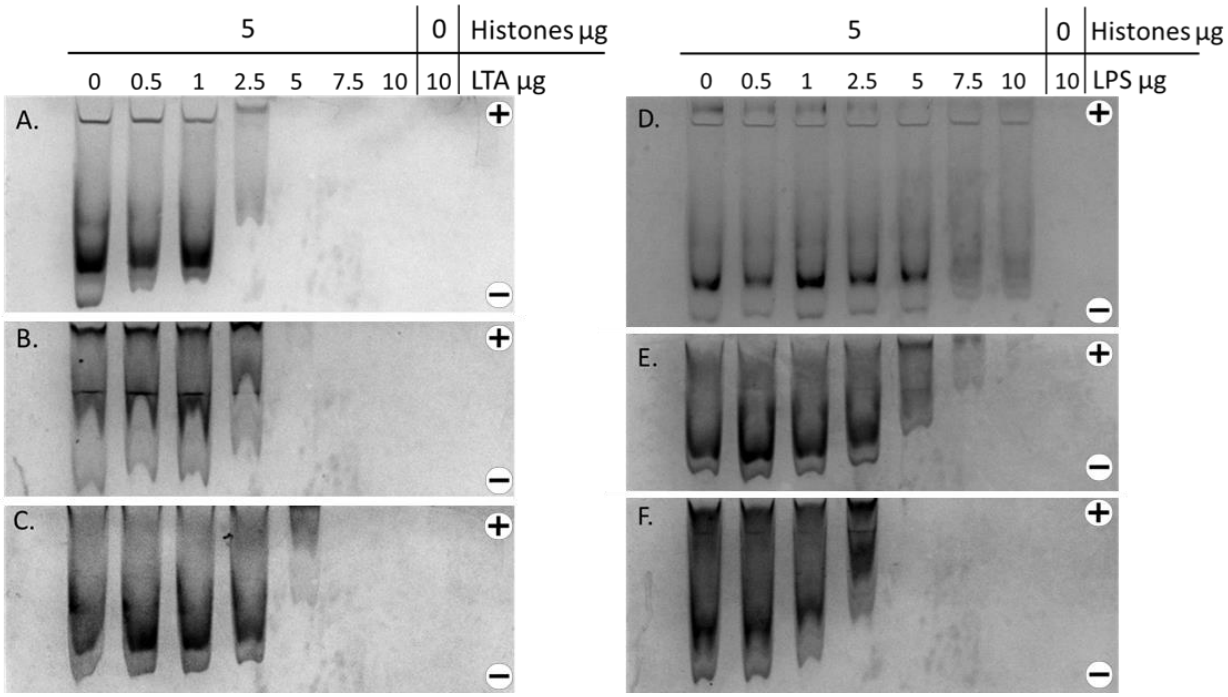

Fig. 8. Mobility shift assay of histone-LTA and histone-LPS complexes in non-denaturing conditions. Purified histones (5µg) were incubated with increasing amounts of LTA from (A) *B. subtilis*, (B) *S. aureus* and (C) *E. faecalis*, or LPS from (D) *E. coli*, (E) *S. typhimurium* and (F) *P. aeruginosa*. Controls include 5µg of histones and 10µg of LPS/LTA loaded individually on each gel.

3.5. Hemolytic Activity

A hemolytic assay was used to determine whether the histone mixture displayed toxicity towards mammalian cells. A wide range of histone concentrations were tested (from 0.005 – 1.25 mg/ml) which did not damage the RBC cell membranes (Table 3). Histones are non-hemolytic even at the highest concentration tested (1.25 mg/ml). Statistical analysis revealed that treatment with 1.25, 0.25 and 0.005 mg/ml were not significantly higher than the zero hemolysis control.

Table 3. Hemolytic activity of the histone mixture towards mammalian RBCs.

Concentration of histone mixture (mg/ml)	Hemolysis %[a]
1.25	2 ± 2[b]
1	1.5 ± 0.2
0.75	2 ± 1
0.5	2 ± 1
0.25	2 ± 1[b]
0.125	3 ± 1
0.05	3.4 ± 0.3
0.025	2 ± 1
0.0125	1.8 ± 0.3
0.005	0.9 ± 0.8[b]

a. Hemolysis % was calculated according to the equation in Materials and Methods.
b. No significant hemolytic activity of the histone mixture compared to the PBS (no hemolysis) control. A P value ≤ 0.05 was necessary for statistical significance.

4. Discussion

We have shown that histones extracted from chicken erythrocytes have potent antimicrobial activity against both Gram-positive and Gram-negative planktonic bacterial cells as well as Gram-positive biofilms, including MRSA. Moreover, they exhibit strong binding affinity for the negatively charged bacterial cell wall components, LPS and LTA, from a variety of species. Chicken erythrocytes are an ideal source of purified histones; the ease of harvest and lack of connective tissue allow for rapid and simple large-scale acid extraction from nuclei [8, 9]. In this work, we have optimized the protocol to reduce contamination by hemoglobins and other nuclear proteins. The histone mixture assessed in our study contains histones H1, H2B, H2A, H3, H4 and H5. It is relevant that neutrophil extracellular traps (NETs), which are key players in the innate immune response in a variety of vertebrate species, also contain a variety of histones (H1, H2A, H2B, H3 and H4) [18]. NETs are composed of the neutrophil nuclear contents that have been released extracellularly to create an elevated concentration of antimicrobial proteins at the site of infection. In addition to a bactericidal function, they also prevent further microbial spreading within the organism [18]. Our results clearly indicate that histones possess antimicrobial activity and could play a role in pathogen recognition by NETs. We can also observe the synergistic effects of different histones in a mixture already existing in the vertebrate immune system.

E. faecalis and MRSA are major causes of nosocomial infections due to their resistance to numerous current antibiotics [19]. To our knowledge, *E. faecalis* susceptibility to antimicrobial histones has never been previously investigated. We found that *E. faecalis* was the least sensitive bacterial species to the histones, with a MIC of 700 μg/ml. This is similar to

human β-defensin 3, a cationic antimicrobial peptide that is unable to completely inhibit the growth of wild-type *E. faecalis* with concentrations as high as 512 µg/ml [20]. However, melittin, an antimicrobial peptide from bee venom, and nisin, a well-known bacteriocin, have MICs in the range of 1 – 8 µg/ml and 4 – 32 µg/ml, respectively, for *E. faecalis* [19].

Melittin and nisin are also effective against MRSA with MICs from 0.5 – 4 µg/ml and 2 – 32 µg/ml, respectively [19]; this is comparable to our histone results with MIC = 8 ± 2 µg/ml. We found similar MICs for wild-type *S. aureus* and MRSA sensitivity to histones, as demonstrated for mellitin and nisin, which suggests that mechanisms responsible for MRSA antibiotic resistance are distinct from the mechanisms which CAMPs, such as histones, target bacteria.

Biofilm formation occurs in several steps that can eventually become a pathological cycle. As a reaction to environmental triggers, planktonic bacteria reversibly attach themselves to a solid surface and form microcolonies [21]. These colonies, now irreversibly attached, will adapt to the surface-attached environment and mature into a biofilm by cell division and increasing the expression of exopolysaccharides (EPS) [21]. Environmental cues from within a mature and established biofilm can activate dispersal mechanisms, where some bacteria are reverted back to a planktonic state and shed from the biofilm [22]. These planktonic bacteria can cause acute infections, including sepsis, or form new biofilms at secondary sites which leads to chronic infections [22].

Our data indicates that the biofilm cultures of Gram-positive *S. aureus* and MRSA were susceptible to the histone mixture; however, biofilm cultures displayed more resistance when compared to the same bacteria in planktonic state. Comparisons of the MIC/MBC and MBEC values revealed a 4.5-fold increase in *S. aureus* resistance and 3-fold increase in MRSA (Table

2). Studies examining the effect of human β-defensin 3 against MRSA biofilms were able to detect reduced colony numbers after treatment with a 6xMIC concentration; however, complete eradication of bacteria in biofilm was not observed [23]. The increase in resistance attributed to the biofilms in my study could be attributed to a decrease in antimicrobial dispersion through the EPS matrix. An increase in diffusional resistance can reduce the ability of antimicrobial agents to reach the cells within the biofilm [24]. Biofilm matrices also contain extracellular DNA which could bind to positively charged peptides, reducing their effectiveness [25]. To our knowledge, this is the first study to demonstrate the biofilm-eradication properties of antimicrobial histones.

We were unable to determine the MBEC value for *P. aeruginosa* biofilms which displayed at least a 100-fold increase in resistance when compared to the MIC. This is similar to results obtained from a previous study examining the anti-biofilm properties of several CAMPs, including LL-37, cecropin A-melittin A amide (CAMA), melittin, defensin and magainin II, against *P. aeruginosa* biofilms. MBEC values could only be reported for LL-37 and CAMA, both 640 µg/ml [26]. In addition to extracellular DNA in the biofilm matrix, *P. aeruginosa* uses another mechanism to reduce its interactions with CAMPs. Previous studies indicate that *P. aeruginosa* biofilms activate the *tolA* gene [27]; its gene product is said to be responsible for altering the LPS structure in order to reduce its affinity to polycations [28].

P. aeruginosa was not only resistant to the histone mixture but also displayed an increase in biofilm growth at subinhibitory concentrations of antimicrobial agents. This phenomenon was also observed in *P. aeruginosa* biofilms treated with tobramycin, amikacin, streptomycin and gentamicin [29]. The same study also observed this response in *E. coli* biofilms treated with tobramycin. This defensive response to the presence of subinhibitory levels of antibiotics involves Arr (aminoglycoside response regulator)—a regulator that alters c-di-GMP levels [29].

Whether Arr in responsible for *P. aeruginosa* biofilm resistance to CAMPs needs to be investigated further.

With respect to the bactericidal mechanism of histones, this study is the first demonstration, to our knowledge, that avian histones bind LTA, particularly that of *B. subtilis* and *E. faecalis*. LTA is highly variable among Gram-positive species, consisting of a polymer of ribitol and glycerol phosphates and anchored to the bacterial membrane by a glycolipid anchor [30]. Studies examining various LTA mutations revealed that the presence of D-alanine esters conferred resistance on *S. aureus* against a variety of CAMPs by reducing the overall negative charge of the LTA [31]. However, resistance to cationic antimicrobial peptides due to low LTA binding affinity was not demonstrated by the MRSA clinical isolate used in this study. Our demonstration of histone binding to LTA is in line with studies demonstrating that histone-like protein A, of bacterial origin, interacts with *S. mutans* LTA [14]. A recent study revealed that histones H2B, H3 and H4 individually can bind *S. aureus* LTA, however a lower affinity between histone H3 and *S. aureus* LTA was observed [32]. They determined that 1-2µg of *S. aureus* LTA was able pull histones H2B, H3 or H4 down into the gel, needing 4-8µg to completely bind 4µg of histones [32]. We demonstrated that 2.5µg of *S. aureus* LTA is necessary to bind and neutralize the positive charges of the histone mixture, with 5µg of LTA needed for complete binding of 5µg of the histone mixture.

We also examined the correlation between LTA-histone binding and the antimicrobial susceptibility of Gram-positive bacteria. The mobility shift assay clearly indicates that purified histones bind *B. subtilis* and *S. aureus* LTA more strongly than that of *E. faecalis* LTA (Fig. 6A, B and C). This is mirrored in the antimicrobial assay with *E. faecalis* having the highest MIC (Table 2).

No correlation was observed between the antimicrobial activity and LPS binding affinity for Gram-negative bacteria. Our results show that histones strongly bind to *P. aeruginosa* LPS with a weaker affinity for *S. typhimurium* LPS and *E. coli* LPS. However, previous studies have shown that histones H2A and H2B, isolated from human placenta, have a higher affinity for the core and lipid A sections of the LPS and possess anti-endotoxin activity [33]. Further studies will determine whether the LPS and LTA binding activity of the chicken histone mixture can sequester these molecules to prevent the release of pro-inflammatory cytokines which can lead to septic shock.

Important factors to consider for an antibiotic alternative are antimicrobial potency and low host cell toxicity to ensure selectivity for pathogens. We used a hemolytic assay to test concentrations up to 50X the highest determined MBEC value, and clearly demonstrated that histones possess little to no significant toxicity towards mammalian cells. Multicellular organisms also possess negatively charged membrane components, although these are typically located in the inner leaflet of the lipid bilayer, resulting in a more neutral charge for the outer membrane [8]. This difference limits the electrostatic interactions between host cells and CAMPs, and increases CAMP selectivity for pathogens.

This study demonstrates that histones extracted from chicken erythrocytes have the potential not only as novel antimicrobial agents against both Gram-positive and Gram-negative bacteria by targeting negatively charged membrane components, but also as novel biofilm eradication agents against Gram-positive biofilms. Insight into the antimicrobial mechanism of CAMPs is essential to the development of novel antimicrobial agents, novel therapeutic application and the identification of the amino acid sequences with the most potent antimicrobial

activity. This information is necessary to combat the emerging antibiotic-resistant bacterial strains and biofilms which have forced exploration of alternatives to inhibit microbial growth.

References

[1] Simor AE, Gilbert NL, Gravel D, Mulvey MR, Bryce E, Loeb M et al. Methicillin-resistant Staphylococcus aureus colonization or infection in Canada: National Surveillance and Changing Epidemiology, 1995-2007. Infect Control Hosp Epidemiol 2010;31:348-56.

[2] Reardon S. WHO warns against "post-antibiotic" era. Nature 2014;doi:10.1038/nature.2014.15135

[3] Mah TC, O'Toole GA. Mechanisms of biofilm resistance to antimicrobial agents. Trends Microbiol. 2001 1/1;9(1):34-9.

[4] Donlan RM. Biofilm formation: A clinically relevant microbiological process. Clin Infect Dis. 2001 Oct 15;33(8):1387-92.

[5] Hall-Stoodley L, Costerton JW, Stoodley P. Bacterial biofilms: From the natural environment to infectious diseases. Nature Reviews Microbiology. 2004;2(2):95-108.

[6] Hirsch JG. Bactericidal action of histone. Jour Exp Med 1958;108:925-44.

[7] Kawasaki H, Iwamuro S. Potential roles of histones in host defense as antimicrobial agents. Infect Disord Drug Targets 2008;8:195-205.

[8] Zasloff M. Antimicrobial peptides of multicellular organisms. Nature 2002;415:389-95.

[9] Teixeira V, Feio MJ, Bastos M. Role of lipids in the interaction of antimicrobial peptides with membranes. Prog Lipid Res 2012;51:149-77.

[10] Helliger W, Lindner H, Hauptlorenz S, Puschendorf B. A new HPLC isolation procedure for chicken and goose erythrocyte histones. Biochem J 1988;255:647-52.

[11] Shechter D, Dormann HL, Allis CD, Hake SB. Extraction, purification and analysis of histones. Nat Protoc 2007;2:1445-57.

[12] Rose-Martel M, Du J, Hincke MT. Proteomic analysis provides new insight into the chicken eggshell cuticle. J Proteomics 2012;75:2697-706.

[13] Jang SA, Kim H, Lee JY, Shin JR, Kim DJ, Cho JH et al. Mechanism of action and specificity of antimicrobial peptides designed based on buforin IIb. Peptides 2012;34:283-9.

[14] Stinson MW, McLaughlin R, Choi SH, Juarez ZE, Barnard JJ. Streptococcal Histone-Like Protein: Primary Structure of hlpA and Protein Binding to Lipoteichoic Acid and Epithelial Cells. Infect Immun 1998;66:259–65.

[15] Kim JK, Lee E, Shin S, Jeong KW, Lee JY, Bae SY et al. Structure and function of papiliocin with antimicrobial and anti-inflammatory activities isolated from the swallowtail butterfly, Papilio xuthus. J Biol Chem 2011;286:41296-311.

[16] Kamio Y, Nikaido H. Outer membrane of Salmonella typhimurium: Accessibility of phospholipid head groups to phospholipase c and cyanogen bromide activated dextran in the external medium. Biochemistry 1976;15:2561–70.

[17] Neuhaus F. A continuum of anionic charge: Structures and functions of d-alanyl-teichoic acids in Gram-positive bacteria. Micro Molec Biol Rev 2003;67:686–723.

[18] Brinkmann V, Reichard U, Goosmann C, Fauler B, Uhlemann Y, Weiss DS et al. Neutrophil extracellular traps kill bacteria. Science 2004;303:1532-5.

[19] Dosler S, Gerceker AA. In vitro activities of antimicrobial cationic peptides; melittin and nisin, alone or in combination with antibiotics against Gram-positive bacteria. 2012;24:137-43.

[20] Bao Y, Sakinc T, Laverde D, Wobser D, Benachour A, Theilacker C et al. Role of mprF1 and mprF2 in the pathogenicity of Enterococcus faecalis. PLoS One 2012;7:e38458.

[21] O'Toole G, Kaplan HB, Kolter R. Biofilm formation as microbial development. Annu Rev Microbiol. 2000;54:49-79.

[22] Lister JL, Horswill AR. Staphylococcus aureus biofilms: Recent developments in biofilm dispersal. Frontiers in Cellular and Infection Microbiology. 2014;4:178.

[23] Zhu C, Tan H, Cheng T, Shen H, Shao J, Guo Y, et al. Human β-defensin 3 inhibits antibiotic-resistant< i> staphylococcus biofilm formation. J Surg Res. 2013;183(1):204-13.

[24] Mulcahy LR, Isabella VM, Lewis K. Pseudomonas aeruginosa biofilms in disease. Microb Ecol. 2013:1-12.

[25] Lewenza S. Extracellular DNA-induced antimicrobial peptide resistance mechanisms in pseudomonas aeruginosa. Frontiers in microbiology. 2013;4.

[26] Dosler S, Karaaslan E. Inhibition and destruction of pseudomonas aeruginosa biofilms by antibiotics and antimicrobial peptides. Peptides. 2014 Dec;62:32-7.

[27] Whiteley M, Bangera MG, Bumgarner RE, Parsek MR, Teitzel GM, Lory S, et al. Gene expression in pseudomonas aeruginosa biofilms. Nature. 2001;413(6858):860-4.

[28] Rivera M, Hancock RE, Sawyer JG, Haug A, McGroarty EJ. Enhanced binding of polycationic antibiotics to lipopolysaccharide from an aminoglycoside-supersusceptible, tolA mutant strain of pseudomonas aeruginosa. Antimicrob Agents Chemother. 1988 May;32(5):649-55.

[29] Hoffman LR, D'Argenio DA, MacCoss MJ, Zhang Z, Jones RA, Miller SI. Aminoglycoside antibiotics induce bacterial biofilm formation. Nature. 2005 Aug 25;436(7054):1171-5.

[30] Ginsburg I. Role of lipoteichoic acid in infection and inflammation. Lancet Infect Dis 2002;2:171-9.

[31] Peschel A, Otto M, Jack RW, Kalbacher H, Jung G, Götz F. Inactivation of the dlt operon in Staphylococcus aureus confers sensitivity to defensins, protegrins, and other antimicrobial peptides. J Biol Chem 1999;274:8405-10.

[32] Morita S, Tagai C, Shiraishi T, Miyaji K, Iwamuro S. Differential mode of antimicrobial actions of arginine-rich and lysine-rich histones against Gram-positive Staphylococcus aureus. Peptides 2013;48:75-82.

[33] Kim HS, Cho JH, Park HW, Yoon H, Kim MS, Kim SC. Endotoxin-neutralizing antimicrobial proteins of the human placenta. J Immunol 2002;168:2356-64.

Peer-reviewed Letter to the Editor:

"Antimicrobial Histones from Chicken Erythrocytes Bind Bacterial Cell Wall Lipopolysaccharides and Lipoteichoic Acids."

Rose-Martel M and Hincke MT (2014) *International Journal of Antimicrobial Agents*, 44(5):470-472

Sir,

Extensive use of antibiotics has selected for a variety of multi-drug resistant bacteria, which is a pressing concern due to their increasing prevalence. From 1995 to 2007, Canadian hospitals experienced a 17-fold increase in MRSA incidence, of which >75% were thought to be acquired in a hospital or health-care setting [1]. The gravity of the situation was recently highlighted by the World Health Organization (WHO) [2]. Moreover, 12% of hospital-acquired infections in the USA are from the species *Enterococcus*, of which 80-90% are *E. faecalis* [3]. Promising alternatives to antibiotics are cationic antimicrobial peptides (CAMPs), which are key players in the innate immune defense system of many species that target pathogen components that cannot be easily mutated. Histones are an archetypal CAMP.

This study reports the MIC (minimum inhibitory concentration) and MBC (minimum bactericidal concentration) values of histones purified from chicken erythrocytes against Gram-negative and Gram-positive bacterial strains, including *E. faecalis* and methicillin-resistant *S. aureus* (Fig. 1A-G). The most susceptible Gram-positive bacterial species was *B. subtilis*, with a MIC of 3 ± 1 µg/ml; the least susceptible was *E. faecalis*, requiring 700 ± 100 µg/ml to inhibit bacterial growth (MIC) and 1100 ± 200 µg/ml to cause bacterial cell death (MBC) (Fig. 1A and B). The MICs of *S. aureus* and MRSA were not significantly different from each other,

demonstrating similar susceptibilities at 6 ± 1 μg/ml and 8 ± 2 μg/ml, respectively (Fig. 1C and D). The histone mixture was significantly more potent in inhibiting the growth of Gram-negative *S. typhimurium* and *P. aeruginosa* when compared to *E. coli* (Fig 1E, F and G). *E. coli, S. typhimurium* and *P. aeruginosa* have MICs of 21 ± 3 μg/ml, 3.6 ± 0.4 μg/ml and 5 ± 1 μg/ml, respectively, which are not statistically different from their MBCs. Therefore histones exert potent antimicrobial activity towards both Gram-negative and Gram-positive bacteria, with *E. faecalis* demonstrating markedly less susceptibility.

The first step in the antimicrobial mechanism of CAMPs is the electrostatic interaction between the positive charges of the antimicrobial and the negatively charged molecules located on the surface of the bacterial cell wall. We investigated the mechanism for this interaction using a mobility shift assay to determine the affinity of histones for *S. aureus, E. faecalis* and *B. subtilis* lipoteichoic acids (LTA), as well as *E. coli, S. typhimurium* and *P. aeruginosa* lipopolysaccharides (LPS) (Fig. 1K, L and M). Fig. 1 (H, I and J) demonstrates that histones bind strongly to *B. subtilis* and *S.aureus* LTA, with saturated binding at 5μg of LTA, compared with *E. faecalis* LTA which required 7.5μg of LTA. Similarly, 5μg of *P. aeruginosa* LPS completely bound to and neutralized the positive charges of the histone molecules (Fig. 1M). However, the lowest histone-LPS binding affinities observed were for *S. typhimurium* LPS, requiring 10μg of LPS to saturate the charge on histone molecules; while more than 10μg of *E. coli* LPS is necessary (Fig. 6K and L). Overall, these results suggested that histones target pathogens via conserved negatively charged components imbedded in their cellular membranes. A correlation between the antimicrobial activity of histones towards Gram-positive bacteria and LTA-histone binding affinity was observed.

A hemolytic assay was used to determine whether the histone mixture displayed toxicity towards mammalian cells, over a wide range of histone concentrations were tested (from 0.005 – 1.25 mg/ml). Histones did not damage the RBC cell membranes, and were non-hemolytic even at the highest concentration tested (1.25 mg/ml).

Chicken erythrocytes are an ideal source of purified histones; the ease of harvest and lack of connective tissue allow for rapid and simple large-scale acid extraction from nuclei [4]. Proteomic analysis revealed that the histone mixture assessed in our study contains histones H1, H2B, H2A, H3, H4 and H5. Neutrophil extracellular traps (NETs), which are key players in the innate immune response in a variety of vertebrate species, also contain a variety of histones (H1, H2A, H2B, H3 and H4) [5]. NETs are composed of the neutrophil nuclear contents that have been released extracellularly to create an elevated concentration of antimicrobial proteins at the site of infection. In addition to a bactericidal function, they also prevent further microbial spreading within the organism [5]. Our results clearly indicate that histones possess antimicrobial activity, potentially of a synergistic nature, and could play a role in pathogen recognition in the vertebrate immune system. Development of antimicrobial peptides is essential to combat emerging antibiotic-resistant bacterial strains which have forced exploration of alternatives for inhibition of microbial growth. These results demonstrate that histone-derived molecules have the possibility for development of novel antibiotics.

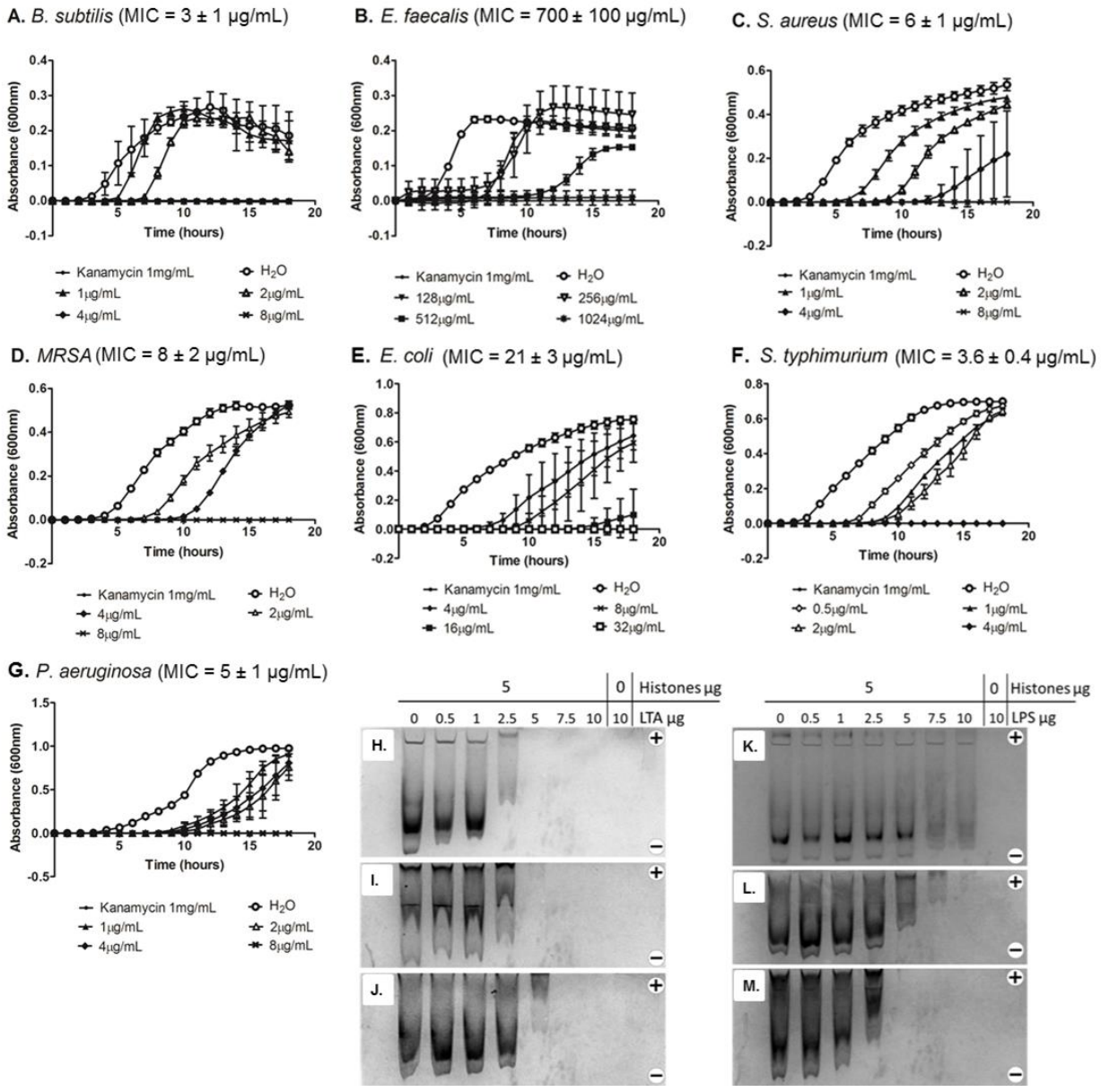
A. B. subtilis (MIC = 3 ± 1 μg/mL)
B. E. faecalis (MIC = 700 ± 100 μg/mL)
C. S. aureus (MIC = 6 ± 1 μg/mL)
D. MRSA (MIC = 8 ± 2 μg/mL)
E. E. coli (MIC = 21 ± 3 μg/mL)
F. S. typhimurium (MIC = 3.6 ± 0.4 μg/mL)
G. P. aeruginosa (MIC = 5 ± 1 μg/mL)
Absorbance (600nm)
Time (hours)
Kanamycin 1mg/mL
H2O
1μg/mL
2μg/mL
4μg/mL
8μg/mL
128μg/mL
256μg/mL
512μg/mL
1024μg/mL
16μg/mL
32μg/mL
0.5μg/mL
Histones μg
LTA μg
LPS μg
H.
I.
J.
K.
L.
M.

Fig. 1. Dose-dependent growth inhibition of Gram-positive and Gram-negative bacteria treated with histone mixture from chicken erythrocytes, as well as Minimum Inhibitory Concentration (MIC), determined by a microbroth dilution assay. (A, B, C and D) Four Gram-positive bacterial strains were tested as well as (E, F and G) three Gram-negative strains with H_2O and kanamycin as negative and positive controls for inhibition, respectively. Results are representative of three independent trials, each in triplicate. (H-M) Mobility shift assay of histone-LTA and histone-LPS complexes in non-denaturing conditions. Purified histones (5µg) were incubated with increasing amounts of LTA from (H) *B. subtilis*, (I) *S. aureus* and (J) *E. faecalis*, or LPS from (K) *E. coli*, (L) *S. typhimurium* and (M) *P. aeruginosa*. Controls include 5µg of histones and 10µg of LPS/LTA loaded individually on each gel.

Acknowledgments

The authors would like to thank Dr. Sattar and Richard Kibbee from the University of Ottawa's Centre for Research on Environmental Microbiology (CREM) for the gift of the bacterial species used in this study. They are also grateful to Tom Henderson of Tom Henderson Custom Meat (Chesterville, Ontario) and Robert Laplante from Laplante Poultry Farms Ltd. (Monkland, Ontario) for assisting with collection of fresh chicken blood.

Declarations

Funding: This study was funded by the Poultry Industry Council (PIC) and the Agriculture and Agri-Food Canada (AAFC) - Canadian Poultry Research Council (CPRC) poultry cluster. MRM would also like to thank the CPRC for a student scholarship.

Competing interests: None declared.

Ethical approval: All procedures involving chickens were in accordance with CFIA guidelines and regulations and all procedures involving rats were carried out in accordance with the University of Ottawa Animal Care Committee guidelines.

References

[1] Rose ML, Hincke MH. Protein constituents of the eggshell: eggshell-specific matrix proteins. Cell Mol Life Sci 2009;66:2707–19.

[2] Dennis JM, Xiao SQ, Agarwal M, Fink DJ, Heuer AH, Caplan AI. Microstructure of matrix and mineral components of eggshells from White Leghorn Chickens (Gallus gallus). J Morphol 1996;228:287–306.

[3] Hincke MT, Chien Y-C, Gerstenfeld LC, McKee MD. Colloidal-gold immunocytochemical localization of osteopontin in avian eggshell gland and eggshell. J Histochem Cytochem 2008;56:467–76.

[4] Romanoff AL, Romanoff AJ. The avian egg. New York: John Wiley and Sons Inc.; 1949.

[5] Ruiz J, Lunam CA. Ultra structural analysis of the eggshell: contribution of the individual calcified layers and the cuticle to hatchability and egg viability in broiler breeders. Br Poult Sci 2000;41:584–92.

Supplementary Data

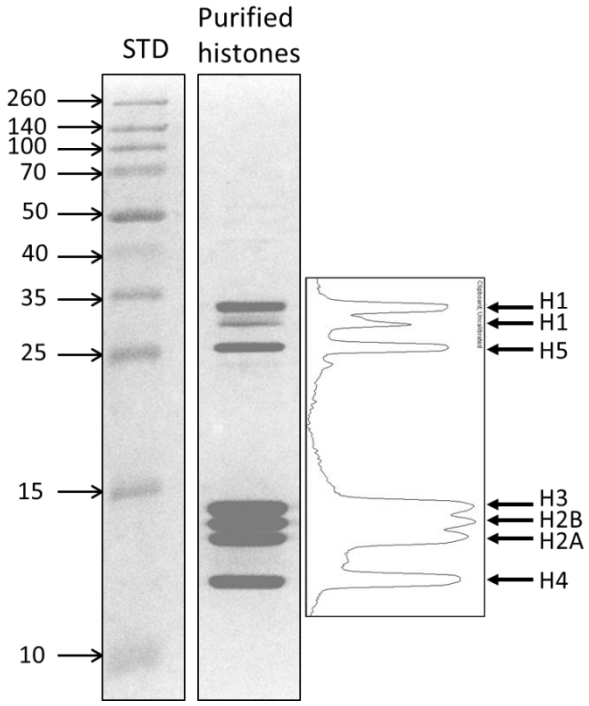

Fig. S1. SDS-PAGE analysis of TCA-precipitated histone mixture extracted from turkey erythrocytes. (A) A 15% acrylamide gel revealed 7 distinct bands which were analyzed using densitometry as well as cut out and sent for proteomics LC/MS/MS analysis. Results allowed us to distinguish two bands for histone H1 as well as a single band for histones H2A, H2B, H3, H4 and H5 (see Table S1 for proteomics and densitometry results). STD: molecular weight standards (kDa).

Table S1. Densitometry and LC/MS/MS proteomics analysis results of sequenced turkey histone bands (Fig. S1).

Bands[a]	Identified proteins[b]	# of unique peptides[b]	UniProt ID[b]	% of total histone sample[c]	Coverage (%)[b]
Band 1	Histone H1	16	G1NH14	11	36
Band 2	Histone H1	22	G1NH14	5	34
Band 3	Histone H5	30	G1NRW6	9	46
Band 4	Histone H3	25	G1N7D3	22	64
Band 5	Histone H2B	35	G1NRI6	17	75
Band 6	Histone H2A	8	H9H207	19	55
Band 7	Histone H4	38	G1NRJ0	17	73

d. Bands are depicted in Fig. S1.
e. Data obtained from Scaffold version 4.3.4, Proteome Software Inc
f. Results obtained from densitometry analysis using ImageJ densitometry software version 1.6

Table S2. Identity scores for sequence alignments between histones extracted from chicken and turkey erythrocytes.

Bands[a]	Chicken		Turkey		UniProt Identity Score (%)[d]
	Identified proteins[b]	UniProt ID[b]	Identified proteins[c]	UniProt ID[c]	
Band 1	Histone H1.11L	P08287	Histone H1	G1NH14	81
Band 2	Histone H1.11R	P08288	Histone H1	G1NH14	79
Band 3	Histone H5	P02259	Histone H5	G1NRW6	96
Band 4	Histone H3	P84229	Histone H3	G1N7D3	100
Band 5	Histone H2B	P0C1H3	Histone H2B	G1NRI6	98
Band 6	Histone H2A	P70082	Histone H2A	H9H207	91
Band 7	Histone H4	P62801	Histone H4	G1NRJ0	100

a. Bands are depicted in Fig. 1 and S1.
b. Data obtained from Scaffold version 3.00.08, Proteome Software Inc
c. Data obtained from Scaffold version 4.3.4, Proteome Software Inc
d. Results obtained from UniProt sequence alignment software.

Chapter 5 – General Discussion

A pathogen-free egg is not only vital for reproductive success of avian species, but also critical for human safety as unfertilized eggs are a nutritious, functional food for human consumption. Eggs are a significant source of dietary cholesterol and, for this reason, were discouraged from regular consumption in order to prevent elevated levels of blood low density lipoprotein cholesterol (Krauss et al., 2000). Studies are now revealing that increased egg consumption, up to one egg per day, is not associated with an increased risk of heart disease (Rong et al., 2013). Increased awareness of the beneficial effects of functional foods in promoting health and preventing chronic illnesses has furthered the fast-growing functional food and natural health product industry in Canada (Khamphoune, 2013). Eggs can be categorized as enhanced commodities since their nutritional components are naturally enhanced using different feed formulations (Siró et al., 2008). A good example of enhanced eggs is eggs rich in omega-3 fatty acids, obtained by introducing flax seeds or fish oil into the feed of the laying hens (Surai and Sparks, 2001). An increased dietary intake of omega-3 fatty acids can aid in the prevention and management of coronary heart diseases, hypertension and many other human diseases (Simopoulos, 2000), and a recent survey found that eggs with omega-3 fatty acids were among the top three functional food products consumed by participants (Vella et al., 2013). For all of these reasons, Canadian yearly egg consumption has risen from 205 to 256 eggs per person from 1995-2013.

The egg possesses numerous barriers which ensure the protection of the developing embryo; these in turn, have been beneficial in respect to food safety. This thesis has described the many physical and chemical barriers that prevent bacterial contamination of the interior, with

particular focus on the biomineralized eggshell. Proteomics and transcriptomics analyses performed by myself and others have provided valuable insight into eggshell specific-matrix proteins and their function in biomineralization and/or antimicrobial protection. The following discussion will describe the future directions of this study and its potential applications for human health.

1. Enhancing the Innate Barriers of the Eggshell

Deficiencies in the eggshell biomechanical integrity and antimicrobial constituents can lead to an increase in horizontal bacterial transmission from pathogens associated with chicken feces, nesting environment or egg processing facilities (Messens et al., 2005). The primary concern of the food industry is preventing human illness caused by food-borne pathogens. With regards to the table egg industry, the major bacterial concerns are *Salmonella* spp., *Listeria* spp., *Staphylococcus* spp., *Bacillus* spp., *Campylobacter* spp. and *Escherichia* spp. The consumption of eggs or egg products contaminated with these pathogens can result in gastrointestinal symptoms including abdominal pain, diarrhea, nausea and vomiting.

Eggs with incomplete or absent cuticles are known to be more susceptible to bacterial contamination (Sparks and Board, 1984); which led to my hypothesis that the cuticle layer is an important antimicrobial barrier of the avian egg. Since cuticle deposition is a moderately heritable trait (Bain et al., 2013), genetic selection to improve cuticle quality can be a promising technique to enhance food safety. Using mass spectrometry-based technology and bioinformatics analysis we identified multiple cuticle-resident antimicrobials (Rose-Martel et al., 2012). The two most abundant cuticle proteins identified were OCX-25 (similar to Kunitz-like protease

inhibitor) and OCX-32, both eggshell-specific matrix proteins. A large variety of nonsynonymous SNPs in *OCX-32* were detected in multiple commercial layer chicken lines (Fulton et al., 2012). Certain OCX-32 haplotypes were associated with calcium carbonate crystal orientation (Dunn et al., 2012) and eggshell mammillary layer thickness (Dunn et al., 2009). Our cross-analysis of proteomics data isolated from fertilized and unfertilized egg models revealed OCX-32 as one of the proteins enriched in the mammillary cones (Rose-Martel et al., 2015). Recombinant OCX-32 inhibits bacterial growth (Xing et al., 2007); however, it is unclear whether naturally occurring OCX-32 haplotypes will demonstrate variability in antimicrobial protection.

Our proteomics analysis of the eggshell cuticle also identified ovocleidin-116 (OC-116), an eggshell-specific matrix protein suggested to have a crucial function in calcitic biomineralization (Hincke et al., 1999). OC-116 haplotypes were also shown to be associated with calcium carbonate crystal orientation (Dunn et al., 2012), as well as cuticle deposition (Bain et al., 2013), eggshell thickness and elasticity (Dunn et al., 2009).

Shell strength and quality can be affected by several factors including nutritional and physiological changes in the laying hen. It is well known that eggshell quality declines as the laying hens advance in age due to an increase in egg weight (size), without an increase in shell deposition (Roland, 1979). It was established that the decrease in shell quality could be associated with variations in the proportions of eggshell matrix proteins as well as alterations in crystal size and orientation (Panheleux et al., 2000). These effects are reversed following an induced moult in the laying hens. Studies evaluating the lev els of eggshell matrix proteins before and after moulting have associated the change in eggshell quality to an increase in OC-116 and OC-17 shell matrix proteins after moulting (Ahmed et al., 2005).

Due to substantial amounts of genetic variation in commercial layer chicken lines (Wong et al., 2004), selection breeding programs could be developed for specific gene targets to enhance shell quality and resistance to microbial invasion. Comprehensive proteomics studies are the first step towards understanding the role of the eggshell matrix proteins in the resistance to microbial contamination of the table egg as well as provide possible targets for selection breeding programs.

2. The Avian Eggshell as a Model for Calcitic Biomineralization

Living organisms can direct organized crystal formation from a supersaturated solution, a process known as biomineralization. This process is characterized by protein-crystal interactions that modulate crystal growth on an extracellular matrix, and is essential for the formation of biological hard tissues including bone, teeth, and the calcareous shell (Arias et al., 1990). The fastest calcitic biomineralization process is avian eggshell formation; in the chicken approximately 6g of calcium carbonate is deposited within a 17-hour period while the egg is in the hen uterus (Arias et al., 1990). Chicken eggshell formation is therefore an accessible model for the study of this process due to the rapid rate of mineralization, the ease of protein extraction and the availability of this biomaterial.

Proteomics analysis of shell matrix proteins, combined with our analysis of proteins involved in the initial stages of eggshell formation, drew attention to key similarities between the proteins involved in the calcitic biomineralization process in both eggshell and otoconia formation. Otoconia are bio-crystals associated with the gravity receptor organs of the inner ear of vertebrates. The gravity receptor organs are known as the utricle and saccule, and are localized to the vestibule of the inner ear along with three semicircular canals. The semicircular

canals sense rotational acceleration, such as head turning, while the gravity receptor organs sense gravity and linear acceleration (Lundberg et al., 2014).

Otoconia formation requires precise interactions between calcium carbonate, matrix proteins and the otoconial membrane localized to the inner ear of vertebrates. Each otoconium consists of a proteinaceous core around which calcium carbonate was precipitated (Hughes et al., 2006). Similar to the avian eggshell, the cells of the surrounding tissues secrete the necessary ionic and protein components for the biomineralization process. Within the inner ear, the epithelial cells in the saccule and utricle synthesize the necessary regulatory proteins such as otoconins (Lundberg et al., 2014). Otoconins are otoconia-specific proteins involved in crystal-protein interactions that modulate crystal formation and growth (Kawasaki et al., 2009). These crystals are embedded in an extracellular matrix responsible for connecting the shearing force provided by the otoconia to the sensory hair cells (Hughes et al., 2006). These cells send electrical signals to the central nervous system which leads to the initiation of neuronal responses for sustaining body balance (Lundberg et al., 2014).

Benign paroxysmal position vertigo (BPPV), the most common cause of vertigo in humans, is caused by the detachment of degenerated otoconia from the utricle and their migration to the semicircular canals (Walther et al., 2014). An epidemiological study conducted in Germany revealed a cumulative incidence of BPPV at 10% by the age of 80 years (von Brevern et al., 2007). A Swedish study identified a prevalence of 11% in a population of 75 year-olds (Kollén et al., 2012) and finally, a prevalence of 9% of unrecognized BPPV was identified in a study of an elderly population in the United States (Oghalai et al., 2000). BPPV is characterized by dizziness, imbalance and severe attacks of vertigo brought on by specific head movements including lying down and turning over in bed (von Brevern, 2013). Previous studies

have described an increase in the occurrence of falls in patients with BPPV (Oghalai et al., 2000), which, in the elderly, can often lead to fractures and hospitalization.

Otoconia can become dislodged due to head trauma or can be damaged by drugs and inflammation (Andrade et al., 2012). However, the most common source of otoconial damage is age-related degeneration. Intact otoconia crystals possess a slightly coarsened surface due to the presence of tiny pores. Studies examining degenerative changes in vital specimens determined that otoconia degenerate gradually over a lifetime (Walther et al., 2013). Initial indications of degeneration include fissures and increase in surface roughness. These characteristics eventually worsen leading to deeper fissures and pores (formation of holes), with dissolution leading to the loss of otoconial material. Eventually the otoconia become completely dissolved resulting in a decrease in volume and number of otoconia (Igarashi et al., 1993).

Several studies have described potential causes for otoconia detachment and degeneration including partial demineralization of the subsurface layer which weakens the fibrils that anchor the otoconia to each other, as well as to the otoconial membrane (Andrade et al., 2012). Researchers also found that women who suffer from osteoporosis were more likely to suffer from BPPV possibly due to variations in the calcium metabolism of post-menopausal women (Vibert et al., 2003). The effect of an imbalanced calcium homeostasis in the endolymph of the inner ear on matrix proteins in otoconia is unknown. Many studies have clearly demonstrated the age-induced degeneration of ocotonia; however, no studies have been able to determine the precise cause of otoconial demineralization.

Eggshell formation is an accessible model for studying calcitic biomineralization and our study has demonstrated key similarities in the proteinaceous organic matrices of both these calcitic structures. Further studies of eggshell matrix proteins and their function in

biomineralization can lead to new technologies to regulate biomineralization in a variety of hard tissues, including otoconia, and can offer new insights into protein-crystal interactions for treatment of human diseases such as otoconial degeneration.

3. Eggshell-Inspired Antimicrobial Proteins

In-depth analysis of the comprehensive proteomes generated by this study, together with the previously characterized proteomes from other egg compartments, revealed the presence of histones in the egg yolk, egg white, shell membranes, eggshell and cuticle (Mann and Mann, 2008; D'Ambrosio et al., 2008; Mann, 2007; Mann and Mann, 2011; Mann et al., 2006; Sun et al., 2013). However, the concentration of histones in each of the egg compartments is currently unknown; further studies are necessary to confirm whether histones levels are sufficiently high to provide these egg compartments with antimicrobial protection. For this reason, highly purified histones were prepared from a suitable tissue source in order to investigate dose-response and bacterial specificity.

Therefore, applications of antimicrobial histones can be extended further than just to innate protection for the egg. My studies have described the potent antimicrobial activity of avian histones towards Gram-positive and Gram-negative planktonic, and biofilm-forming bacteria, as well as low mammalian cell toxicity. Most importantly, the histone mixture extracted from avian erythrocytes inhibited the growth of planktonic methicillin-resistant *S. aureus* (MRSA) and its corresponding biofilm. Histones have ideal characteristics for development as novel therapeutic agents for the treatment of multi-drug resistant bacteria and their corresponding biofilms.

Extensive use of antibiotics in health care settings and agricultural industry has selected for a variety multi-drug resistant bacteria (Laxminarayan and Heymann, 2012). From 1995-2009, Canadian hospitals have observed a 19-fold increase in the incidence of MRSA in admitted patients (Canadian Nosocomial Infection Surveillance Program, 2011). The emergence of multi-drug resistant bacteria has promoted research for new antimicrobial strategies to treat antibiotic-resistant infections that lead to prolonged illnesses and elevated rates of mortality. Cationic antimicrobial peptides (CAMPs) are emerging as a new class of antimicrobial agents that could have potential in a clinical setting.

CAMPs have several advantages over conventional antibiotics, including a broader spectrum of antimicrobial activity and reduced potential for development of resistance mechanisms. As demonstrated by this study, one of the major advantages of histones is their capacity to inhibit the growth of both susceptible and antibiotic-resistant bacteria, at similar concentrations. This demonstrates that the current bacterial resistance mechanisms that diminish the efficacy of traditional antibiotics, such as diminished uptake, improved efflux and chemical modification/degradation of the antibiotic, would have no effect on the activity of CAMPs (Marr et al., 2006).

The correspondence between the minimum inhibitory concentration (MIC) and minimum bactericidal concentration (MBC) values for histones identified in this study support a bacteriolytic mechanism of action (Rose-Martel and Hincke, 2014). The bactericidal mechanism of histones was suggested to originate from electrostatic interactions between histones and negatively charged components of the bacterial cell wall. My study confirmed histone interactions with lipopolysaccharides (LPS) and lipoteichoic acids (LTA), components of the Gram-negative and Gram-positive bacterial cell wall, respectively. Strategies that bacteria use to

evade CAMPs are modifications of these outer membrane components in order to reduce the overall negative charge and decrease the electrostatic interactions with the peptides. For example, Gram-positive bacteria such as *S. aureus* and *L. monocytogenes* can reduce the overall negative charge of their outer cell wall by modifying LTA with D-alanine residues (Peschel et al., 1999). *S. aureus* can also reduce the negative charge of a membrane lipid phosphatidylglycerol following L-lysine modifications (Peschel et al., 2001). Similar modifications to LPS are observed in Gram-negative bacteria with demonstrated resistance to antimicrobial peptides. In the case of *S. typhimurium*, positively charged aminoarabinoses are added to the lipid A components of the bacterial membrane (Ernst et al., 2001). While bacterial resistance mechanisms have appeared against CAMPs, the resulting increase in resistance is modest. This was previously confirmed by exposing *P. aeruginosa* to sub-MIC levels of antimicrobial peptides and antibiotics. Following 30 passages, *P. aeruginosa* was 2 to 4-fold more resistant to antimicrobial peptides (Zhang et al., 2005) while 11 passages were sufficient to increase resistance 10 to 190-fold for antibiotics (Steinberg et al., 1997).

Another desirable trait of CAMPs is the possibility of endotoxin-neutralizing function and immune-modulation. Lipopolysaccharides (LPS), or endotoxins, released from Gram-negative bacteria in the blood stream can elicit a significant inflammatory response causing septic shock. This is a common occurrence in bacterial infections treated with antibiotics (Rosenfeld et al., 2006). Histones H2A and H2B isolated from the fetal membrane of human placenta demonstrated endotoxin-neutralizing activity that functioned by binding to the lipid A component of bacterial LPS and thus preventing tumor necrosis factor (TNF)-α secretion induced by LPS (Kim et al., 2002). Antimicrobial peptides LL-37, a human cathelicidin, and DEFB126, human β-defensin 126, are also able to significantly diminish LPS-induced

production of TNF-α as well as interleukin (IL)-6 (Liu et al., 2013). This suggests a dual protective role for CAMPs by preventing LPS from activating Toll-Like receptors and inhibiting the release of inflammatory cytokines. LL-37 also has chemoattractant properties for monocytes, neutrophils and T cells (Yang et al., 2000) as well as up-regulates chemokine and chemokine receptor expression *in vivo* in the mouse lung (Scott et al., 2022). Additionally, human α-defensins human neutrophil peptide (HNP)-1 and HNP-2 possess chemotactic activity towards T cells (Chertov et al., 1996). These findings suggest that CAMPs can play several beneficial roles in eradicating bacterial infections. They have direct bacteriolytic activity against invading pathogens, prevent inflammatory responses induced by endotoxins and recruit immune cells to the site of infection.

Some of the disadvantages of using antimicrobial peptides in clinical use for systemic applications are the costs associated with peptide production and their susceptibility to proteolytic digestion (Zhang and Falla, 2006). While low-cost commercial-scale peptide production systems are being explored, several strategies are being used to reduce the size of the peptides to the most antimicrobially active sequence. Some researchers have described modifying the original sequence of the antimicrobial peptides to increase hydrophobicity and α-helical content in order to improve the antimicrobial properties of the peptide or to decrease cytotoxicity (Jang et al., 2012). The incorporation of fluorinated amino acids has also been explored as an approach to increase hydrophobicity and the stability of secondary structures. Importantly, antimicrobial peptides synthesized with fluorinated amino acids have shown an increase in activity as well as resistance to proteolytic digestion due to steric obstruction (Meng and Kumar, 2007). Lipidic and polymeric encapsulation methods for the improved resistance of

orally administered CAMPs to digestive enzymes show promising results in target delivery and uptake by enterocytes, hence increasing CAMP bioavailability (Delie and Blanco-Príeto, 2005).

Therefore, histones are exciting candidates for therapeutic agents for several reasons. (1) They possess a broad spectrum of antimicrobial activity with low toxicity towards mammalian cells. (2) Only a few resistance mechanisms have been detected against CAMPs and the resulting resistance is limited. (3) They can be utilized in a variety of potential applications as LPS-neutralizing and immune-modulating compounds. Histones have therapeutic potential in medical applications: they can be used individually or in synergy with antibiotics to combat infection or aid in the prevention of biofilm formation on medical devices such as implants and catheters. In fact, MX-226, a peptide derived from bovine indolicidin, has shown efficacy in clinical trials for the prevention of infections associated with central venous catheters (Marr et al., 2006). Clinical trials with CAMPs have been mostly limited to topical applications due to the unknown toxicity effects of systemic use or poor pharmacokinetics due to their proteolytic digestion after oral ingestion. Interestingly, antimicrobial peptides are now being incorporated into hydrogels and other biological scaffolds, and studied for wound healing properties (Song et al., 2011). Histones also have potential applications in the food and agricultural industry, either as a preservative or as an alternative to antibiotics in animal feed. Emerging antibiotic-resistant bacteria are a growing concern in all of these industries and the discovery and development of alternative antimicrobial agents is essential for human health.

Future considerations for development of this project involve identifying histone fragments with potent antimicrobial and biofilm eradicating activity, and their chemical synthesis. Candidate peptides will be assessed for immune-modulating activity and modifications

to the peptide sequence will be evaluated for decreased susceptibility to proteolysis, decrease in cytotoxicity and increase in therapeutic activity.

4. Conclusions

My comprehensive proteomics analyses have provided significant insight into the protein constituents of the avian eggshell. Thorough analysis of proteins associated with shell membranes, mineralized shell and organic cuticle reveal two important clusters of proteins that participate in the innate defense of the egg against microbial contamination. The first group consists of proteins that enhance the physical barriers of the egg. These include proteins that are involved in the formation of shell membranes, eggshell calcification and cuticle deposition. The second group corresponds to proteins that contribute to the antimicrobial protection of the egg by inhibiting bacterial growth, either directly or indirectly. Continued research of these proteins and functions can provide increased knowledge of the defense mechanisms operating at biomineralized barriers and lead to valuable insight as a model for human biological hard tissues as well as provide new therapeutic alternatives for combatting multi-drug resistant bacteria.

References

Ahmed A, Rodriguez-Navarro A, Vidal M, Gautron J, García-Ruiz JM, Nys Y (2005) Changes in eggshell mechanical properties, crystallographic texture and in matrix proteins induced by moult in hens. Br Poult Sci 46: 268-279

Andrade LR, Lins U, Farina M, Kachar B, Thalmann R (2012) Immunogold TEM of otoconin 90 and otolin–relevance to mineralization of otoconia, and pathogenesis of benign positional vertigo. Hear Res 292: 14-25

Ar A, Rahn H (1985) Pores in avian eggshells: gas conductance, gas exchange and embryonic growth rate. Respir Physiol 61: 1-20

Ar A, Rahn H, Paganelli CV (1979) The avian egg: mass and strength. Condor: 331-337

Arias JL, Fernandez MS, Dennis JE, Caplan AI (1991) Collagens of the chicken eggshell membranes. Connect Tissue Res 26: 37-45

Arias JL, Fernandez MS, Laraia VJ, Janicki J, Heuer AH, Caplan AI (1990) The Avian Eggshell as a Model of Biomineralization. MRS Online Proceedings Library 218

Arias JL, Fink DJ, Xiao S, Heuer AH, Caplan AI (1993) Biomineralization and eggshells: cell-mediated acellular compartments of mineralized extracellular matrix. Int Rev Cytol 145: 217-250

Bain MM, McDade K, Burchmore R, Law A, Wilson PW, Schmutz M, Preisinger R, Dunn IC (2013) Enhancing the egg's natural defence against bacterial penetration by increasing cuticle deposition. Anim Genet 44: 661-668

Birkhead TR, Sheldon BC, Fletcher F (1994) A comparative study of sperm-egg interactions in birds. J Reprod Fertil 101: 353-361

Board R, Fuller R (1974) Non-specific antimicrobial defences of the avian egg, embryo and neonate. Biological Reviews 49: 15-49

Board R, Halls N (1973) The cuticle: a barrier to liquid and particle penetration of the shell of the hen's egg. Br Poult Sci 14: 69-97

Board R, Tranter H (1995) The Microbiology of Eggs. In "Egg Science and Technology" Ed by Staddelman W, Cotterill O, Food Products Press/ The Haworth Press Inc., New York, NY, pp 81-104

Burley RW, Vadehra DV (1989). The Avian Egg: Chemistry and Biology, Wiley-Interscience Publication, p 472

Camarda A, Newell D, Nasti R, Di Modugno G (2000) Genotyping Campylobacter jejuni strains isolated from the gut and oviduct of laying hens. Avian Dis: 907-912

Canadian Nosocomial Infection Surveillance Program (2011) Surveillance for methicillin-resistant Staphylococcus aureus in Canadian hospitals—a report update from the Canadian Nosocomial Infection Surveillance Program. Can Commun Dis Rep 2015: 14

Chemaly M, Toquin M, Le Nôtre Y, Fravalo P (2008) Prevalence of Listeria monocytogenes in poultry production in France. Journal of Food Protection 71: 1996-2000

Chertov O, Michiel DF, Xu L, Wang JM, Tani K, Murphy WJ, Longo DL, Taub DD and Oppenheim JJ (1996) Identification of defensin-1, defensin-2, and CAP37/azurocidin as T-cell chemoattractant proteins released from interleukin-8-stimulated neutrophils. J Biol Chem 271: 2935-2940

Chien Y, Hincke MT, Vali H, McKee MD (2008) Ultrastructural matrix–mineral relationships in avian eggshell, and effects of osteopontin on calcite growth in vitro. J Struct Biol 163: 84-99

Chousalkar KK, Flynn P, Sutherland M, Roberts JR, Cheetham BF (2010) Recovery of Salmonella and Escherichia coli from commercial egg shells and effect of translucency on bacterial penetration in eggs. Int J Food Microbiol 142: 207-213

Cordeiro CM, Esmaili H, Ansah G, Hincke MT (2013) Ovocalyxin-36 is a pattern recognition protein in chicken eggshell membranes. PloS one 8: e84112

Cuperus T, Coorens M, van Dijk A, Haagsman HP (2013) Avian host defense peptides. Developmental & Comparative Immunology 41: 352-369

D'Ambrosio C, Arena S, Scaloni A, Guerrier L, Boschetti E, Mendieta ME, Citterio A, Righetti PG (2008) Exploring the chicken egg white proteome with combinatorial peptide ligand libraries. J Proteome Res 7: 3461-3474

Danielsson-Tham M (2013) Staphylococcal Food Poisoning. Food Associated Pathogens: 250

De Reu K, Messens W, Heyndrickx M, Rodenburg T, Uyttendaele M, Herman L (2008) Bacterial contamination of table eggs and the influence of housing systems. Worlds Poult Sci J 64: 5-19

Delie F, Blanco-Príeto MJ (2005) Polymeric particulates to improve oral bioavailability of peptide drugs. Molecules 10: 65–80

Dennis JE, Xiao S, Agarwal M, Fink DJ, Heuer AH, Caplan AI (1996) Microstructure of matrix and mineral components of eggshells from white leghorn chickens (Gallus gallus). J Morphol 228: 287-306

DeWinter LM, Ross WH, Couture H, Farber JF (2011) Risk assessment of shell eggs internally contaminated with Salmonella Enteritidis. International Food Risk Analysis Journal 1: 40-81

Dunn IC, Joseph NT, Bain M, Edmond A, Wilson PW, Milona P, Nys Y, Gautron J, Schmutz M, Preisinger R, Waddington D (2009) Polymorphisms in eggshell organic matrix genes are associated with eggshell quality measurements in pedigree Rhode Island Red hens. Anim Genet 40: 110-114

Dunn IC, Rodriguez-Navarro AB, Mcdade K, Schmutz M, Preisinger R, Waddington D, Wilson PW, Bain MM (2012) Genetic variation in eggshell crystal size and orientation is large and these traits are correlated with shell thickness and are associated with eggshell matrix protein markers. Anim Genet 43: 410-418

Ernst RK, Guina T, Miller SI (2001) Salmonella typhimurium outer membrane remodeling: role in resistance to host innate immunity. Microb Infect 3: 1327-1334

Farinazzo A, Restuccia U, Bachi A, Guerrier L, Fortis F, Boschetti E, Fasoli E, Citterio A, Righetti PG (2009) Chicken egg yolk cytoplasmic proteome, mined via combinatorial peptide ligand libraries. J Chromatogr A 1216: 1241-1252

Fulton JE, Soller M, Lund AR, Arango J, Lipkin E (2012) Variation in the ovocalyxin-32 gene in commercial egg-laying chickens and its relationship with egg production and egg quality traits. Anim Genet 43 Suppl 1: 102-113

Gast RK, Benson ST (1995) The comparative virulence for chicks of Salmonella enteritidis phage type 4 isolates and isolates of phage types commonly found in poultry in the United States. Avian Dis 39: 567-574

Gautron J, Hincke M, Panheleux M, Garcia-Ruiz J, Boldicke T, Nys Y (2001) Ovotransferrin is a matrix protein of the hen eggshell membranes and basal calcified layer. Connect Tissue Res 42: 255-267

Hellgren O, Ekblom R (2010) Evolution of a cluster of innate immune genes (beta-defensins) along the ancestral lines of chicken and zebra finch. Immunome Res 6: 3-7580-6-3

Hernandez-Milian A, Payeras-Cifre A (2014) What is new in listeriosis?. Biomed Res Int 2014: 358051

Herve-Grepinet V, Rehault-Godbert S, Labas V, Magallon T, Derache C, Lavergne M, Gautron J, Lalmanach AC, Nys Y (2010) Purification and characterization of avian beta-defensin 11, an antimicrobial peptide of the hen egg. Antimicrob Agents Chemother 54: 4401-4409

Hincke M, Gautron J, Mann K, Panhéleux M, McKee M, Bain M, Solomon S, Nys Y (2003) Purification of ovocalyxin-32, a novel chicken eggshell matrix protein. Connect Tissue Res 44: 16-19

Hincke M, Gautron J, Panheleux M, Garcia-Ruiz J, McKee M, Nys Y (2000) Identification and localization of lysozyme as a component of eggshell membranes and eggshell matrix. Matrix Biology 19: 443-453

Hincke M, Tsang C, Courtney M, Hill V, Narbaitz R (1995) Purification and immunochemistry of a soluble matrix protein of the chicken eggshell (ovocleidin 17). Calcif Tissue Int 56: 578-583

Hincke MT, Chien YC, Gerstenfeld LC, McKee MD (2008) Colloidal-gold immunocytochemical localization of osteopontin in avian eggshell gland and eggshell. J Histochem Cytochem 56: 467-476

Hincke MT, Gautron J, Tsang CP, McKee MD, Nys Y (1999) Molecular cloning and ultrastructural localization of the core protein of an eggshell matrix proteoglycan, ovocleidin-116. J Biol Chem 274: 32915-32923

Hincke MT, Nys Y, Gautron J, Mann K, Rodriguez-Navarro AB, McKee MD (2012) The eggshell: structure, composition and mineralization. Front Biosci (Landmark Ed) 17: 1266-1280

Hirsch JG (1958) Bactericidal action of histone. J Exp Med 108: 925-944

Hogue A, White P, Guard-Petter J, Schlosser W, Gast R, Ebel E, Farrar J, Gomez T, Madden J, Madison M, McNamara AM, Morales R, Parham D, Sparling P, Sutherlin W, Swerdlow D (1997) Epidemiology and control of egg-associated Salmonella enteritidis in the United States of America. Rev Sci Tech 16: 542-553

Hughes I, Thalmann I, Thalmann R, Ornitz DM (2006) Mixing model systems: Using zebrafish and mouse inner ear mutants and other organ systems to unravel the mystery of otoconial development. Brain Res 1091: 58-74

Igarashi M, Saito R, Mizukoshi K, Alford BR (1993) Otoconia in young and elderly persons: a temporal bone study. Acta Otolaryngol 113: 26-29

Jan S, Brunet N, Techer C, Le Maréchal C, Koné AZ, Grosset N, Cochet MF, Gillard A, Gautier M, Puterflam J, Baron F (2011) Biodiversity of psychrotrophic bacteria of the Bacillus cereus group collected on farm and in egg product industry. Food Microbiol 28: 261-265

Jang SA, Kim H, Lee JY, Shin JR, Kim DJ, Cho JH, Kim SC (2012) Mechanism of action and specificity of antimicrobial peptides designed based on buforin IIb. Peptides 34: 283-289

Jones D, Anderson K, Guard J (2012) Prevalence of coliforms, Salmonella, Listeria, and Campylobacter associated with eggs and the environment of conventional cage and free-range egg production. Poult Sci 91: 1195-1202

Jones D, Musgrove M (2005) Correlation of eggshell strength and Salmonella Enteritidis contamination of commercial shell eggs. Journal of Food Protection 68: 2035-2038

Jones D, Musgrove M (2007) Pathogen prevalence and microbial levels associated with restricted shell eggs. Journal of Food Protection 70: 2004-2007

Kawasaki H, Iwamuro S (2008) Potential roles of histones in host defense as antimicrobial agents. Infectious Disorders-Drug Targets (Formerly Current Drug Targets-Infectious Disorders) 8: 195-205

Kawasaki K, Buchanan AV, Weiss KM (2009) Biomineralization in humans: making the hard choices in life. Annu Rev Genet 43: 119-142

Kaweewong K, Garnjanagoonchorn W, Jirapakkul W, Roytrakul S (2013) Solubilization and identification of hen eggshell membrane proteins during different times of chicken embryo development using the proteomic approach. Protein J 32: 297-308

Khamphoune B (2013) Results from the 2011 Functional Foods and Natural Health Products Survey. Statistics Canada Working Paper, Catalogue: 18-001

Kim HS, Cho JH, Park HW, Yoon H, Kim MS and Kim SC (2002). Endotoxin-neutralizing antimicrobial proteins of the human placenta. J of Immunol 168: 2356-2364

Kodali VK, Gannon SA, Paramasivam S, Raje S, Polenova T, Thorpe C (2011) A novel disulfide-rich protein motif from avian eggshell membranes. PLoS One 6: e18187

Kollén L, Frändin K, Möller M, Olsén MF, Möller C (2012) Benign paroxysmal positional vertigo is a common cause of dizziness and unsteadiness in a large population of 75-year-olds. Aging clinical and experimental research 24: 317-323

Kone A, Jan S, Le Maréchal C, Grosset N, Gautier M, Puterflam J, Baron F (2013) Identifying risk factors for eggshell contamination by Bacillus cereus group bacteria in French laying farms. Br Poult Sci 54: 298-305

Kovacs-Nolan J, Mine Y (2012) Egg yolk antibodies for passive immunity. Annual review of food science and technology 3: 163-182

Krauss RM, Eckel RH, Howard B, Appel LJ, Daniels SR, Deckelbaum RJ, et al. (2000) AHA Dietary Guidelines: revision 2000: a statement for healthcare professionals from the Nutrition Committee of the American Heart Association. Stroke 31: 2751-2766

Laxminarayan R, Duse A, Wattal C, Zaidi AK, Wertheim HF, Sumpradit N, Vlieghe E, Hara GL, Gould IM, Goossens H (2013) Antibiotic resistance—the need for global solutions. The Lancet infectious diseases 13: 1057-1098

Laxminarayan R, Heymann DL (2012) Challenges of drug resistance in the developing world. BMJ-British Medical Journal 344: e1567

Le Loir Y, Baron F, Gautier M (2003) Staphylococcus aureus and food poisoning. Genet Mol Res 2: 63-76

Lemaire S, Trinh T, Le H, Tang S, Hincke M, Wellman-Labadie O, Ziai S (2008) Antimicrobial effects of H4-(86–100), histogranin and related compounds–possible involvement of DNA gyrase. FEBS journal 275: 5286-5297

Li G, Mine Y, Hincke MT, Nys Y (2007) Isolation and characterization of antimicrobial proteins and peptide from chicken liver. Journal of Peptide Science 13: 368-378

Liu H, Yu H, Gu Y, Xin A, Zhang Y, Diao H, Lin D (2013) Human beta-defensin DEFB126 is capable of inhibiting LPS-mediated inflammation. Appl Microbiol Biotechnol 97: 3395-3408

Logan N (2012) Bacillus and relatives in foodborne illness. J Appl Microbiol 112: 417-429

Lundberg YW, Xu Y, Thiessen KD, Kramer KL (2014) Mechanisms of otoconia and otolith development. Developmental Dynamics

Mageed AA, Isobe N, Yoshimura Y (2008) Expression of avian β-defensins in the oviduct and effects of lipopolysaccharide on their expression in the vagina of hens. Poult Sci 87: 979-984

Mann K (2007) The chicken egg white proteome. Proteomics 7: 3558-3568

Mann K (2008) Proteomic analysis of the chicken egg vitelline membrane. Proteomics 8: 2322-2332

Mann K, Macek B, Olsen JV (2006) Proteomic analysis of the acid-soluble organic matrix of the chicken calcified eggshell layer. Proteomics 6: 3801-3810

Mann K, Mann M (2008) The chicken egg yolk plasma and granule proteomes. Proteomics 8: 178-191

Mann K, Mann M (2011) In-depth analysis of the chicken egg white proteome using an LTQ Orbitrap Velos. Proteome Sci 9: 7-5956-9-7

Marr AK, Gooderham WJ, Hancock RE (2006) Antibacterial peptides for therapeutic use: obstacles and realistic outlook. Current Opinion in Pharmacology 6: 468-472

Matsuzaki K (1998) Magainins as paradigm for the mode of action of pore forming polypeptides. Biochimica et Biophysica Acta (BBA)-Reviews on Biomembranes 1376: 391-400

Mayes F, Takeballi M (1983) Microbial contamination of the hen's egg: a review. Journal of Food Protection (USA)

Meng H, Kumar K (2007) Antimicrobial activity and protease stability of peptides containing fluorinated amino acids. J Am Chem Soc 129: 15615-15622

Messens W, Grijspeerdt K, Herman L (2005) Eggshell characteristics and penetration by Salmonella enterica serovar Enteritidis through the production period of a layer flock. Br Poult Sci 46: 694-700

Messens W, Grijspeerdt K, Herman L (2005) Eggshell penetration by Salmonella: a review. Worlds Poult Sci J 61: 71-86

Miksik I, Sedlakova P, Lacinova K, Pataridis S, Eckhardt A (2010) Determination of insoluble avian eggshell matrix proteins. Anal Bioanal Chem 397: 205-214

Moats WA (1980) Classification of bacteria from commercial egg washers and washed and unwashed eggs. Appl Environ Microbiol 40: 710-714

Musgrove MT, Jones DR, Northcutt JK, Harrison MA, Cox NA (2005) Impact of commercial processing on the microbiology of shell eggs. Journal of Food Protection 68: 2367-2375

Nys Y, Gautron J, Garcia-Ruiz JM, Hincke MT (2004) Avian eggshell mineralization: biochemical and functional characterization of matrix proteins. Comptes Rendus Palevol 3: 549-562

Nys Y, Hincke MT, Arias JL, Garcia-Ruiz JM, Solomon SE (1999) Avian Eggshell Mineralization. Avian and Poultry Biology Reviews 10: 143-166

Ofner-Agostini M, Johnston BL, Simor AE, Embil J, Matlow A, Mulvey M, Ormiston D, Conly J, Canadian Nosocomial Infection Surveillance Program (2008) Vancomycin-resistant enterococci in Canada: results from the Canadian nosocomial infection surveillance program, 1999-2005. Infect Control Hosp Epidemiol 29: 271-274

Oghalai JS, Manolidis S, Barth JL, Stewart MG, Jenkins HA (2000) Unrecognized benign paroxysmal positional vertigo in elderly patients. Otolaryngol Head Neck Surg 122: 630-634

Panheleux M, Nys Y, Williams J, Gautron J, Boldicke T, Hincke M (2000) Extraction and quantification by ELISA of eggshell organic matrix proteins (ovocleidin-17, ovalbumin, ovotransferrin) in shell from young and old hens. Poult Sci 79: 580-588

Park CB, Yi KS, Matsuzaki K, Kim MS, Kim SC (2000) Structure-activity analysis of buforin II, a histone H2A-derived antimicrobial peptide: the proline hinge is responsible for the cell-penetrating ability of buforin II. Proc Natl Acad Sci U S A 97: 8245-8250

Parseghian MH, Luhrs KA (2006) Beyond the walls of the nucleus: the role of histones in cellular signaling and innate immunity This paper is one of a selection of papers published in this Special Issue, entitled 27th International West Coast Chromatin and Chromosome Conference, and has undergone the Journal's usual peer review process. Biochemistry and cell biology 84: 589-595

Peschel A, Jack RW, Otto M, Collins LV, Staubitz P, Nicholson G, Kalbacher H, Nieuwenhuizen WF, Jung G, Tarkowski A, van Kessel KP, van Strijp JA (2001) Staphylococcus aureus resistance to human defensins and evasion of neutrophil killing via the novel virulence factor MprF is based on modification of membrane lipids with l-lysine. J Exp Med 193: 1067-1076

Peschel A, Otto M, Jack RW, Kalbacher H, Jung G, Gotz F (1999) Inactivation of the dlt operon in Staphylococcus aureus confers sensitivity to defensins, protegrins, and other antimicrobial peptides. J Biol Chem 274: 8405-8410

Reyes-Grajeda JP, Moreno A, Romero A (2004) Crystal structure of ovocleidin-17, a major protein of the calcified Gallus gallus eggshell: implications in the calcite mineral growth pattern. J Biol Chem 279: 40876-40881

Rivoal K, Fablet A, Courtillon C, Bougeard S, Chemaly M, Protais J (2013) Detection of Listeria spp. in liquid egg products and in the egg breaking plants environment and tracking of Listeria monocytogenes by PFGE. Int J Food Microbiol 166: 109-116

Rodriguez-Navarro A, Kalin O, Nys Y, Garcia-Ruiz J (2002) Influence of the microstructure on the shell strength of eggs laid by hens of different ages. Br Poult Sci 43: 395-403

Roland DA (1979) Factors influencing shell quality of aging hens. Poult Sci 58: 774-777

Romanoff AL, Romanoff AJ (1949) The Avian Egg. John Wiley & Sons, New York

Rong Y, Chen L, Zhu T, Song Y, Yu M, Shan Z, et al. (2013) Egg consumption and risk of coronary heart disease and stroke: dose-response meta-analysis of prospective cohort studies. BMJ 346: e8539

Rose ML, Hincke MT (2009) Protein constituents of the eggshell: eggshell-specific matrix proteins. Cell Mol Life Sci 66: 2707-2719

Rose-Martel M, Du J, Hincke MT (2012) Proteomic analysis provides new insight into the chicken eggshell cuticle. J Proteomics 75: 2697-2706

Rose-Martel M, Hincke MT (2014) Antimicrobial histones from chicken erythrocytes bind bacterial cell wall lipopolysaccharides and lipoteichoic acids. Int J Antimicrob Agents 44: 470-472

Rose-Martel M, Smiley S, Hincke MT (2015) Novel identification of matrix proteins involved in calcitic biomineralization. Journal of Proteomics 116: 81-96

Rosenfeld Y, Papo N, Shai Y (2006) Endotoxin (lipopolysaccharide) neutralization by innate immunity host-defense peptides. Peptide properties and plausible modes of action. J Biol Chem 281: 1636-1643

Ruiz J, Lunam CA (2000) Ultrastructural analysis of the eggshell: contribution of the individual calcified layers and the cuticle to hatchability and egg viability in broiler breeders. Br Poult Sci 41: 584-592

Rusnak JM, Kortepeter M, Ulrich R, Poli M, Boudreau E (2004) Laboratory exposures to staphylococcal enterotoxin B. Emerging Infect Dis 10: 1544-1549

Sahin O, Kobalka P, Zhang Q (2003) Detection and survival of Campylobacter in chicken eggs. J Appl Microbiol 95: 1070-1079

Schroeder CM, Naugle AL, Schlosser WD, Hogue AT, Angulo FJ, Rose JS, Ebel ED, Disney WT, Holt KG, Goldman DP (2005) Estimate of illnesses from Salmonella enteritidis in eggs, United States, 2000. Emerg Infect Dis 11: 113-115

Scott MG, Davidson DJ, Gold MR, Bowdish D and Hancock RE (2002) The human antimicrobial peptide LL-37 is a multifunctional modulator of innate immune responses. Journal of Immunology 169: 3883-3891

Silphaduang U, Hincke MT, Nys Y, Mine Y (2006) Antimicrobial proteins in chicken reproductive system. Biochem Biophys Res Comm 340: 648

Simopoulos A (2000) Human requirement for N-3 polyunsaturated fatty acids. Poult Sci 79: 961-970

Siró I, Kápolna E, Kápolna B, Lugasi A (2008) Functional food. Product development, marketing and consumer acceptance—A review. Appetite 51: 456-467

Smith MM (1991) Histone structure and function. Curr Opin Cell Biol 3: 429-437

Solomon SE (1999) Gordon Memorial Lecture. An egg ist ein ei, es un huevo, est un oeuf. Br Poult Sci 40: 5-11

Song A, Rane AA and Christman KL (2012) Antibacterial and cell-adhesive polypeptide and poly (ethylene glycol) hydrogel as a potential scaffold for wound healing. Acta biomaterialia 8: 41-50

Sparks N (1994) Shell accessory materials: structure and function. In "Microbiology of the avian egg" Ed by Anonymous Springer, pp 25-42

Sparks N, Board R (1984) Cuticle, shell porosity and water uptake through hens' eggshells. Br Poult Sci 25: 267-276

Steinberg DA, Hurst MA, Fujii CA, Kung AH, Ho JF, Cheng FC, Loury DJ, Fiddes JC (1997) Protegrin-1: a broad-spectrum, rapidly microbicidal peptide with in vivo activity. Antimicrob Agents Chemother 41: 1738-1742

Sun C, Xu G, Yang N (2013) Differential label-free quantitative proteomic analysis of avian eggshell matrix and uterine fluid proteins associated with eggshell mechanical property. Proteomics 13: 3523-3536

Surai PF, Sparks NHC (2001) Designer eggs: from improvement of egg composition to functional food. Trends Food Sci Technol 12: 7-16

Swaminathan B, Gerner-Smidt P (2007) The epidemiology of human listeriosis. Microb Infect 9: 1236-1243

Teixeira V, Feio MJ, Bastos M (2012) Role of lipids in the interaction of antimicrobial peptides with membranes. Prog Lipid Res 51: 149-177

Todd EC (1996) Risk assessment of use of cracked eggs in Canada. Int J Food Microbiol 30: 125-143

Tyler C (1956) Studies on egg shells. VII.—Some aspects of structure as shown by plastic models. J Sci Food Agric 7: 483-493

Vella MN, Stratton LM, Sheeshka J, Duncan AM (2013) Exploration of functional food consumption in older adults in relation to food matrices, bioactive ingredients, and health. J Nutr Gerontol Geriatr 32: 122-144

Vibert D, Kompis M, Hausler R (2003) Benign paroxysmal positional vertigo in older women may be related to osteoporosis and osteopenia. ANNALS OF OTOLOGY RHINOLOGY AND LARYNGOLOGY 112: 885-889

Volentine KK, Yao HH, Bahr JM (1998) Epidermal growth factor in the germinal disc and its potential role in follicular development in the chicken. Biol Reprod 59: 522-526

von Brevern M (2013) Benign paroxysmal positional vertigo. Semin Neurol 33: 204-211

von Brevern M, Radtke A, Lezius F, Feldmann M, Ziese T, Lempert T, Neuhauser H (2007) Epidemiology of benign paroxysmal positional vertigo: a population based study. J Neurol Neurosurg Psychiatry 78: 710-715

Walther LE, Blödow A, Buder J, Kniep R (2014) Principles of Calcite Dissolution in Human and Artificial Otoconia. PloS one 9: e102516

Walther LE, Wenzel A, Buder J, Bloching MB, Kniep R, Blödow A (2013) Detection of human utricular otoconia degeneration in vital specimen and implications for benign paroxysmal positional vertigo. European Archives of Oto-Rhino-Laryngology: 1-6

Wellman-Labadie O, Lakshminarayananb R, Hincke MT (2008) Antimicrobial properties of avian eggshell-specific C-type
lectin-like proteins. FEBS let 582

Wellman-Labadie O, Lemaire S, Mann K, Picman J, Hincke MT (2010) Antimicrobial activity of lipophilic avian eggshell surface extracts. J Agric Food Chem 58: 10156-10161

Wellman-Labadie O, Picman J, Hincke MT (2008) Antimicrobial activity of cuticle and outer eggshell protein extracts from three species of domestic birds. Br Poult Sci 49

Whittow GC (1999) Sturkie's avian physiology. Academic press, New York

Wong GKS, Liu B, Wang J, Zhang Y, Yang X, Zhang Z, et al. (2004) A genetic variation map for chicken with 2.8 million single-nucleotide polymorphisms. Nature 432: 717-722

Xing J, Wellman-Labadie O, Gautron J, Hincke MT (2007) Recombinant eggshell ovocalyxin-32: Expression, purification and biological activity of the glutathione S-transferase fusion protein. Comparative Biochemistry and Physiology Part B: Biochemistry and Molecular Biology 147: 172-177

Yang D, Chen Q, Schmidt AP, Anderson GM, Wang JM, Wooters J, Oppenheim JJ and Chertov O (2000) LL-37, the neutrophil granule–and epithelial cell–derived cathelicidin, utilizes formyl peptide receptor–like 1 (FPRL1) as a receptor to chemoattract human peripheral blood neutrophils, monocytes, and T cells. J Exp Med 192: 1069-1074

Zasloff M (2002) Antimicrobial peptides of multicellular organisms. Nature 415: 389-395

Zhang L, Falla TJ (2006) Antimicrobial peptides: therapeutic potential. Expert Opin Pharmacother 7: 653-663

Zhang L, Parente J, Harris SM, Woods DE, Hancock RE, Falla TJ (2005) Antimicrobial peptide therapeutics for cystic fibrosis. Antimicrob Agents Chemother 49: 2921-2927

Authorizations

SPRINGER LICENSE
TERMS AND CONDITIONS

Jan 24, 2015

This is a License Agreement between Megan Rose-Martel ("You") and Springer ("Springer") provided by Copyright Clearance Center ("CCC"). The license consists of your order details, the terms and conditions provided by Springer, and the payment terms and conditions.

All payments must be made in full to CCC. For payment instructions, please see information listed at the bottom of this form.

License Number	3555140387502
License date	Jan 23, 2015
Licensed content publisher	Springer
Licensed content publication	Cellular and Molecular Life Sciences
Licensed content title	Protein constituents of the eggshell: eggshell-specific matrix proteins
Licensed content author	Megan L. H. Rose
Licensed content date	Jan 1, 2009
Volume number	66
Issue number	16
Type of Use	Thesis/Dissertation
Portion	Full text
Number of copies	5
Author of this Springer article	Yes and you are the sole author of the new work
Order reference number	None
Title of your thesis / dissertation	Innate Mechanisms of Antimicrobial Defense Associated with the Avian Eggshell
Expected completion date	Jan 2015
Estimated size(pages)	300

ELSEVIER LICENSE
TERMS AND CONDITIONS

Jan 24, 2015

This is a License Agreement between Megan Rose-Martel ("You") and Elsevier ("Elsevier") provided by Copyright Clearance Center ("CCC"). The license consists of your order details, the terms and conditions provided by Elsevier, and the payment terms and conditions.

All payments must be made in full to CCC. For payment instructions, please see information listed at the bottom of this form.

Supplier	Elsevier Limited The Boulevard,Langford Lane Kidlington,Oxford,OX5 1GB,UK
Registered Company Number	1982084
Customer name	Megan Rose-Martel
License number	3555141291974
License date	Jan 24, 2015
Licensed content publisher	Elsevier
Licensed content publication	Journal of Proteomics
Licensed content title	Proteomic analysis provides new insight into the chicken eggshell cuticle
Licensed content author	Megan Rose-Martel,Jingwen Du,Maxwell T. Hincke
Licensed content date	17 May 2012
Licensed content volume number	75
Number of pages	10
Start Page	2697
End Page	2706
Type of Use	reuse in a thesis/dissertation
Intended publisher of new work	other
Portion	full article
Format	both print and electronic
Are you the author of this Elsevier article?	Yes
Will you be translating?	No
Title of your thesis/dissertation	Innate Mechanisms of Antimicrobial Defense Associated with the Avian Eggshell
Expected completion date	Jan 2015
Estimated size (number of pages)	300
Elsevier VAT number	GB 494 6272 12

ELSEVIER LICENSE
TERMS AND CONDITIONS

Jan 28, 2015

This is a License Agreement between Megan Rose-Martel ("You") and Elsevier ("Elsevier") provided by Copyright Clearance Center ("CCC"). The license consists of your order details, the terms and conditions provided by Elsevier, and the payment terms and conditions.

All payments must be made in full to CCC. For payment instructions, please see information listed at the bottom of this form.

Supplier	Elsevier Limited The Boulevard,Langford Lane Kidlington,Oxford,OX5 1GB,UK
Registered Company Number	1982084
Customer name	Megan Rose-Martel
License number	3557430643510
License date	Jan 28, 2015
Licensed content publisher	Elsevier
Licensed content publication	Journal of Proteomics
Licensed content title	Novel identification of matrix proteins involved in calcitic biomineralization
Licensed content author	None
Licensed content date	Available online 10 January 2015
Licensed content volume number	n/a
Licensed content issue number	n/a
Number of pages	1
Start Page	None
End Page	None
Type of Use	reuse in a thesis/dissertation
Intended publisher of new work	other
Portion	full article
Format	both print and electronic
Are you the author of this Elsevier article?	Yes
Will you be translating?	No
Title of your thesis/dissertation	Innate Mechanisms of Antimicrobial Defense Associated with the Avian Eggshell
Expected completion date	Jan 2015

ELSEVIER LICENSE
TERMS AND CONDITIONS

Jan 28, 2015

This is a License Agreement between Megan Rose-Martel ("You") and Elsevier ("Elsevier") provided by Copyright Clearance Center ("CCC"). The license consists of your order details, the terms and conditions provided by Elsevier, and the payment terms and conditions.

All payments must be made in full to CCC. For payment instructions, please see information listed at the bottom of this form.

Supplier	Elsevier Limited The Boulevard,Langford Lane Kidlington,Oxford,OX5 1GB,UK
Registered Company Number	1982084
Customer name	Megan Rose-Martel
License number	3557421401186
License date	Jan 28, 2015
Licensed content publisher	Elsevier
Licensed content publication	International Journal of Antimicrobial Agents
Licensed content title	Antimicrobial histones from chicken erythrocytes bind bacterial cell wall lipopolysaccharides and lipoteichoic acids
Licensed content author	None
Licensed content date	November 2014
Licensed content volume number	44
Licensed content issue number	5
Number of pages	3
Start Page	470
End Page	472
Type of Use	reuse in a thesis/dissertation
Intended publisher of new work	other
Portion	full article
Format	both print and electronic
Are you the author of this Elsevier article?	Yes
Will you be translating?	No
Title of your thesis/dissertation	Innate Mechanisms of Antimicrobial Defense Associated with the Avian Eggshell
Expected completion date	Jan 2015